Title

Part 1: Method Development for the Analysis of Polyamines by Derivatives with Benzoyl Chloride by HPLC Tandem Mass Spectrometry Part 2: Detection of Volatile Organic Compound Tracers in Human Breath

Author

Van, Jenny Kim

Publication Date

2015

Peer reviewed|Thesis/dissertation

UNIVERSITY OF CALIFORNIA, SAN DIEGO

SAN DIEGO STATE UNIVERSITY

Part 1: Method Development for the Analysis of Polyamines by Derivatives with Benzoyl Chloride by HPLC Tandem Mass Spectrometry

Part 2: Detection of Volatile Organic Compound Tracers in Human Breath

A dissertation submitted in partial satisfaction of the

requirements for the degree Doctor of Philosophy in

Chemistry

by

Jenny Kim Van

Committee in charge:

University of California, San Diego

Professor Charles L. Perrin
Professor Amitabha Sinha

San Diego State University

Professor Dale A. Chatfield, Chair
Professor Christopher R. Harrison
Professor Eunha Hoh

2015

The Dissertation of Jenny Kim Van is approved, and it is acceptable in quality and form for publication on microfilm and electronically:

_____

_____

_____

_____

_____
Chair

University of California, San Diego

San Diego State University

2015

DEDICATION

I dedicate this work to the memory of my parents, Phat Gia Van and Hoa Trinh. Without their courage, sacrifice, and love I would not achieve what I have accomplished and become who I am today. I am forever indebted to them for the chance they gave me to pursue life and career goals.

I will always miss them dearly.

To my husband, Thomas Lee, there are no words to describe how grateful and blessed I am to have your patience, support, and love.

TABLE OF CONTENTS

SIGNATURE PAGE iii

DEDICATION iv

TABLE OF CONTENTS v

LIST OF ABBREVIATIONS xi

LIST OF TABLES xiv

LIST OF FIGURES xxii

LIST OF GRAPHS xxx

ACKNOWLEDGEMENTS xxxii

VITA xxxiv

ABSTRACT OF THE DISSERTATION xxxvi

PART 1: METHOD DEVELOPMENT FOR THE ANALYSIS OF POLYAMINES BY DERIVATIVES WITH BENZOYL CHLORIDE BY HPLC TANDEM MASS SPECTROMETRY 1

CHAPTER 1. INTRODUCTION 2

1.1. Relevance of Polyamine Analysis 2

1.2. Analyses of Polyamines in Fruit Flies 3

1.3. Review of Literature of Analytical Methods for Polyamine Analysis 4

1.3.1. Pre-treatment of Amines for Analysis 4

1.3.2. Detectors Used for Derivatized Products 7

1.4. Electrospray Ionization and Triple Stage Quadrupole 8

1.5. Objectives 12

CHAPTER 2. EXPERIMENTAL 16

2.1. Chemicals, Materials, and Instruments 16
2.2. Preparation of Standards and Internal Standards 18
2.3. Sample Preparation and Instrument Operating Optimized Conditions 18
2.3.1. Preparation of Samples 19
2.3.2. Derivatization Procedure 19
2.3.3. Liquid Chromatography 20
2.3.4. Selection of Fragment Ions 21
CHAPTER 3. RESULTS AND DISCUSSION 23
3.1. Internal Standards 23
3.1.1. Types of Internal Standards 23
3.1.2. Internal Standard Method 24
3.1.2.1 DAH vs. BEN to determine quantitation accuracy of PUT and SPD 26
3.1.3. Isotope Dilution Method 27
3.1.4. Accuracy of Internal Standard Versus Isotope Dilution Method 30
3.2. Optimization of the Derivatization Procedure 31
3.2.1. Reagent (Benzoyl Chloride) Reaction Solvent and Mole Ratio 32
3.2.2. Reaction Time and Temperature 36
3.2.3. Removal of Reaction By-Products 36
3.2.4. Product Extraction 40
3.3. Optimizing Liquid Chromatography Steps 40
3.3.1. Gradient Elution 40
3.3.2. Sample Solvent Reconstitution 44
3.3.3. Sample Injection Volume 46
3.3.4. Blanks & Carryover 47
3.4. Optimization of Mass Spectrometer Parameters 49

3.4.1. Fragmentation and Collision Energy Optimization of PAs and Internal Standards 49
3.4.2. Formic Acid versus Acetic Acid 52
3.4.3. Optimization of Collision Energy (CE) for Isotopic Internal Standards (PUT-d8 and SPD-d8) 52
3.5. Matrix Effect 55
3.5.1. Filtered Versus Unfiltered Homogenized Flies 56
3.5.2. Full Scan and Single Reaction Monitoring for Phospholipids 59
3.6. Method Validation 69
3.6.1. Linearity 69
3.6.2. Accuracy and Precision 70
3.6.2.1 Derivatization method accuracy and precision 70
3.6.2.2 Instrument accuracy and precision 71
3.6.3. Limit of Detection (LOD) and Limit of Quantitation (LOQ) 72
3.6.4. Stability and Storage (Ruggedness) 74
3.7. Fly Samples 77
3.8. Rat Liver Cell Lysate 79
CHAPTER 4. CONCLUSION 87
Appendix 91
A. Comparison of Four Internal Standards Investigated 91
B. Raw Data Collected from Optimization Experiments 92
B.1. Raw Data of Different Treatments of Benzoyl Chloride 92
B.2. Raw Data of Optimized Ratio of Benzoyl Chloride to Each PA 94
B.3. Raw Data of Optimization of Reaction Time and Temperature 96
B.4. Methylene Chloride Extracts of Products 98
C. Chromatograms of Liquid Chromatography Experiments 99

C.1. Chromatograms of Solvent Ratio Reconstitution of Samples 99
C.2. Chromatograms of Individually Prepared PAs and Internal Standards 100
D. Mass Spectra and Raw Data from Collision Energy Optimization Experiments 102
E. Raw Data of Collision Energy Experiments of PUT and SPD 107
F. Full scan spectra from matrix effect experiments 108
G. Calibration Curve of Each Analyte Relative to an Internal Standard 109
H. Raw Data from Intra-day and Inter-day Experiments 114
I. Raw Data from Stability Experiments 116
J. Raw Data from Analysis of Fruit Flies 124
K. Raw Data from Analysis of Rat Liver Cell Lysates 126
PART 2: DETECTION OF VOLATILE ORGANIC COMPOUND TRACERS IN HUMAN BREATH 128
CHAPTER 5. INTRODUCTION 129
5.1. Review of Literature 131
5.1.1. Breath Sample Types for BCA 131
5.1.2. Standardization of Sample Collection 132
5.1.3. Normalization of Data 133
5.1.4. 'Background' Sample 134
5.2. Objectives 135
CHAPTER 6. EXPERIMENTAL 140
6.1. Subject(s) Recruitment Protocol 140
6.2. Chemicals, Materials, and Instruments 141
6.3. Preparation of Internal Standards 143
6.4. Preparation of Chemical Tracers in Exposure Device 144

6.5. Canister Cleaning Apparatus and Protocol 146
6.6. Breath and Exhaled Breath Condensate (EBC) Collection Apparatus 147
6.6.1. Breath Sample Collection (Canisters) Protocol 149
6.6.2. EBC Collection 150
6.6.2.1 Preparation of adsorbent traps 150
6.6.2.2 EBC collection protocol 151
6.6.3. Sample Concentration 152
6.7. Gas Chromatography 153
6.8. Mass Spectrometry 154
CHAPTER 7. RESULTS AND DISCUSSION 156
7.1. Tracer Compound Selection 156
7.1.1. Gas Anesthetics 157
7.1.2. Fluorinated Compounds 158
7.2. Gas Chromatography 160
7.3. Mass Spectrometry 162
7.4. Blanks 163
7.4.1. Canister Blanks 163
7.4.2. Adsorbent Traps 166
7.4.2.1 Breakthrough experiments of adsorbent traps 168
7.4.3. Carryover From Subject to Subject 171
7.5. Reproducibility of Results from Canisters and Adsorbent Traps 173
7.5.1. Reproducibility of Internal Standards with Canisters 173
7.5.2. Reproducibility of Internal Standards with Adsorbent Traps 174
7.6. Sensitivity of Canisters versus Adsorbent Traps 175
7.7. Linearity of Instrument 175

7.8. Normalization of Data 177
7.8.1. Quantifying Results Using Ratios of Tracer Compound to Internal Standard 178
7.8.1.1 Pharmacokinetic modeling 179
7.8.2. Quantifying Results Using Only Peak Area of Tracer Compound 181
7.8.3. Quantifying Results Using Ratios of Tracer Compound and a Compound that was Assumed to be Constant in Breath 182
7.9. Decay of Compounds in Breath Samples 184
CHAPTER 8. CONCLUSION 191
Appendix 196
A. Institutional Review Board (IRB) Approval For Outside Subject(s) 196
B. Spectra of Analytes and Internal Standards 197
C. Canister Cleaning Cycle Raw Data 201
D. Data of Reproducibility Experiments from Canisters and Adsorbent Traps 202
D.1. Reproducibility of Canisters 202
D.2. Reproducibility of Adsorbent Traps 204
E. Linearity graphs 206
F. Elimination Graphs of EBC from Subject 1 and Subject 2 212

LIST OF ABBREVIATIONS

$[M+H]^+$	Protonated molecular ion
3-FBT	3-Fluorobenzotrifluoride
4-CBT	4-Chlorobenzotrifluoride
AA	Acetic acid
ACGIH	American Conference of Governmental Industrial Hygienists
ACN	Acetonitrile
BCA	Breath component analysis
BEN	Benzanilide
BEN-105	Benzanilide with m/z of 105.1
BEN-77	Benzanilide with m/z of 77.1
BEN-d6	Benzene-d6
CAD	Cadaverine
CE	Collision energy
CRM	Charged residue model
DAH	1,7-diaminoheptane
EBC	Exhaled breath condensate
EE	Even electron species
ENF	Enflurane
ESI	Electrospray ionization
FA	Formic acid
HCF	Hydrocarbon free air
HPLC	High performance liquid chromatography

IDMS	Isotope dilution mass spectrometry
IEM	Ion evaporation model
IR	Infrared
IRB	Internal Review Board
LC	Liquid chromatography
LOD	Limit of detection
LOQ	Limit of quantitation
m/z	mass to charge ratio
MET	Methoxyflurane
MS	Mass spectrometry
MS/MS	Tandem mass spectrometry
N1-ASPM	N1-acetylspermine
N8-ASPD	N8-acetylspermidine
OE	Odd electron species
P	Octanol to water partition coefficient
P/d8	Ratio of putrescine to putrescine-d8
PA(s)	Polyamines: CAD, N1-ASPM, N8-ASPD, PUT, SPD, and SPM
PDMS	Polydimethylsiloxane
ppb	parts per billion
ppm	parts per million
PUT	Putrescine
PUT-d8	Putrescine-d8
Q1	Quadrupole 1

Q2	Quadrupole 2
Q3	Quadrupole 3
RF(s)	Response factor, radio frequency
RSD	Relative standard deviation
S/d8	Ratio of spermidine to spermidine-d8
SEV	Sevoflurane
SPD	Spermidine
SPD-d8	Spermidine-d8
SPM	Spermine
SRM	Single reaction monitoring
TFT	α,α,α- Trifluorotoluene
TOL-d8	Toluene-d8
TSQ	Triple stage quadrupole
TSQ	Triple stage quadrupole
UV-vis	Ultraviolet-visible spectroscopy
VOC(s)	Volatile organic compound(s)
XYL-d10	ρ-Xylene-d10
$\lambda_{b/g}$	Blood to gas partition coefficient

LIST OF TABLES

Table 2.1. Gradient profile for chromatography. 21

Table 2.2. Table with each derivatized analyte and internal standard's parent ion, quantifying ion, confirming ion, and collision energy. 22

Table 3.1. Accuracy, expressed as % error, of PUT and SPD calculated with PUT-d8, SPD-d8, DAH, and BEN (both ions compared).* 31

Table 3.2. The final concentration of each compound and internal standard used for optimization of solvents and ratios used to prepare benzoyl chloride for derivatization. All compounds were prepared in 0.1M $HClO_4$, and BEN was prepared in acetonitrile. 32

Table 3.3. Benzoyl chloride treatment variations. 33

Table 3.4. Mole ratio of benzoyl chloride to each polyamine. 34

Table 3.5. Two gradient profiles compared. 41

Table 3.6. Peak area of each analyte analyzed with either gradient X (slow gradient) or Y (fast gradient). 43

Table 3.7. Peak area ratio of PUT to PUT-d8 and SPD to SPD-d8. 44

Table 3.8. Peak area of analytes using either acetic acid (AA) or formic acid (FA). 52

Table 3.9. Results from CE experiment comparing the CE used for accuracy comparison. 54

Table 3.10. Concentration of calibration solutions.* 70

Table 3.11. R^2 of each PA using PUT-d8 and SPD-d8 as an internal standard. 70

Table 3.12. Accuracy and precision of derivatization method. Each level was derivatized in triplicate (n=3). 71

Table 3.13. Results from 3 levels of PUT and SPD for intra-day and inter-day experiments.* 72

Table 3.14. LOD and LOQ for the method developed. 73

Table 3.15. LOD of 4 published methods. 73

Table 3.16. Calculated concentrations of PUT on different days, with different treatments. One set was stored in 50:50 ACN:H_2O and the other set stored in 100% acetonitrile. The expected concentration was 11.9 ng/mL. 75

Table 3.17. Calculated concentrations of SPD on different days, with different treatments. One set was stored in 50:50 ACN:H_2O and the other set stored in 100% acetonitrile. The expected concentration was 12.4 ng/mL. 76

Table 3.18. Results from two levels of isotopic internal standards. 78

Table 3.19. Concentration of PUT in fruit fly homogenate in a 100 µL aliquot and 20 µL aliquot of the same sample (n=3). 79

Table 3.20. Concentration of SPD in fruit fly homogenate in a 100 µL aliquot and 20 µL aliquot of the same sample (n=3). 79

Table 3.21. Concentration of PUT in rat liver cell lysate in a 50 µL aliquot and 10 µL aliquot of the same sample (n=3). 82

Table 3.22. Concentration of SPD in rat liver cell lysate in a 50 µL aliquot and 10 µL aliquot of the same sample (n=3). 82

Table 6.1. GC temperature program used for separation. 154

Table 6.2. Compounds with its corresponding quantifying ion and qualifying ion, with observed retention times. 155

Table 7.1. Properties of the 6 prospective compounds (tracers) studied, and three comparative compounds. 160

Table 7.2. Retention time of each compound from the previous chromatogram. 162

Table 7.3. NIST library search 'fit' values to confirm the spectrum comparisons..... 163

Table 7.4. Table of 3 three subjects. 172

Table 7.5. Results from reproducibility experiments of canisters. 174

Table 7.6. Area counts of internal standards for each trial of the experiment carried out for adsorbent traps..... 175

Table 7.7. Concentration levels of each analyte used for the calibration curve. 176

Table 7.8. Concentration of internal standards. 176

Table 7.9. The R^2 value of the regression line for each analyte and the corresponding internal standards. Table A) represents the concentration levels 2-5 and Table B) represents all concentration levels. 177

Table 7.10. Rate constants from the 1st order kinetic graphs of subject 2's EBC sample (n=3)..... 188

Table 8.1. Comparison of sample collection with canisters and adsorbent traps. 193

Table. A.1. Accuracy calculated for SPD and PUT using all 4 internal standards to show that DAH and BEN are not suitable internal standards. 91

Table. B.1. Reagent Amount Experiment – Peak area of 6 polyamines prepared with 5µL pure benzoyl chloride, 25 µL pure benzoyl chloride, benzoyl chloride prepared in acetonitrile (ACN), methylene chloride (CH_2Cl_2), and diethyl ether (Ether)..... 92

Table. B.2. Reagent Amount Experiment – Peak area of 4 internal standards prepared with 5μL pure benzoyl chloride, 25 μL pure benzoyl chloride, benzoyl chloride prepared in acetonitrile (ACN), methylene chloride (CH_2Cl_2), and diethyl ether (Ether). 93

Table. B.3. Reagent Mole Ratio Experiment - Peak area of 6 PAs prepared in ratio moles of benzoyl chloride to total amines. Benzoyl chloride reagent was prepared in methylene chloride. 94

Table. B.4. Reagent Mole Ratio Experiment - Peak area of 4 internal standards prepared in ratio moles of benzoyl chloride to total amines. Benzoyl chloride reagent was prepared in methylene chloride. 95

Table. B.5. Derivatization Time Experiment - Peak area of 6 PAs derivatized with different reaction times. One set prepared at room temperature and a second set was prepared at 30^{o}C. 96

Table. B.6. Derivatization Time Experiment - Peak area of 4 internal standards derivatized with different reaction times. One set prepared at room temperature and a second set was prepared at 30^{o}C. 97

Table. E.1. Peak area of PUT, SPM and its isotopic internal standards comparing CE used for quantification. 107

Table. G.1. Concentration of calibration solutions. 109

Table. G.2. Concentration of internal standards used in calibration solutions. 109

Table. G.3. Correlation coefficient (R^2) of each analyte relative to an internal standard. * Indicates a value below the accepted value of 0.96. 109

Table. H.1. Peak areas of PUT, SPD, PUT-d8, and SPD-d8 for intra-day experiment. . 114

Table. H.1. Peak areas of PUT, SPD, PUT-d8, and SPD-d8 for inter-day experiment results. 115

Table. I.1. Stability Experiment Day 22 - Peak area of 6 PAs derivatized and stored in 50:50 ACN:H_2O. One set stored at room temperature exposed to light, one set stored at room temperature not exposed to light, and a third set stored in the freezer not exposed to light. 116

Table. I.2. Stability Experiment Day 22 - Peak area of 4 internal standards derivatized and stored in 50:50 ACN:H_2O. One set stored at room temperature exposed to light, one set stored at room temperature not exposed to light, and a third set stored in the freezer not exposed to light. 116

Table. I.3. Stability Experiment Day 22 - Peak area of 6 PAs derivatized and stored in 100% ACN. One set stored at room temperature exposed to light, one set stored at room temperature not exposed to light, and a third set stored in the freezer not exposed to light. 117

Table. I.4. Stability Experiment Day 22 - Peak area of 4 internal standards derivatized and stored in 100% ACN. One set stored at room temperature exposed to light, one set stored at room temperature not exposed to light, and a third set stored in the freezer not exposed to light. 117

Table. I.5. Stability Experiment Day 15 - Peak area of 6 PAs derivatized and stored in 50:50 ACN:H_2O. One set stored at room temperature exposed to light, one set stored at room temperature not exposed to light, and a third set stored in the freezer not exposed to light. 118

Table. I.6. Stability Experiment Day 15 - Peak area of 4 internal standards derivatized and stored in 50:50 ACN:H_2O. One set stored at room temperature exposed to light, one set stored at room temperature not exposed to light, and a third set stored in the freezer not exposed to light. 118

Table. I.7. Stability Experiment Day 15 - Peak area of 6 PAs derivatized and stored in 100% ACN. One set stored at room temperature exposed to light, one set stored at room temperature not exposed to light, and a third set stored in the freezer not exposed to light. 119

Table. I.8. Stability Experiment Day 15 - Peak area of 4 internal standards derivatized and stored in 100% ACN. One set stored at room temperature exposed to light, one set stored at room temperature not exposed to light, and a third set stored in the freezer not exposed to light. 119

Table. I.9. Stability Experiment Day 8 - Peak area of 6 PAs derivatized and stored in 50:50 ACN:H_2O. One set stored at room temperature exposed to light, one set stored at room temperature not exposed to light, and a third set stored in the freezer not exposed to light. 120

Table. I.10. Stability Experiment Day 15 - Peak area of 4 internal standards derivatized and stored in 50:50 ACN:H_2O. One set stored at room temperature exposed to light, one set stored at room temperature not exposed to light, and a third set stored in the freezer not exposed to light. 120

Table. I.11. Stability Experiment Day 8 - Peak area of 6 PAs derivatized and stored in 100% ACN. One set stored at room temperature exposed to light, one set stored at

room temperature not exposed to light, and a third set stored in the freezer not exposed to light. 121

Table. I.12. Stability Experiment Day 8 - Peak area of 4 internal standards derivatized and stored in 100% ACN. One set stored at room temperature exposed to light, one set stored at room temperature not exposed to light, and a third set stored in the freezer not exposed to light. 121

Table. I.13. Stability Experiment Day 1 - Peak area of 6 PAs derivatized and stored in 50:50 ACN:H_2O. One set stored at room temperature exposed to light, one set stored at room temperature not exposed to light, and a third set stored in the freezer not exposed to light. 122

Table. I.14. Stability Experiment Day 1 - Peak area of 4 internal standards derivatized and stored in 50:50 ACN:H_2O. One set stored at room temperature exposed to light, one set stored at room temperature not exposed to light, and a third set stored in the freezer not exposed to light. 122

Table. I.15. Stability Experiment Day 1 - Peak area of 6 PAs derivatized and stored in 100% ACN. One set stored at room temperature exposed to light, one set stored at room temperature not exposed to light, and a third set stored in the freezer not exposed to light. 123

Table. I.16. Stability Experiment Day 1 - Peak area of 4 internal standards derivatized and stored in 100% ACN. One set stored at room temperature exposed to light, one set stored at room temperature not exposed to light, and a third set stored in the freezer not exposed to light. 123

Table. J.1. Raw data of two whole fruit fly homogenate with a high and low amount of internal standard added. 124

Table. J.2. Raw data of two aliquot volumes studied for whole fruit fly homogenate. .. 125

Table. K.1. Raw data of peak area of PUT and SPD for old and young rat liver cell lysates..... 126

Table. K.2. Raw data of peak area of two aliquot volumes for rat liver cell lysate..... 127

Table. D.1. Compiled peak areas of each internal standard from the chromatograms shown above..... 203

Table. D.2. Ratios of internal standards for each trial. The mean and standard deviation, and % RSD for each ratio. 203

Table. D.3. Compiled area counts of each internal standard from the chromatograms shown above..... 205

Table. D.4. Ratios of internal standards for each trial. The mean and standard deviation, and % RSD for each ratio. 205

LIST OF FIGURES

Figure 1.1. Biogenic polyamine structures. 3

Figure 1.2. Reaction of dansyl chloride and a primary amine. 5

Figure 1.3. Reaction of o-phthaldialdehyde with a primary amine producing a fluorescent product. The fluorescent product can degrades forming a non-fluorescent product.[25] 6

Figure 1.4. Reaction benzoyl chloride with a primary amine. 7

Figure 1.5. General schematic of a single quadrupole mass analyzer. 9

Figure 1.6. Schematic of a triple stage quadrupole. 11

Figure 1.7. Inlet, ion optics, and quadrupoles of the mass analyzer.[40] 11

Figure 1.8. MS/MS predicted fragmentation pathways of derivatized putrescine. 12

Figure 3.1. Structures of DAH, a derivatizable internal standard, and BEN, a non-derivatizable. 24

Figure 3.2. Chromatogram of BEN treated without and with the derivatization process. Both samples were analyzed by MS/MS. 25

Figure 3.3. Structures of isotopically labeled internal standards. 28

Figure 3.4. Schotten-Baumann reaction mechanism. 37

Figure 3.5. Common side-products from the Schotten-Baumann reaction. 38

Figure 3.6. Predicted fragmentation of by-products, benzoic anhydride and benzoic acid. 38

Figure 3.7. Hydrolysis of benzoic anhydride. 39

Figure 3.8. Chromatogram of a single run with all polyamines and all internal standards shown in two panels using gradient X, the longer run time. 42

Figure 3.9. Chromatogram of a single run with all polyamines and all internal standards shown in two panels using gradient Y, the shorter run time. 42

Figure 3.10. Components of a peak to calculate peak asymmetry..... 45

Figure 3.11. Peak asymmetry factor calculated for each analyte. 46

Figure 3.12. Sample injection volume and corresponding area of spermine. 47

Figure 3.13. Total ion chromatogram from MS/MS data of 3 consecutive runs: A) blank sample, B) 50-µL injection of derivatized fly sample, and C) blank sample. 48

Figure 3.14. Structures of derivatized PAs and their corresponding MS/MS fragmentations.* 50

Figure 3.15. Structures of internal standards and their corresponding MS/MS fragmentations..... 51

Figure 3.16. IR of A) whole butter lipid sample, B) unfiltered homogenized flies, and C) filtered homogenized flies..... 58

Figure 3.17. Structure of two classes of phospholipids that have a fragmentation that interferes with putrescine-d8.[45,51] 60

Figure 3.18. Flow chart of the three types of fly samples injected for the matrix effect experiment. The items in bold are the three types of samples. 61

Figure 3.19. MS/MS ion channels of all PAs to show if *m/z* 184 is an interferent (A,C, & E) internal standards (B, D, & F) and the phospholipid *m/z* 184 ion channel (first ion channel of each figure). A) & B) chromatogram of the matrix with a multi-step cleanup underivatized; C) & D) chromatogram of underivatized matrix without cleanup; E) & F) chromatogram of derivatized flies. 63

Figure 3.20. Infusion experiment result of a published method. A is of the infusion solution they investigated , B and C are of the same matrices treated two different ways. Permission to reproduce this figure was authorized. [53] 64

Figure 3.21. Post-column infusion set-up for the matrix effect experiment. 65

Figure 3.22. Infusion experiment of 6 PAs (A, C, & E); 4 internal standards (B, D & F). Figure A & B is only the infusion solution; figure C & D is underivatized flies without cleanup; figure E & F underivatized flies without..... 67

Figure 3.23. Chromatogram of matrix effect using a post-column infusion set-up. A derivatized sample was injected. Red arrows indicate where the analyte of the respective ion channel should be. 68

Figure 3.24. Proposed mechanism of amide hydrolysis in water.[60]..... 77

Figure 6.1. Analysis set-up. Left to right: Agilent 5973 mass spectrometer, HP 5890 gas chromatograph, and Tekmar Sample Concentrator. 143

Figure 6.2. Structure of internal standards. 144

Figure 6.3. Scotty tank used for preparing analytes at varying concentrations. A) Schematic of the tank, B) Picture of the tank used. 145

Figure 6.4. Structure of chemical tracers. 146

Figure 6.5. Canister cleaning apparatus. 147

Figure 6.6. Breath and EBC collection apparatus. 149

Figure 6.7. Adsorbent trap and approximate length of each adsorbent material. 151

Figure 6.8. Subliminator device for EBC collection, gas flow direction for the desorption of EBC onto an adsorbent trap. 152

Figure 6.9. Sample concentration steps on a trap carried out inside the Tekmar sample concentrator..... 153

Figure 6.10. Schematic of the Tekmar concentrator, modified gas chromatograph and mass spectrometer..... 154

Figure 7.1. Chromatogram of the L5 (lowest level standard), concentrations found in Table 7.7 and Table 7.8, standard solution with all analytes and internal standards present..... 161

Figure 7.2. A) Chromatogram of a canister cleaned with dry gas. Contaminant peaks can be observed. B) Chromatogram of the same canister after the application of proper cleaning cycles..... 164

Figure 7.3. A) Chromatogram shows a breath sample after TFT exposure, B) Chromatogram shows the same canister after 3 cleaning cycles..... 165

Figure 7.4. A) Chromatogram of a cleaned canister that was stored for 30 days. B) Chromatogram of canister that was cleaned and analyzed on the same day. 166

Figure 7.5. A) Chromatogram of a breath sample analyzed from a trap. B) Chromatogram of the same trap..... 167

Figure 7.6. Breakthrough experiment with resulting chromatogram from each trap. 170

Figure 7.7. Breakthrough experiment with resulting chromatogram from each trap. 170

Figure 7.8. Ion extracted chromatograms of TFT for three different samples. 172

Figure 7.9. Models for one compartment model (route A), and a two compartment model (route B)..... 180

Figure 7.10. Compiled data of decay of tracers: A) SEV, ENF, and MET (n=4), B) 4-CBT and 3-FBT (n=3), and C) TFT for subject 1 (principal investigator, n=3) and subject 2 (myself, n=4). 187

Figure. B.1. Chromatogram of the A) first extraction, B) second extraction, C) third extraction, D) fourth extraction, and E) fifth extraction. 98

Figure. C.1. Chromatogram of analytes reconstituted with: A) 50:50 ACN:H_2O, B) 40:60 ACN:H_2O, C) 30:70 ACN:H_2O, D) 30:70 ACN:H_2O. 99

Figure. C.2. Chromatogram of each standard individually prepared. A) blank-no reagent added, B) blank-benzoyl chloride added, C) SPD-d8, D) PUT-d8, E) SPM, F) CAD, G) SPD, H) N1-ASPM, I) N8-ASPD, and J) PUT. 100

Figure. D.1. MS/MS full scan spectrum of PUT with optimized CE of 20 volts showing *m/z* 297 (parent ion), 176 (quantifying ion), and 105 (confirming ion). 102

Figure. D.2. MS/MS full scan spectrum of N8-ASPD with optimized CE of 21 volts showing *m/z* 396 (parent ion), 274 (quantifying ion), and 162 (confirming ion). 102

Figure. D.3. MS/MS full scan spectrum of N1-ASPM with optimized CE of 32 volts showing *m/z* 557 (parent ion), 435 (quantifying ion), and 161 (confirming ion). 103

Figure. D.4. MS/MS full scan spectrum of SPD with optimized CE of 23 volts showing *m/z* 458 (parent ion), 36 (quantifying ion), and 162 (confirming ion). 103

Figure. D.5. MS/MS full scan spectrum of CAD with optimized CE of 19 volts showing *m/z* 311 (parent ion), 190 (quantifying ion), and 105 (confirming ion). 104

Figure. D.6. MS/MS full scan spectrum of SPM with optimized CE of 30 volts showing *m/z* 619 (parent ion), 497 (quantifying ion), and 162 (confirming ion)..... 104

Figure. D.7. MS/MS full scan spectrum of DAH with optimized CE of 20 volts showing *m/z* 339 (parent ion), 218 (quantifying ion), and 105 (confirming ion)..... 105

Figure. D.8. MS/MS full scan spectrum of BEN with optimized CE of 27 volts showing *m/z* 198 (parent ion), 77 and 105 (both can be the quantifying ion)..... 105

Figure. D.9. MS/MS spectrum of PUT-d8 with optimized CE of 17 volts showing *m/z* 305 (parent ion), 184 (quantifying ion), and 105 (confirming ion). 106

Figure. D.10. MS/MS spectrum of SPD-d8 with optimized CE of 18 volts showing *m/z* 297 (parent ion), 344 (quantifying ion), and 162 (confirming ion). 106

Figure. F.1. Full scan of A) filtered & cleaned fly matrix, B) filtered fly matrix, and C) derivatized fly matrix. 108

Figure. G.1. Calibration curve of each amine with PUT-d8 or SPD-d8 as the internal standard. 110

Figure. G.2. Calibration curve of each amine with DAH as the internal standard. 111

Figure. G.3. Calibration curve of each amine with BEN-77 as the internal standard. ... 112

Figure. G.4. Calibration curve of each amine with BEN-105 as the internal standard. . 113

Figure. B.1. Chromatogram of standards and internal standards..... 197

Figure. B.2. A) Spectrum of SEV from the NIST MS Search Program, and B) spectrum from a sample standard of SEV at a retention time of ~6.0 minutes. 197

Figure. B.3. A) Spectrum of ENF from the NIST MS Search Program, and B) spectrum from a sample standard of ENF at a retention time of ~6.5 minutes. 198

Figure. B.4. A) Spectrum of 3-FBT from the NIST MS Search Program, and B) spectrum from a sample standard of 3-FBT at a retention time of ~9.4 minutes. 198

Figure. B.5. A) Spectrum of TFT from the NIST MS Search Program, and B) spectrum from a sample standard of TFT at a retention time of ~9.8 minutes..... 198

Figure. B.6. A) Spectrum of MET from the NIST MS Search Program, and B) spectrum from a sample standard of MET at a retention time of ~10.0 minutes. 199

Figure. B.7. A) Spectrum of 4-CBT from the NIST MS Search Program, and B) spectrum from a sample standard of 4-CBT at a retention time of ~12.5 minutes..... 199

Figure. B.8. A) Spectrum of BEN-d6 from the NIST MS Search Program, and B) spectrum from a sample standard of BEN-d6 at a retention time of ~9.1 minutes. 199

Figure. B.9. A) Spectrum of TOL-d8 from the NIST MS Search Program, and B) spectrum from a sample standard of TOL-d8 at a retention time of ~10.9 minutes. 200

Figure. B.10. A) Spectrum of XYL-d10 from the NIST MS Search Program, and B) spectrum from a sample standard of XYL-d10..... 200

Figure. C.1. A) Chromatogram of a canister with a sample collected, B) chromatogram of the same canister after 1 cleaning cycle, C) chromatogram of the same canister after 2 cleaning cycles, and D) chromatogram after 3 cleaning cycles. 201

Figure. D.1. Chromatogram of 1st replicate of reproducibility experiment with canisters. 202

Figure. D.2. Chromatogram of 2nd replicate of reproducibility experiment with canisters. 202

Figure. D.3. Chromatogram of 3rd replicate of reproducibility experiment with canisters. 203
Figure. D.4. Chromatogram of 1st replicate of reproducibility experiment with adsorbent traps. 204
Figure. D.5. Chromatogram of 2nd replicate of reproducibility experiment with adsorbent traps. 204
Figure. D.6. Chromatogram of 3rd replicate of reproducibility experiment with adsorbent traps. 205

LIST OF GRAPHS

Graph 3.1. RF comparison of PUT vs. PUT-d8 and PUT vs. DAH for each trial.* 29

Graph 3.2. RF comparison of SPD vs. SPD-d8 and SPD vs. DAH for each trial.* 29

Graph 3.3. Reaction ratio treatment results for PAs.* 35

Graph 3.4. Reaction ratio treatment results for internal standards.* 35

Graph 7.1. Ratio of analyte to internal standard: A) Decay of TFT (green), MET (blue), and SEV (red) vs. time. B) First order kinetics of the decay of the same compounds. 179

Graph 7.2. A) Decay of TFT B) First order kinetics of the decay. 182

Graph 7.3. Ratio of area of TFT to toluene: A) Decay of TFT B) First order kinetics of the decay. 184

Graph. E.1.Calibration curve of all 6 analytes and benzene-d6 as the internal standard. Levels 2-5 represented in the graph (concentrations listed in Table 7.7).* 206

Graph. E.2. Calibration curve of all 6 analytes and toluene-d8 as the internal standard. Levels 2-5 represented in the graph (concentrations listed in Table 7.7).* 207

Graph. E.3. Calibration curve of all 6 analytes and ρ-xylene-d10 as the internal standard. Levels 2-5 represented in the graph (concentrations listed in Table 7.7).* 208

Graph. E.4. Calibration curve of all 6 analytes and benzene-d6 as the internal standard. Levels 1-5 represented in the graph (concentrations listed in Table 7.7).* 209

Graph. E.5. Calibration curve of all 6 analytes and toluene-d8 as the internal standard. Levels 1-5 represented in the graph (concentrations listed in Table 7.7).* 210

Graph. E.6. Calibration curve of all 6 analytes and ρ-xylene-d10 as the internal standard. Levels 1-5 represented in the graph (concentrations listed in Table 7.7).* 211

Graph. F.1. Elimination graph of tracer compound from subject 2's breath, who was exposed to 1 ppm of TFT. 212

Graph. F.2. Elimination graph of tracer compounds from 1's breath, who was exposed to 1 ppm each of A) MET, SEV, and TFT; and B) ENF. 212

Graph. F.3. Elimination graph of tracer compound from subject 2's breath, who was exposed to 1 ppm of TFT. 213

Graph. F.4. Elimination graph of tracer compound from subject 1's breath, who was exposed to 1 ppm of TFT. 213

Graph. F.5. Elimination graph of tracer compound from subject 1's breath, who was exposed to 1 ppm of TFT. 214

Graph. F.6. Elimination of MET, SEV, ENF, 4-CBT, 3-FBT, and TFT from EBC of subject 2, trial 1.* 215

Graph. F.7. Elimination of MET, SEV, ENF, 4-CBT, 3-FBT, and TFT from EBC of subject 2, trial 2.* 216

Graph. F.8. Elimination of MET, SEV, ENF, 4-CBT, 3-FBT, and TFT from EBC of subject 2, trial 3.* 217

ACKNOWLEDGEMENTS

First and foremost I want like to thank my advisor, Dale Chatfield, for guiding me through the long arduous path of graduate school. I have never worked for such a caring and helpful person as him. His interest and enthusiasm for chemistry pushes me to be a better analytical chemist. He is a very encouraging advisor who is also supportive and understanding of all the highs and lows in my graduate career. Without his endless patience and willingness to teach me, I would have never seen the end of this graduate education path.

I would also like to thank Dr. Harrison, Dr. Hoh, Dr. Perrin, and Dr. Sinha for being a part of my committee and for their valuable time.

It has been such an enjoyment to spend my graduate studies in a great environment filled with great people. The professors I had the honor to work with showed me what dedication and hard work means and helped me see what a genuine role model in the Chemistry field should embody. My peers were some of the best I had worked with, and fun to say the least. Throughout the years I am grateful for all the friendships that cultivated, professional relationships that developed, and support that was offered. It has been a great pleasure to be part of a unique camaraderie.

Part 1, in full, is being prepared to submit for publication. I was the primary researcher and will be first author on this paper. Van, Jenny K.; Chatfield, Dale A. "Method Development for the Analysis of Polyamines by Derivatives with Benzoyl Chloride by HPLC Tandem Mass Spectrometry" *Manuscript in preparation.*

Part 2 contains material, which will also be prepared to submit for publication. I was the primary researcher and will be the first author on this paper. Van, Jenny K.;

Chatfield, Dale A. “Detection of Volatile Organic Compound Tracers in Human Breath” *Manuscript in preparation.*

VITA

2005-2006	Undergraduate research assistant, Advisor: Dr. Sean Liu California Polytechnic State University, Pomona
2006	Bachelor of Science, Chemical Sciences California Polytechnic State University, Pomona
2006-2007	Chemist, Energetics, Inc.
2008-2015	Research Assistant, Advisor: Dr. Dale A. Chatfield San Diego State University
2013	Master of Arts, Chemistry San Diego State University
2015	Doctor of Philosophy, Chemistry University of California, San Diego San Diego State University

Oral Presentations

Van, J. K.; Chatfield, D.A., "Detection of Chemical Tracers in Human Breath by Mass Spectrometry for Development of a New Forensic Technique," American Society for Mass Spectrometry Sanibel Conference, Clearwater Beach, FL, January 22-25, 2015.

Poster Presentations

Van, J. K.; Chatfield, D. A., "Breath Component Analysis: A Sensitive Method to Detect VOCs in Exhaled Breath using Gas Chromatography-Mass Spectrometry", The 8th Annual Student Research Symposium, San Diego, CA, Mar 6-7, 2015.

Van, J. K.; Chatfield, D.A., "Method Development for a Sensitive Assay of Benzoylated Polyamine Derivatives by LC-MS/MS-ESI," Mass Spectrometry: Applications to the Clinical Lab Meeting, San Diego, CA, February Feb 9-13, 2013.

Van, J. K.; Chatfield, D.A., "Detection of Chemical Tracers in Human Breath by Mass Spectrometry for Development of a New Forensic Technique," American Society for Mass Spectrometry Sanibel Conference, Clearwater Beach, FL, January 22-25, 2015.

Awards

January 2015 American Society for Mass Spectrometry Sanibel Conference Travel Stipend (National Science Foundation Funding)

Major Fields of Study

Major Field: Chemistry (Analytical)

Studies in Analytical Method Development and Small Molecule Analysis
Professor Dale A. Chatfield

ABSTRACT OF THE DISSERTATION

Part 1: Method Development for the Analysis of Polyamines by Derivatives with Benzoyl Chloride by HPLC Tandem Mass Spectrometry

Part 2: Detection of Volatile Organic Compound Tracers in Human Breath

by

Jenny Kim Van

Doctor of Philosophy in Chemistry

University of California, San Diego, 2015
San Diego State University, 2015

Professor Dale A. Chatfield, Chair

Part 1: Development and validation of an analytical method by liquid chromatography-tandem mass spectrometry to detect putrescine, cadaverine, spermidine, spermine, n8-acetylspermidine, and n1-acetylspermine as benzyl amide derivatives in

biological samples were completed. The derivatization conditions were optimized for all PAs, and method validation was completed for putrescine (PUT) and spermidine (SPD) using isotope dilution techniques. The method exhibited: high accuracy (<±15% error) and precision (<±10% RSD); product stability of >22 days; linearity within concentration range of 0.40-50 ng/mL for PUT and 0.42-530 ng/mL for SPD; level of detection (LOD) of 2.8 and 2.4 picograms (pg); and level of quantitation (LOQ) of 20 and 21 pg for PUT and SPD, respectively. Matrix effects and interferences were shown to not affect accuracy. The method developed provided superior with shorter analysis time than other published methods. Levels of PUT and SPD were determined to be 5.75 ± 0.1 and 43.8 ± 1 ng/mL, respectively in a sample as small as 4 fruit flies.

Part 2: This project was a proof of concept study that used breath component analysis (BCA) to determine if a unique volatile organic compound (VOC) could be measured in human breath 72 hours or longer following a brief exposure. A portable breathing mask with a pressurized canister was constructed to provide 1-2 ppm exposures of the tracer chemicals to the subjects. An EBC sample collection device and canister cleaning system were modified to provide clean sample blanks. Analytical protocols were established to collect BCA from subjects using canisters and adsorbent traps. The chemicals tested and the maximum duration they were detectable in a subjects' breath (days) were methoxyflurane (1.2), enflurane (7.7), sevoflurane (1.2), α,α,α-trifluorotoluene (14), 4-chlorobenzotrifluoride (7.2), and 3-fluorobenzotrifluoride (1.2). The rate constants for the most promising candidate chemicals followed a one-compartment (first order kinetics) model. Other compounds of similar chemical properties are potential candidates for further study. The applications of this proof of

concept study may lead to the development of tools for use in toxicology, forensics, and security.

PART 1: METHOD DEVELOPMENT FOR THE ANALYSIS OF POLYAMINES BY DERIVATIVES WITH BENZOYL CHLORIDE BY HPLC TANDEM MASS SPECTROMETRY

CHAPTER 1. INTRODUCTION

1.1. Relevance of Polyamine Analysis

Polyamines (PAs) are found in all living organisms at low levels and its analysis provides an abundance of information relating to stages in cell growth and developmental processes.[1-4] The exact roles, mechanisms, and pathways of the biogenic amines are still unknown for many organisms,[5,6] therefore an accurate method of analysis will provide a vital tool for the study of these compounds at low levels.

The relationship of cell viability and concentration changes of PAs in living cells have attracted much attention.[7-9] As one specific example, San Diego State University Bioscience Center has been studying the relationship between feeding spermidine rich diets and aging in *Drosophila melanogaster* (fruit flies). The relationship of age and concentrations of PAs in rats was another focus of their research. They hypothesized, along with many other published works, that feeding diets rich in spermidine induces early cellular autophagy which in turn maintains the normal cycle of cellular degradation and formation which promotes longevity.[7,8,10,11] An accurate method to analyze PA concentrations in small sample sizes would be needed to further this work. The six most biologically relevant PAs have been defined as putrescine (PUT), cadaverine (CAD), spermidine (SPD), spermine (SPM), n8-acetylspermidine (N8-ASPD), and n1-acetylspermine (N1-ASPM) and their structures are shown in Figure 1.1.

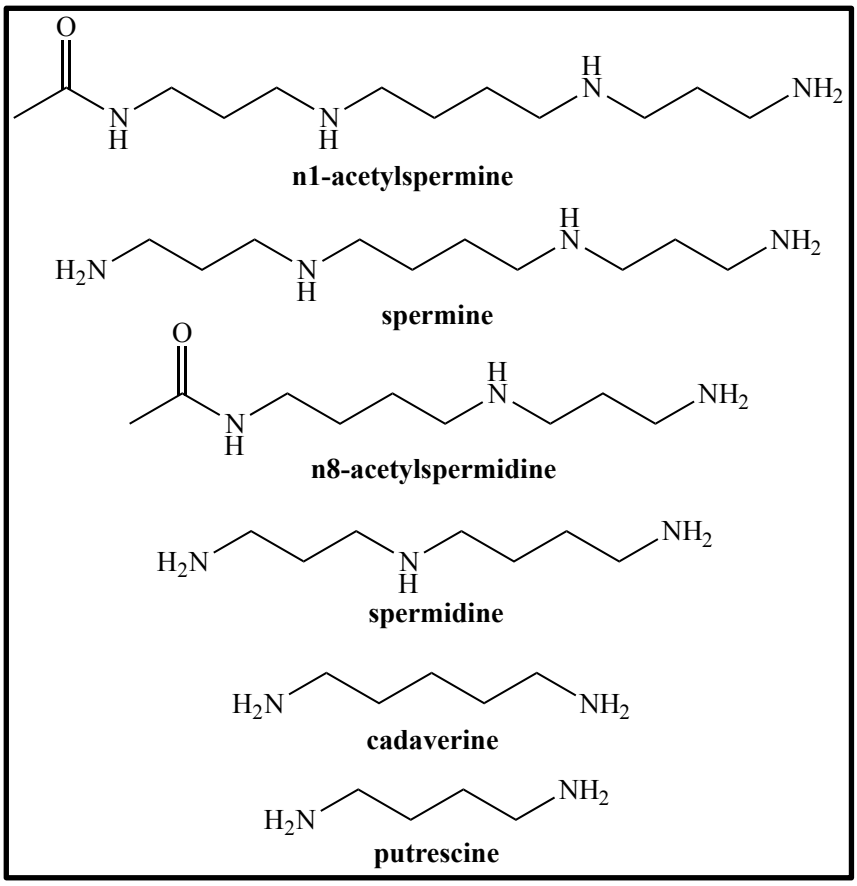

Figure 1.1. Biogenic polyamine structures.

1.2. Analyses of Polyamines in Fruit Flies

Analyses of PAs have been carried out in a number of sample types like food and drink, bacteria, plants, and urine. However, there are very few works that focus on measuring the concentrations of biogenic amines in *Drosophila melanogaster* (fruit flies); the published studies mainly focused on the genotypic and phenotypic affects of feeding fruit flies different amounts of PAs.[12-14]

Fruit flies are a good and common model used for studies in pharmacology, gene therapy, neurology, and biological pathway screening to name a few.[15,16] The flies are

easily modified genetically and the short life cycle allows for studying different generations. Determining concentrations of PAs in fruit flies would provide an abundance of information. An ongoing study by Dr. Kim Finley at the SDSU Bioscience Center was to determine if fruit flies of a specific genotype, upon being fed a PA enriched diet, naturally have high amounts of one or all of the PAs that may contribute to its increased life span. This thesis will focus on the method development and validation of PAs for whole fruit flies, which has not been reported in literature.

1.3. Review of Literature of Analytical Methods for Polyamine Analysis

The following sections will review the common chemical pre-treatment methods applied to increase the chromatographic properties of amines and the types of detectors frequently used to measure polyamine concentrations.

1.3.1. Pre-treatment of Amines for Analysis

The purpose of pre-treatment procedures was to reduce the polarity of the PAs and to isolate them from other interfering compounds that are present in the sample. Amines are difficult to chemically analyze without pre-treatment because they are water-soluble except at a high pH. Amines hydrogen bond to acidic sites on glass and tenaciously adheres to metal and plastic surfaces. This greatly affects the accuracy of analysis especially in the nanomolar to picomolar concentration ranges. Hydrogen bonding also causes chromatographic peak tailing, which is a distortion of the peak shape in chromatography.

Some studies have utilized ion-pairing methods to improve their extraction from solutions with organic solvents. Heptafluorobutyric acid is an often used volatile ion-pair

reagent for polyamines, but sensitivity to mass spectrometric analysis was not comparable to derivatized methods due to ion suppression of signals.[17,18] There are several post and pre-column derivatization methods available for polyamines; but each suffers from shortfalls in terms of, analysis time, sensitivity, sample preparation and/or sample cleanup are problems that make them problematic trying to achieve a lower limit of detection and quantification.[19,20]

The most common methods are reactions with dansyl chloride, *o*-phthaldialdehyde, and benzoyl chloride.[1,6,20,21] Dansyl derivatives have been extensively studied and used due to its ease in derivatization and good stability relative to *o*-phthaldialdehyde derivatives.[22] Dansylation reactions produce many side reactions that decreases sensitivity, selectivity, and specificity of the analysis.[23] The reaction of dansyl chloride with an amine is shown in Figure 1.2.

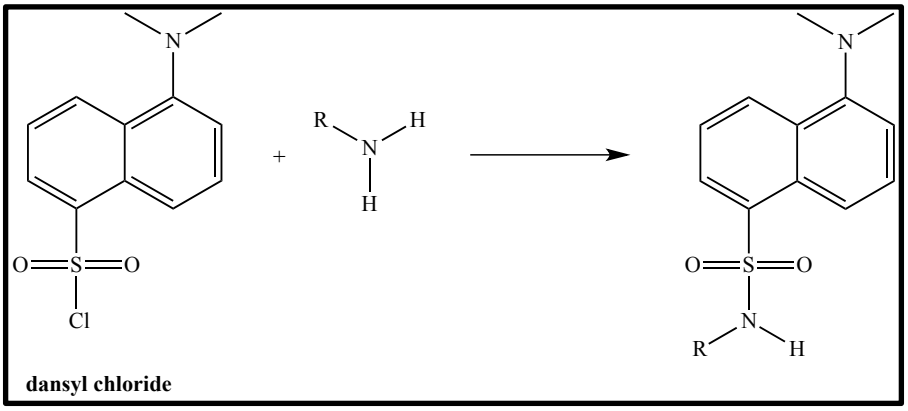

Figure 1.2. Reaction of dansyl chloride and a primary amine.

O-phthaldialdehyde derivatives are also commonly prepared for PA analysis; however, the products are highly unstable once formed.[24-26] The fluorescent product readily forms at room temperature, but the product is short lived and it is degraded to the

non-fluorescent product as shown in Figure 1.3. Instability of *o*-phthaldialdehyde derivatives requires samples to be freshly prepared. The degraded product can likewise be detected but it has not been established to be a quantitative measure. It has also been reported that degradation occured much faster for SPM and SPD, this is a problem if quantitation of a large amine profile is of interest.[27]

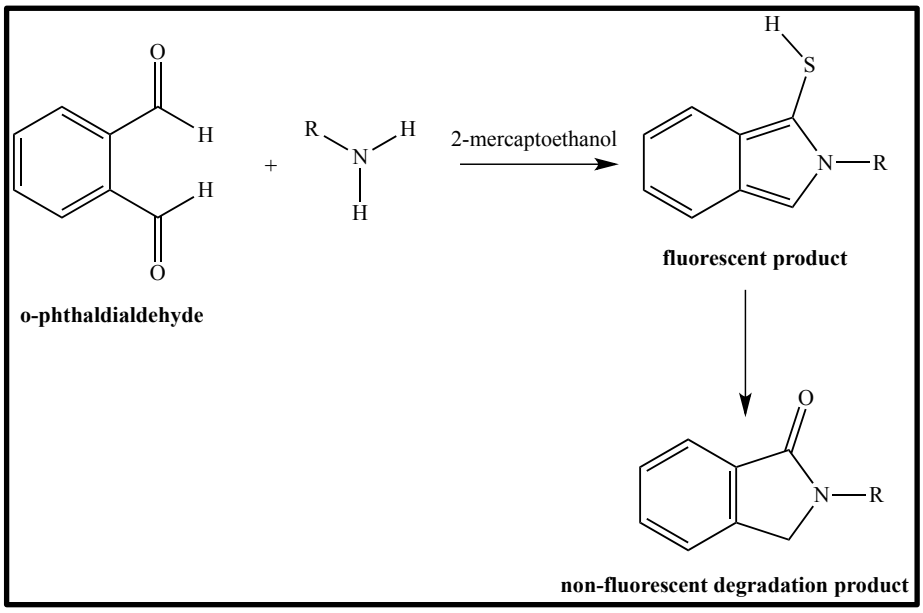

Figure 1.3. Reaction of o-phthaldialdehyde with a primary amine producing a fluorescent product. The fluorescent product can degrades forming a non-fluorescent product.[25]

Benzoyl chloride is another common derivatization reagent because it results in the formation of a stable amide as shown in Figure 1.4. Among the many reagents, benzoyl chloride derivatized products are claimed to be most stable and the reaction can be carried out quantitatively on secondary and primary amines.[28-31] Due to the lack of specificity of the reaction, side-products have been reported that could interfere with analysis.[32,33] This method was investigated due to the reported stability of the benzamide

products. Since side-products could cause inaccurate results, a cleanup procedure was included. Side-products not only cause discrepancies in results, but the lifetime and performance of the instrument would also be affected.

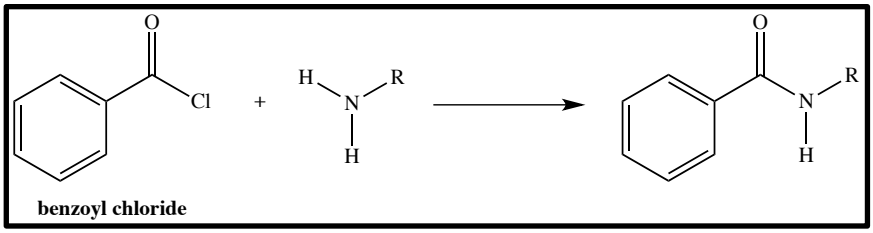

Figure 1.4. Reaction benzoyl chloride with a primary amine.

1.3.2. Detectors Used for Derivatized Products

The types of detectors usually used for derivatized analytes are ultraviolet-visible (UV-vis) or fluorescence spectroscopy. UV-vis, the most common detector, detects analytes by its absorbance of light at a particular wavelength, whereas the fluorescence detector is based on the principle that compounds with a fluorophore will fluoresce when excited with energy.[34]

UV-vis and fluorescence detectors are simple and inexpensive, but do have disadvantages. Many compounds, especially solvents used in mobile phases for liquid chromatography absorb in the UV-vis spectral range, which causes high noise levels that affect sensitivity. Fluorescence detectors on the other hand do not have this problem but are limited to compounds with a fluorophore.

Sensitivity of mass spectrometry in many cases are comparable to fluorescence, but it provides much more specificity and selectivity. Mass spectrometry can detect

compounds with or without a chromophore or fluorophore, and also allows for structural elucidation whereas UV-vis and fluorescence do not. Mass spectrometry in conjunction with stable derivatized products further increases specificity and sensitivity of PA analysis. In this project mass spectrometry was used with derivatized PAs as an effort to produce highly specific and sensitive means of detection.

1.4. Electrospray Ionization and Triple Stage Quadrupole

In mass spectrometry there are a wide array of ionization techniques and mass analyzers used with high-performance liquid chromatography (HPLC). The method developed used electrospray ionization (ESI) with a triple quadrupole mass analyzer. Electrospray ionization, the most widely used liquid chromatography–mass spectrometry (LC-MS) technique, is a "soft ionization" method, which means that little to no fragmentation of the protonated molecular ion occurs. In ESI, the LC flow was pumped through a small orifice surrounded by a curtain of gas to achieve nebulization of sample into small charged droplets. The primary parameters that control ion formation are the curtain gas flow rate and voltage applied to the liquid orifice. Ions are hypothesized to form via two similar but slightly different theoretical models. In the ion evaporation model (IEM) the radius of the droplet reduces via solvent evaporation to a critical size (the Raleigh Limit) where the charge on the surface becomes so high that small ion droplets are expelled.[35,36] In the second proposed mechanism, the charged residue model (CRM), the charged droplet formed from the nebulization shrinks from solvent evaporation, leaving a fine mist of charged droplets. As evaporation proceeds the Raleigh limit is reached for each droplet and a cascade of Columbic explosions occur that produce

smaller and smaller droplets. This process continues until only the charged analyte will remain.[35,37] The benefit of ESI is that the molecules are not generally fragmented, leaving still intact molecular ions as, either protonated $[M+H]^+$ cations or deprotonated $[M-H]^-$ anions, depending on the (+) or (-) charge applied to the liquid orifice.

Once ionization has occurred the ions must be mass selected and detected. A quadrupole mass analyzer acts like a filter to isolate specific mass to charge ions (symbols *m/z* or Da). A general schematic of a single quadrupole is shown in Figure 1.5. Application of a direct current (DC) and a radio frequency (RF) voltage generates an oscillating quadrupolar electric field that allows specific *m/z* ratio ions to pass between the poles to a detector (electron multiplier). In this work we used an advanced form of LC-MS called LC-tandem mass spectrometry (LC-MS/MS).

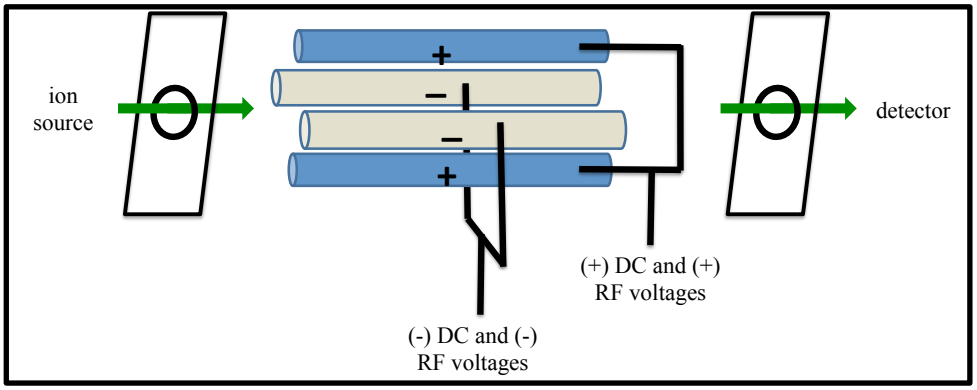

Figure 1.5. General schematic of a single quadrupole mass analyzer.

In LC-MS/MS, a triple stage quadrupole mass filter arrangement allows for the fragmentation of a protonated molecular ions $[M+H]^+$ by collision with inert gas

molecules, thus undergoing collision-induced dissociation. Upon collision two possible results could occur:

$$[M+H]^+ \xrightarrow{collision\ gas} N^+ + O \quad (1.1)$$

$$[M+H]^+ \xrightarrow{collision\ gas} P^{\bullet+} + O^{\bullet} \quad (1.2)$$

The protonated molecular ion $[M+H]^+$ is an even electron (EE) species, and the product ions N^+ and $P^{\bullet+}$ are even and odd electron (OE) species, respectively. Equation 1.1 is the thermodynamically preferred pathway, so fragmentation almost always results in the ions that undergo the loss of neutral small molecules.[38,39] The advantage of applying MS/MS to chemical analysis are that a unique fragmentation pattern often exists that are specific to a particular molecule.

A typical MS/MS instrument such as the one shown in Figure 1.6 contains additional quadrupole focusing lenses. The ions were drawn by an electric field from the ion source interface, passing through the optics (Q00 and Q0), before entering the quadrupole Q1 where selection of the specific protonated molecular ion $[M+H]^+$ took place. The mass selected $[M+H]^+$ cation then enters a collision cell (Q2) in which fragmentation occurred by collision induced dissociation. The final quadrupole (Q3) was used to mass select the *m/z* of the fragment ions (daughter ions), which were then detected at the electron multiplier. Figure 1.7 shows the schematic of the Thermo-Finnigan TSQ quantum triple stage quadrupole that was used for this research.

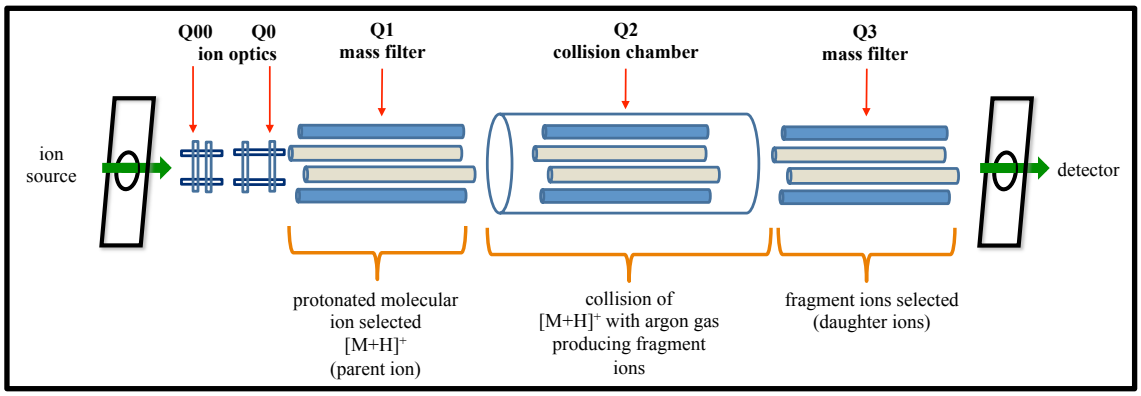

Figure 1.6. Schematic of a triple stage quadrupole.

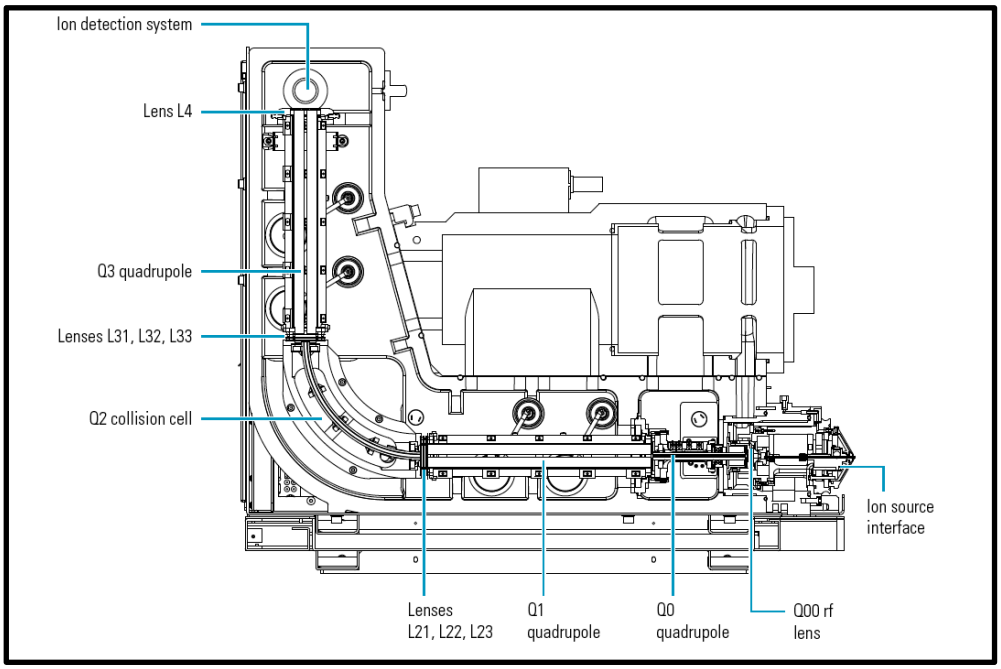

Figure 1.7. Inlet, ion optics, and quadrupoles of the mass analyzer.[40]

An example of the fragmentation and mode of detection specific to this project is shown in Figure 1.8. Derivatized putrescine molecules were protonated at the ESI source and the $[M+H]^+$ ions were passed through the optics and mass selected in Q1 at *m/z* of

297.1. Collision of the $[M+H]^+$ ion with 1.5 torr of argon, gas in Q2 produced multiple fragment ions. The two most intense fragment ions were selected in this example *m/z* 176.1 and *m/z* 105.1 were mass selected and their abundance measured at the electron multiplier. The ions of *m/z* 176.1 and *m/z* 105.1 were both positively charged even electron species produced from an even electron protonated molecular ion, which followed the thermodynamically favored Equation 1.1.

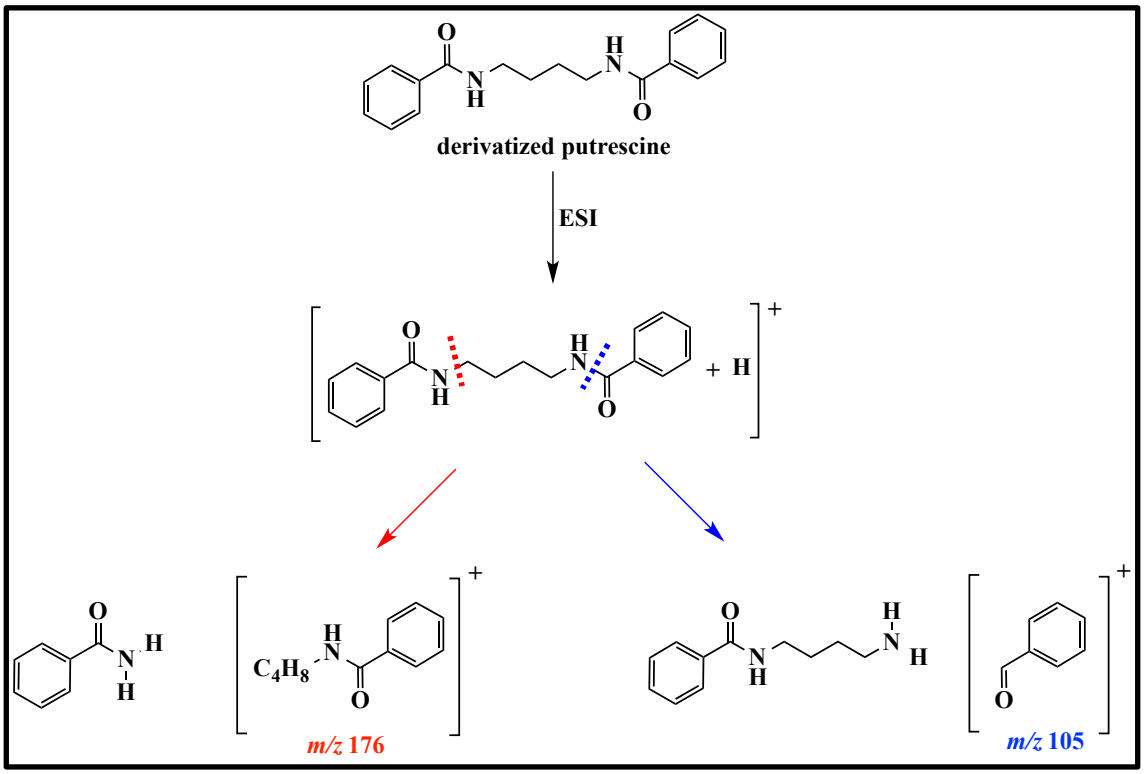

Figure 1.8. MS/MS predicted fragmentation pathways of derivatized putrescine.

1.5. Objectives

The objective of this study was to develop and validate a rapid and sensitive method for the analysis of putrescine (PUT), cadaverine (CAD), spermidine (SPD), N8-acetylspermidine (N8-ASPD), spermine (SPM), and N1-acetylspermine (N1-ASPM) as

their benzoylated derivatives in fruit fly samples with HPLC-ESI MS/MS. This thesis will focus on the primary aspects of method validation, which include linearity, accuracy and precision of the procedure and instrument, limit of detection and quantification, and ruggedness (stability). It also addresses the important aspects of optimization of the derivatization procedure, reduction of the chromatographic time, optimizing sensitivity of all the analytes, and the minimization of matrix interferents in a fruit fly matrix.

References

1 Pegg, A. E.; Casero, R. A., Jr. *Methods in Molecular Biology* 2011, *720*, 3.

2 Heby, O. *Differentiation* 1981, *19*, 1.

3 Jia, S.; Ryu, Y.; Kwon, S. W.; Lee, J. *Journal of Chromatography A* 2013, *1282*, 1.

4 Mayr, C. M.; Schieberle, P. *Journal of Agricultural and Food Chemistry* 2012, *60*, 3026.

5 Gugliucci, A. *Clinica Chimica Acta* 2004, *344*, 23.

6 Jeevanandam, M.; Petersen, S. R. *Current Opinion in Clinical Nutrition and Metabolic Care* 2001, *4*, 385.

7 Minois, N. *Gerontology* 2014, *60*, 319.

8 Minois, N.; Carmona-Gutierrez, D.; Madeo, F. *Aging* 2011, *3*, 716.

9 Nishimura, K.; Shiina, R.; Kashiwagi, K.; Igarashi, K. *Journal of biochemistry* 2006, *139*, 81.

10 Minois, N.; Rockenfeller, P.; Smith, T. K.; Carmona-Gutierrez, D. *PLoS ONE* 2014, *9*, e102435.

11 Minois, N.; Carmona-Gutierrez, D.; Bauer, M. A.; Rockenfeller, P.; Eisenberg, T.; Brandhorst, S.; Sigrist, S. J.; Kroemer, G.; Madeo, F. *Cell Death and Disease* 2012, *3*, e401.

12 Sigrist, S. J.; Carmona-Gutierrez, D.; Gupta, V. K.; Bhukel, A.; Mertel, S.; Eisenberg, T.; Madeo, F. *Autophagy* 2014, *10*, 178.

13 Buttner, S.; Broeskamp, F.; Sommer, C.; Markaki, M.; Habernig, L.; Alavian-Ghavanini, A.; Carmona-Gutierrez, D.; Eisenberg, T.; Michael, E.; Kroemer, G.; Tavernarakis, N.; Sigrist, S. J.; Madeo, F. *Cell Cycle* 2014, *13*, 3903.

14 Gupta, V. K.; Scheunemann, L.; Eisenberg, T.; Mertel, S.; Bhukel, A.; Koemans, T. S.; Kramer, J. M.; Liu, K. S. Y.; Schroeder, S.; Stunnenberg, H. G.; Sinner, F.; Magnes, C.; Pieber, T. R.; Dipt, S.; Fiala, A.; Schenck, A.; Schwaerzel, M.; Madeo, F.; Sigrist, S. J. *Nature Neuroscience* 2013, *16*, 1453.

15 Nichols, C. D. *Pharmacology & Therapeutics* 2006, *112*, 677.

16 Tickoo, S.; Russell, S. *Current Opinion in Pharmacology* 2002, *2*, 555.

17 Haekkinen, M. R.; Keinaenen, T. A.; Vepsaelaeinen, J.; Khomutov, A. R.; Alhonen, L.; Jaenne, J.; Auriola, S. *Journal of Pharmaceutical and Biomedical Analysis* 2007, *45*, 625.

18 Sanchez-Lopez, J.; Camanes, G.; Flors, V.; Vicent, C.; Pastor, V.; Vicedo, B.; Cerezo, M.; Garcia-Agustin, P. *Plant Physiology and Biochemistry* 2009, *47*, 592.

19 Bomke, S.; Seiwert, B.; Dudek, L.; Effkemann, S.; Karst, U. *Analytical and Bioanalytical Chemistry* 2009, *393*, 247.

20 Conca, R.; Bruzzoniti, M. C.; Mentasti, E.; Sarzanini, C.; Hajos, P. *Analytica Chimica Acta* 2001, *439*, 107.

21 Ducros, V.; Ruffieux, D.; Belva-Besnet, H.; de, F. F.; Berger, F.; Favier, A. *Analytical Biochemistry* 2009, *390*, 46.

22 Kang, X.; Xiao, J.; Huang, X.; Gu, Z. *Clinica Chimica Acta* 2006, *366*, 352.

23 Merali, S.; Clarkson, A. B., Jr. *Journal of Chromatography B: Biomedical Applications* 1996, *675*, 321.

24 Cooper, J. D. H.; Ogden, G.; McIntosh, J.; Turnell, D. C. *Analytical Biochemistry* 1984, *142*, 98.

25 García Alvarez-Coque, M. C.; Medina Hernández, M. J.; Villanueva Camañas, R. M.; Mongay Fernández, C. *Analytical Biochemistry* 1989, *178*, 1.

26 Teti, D.; Visalli, M.; McNair, H. *Journal of Chromatography B* 2002, *781*, 107.

27 Khuhawar, M. Y.; Qureshi, G. A. *Journal of Chromatography B* 2001, *764*, 385.

28 Hockl, P. F.; Thyssen, S. M.; Libertun, C. *Journal of Liquid Chromatography & Related Technologies* 2000, *23*, 693.

29 Liu, R.; Jia, Y.; Cheng, W.; Ling, J.; Liu, L.; Bi, K.; Li, Q. *Talanta* 2011, *83*, 751.

30 Mei, Y. H. *Journal of Liquid Chromatography* 1994, *17*, 2413.

31 Roberts, D. R.; Walker, M. A.; Dumbroff, E. B. *Phytochemistry* 1985, *24*, 1089.

32 Watanabe, S.; Saito, T.; Sato, S.; Nagase, S.; Ueda, S.; Tomita, M. *Journal of Chromatography* 1990, *518*, 264.

33 Morgan, D. M. L. *Methods in Molecular Biology* 1998, *79*, 111.

34 Venn, R. F. *HPLC detectors*, 2000.

35 Wilm, M. *Molecular & Cellular Proteomics : MCP* 2011, *10*, M111.009407.

36 Nguyen, S.; Fenn, J. B. *Proceedings of the Natiocal Academy of Sciences* 2007, *104*, 1111.

37 Konermann, L.; Ahadi, E.; Rodriguez, A. D.; Vahidi, S. *Analytical Chemistry* 2013, *85*, 2.

38 Thurman, E. M.; Ferrer, I.; Pozo, O. J.; Sancho, J. V.; Hernandez, F. *Rapid Communications in Mass Spectrometry* 2007, *21*, 3855.

39 McLafferty, F. W.; Tureček, F. *Interpretation of Mass Spectra*; University Science Books, 1993.

40 Thermo Fisher Scientific Inc. *TSQ Series Hardware Manual*, 2010.

CHAPTER 2. EXPERIMENTAL

2.1. Chemicals, Materials, and Instruments

Putrescine dihydrochloride (≥99% purity, CAS# 333-93-7), N^1-acetylspermine trihydrochloride (≥97% purity, CAS# 77928-70-2), spermidine trihydrochloride (≥98% purity, CAS# 334-50-9), cadaverine (≥97% purity, CAS# 462-94-2), spermine tetrahydrochloride (≥99% purity, CAS# 306-67-2), N^8-acetylspermidine dihydrochloride (≥99% purity, CAS# 34450-15-2), benzanilide (≥98% purity, CAS# 93-98-1), and 1,7-diaminoheptane (≥98% purity, CAS# 646-19-5), anhydrous sodium sulfate (≥99% purity, CAS# 7757-82-6), and benzoyl chloride (≥99% purity, CAS# 98-88-4) were purchased from Sigma-Aldrich (Fluka, St. Louis, MO). N^1-(3-aminopropyl)butane-d_8-1,4-diamine trihydrochloride (99% purity, spermidine-d_8, CAS# 1173019-26-5) was purchased from IsoSciences (King of Prussia, PA), and 1,4-butane-d_8-diamine dihydrochloride (99% purity, putrescine-d_8, CAS# 284665-22-1) was purchased from C/D/N Isotopes (Pointe-Claire, Quebec). Acetonitrile (CAS# 75-05-8) was purchased from Pharmco-Aaper (distilled in glass HPLC grade, Brookfield, CT). Methylene chloride (CAS# 75-09-2) was purchased from Fisher Scientific (HPLC grade, Fair Lawn, NJ). Sodium hydroxide (≥98% purity, CAS# 1310-73-2), ACS grade formic acid (88% purity, CAS# 64-18-6) and perchloric acid (70% purity, CAS# 7601-90-3) were purchased from Thermo Fisher Scientific (Pittsburg, PA). Ultrapure water was obtained from a Barnstead Easypure UV Compact Ultrapure water system (Thermo Scientific).

All solutions and samples were prepared in glassware that was thoroughly washed with soap, rinsed with hot tap water, several rinses with deionized water, then dried at

100°C to evaporate the water, and then baked in a muffle furnace at 420°C for ≥20 minutes before use. Quantitative filter paper grade Q5 purchased from Supelco (Bellefonte, PA) was cut into 0.5-inch diameter circles and used in 5 mL glass filtration columns (Popper & Sons, Inc., New Hyde Park, NY). Centrifugation was carried on a Fisher Scientific Centrific Model 225 Benchtop Centrifuge (Pittsburgh, PA). Evaporation of solvents was carried out in a sample evaporator vacuum manifold purchased from Alltech Associates, Inc. (Bellefonte, PA) that was connected to house vacuum. Solutions were mixed using a vortex mixer made by Scientific Industries, Inc. (Bohemia, NY), and long term mixing was carried out by rocking on a table mixer (Barnstead International, Dubuque, IA).

Infrared spectroscopy was carried out with a PerkinElmer RX1 Fourier Transform – Infrared spectrometer (PerkinElmer, Boston, MA), and data acquisition was performed on the Spectrum software version 5.3.1 (PerkinElmer).

Analysis of samples and standards were carried out on a Thermo Finnigan high performance liquid chromatography tandem mass spectrometry (HPLC-MS/MS) system that was a combination of a Surveyor autosampler, Surveyor MS pump, and a modified Quantum Triple Stage Quadrupole (TSQ) detector with an electrospray ionization source (ESI) (Thermo-Finnigan, San Jose, CA). Mass spectrometer ion optics was modified to improve sensitivity by passing twice as many ions from the ESI source into the analyzer. Automation and data analysis were accomplished by using Xcalibur Version 2.0.7 software (Thermo-Finnigan). Samples were injected onto a 10 mm x 2.1 mm, 5 µm particle Biobasic-C18 Thermo Scientific guard column coupled to a 50 mm x 2.1 mm, 5 µm particle Betabasic-C18 Thermo-Hypersil analytical column.

2.2. Preparation of Standards and Internal Standards

Putrescine dihydrochloride, N^1-acetylspermine trihydrochloride, spermidine trihydrochloride, cadaverine, spermine tetrahydrochloride, and N^8-acetylspermidine standards were gravimetrically prepared on an analytical balance to ±0.1 mg precision in 0.10 M perchloric acid. Concentrations of the standard stock solution mixtures were serially diluted on an analytical balance to prepare working solution mixtures between 1 ng/mL -10 μg/mL.

Three internal standards, 1, 7-diaminoheptane (DAH), putrescine-d8 (PUT-d8), and spermidine-d8 (SPD-d8) were prepared in 0.10 M perchloric acid at concentrations of 831. ng/mL, 305. ng/mL, and 309. ng/mL respectively. Benzanilide (BEN) was prepared as an internal standard in acetonitrile at 2.51 mg/mL. The derivatization reagent benzoyl chloride was dissolved in methylene chloride (CH_2Cl_2) to prepare a working solution in which the mole ratio of benzoyl chloride to amines was about 200 to 1, respectively. All standards and internal standards were prepared and stored at 4^oC and brought to room temperature prior to use.

2.3. Sample Preparation and Instrument Operating Optimized Conditions

This section summarizes the conditions and procedures that were obtained from the many experiments that were run in the course of method validation. These included: preparation of samples, a derivatization protocol, HPLC settings, and mass spectrometry detection parameters. Details of the procedures that were optimized during the course of the work will be described in subsequent sections.

2.3.1. Preparation of Samples

This analytical method was developed for analysis of whole *Drosophila melanogaster* (fruit flies), and the final optimized procedure was also applied to analyze whole rat liver cell lysate. Fruit flies were homogenized in 1.0 M perchloric acid solution with a mortar and pestle. The solution was centrifuged at 4000 rpm (setting at 8) for 10 minutes and the supernatant was gravity filtered twice with the Whatman Q5 grade filter paper, then stored at 4^{o}C in the dark before analysis. Aliquots were spiked with internal standards PUT-d8, SPD-d8, and 1 mL of 1.0 M perchloric acid and then mixed for 10 minutes on the table mixer prior to derivatization.

Rat liver samples were prepared by the Bioscience Center at San Diego State University. Rat liver cell lysates were homogenized in 250 mM sucrose, 10 mM 3-(*N*-morpholino)propanesulfonic acid buffer (MOPS), and 1 mM ethylene glycol tetraacetic acid (EGTA), centrifuged, and the supernatant was used for analysis. Aliquots were spiked with internal standards PUT-d8, SPD-d8, and 1 mL of 1.0 M perchloric acid and placed on the table mixer for 10 minutes prior to derivatization.

2.3.2. Derivatization Procedure

Samples and standards were derivatized and processed concurrently in glass vials with Teflon lined caps. To each vial, four internal standards (DAH, BEN, PUT-d8, and SPD-d8) and 1.5 mL of 2 M sodium hydroxide were added, briefly mixed, followed by the addition of benzoyl chloride and one milliliter of CH_2Cl_2. The solution was placed on the mixing table for 20 minutes at room temperature. One milliliter of a saturated NaCl solution was added immediately to the reaction mixture, and the product was extracted

twice with 2 mL volumes of CH_2Cl_2. The combined CH_2Cl_2 extracts were dried in a vacuum chamber. Then one milliliter of ultrapure water was added to the dried products, and incubated at 30^{o}C overnight. A final extraction was carried out with two aliquots of 2 mL of CH_2Cl_2. The combined extracts were filtered over ~1.0 g of anhydrous sodium sulphate in 10 mL glass filtration columns, dried under vacuum, and then reconstituted with 50:50 acetonitrile:water (ACN:H_2O) for LC-MS analysis.

2.3.3. Liquid Chromatography

The guard column/analytical column combination was attached directly to the inlet of the bypass valve on the MS. The bypass valve was switched to the "waste" position for 1.8 minutes upon injection of a 50-µL injection to divert the earlier eluting compounds to waste, and then switched to the "inject" position to channel the solvent flow into the MS. This configuration kept the early eluting (water soluble) components from contaminating the MS. Separation was achieved by a linear gradient profile by mixing two mobile phases shown in Table 2.1. Mobile phase A was 100% HPLC grade acetonitrile with 0.1% (v/v) formic acid. Mobile phase B was a mixture of 95% (v/v) ultra-pure water and 5% (v/v) HPLC grade acetonitrile and 0.1% (v/v) formic acid. All samples injections were alternated with blank injections consisting of 1:1 ratio of mobile phase A and B, and the injection needle was programmed to rinse two times with acetonitrile before each injection.

Table 2.1. Gradient profile for chromatography.

time (minutes)	% A*	%B†	flow (µL/min)
0.0	0	100	500
0.1	0	100	500
0.2	50	50	250
2.0	100	0	250
2.1	0	100	500
5.0	0	100	500

* %A mobile phase – 100% HPLC grade acetonitrile with 0.1% (v/v) formic acid
† %B mobile phase – 95% ultra-pure water, 5% HPLC grade ACN, and 0.1% (v/v) formic acid

2.3.4. Selection of Fragment Ions

Automation and data integration was accomplished by using the Xcalibur Version 2.0.7 software (Thermo Finnigan). The raw data was exported into Microsoft Excel for final analyses.

For each analyte and internal standard the protonated molecular ion (parent ion, $[M+H]^+$), a quantifying ion, a confirming ion, and optimum collision energy (CE) was established (Table 2.2). Both the quantifying and confirming ions were fragment ions (daughter ions) of the protonated molecular ion. For each analyte the collision energy for each fragment ion was raised to fragment the $[M+H]^+$ ion until the intensity was <5% of the major fragment. The fragment ion chosen for quantification was the base peak, the most intense fragment, of the MS/MS spectrum, and the second most intense fragment ion was chosen as a qualifying ion. BEN has two fragment ions that could be used for quantification because both ions are equally intense.

Table 2.2. Table with each derivatized analyte and internal standard's parent ion, quantifying ion, confirming ion, and collision energy.

Compound	Parent Ion* (*m/z*)	Fragment Ions (*m/z*)		Collision Energy§ (volts)
	$[M+H]^+$	Quantifying Ion†	Confirming Ion‡	
PUT	297.1	176.1	105.1	20
N8-ASPD	396.2	274.2	162.1	21
N1-ASPM	557.2	435.2	162.1	32
SPD	458.2	336.2	162.1	23
CAD	311.1	190.1	105.1	19
SPM	619.3	497.2	162.1	30
DAH¶	339.2	218.1	105.1	20
BEN¶	198.1	105.1, 77.1	105.1, 77.1	27
PUT-d8¶	305.2	184.1	105.1	17
SPD-d8¶	466.2	344.2	162.1	18

* Parent Ion – protonated molecular ion that is selected in Q1
† Quantifying Ion – most intense fragment ion selected in Q3
‡ Confirming Ion – second most intense fragment ion selected in Q3
§ Collision Energy – voltage applied in Q2 that yielded the selected fragment ions
¶ Internal standards

CHAPTER 3. RESULTS AND DISCUSSION

3.1. Internal Standards

Investigation of different types of internal standards used the optimized parameters are discussed in the following sections. The selection of internal standards and quantification method will be first addressed because it will clarify why only PUT-d8 and SPD-d8 were used in lieu of DAH and BEN for method development, accuracy studies, method validation, and in application for sample analysis. Moreover, the following sections about internal standards used only PUT and SPD as the target analyte to properly assess the accuracy since the only isotopic internal standards available were PUT-d8 and SPD-d8.

3.1.1. Types of Internal Standards

Compounds similar in functionality have been widely used as an internal standard for a profile of amines analyzed. Compounds frequently used in the literature to quantify PAs were 1,8-diaminooctane[1], 1,7-diaminoheptane[2-4], norspermidine[5], and or 1,6-diaminohexane[6,7]. There were also papers that used isotope dilution technique with ^{13}C, ^{15}N, and ^{2}H labeled compounds; however, only a limited numbers of published works have ignored or failed to mention how poor accuracy could be when not using isotopically labeled internal standards, especially when derivatization was required. [8-13] This has been shown to be the case in this thesis as well.

Part of this project was to determine which two methods of quantitation, the internal standard method or isotope dilution was most accurate, and provided the most consistent results. This method was developed using DAH, BEN, PUT-d8, and SPD-d8

as internal standards. The selection of internal standards and how DAH and BEN compared will first be discussed, then the selection of isotopic internal standards and its accuracy compared to the internal standard method will be addressed.

3.1.2. Internal Standard Method

Internal standards in known amounts were added to mixtures to allow for quantification even if sample derivatization was not 100% complete, and if any loss of sample occurs during the preparation steps. Two different types of internal standards were added: one that could undergo the derivatization process, and one that remained unaffected by the derivatization process; both internal standards are shown in Figure 3.1.

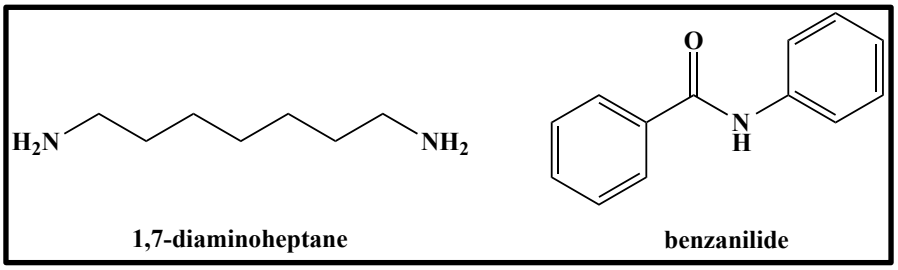

Figure 3.1. Structures of DAH, a derivatizable internal standard, and BEN, a non-derivatizable.

The derivatizable internal standard selected was DAH. Our rationale for the selection of DAH was that it is a diamine and its structure is similar to PUT and CAD only differing by two or three $–CH_2$ groups in chain length respectively. Also, this standard has been commonly used in other published works.[18,44,47] The other internal standard BEN was selected because it is an aromatic amide that does not react with benzoyl chloride. The amide functionality is the same found on the derivatized products of all the analytes.

To be a suitable internal standard, BEN must be fully recovered from the mixture after the derivatized process. An experiment was conducted to determine the recovery of BEN. A 220 ng/mL solution of BEN was prepared in acetonitrile and split into two aliquots. One aliquot was analyzed by MS/MS (sample A), and the second aliquot was processed with the derivatization protocol then analyzed by MS/MS (sample B). Figure 3.2 shows the chromatogram of both aliquots. The area counts were equal showing that BEN was not lost through the assay. It was assumed that if there were any variation in the yield of the analytes it would be from the derivatization steps and not the initial sample preparation procedure.

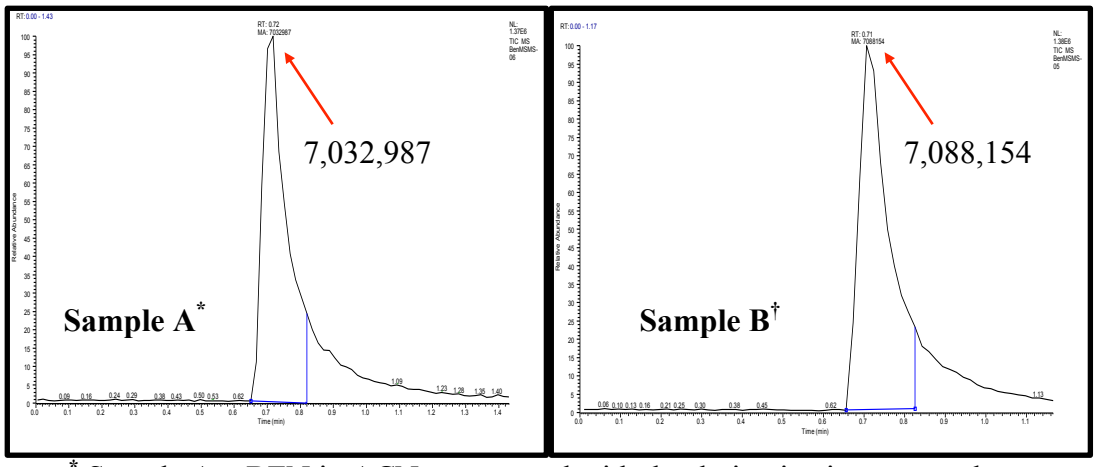

* Sample A – BEN in ACN, not treated with the derivatization protocol
† Sample B – BEN in ACN, treated with the derivatization protocol

Figure 3.2. Chromatogram of BEN treated without and with the derivatization process. Both samples were analyzed by MS/MS.

The purpose of using these standards was to have a similar compound for quantification (DAH) and the second (BEN) was used to determine overall yields. BEN has two MS/MS fragment ions at *m/z* of 77.1 and 105.1 that are of about equal intensities

at the selected CE of 27 volts. Both fragments were used for quantification (BEN-77 and BEN-105) since in an assay there are potential for interferences that may affect intensities.

3.1.2.1 DAH vs. BEN to determine quantitation accuracy of PUT and SPD

Five separate solutions (n=5) containing a mixture of 37.4 ng/mL PUT, 39.1 ng/mL SPD, 49.9 ng/mL DAH, and 125 ng/mL of BEN were prepared and derivatized using the optimized procedures and separated with the longer gradient profile. Each solution was analyzed in triplicate, and the response factor (RF) of PUT and SPD to either BEN or DAH were compared. The RF for PUT and SPD was calculated using the following equation:

$$RF = \frac{A_a}{A_{istd}} X \frac{C_{istd}}{C_a} \quad (3.1)$$

A_a and A_{istd} are the peak areas of the unknown and internal standard respectively, and C_a and C_{istd} are the concentrations of unknown and internal standard respectively.

It was expected that if DAH and BEN were suitable internal standards the RF would be the same from trial to trial. The RF calculated for PUT vs. DAH showed that it would be an appropriate internal standard because the RF did not vary from trial to trial (±1.5%); however the RF calculated for PUT vs. BEN for both ions had very poor precision (±53%). However, the data does confirm that both *m/z* of 77.1 and 105.1 did provide consistent RFs within each trial, but it was not suitable for quantification for PUT due to the low precision.

SPD had poor precision with both DAH and BEN, the RFs varied ±5.7% and ±140%, respectively. Although the RF calculated with DAH does show promise that it

would be an appropriate internal standard, the variation was higher compared to PUT. The variability of DAH may be due to the yield of the derivatized product from DAH. Derivatization for published analytical methods rarely reported product yields, their assumption being that the yields if relatively high would not affect their results. Compounds, even with similar functionalities, do not necessarily have the same product yield, which may significantly affect quantification. In the case of BEN, the underivatizable internal standard, an explanation was not deduced for the lack of precision. Despite this, the data does confirm that both *m/z* of 77.1 and 105.1 would result in the same result within each trial, which was the same observation made in the previous discussion of PUT vs. BEN.

Good precision was observed from one replicate to another for PUT and SPD vs. DAH; however, a good internal standard should work well for all analytes within the same sample, and this was not observed to be true for our dataset since the RF of SPD vs. DAH was not as good compared to PUT vs. DAH. The RF calculated using BEN was the most incompatible internal standard to use because it showed high variability and the RF could not be reproduced within 5 trials.

3.1.3. Isotope Dilution Method

Using isotopes as an internal standard, commonly termed isotope dilution analysis (IDMS), is the most reliable technique because it has been accepted that an isotopic analogue will have the same recovery, chromatographic retention time, and signal response as the analyte.[14] Also, theoretically in the analysis of derivatized products isotope dilution removes any doubts of yield because structurally there are little

differences affecting product formation, provided there are no evidence of kinetic isotope effects. IDMS is generally considered as the "gold standard" for quantification in the LC-MS/MS community. In this thesis two isotopically labeled commercially available internal standards were used, PUT-d8 and SPD-d8, shown in Figure 3.3. Due to the cost and availability these were the only two isotopes investigated.

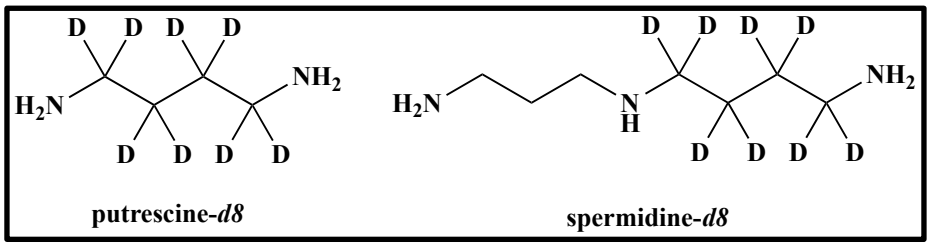

Figure 3.3. Structures of isotopically labeled internal standards.

Five separate solutions containing a mixture of 37.4 ng/mL PUT, 39.1 ng/mL SPD, 36.6 ng/mL PUT-d8, and 39.5 ng/mL of SPD-d8 were prepared (n=5) and derivatized using the optimized procedure and separated using the shorter gradient profile. The collision energies used for PUT, SPD, PUT-d8, and SPD-d8 were of the optimized values found in Table 2.2. Each solution was analyzed in triplicate, and the RFs of PUT vs. PUT-d8 and SPD vs. SPD-d8 were determined. The RF for the isotopically labeled compound was assumed to be 1.00 therefore the concentration of the unknown was determined by the equation:

$$C_a = C_{istd}\, X\, \frac{A_a}{A_{istd}} \qquad (3.2)$$

Where A_a and A_{istd} are the peak areas of the unknown and internal standard respectively, and C_a and C_{istd} are the concentrations of unknown and internal standard respectively.

We first wanted to demonstrate that the RF of PUT and SPD could be set equal to 1.00. Graph 3.1 and Graph 3.2 show the RFs calculated for PUT vs. PUT-d8 and SPD vs. SPD-d8 respectively. The RF for PUT and SPD vs. DAH, from the previous experiment, is also shown in each graph to show that although DAH showed some promise to be a suitable internal standard for PUT but was inconsistent for SPD. IDMS, on the other hand, produced RFs of 0.935 ± 0.04 and 1.03 ± 0.04 for PUT and SPD, respectively.

Graph 3.1. RF comparison of PUT vs. PUT-d8 and PUT vs. DAH for each trial.*

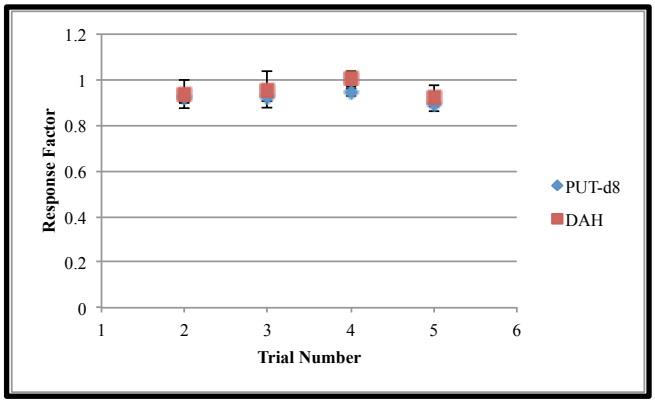

*Each "Trial Number" represents a separate sample prepared. Within each sample triplicate analysis was carried out, which is represented by the error bars.

Graph 3.2. RF comparison of SPD vs. SPD-d8 and SPD vs. DAH for each trial.*

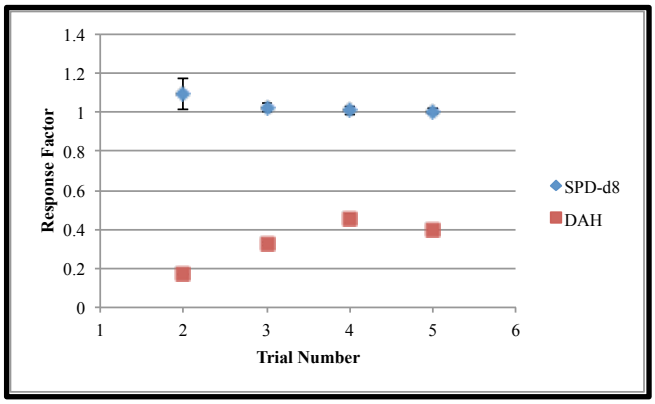

*Each "Trial Number" represents a separate sample prepared. Within each sample triplicate analysis was carried out, which is represented by the error bars.

3.1.4. Accuracy of Internal Standard Versus Isotope Dilution Method

In Sections 3.1.2 - 3.1.4 it was clearly shown that IDMS was the superior method for quantification. To further confirm that isotopic internal standards worked best, solutions of PUT-d8, SPD-d8, DAH, and BEN over a concentration range of 1-80 ng/mL were prepared. High (~80 ng/mL), medium (~12 ng/mL), and low (~1 ng/mL) concentration levels of PUT and SPD were prepared and PUT-d8, SPD-d8, DAH, and BEN were added as internal standards. The samples were derivatized and subjected to HPLC-MS/MS analysis with the optimized procedure. The raw data was used to calculate the concentrations of each sample using Equations 3.1 and 3.2 by solving for C_a (concentration of the analyte). The calculated concentration was compared to the expected concentration and the accuracy was calculated in terms of percent error. Table 3.1 shows the results from these tests for the 3 levels of PUT and SPD along with the accuracy obtained using the internal standards. Appendix A shows the observed and expected concentration of each level corresponding to each internal standard for PUT and SPD.

This data clearly showed that isotope dilution was the only method that consistently produced good accuracy. Combined with the results from the prior Sections 3.1.2 and 3.1.3 it was concluded that isotope dilution methods produced data of high accuracy and precision, and DAH and BEN produced poor accuracy but good precision.

Table 3.1. Accuracy, expressed as % error, of PUT and SPD calculated with PUT-d8, SPD-d8, DAH, and BEN (both ions compared).[*]

			% Error			
	Level	**Expected (ng/mL)**	**d8[†]**	**DAH**	**BEN-77**	**BEN-105**
PUT	High	77.9	12	29	970	770
	Medium	11.9	14	3.7	1400	1100
	Low	1.47	12	25	1100	730
SPD	High	81.4	5.5	84	230	160
	Medium	12.5	6.3	93	120	66
	Low	1.54	27	100	20	4.4

[*]Appendix A lists the calculated concentrations for PUT and SPD with PUT-d8, SPD-d8, DAH, and BEN.
[†]d8 – represents the deuterated internal standard for PUT or SPD

3.2. Optimization of the Derivatization Procedure

Numerous published analytical methods used benzoyl chloride as a derivatization reagent to chemically modify the structures of PAs for detection.[4,5,15-23] Due to the sample type and the number of PAs that were of interest; each published benzoyl chloride derivation method was unique. It was recognized that each PA might provide an optimal yield from derivatization at differing reaction and extraction conditions. Our goal was to measure all PAs and internal standards in one procedure, so a common set of reaction conditions providing overall good yields was desired. For optimization of derivatization conditions, different solvents, benzoyl chloride reagent mole ratios, reaction times and temperatures were investigated.

3.2.1. Reagent (Benzoyl Chloride) Reaction Solvent and Mole Ratio

This series of experiments determined which solvents and what ratio of benzoyl chloride to PAs produced the most reaction products for all the PAs. Many papers used benzoyl chloride either as a pure reagent or diluted different solvents.[4-7,13,17-20,22-29] The following experiments in this thesis used published works as a starting point for optimization. The concentration of each PA, and internal standard used is shown in Table 3.2.

Table 3.2. The final concentration of each compound and internal standard used for optimization of solvents and ratios used to prepare benzoyl chloride for derivatization. All compounds were prepared in 0.1M $HClO_4$, and BEN was prepared in acetonitrile.

Compound	ng/mL
PUT	37.4
N8-ASPD	46.9
N1-ASPM	47.3
SPD	39.1
CAD	68.5
SPM	39.9
DAH	49.9
PUT-D8	36.6
SPD-D8	39.5
BENZ	126

The reaction solvent experiment was carried out by derivatizing the PAs and internal standards that were prepared in 0.1M perchloric acid with 5 different treatments of benzoyl chloride (Table 3.3). Treatment number 1 and 2 used pure benzoyl chloride at different volumes. Treatment number 3-5 used a solution of benzoyl chloride in acetonitrile, methylene chloride, and diethyl ether respectively. These solvents were selected because of their widely divergent solubility parameters. The volumes used for

the diluted treatments were based on the final benzoyl chloride:PAs mole ratio, with at least a ~10% molar excess of benzoyl chloride to react with each PA.[20] The vials were briefly Vortex mixed, placed on a table mixer for 1 hour at room temperature, extracted, then analyzed to compare the area counts.

Table 3.3. Benzoyl chloride treatment variations.

	Benzoyl Chloride Treatment	Benzoyl Chloride Volume (µL)	Solvent	Benzoyl Chloride Concentration (mg/mL)
1	Neat	5	-	-
2	Neat	25	-	-
3	Diluted	-	ACN	1.45
4	Diluted	-	CH_2Cl_2	1.53
5	Diluted	-	Ether	1.46

Appendix B, Table. B.1 and Table. B.2 shows the raw data of each treatment. The largest peak area was observed for all 6 analytes and 4 internal standards when derivatized with benzoyl chloride prepared in CH_2Cl_2. It was initially thought that the use of pure benzoyl chloride would result in better yields, but this was not observed. It was believed that this was due to the solubility of benzoyl chloride. The reaction was carried out in an aqueous environment; upon the addition of pure benzoyl chloride the solution was not homogenous, and there was a visible drop of the reagent at the bottom of the reaction vial. The reaction may have only taken place on the surface of the droplet therefore resulting in a lower yield of products compared to the reaction carried out with benzoyl chloride in CH_2Cl_2 or diethyl ether. Solubility may have also been a problem with the use of acetonitrile. The lowest yield was observed with the use of acetonitrile

compared to the other 4 treatments, because benzoyl chloride was not very soluble in acetonitrile.

The next experiment was carried out by varying the ratios of benzoyl chloride:PAs prepared in CH_2Cl_2. The same concentrations found in Table 3.2 were also used to determine the appropriate benzoyl chloride to PA ratio. The ratios of benzoyl chloride to the total moles of PA investigated are found in Table 3.4. The vials were briefly mixed and placed on a table mixer for 1 hour at room temperature, extracted, analyzed, then the area counts were compared.

Table 3.4. Mole ratio of benzoyl chloride to each polyamine.

Ratio Treatment #*	Benzoyl Chloride†	PA‡
1	10	1
2	20	1
3	50	1
4	100	1
5	200	1

*Each treatment was analyzed in triplicate, the numbers correspond to the ratio treatment found in Graph 3.3 and Graph 3.4
†The mole ratio of benzoyl chloride to each PA
‡The mole ratio of PA to the corresponding benzoyl chloride

The peak areas of all 6 PAs and 4 internal standards is listed in Appendix B.2 and is compared in Graph 3.3 and Graph 3.4, respectively. The peak area counts did not vary much from reaction ratio treatments 3-5, concluding that there must be at least 50 times greater of benzoyl chloride than each PA. This observation was based on data from all of the PAs and internal standards.

Graph 3.3. Reaction ratio treatment results for PAs.*

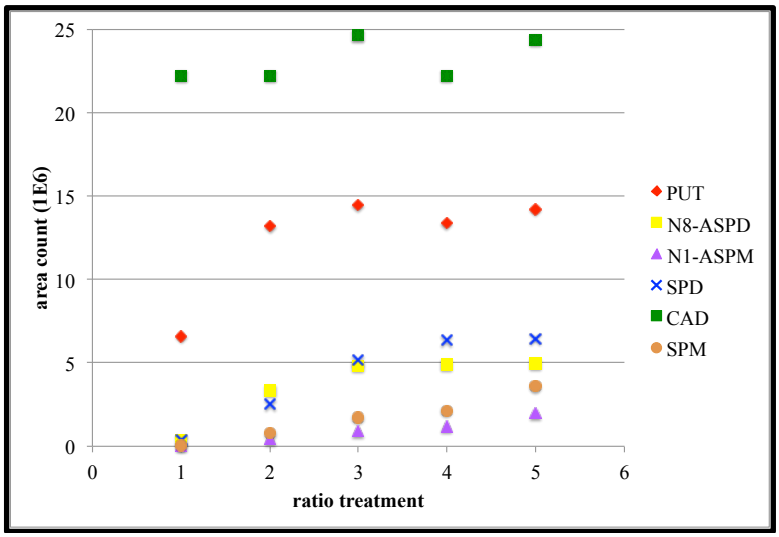

*Ratio treatment – 1) 10:1, 2) 20:1, 3) 50:1, 4) 100:1, and 5) 200:1; mole ratio of benzoyl chloride to each PA

Graph 3.4. Reaction ratio treatment results for internal standards.*

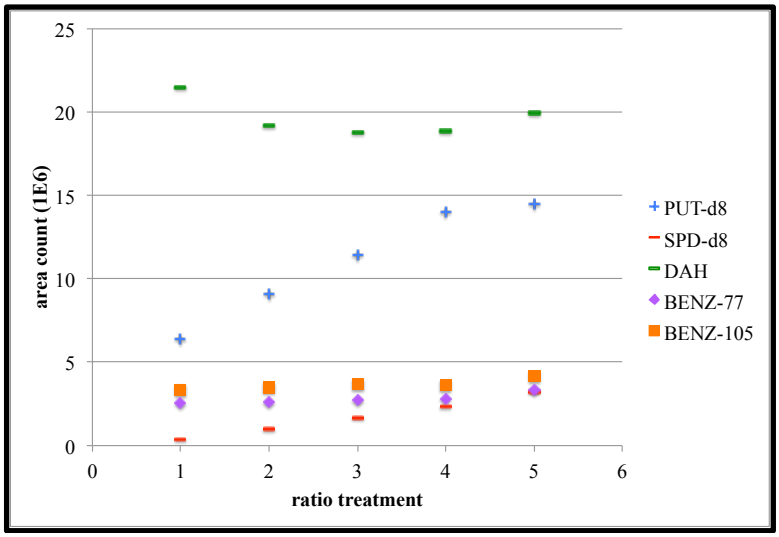

*Ratio treatment – 1) 10:1, 2) 20:1, 3) 50:1, 4) 100:1, and 5) 200:1; mole ratio of benzoyl chloride to each PA

3.2.2. Reaction Time and Temperature

Based on the previous Section 3.2.1, a ratio of at least 200:1 (benzoyl chloride:each PA) was used for the following experiment. Two sets of identical samples were prepared, one set remained at room temperature and the second set was reacted at 30^{o}C. The two temperatures and times used were based on published works. Within each set 4 different reaction times were used: 1) 20-minutes, 2) 60-minutes, 3) 3-hours, and 4) overnight. The compiled raw data can be found in Appendix B, Table. B.5 and Table. B.6. Two obvious observations were made: 1) overnight reaction time resulted in larger peak areas, at most double the peak area compared to the 20-minute reaction time; and 2) the peak areas carried out at 30^{o}C was slightly larger than room temperature, if not comparable, although there was a lower area count for N1-ASPM. Since no significant increase in area counts were observed for all PAs, we decided that keeping reaction at room temperature and mixing for at least 20 minutes was a practical time that produces sufficient yields.

3.2.3. Removal of Reaction By-Products

The method developed required the derivatization of the amines with benzoyl chloride and the mechanism follows the Schotten-Baumann mechanism (Figure 3.4). The reaction involves a nucleophilic attack of the carbon of the acyl chloride, resulting in a formation of tetrahedral intermediate, an alkoxide. The acidic proton was absorbed by the anion (hydroxide ion). The carbon-oxygen double bond was then reformed eliminating the chloride, which resulted in the final derivatized product, the benzoylated derivative or benzamide product. This reaction was classified as a Schotten-Baumann reaction because

it was carried out in a biphasic environment, which is the use of two immiscible solvents in the same reaction container.[30]

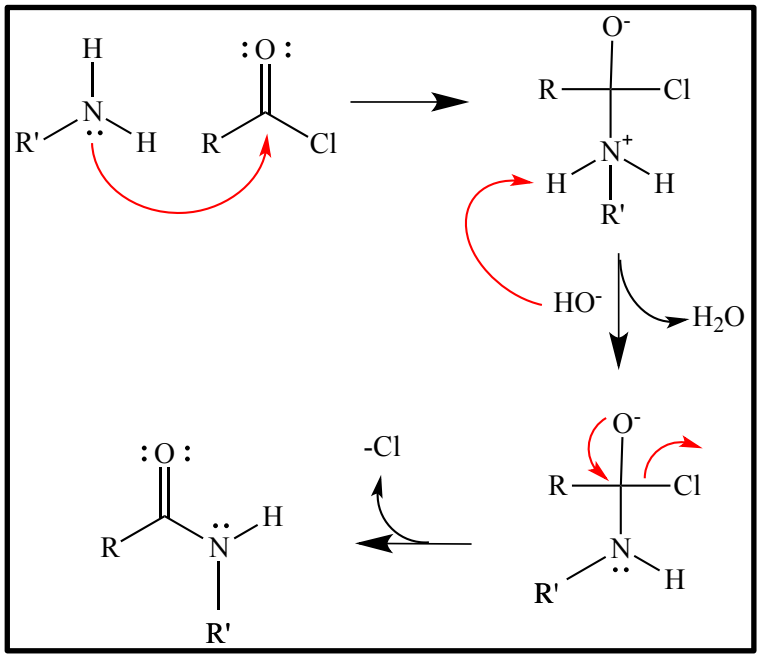

Figure 3.4. Schotten-Baumann reaction mechanism.

Many studies that used derivatization techniques prior to analysis did not take into account interferences from side products and co-eluting analytes that could suppress signal. Only a few papers have investigated the effects of the aforementioned issues.[20,29]

Every different sample type, i.e. plant, organelle, tissue, etc., would generate a varied mixture of compounds that potentially interfere with an analytical measurement. In addition to these are the by-products from the reaction, benzoic acid and benzoic anhydride (Figure 3.5). Benzoic acid was water-soluble and remained in the aqueous phase while the desired products were extracted in the CH_2Cl_2 fraction. Benzoic

anhydride was mostly soluble in CH_2Cl_2, therefore extra steps were required to remove these by-product.

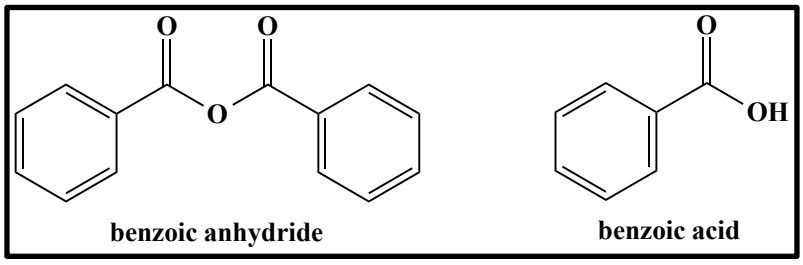

Figure 3.5. Common side-products from the Schotten-Baumann reaction.

The mass spectrometer was not used to check for by-products because the spectrum produced MS/MS ions that were similar to the analytes and internal standards studied. The predicted fragmentation of benzoic anhydride and benzoic acid, shown in Figure 3.6, are the formation of *m/z* 105 and 77, which are common fragments of molecules that contain benzene rings or structures similar to the two compounds.

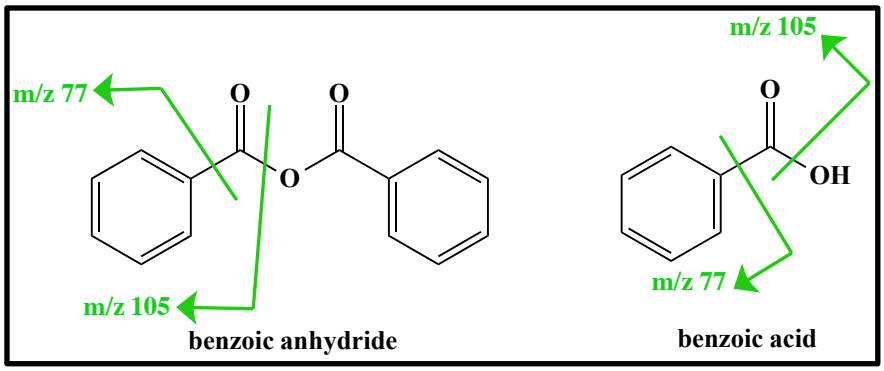

Figure 3.6. Predicted fragmentation of by-products, benzoic anhydride and benzoic acid.

Incubation was a key step in removing water-insoluble by-product(s), specifically benzoic anhydride. Figure 3.7 shows the hydrolysis product expected from benzoic anhydride.[19,29] After the first extraction was vacuum dried, 1 milliliter of water was added and the sample was placed on a heating block set at 30°C overnight. It was noticed that a sharp sweet smell was present before incubation, but the smell was not present the next day. The specific incubation temperature was used for two reasons: 1) the selected temperature was required to hydrolyze benzoic anhydride in the absence of an acid or base catalyst, and 2) 30°C was shown to not degrade the amide products in optimization, discussed in Section 3.2.2.

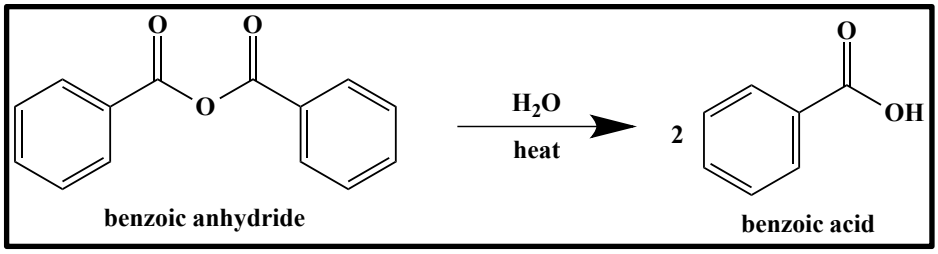

Figure 3.7. Hydrolysis of benzoic anhydride.

The incubation process must have also hydrolyzed other constituents in the biological samples. Benzoyl chloride may also react with lipids and proteins that were not fully removed from the cleanup and filtration step. The final extraction with methylene chloride was filtered through sodium sulphate to remove any possible remaining by-products that were water soluble.

Utilizing two extraction steps and a filtration step not only effectively removed the by-products, but it also removed salts. It was very important to remove as many water-soluble by-products and salts as possible prior to introducing sample into the mass

spectrometer. This procedure prolongs the life of the detector, limits signal suppression and interferences, and improves the detection limits.[31,32]

3.2.4. Product Extraction

Methylene chloride was the best solvent used for the reaction; therefore the logical solvent to use for product extract was CH_2Cl_2. The next step was to determine how many extractions were needed to extract the products. A new batch of PAs were derivatized and each sequential extraction was analyzed, and the area counts were observed (Appendix B, Figure. B.1). It was determined that four extractions of 2 mL each of CH_2Cl_2 were sufficient to remove all of the analytes from the aqueous phase. For the remainder of this study, samples were extracted twice with 2 mL of CH_2Cl_2.

3.3. Optimizing Liquid Chromatography Steps

Appropriate separation conditions were important to achieve good separation and acceptable peak shapes in liquid chromatography. Poor conditions could result in split peaks, tailing and or fronting, and broad peaks; this in turn affects quantitation and efficiency of the method. In this section a comparison between two gradient elution methods, the effect of sample solvent ratio of water and acetonitrile, the sample injection volume used, and sample carry-over was tested.

3.3.1. Gradient Elution

The comparison of two gradient elution profiles used the following optimized conditions: benzoyl chloride mole ratio of at least 200 to 1 for each PA prepared in CH_2Cl_2, a reaction of at least 20 minutes at room temperature, and incubation at 30^{o}C overnight. The final derivatized products were analyzed using both a longer and a shorter

gradient profile. This was carried out to determine if the run time could be reduced to increase sample throughput. Table 3.5 shows the profiles of gradient X, total run-time of 20 minutes, and gradient Y, total run-time of 6 minutes. Mobile phase A was 100% acetonitrile, and mobile phase B was a mixture of 95% water and 5% acetonitrile; both mobile phases contained 0.1% (v/v) formic acid.

Table 3.5. Two gradient profiles compared.

GRADIENT X				GRADIENT Y			
time (minutes)	**% A**	**%B**	**flow (µL/min)**	**time (minutes)**	**% A**	**%B**	**flow (µL/min)**
0.0	0	100	500	0.0	0	100	500
0.5	0	100	500	0.1	0	100	500
0.6	0	100	250	0.2	50	50	250
15.0	100	0	250	2.0	100	0	250
15.1	0	100	500	2.1	0	100	500
20.0	0	100	500	5.0	0	100	500

Figure 3.8 and Figure 3.9 show the chromatogram of the longer and shorter gradient carried out in triplicate, respectively. Gradient X resulted in better separation of the analytes, and gradient Y resulted in less of a separation with a shorter run-time but with virtually no separation of components. This was not an issue since the MS/MS fragment ions used for quantification were different.

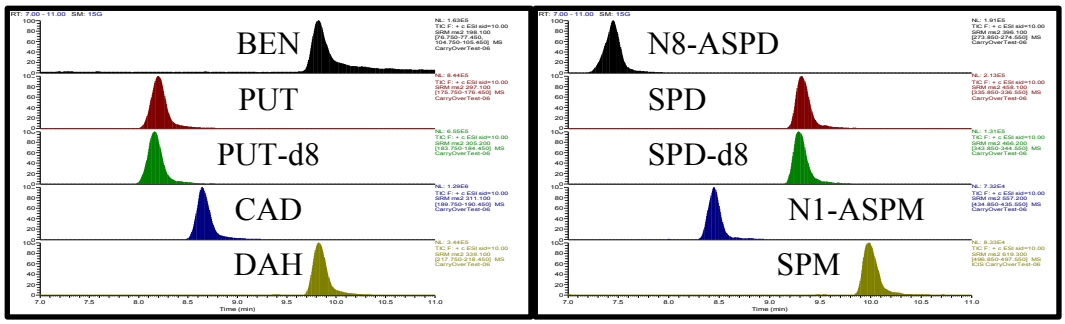

Figure 3.8. Chromatogram of a single run with all polyamines and all internal standards shown in two panels using gradient X, the longer run time.

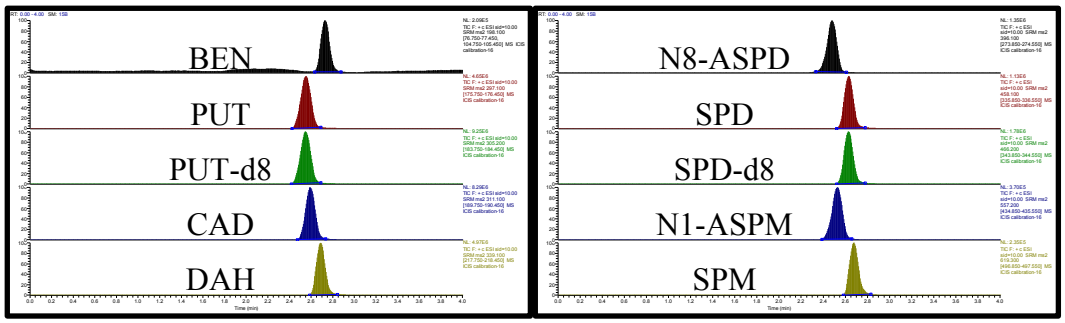

Figure 3.9. Chromatogram of a single run with all polyamines and all internal standards shown in two panels using gradient Y, the shorter run time.

By comparison of the peak area, gradient X has significantly better sensitivity than gradient Y (Table 3.6). Sensitivity in this assay was not a problem as the HPLC injection volume could be increased, but the shorter run time was an overriding factor. The latter, however, may introduce matrix suppression or enhancement effects, so this aspect was further investigated and reported in later sections of this thesis.

Table 3.6. Peak area of each analyte analyzed with either gradient X (slow gradient) or Y (fast gradient).

Gradient$_{\#}$*	PUT	N8-ASPD	N1-ASPM	SPD	CAD	SPM
X_1	4,240,799	729,791	177,336	1,301,449	5,084,562	409,297
X_2	4,789,820	733,394	182,927	1,438,289	5,976,789	423,918
X_3	5,023,783	703,943	156,436	1,376,511	6,446,520	435,624
Y_1	987,892	157,878	22,464	238,908	1,250,310	41,796
Y_2	941,571	147,498	21,280	172,350	1,096,678	23,257
Y_3	1,026,575	134,284	22,222	193,106	1,340,690	38,703

*Gradient$_{\#}$ - each gradient profile was analyzed in triplicate denoted by a subscript, gradient X was the slower gradient, and gradient Y was the faster gradient

From this experiment the accuracy and precision of the assay could be determined. By looking at the area signal ratios of PUT to PUT-d8 (P/d8) and SPD to SPD-d8 (S/d8), both gradients yielded low error, based on standards. Table 3.7 lists the percent error within each run, which indicated that both methods were accurate with no apparent suppression or enhancement. The first peaks didn't elute until 2.5 minutes, so the divert valve could be set to 1.8 minutes to bypass unwanted by-products and salts away from the mass spectrometer.

Table 3.7. Peak area ratio of PUT to PUT-d8 and SPD to SPD-d8.

Expected Ratio		Observed Ratio				
P/d8	S/d8	Gradient$_{\#}$*	P/d8†	% Error	S/d8‡	% Error
		X_1	0.989	0.21	1.13	10
		X_2	0.925	6.6	1.01	1.5
		X_3	0.944	4.7	0.950	7.1
0.991	1.02	Y_1	0.950	4.1	1.05	2.8
		Y_2	0.925	6.7	1.07	4.4
		Y_3	0.916	7.5	1.03	0.86

*Gradient$_{\#}$ - each gradient profile was analyzed in triplicate denoted by a subscript, gradient X was the slower gradient, and gradient Y was the faster gradient
†P/d8 – peak area ratio of PUT to PUT-d8
‡S/d8 – peak area ratio of SPD to SPD-d8

All analysis was completed with the shorter run time, which allowed for higher throughput. It was also shown that separation of the analytes from each other was not necessary since accuracy and peak shape were not compromised.

3.3.2. Sample Solvent Reconstitution

To minimize chromatographic peak distortion it was important to use the correct H_2O:ACN mobile phase ratio to reconstitute the products before injecting them into the HPLC. Since the separation of PAs was carried out using a gradient, the rule of thumb is that the mobile phase composition in which the PAs elute should contain more organic than the solvent of the sample. The final samples consisted of six different PAs, a small change in solvent could either greatly affect the earlier or later eluting analyte. Four different ratios of H_2O:ACN ratio solutions were used 1) 50:50, 2) 40:60 3) 30:70, and 4) 20:80, and the peak shape and width was observed.

The peak shape was measured by calculating the asymmetry factor given by the equation:

$$A_s = \frac{B}{A} \tag{3.3}$$

A_s is peak asymmetry, and B and A is defined as the width of half of the peak at 10% of the total peak height for the right and left side of the peak, respectively (Figure 3.10). This was important because peak shape relates to the height equivalent to a theoretical plate, which is a measure of column efficiency. The larger the plate height the broader the peaks, which means that separation is degraded. So in terms of peak asymmetry, a symmetric peak would result in a narrow peak width increasing the efficiency of separation.[33]

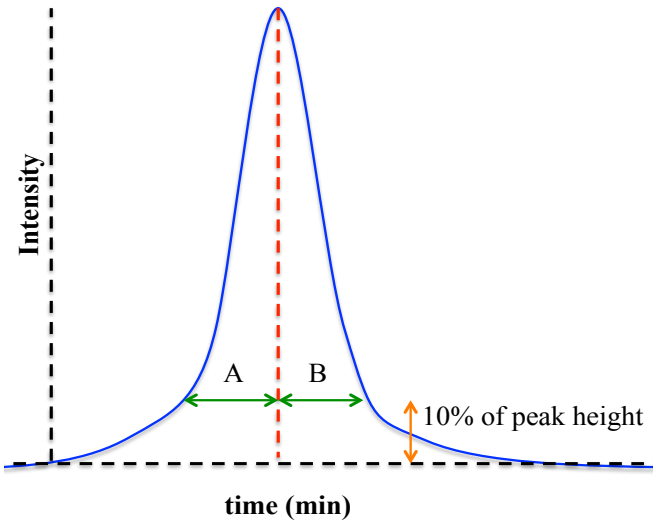

Figure 3.10. Components of a peak to calculate peak asymmetry.

An A_s value of 1.0 indicates a symmetrical peak, a factor greater than 1.0 means there is tailing, and a factor less than 1.0 means there is front tailing. Tailing is usually

caused by interactions of the analyte and residual polar sites on the column or contaminants. Front tailing is commonly due to overloading of the sample. In general A_s values between 0.8 and 1.6 are acceptable, and any value outside this range is unacceptable.[34]

From the peak shape shown in Appendix C, Figure. C.1, at a 50-µL injection volume with sample reconstitution of 50:50 ratio of H_2O:ACN resulted in the best peak shape. The peak asymmetry was calculated for 6 PAs at a 50:50 ratio of H_2O:ACN, the data is shown in Figure 3.11. Although according to the general acceptance of peak asymmetry factor N8ASPD was not within the 0.8-1.60 factor, overall the symmetry was best observed for this solvent reconstitution ratio for the whole profile of PAs.

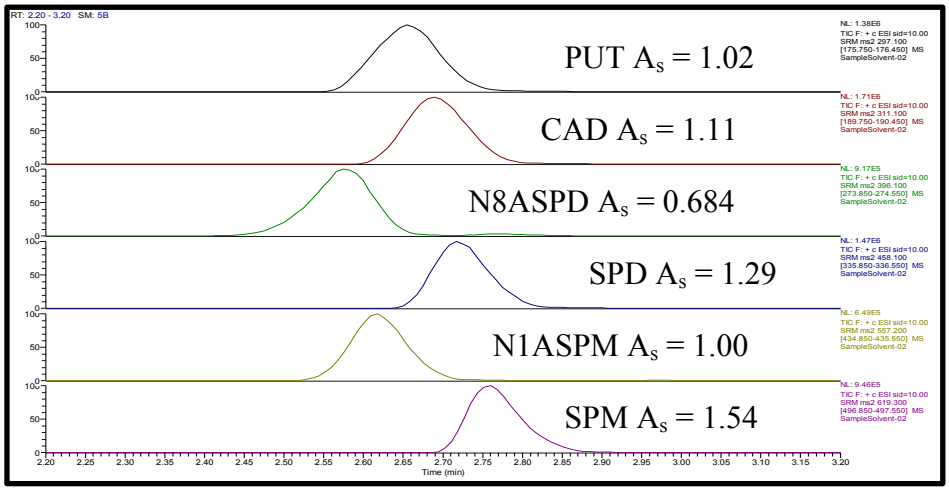

Figure 3.11. Peak asymmetry factor calculated for each analyte.

3.3.3. Sample Injection Volume

Sample injection volume was studied to determine which volume gave the best sensitivity without increasing peak asymmetry or width. The peak shape was greatly affected by the flow rate and gradient. Once a gradient was established the sample

injection volume was investigated to determine which volume resulted the best sensitivity without adversely affecting peak shape for SPM in Figure 3.12. The three volumes chosen were based on the highest and lowest volume that could be injected with a sample loop volume of 70 µL. Only the sensitivity of SPM was monitored because it was the analyte with the lowest sensitivity.

Figure 3.12. Sample injection volume and corresponding area of spermine.

Sample Injection Volume (µL)	SPM peak area
10	3,020,905
25	5,206,627
50	9,004,087

By observing the peak shapes and the peak area of SPM it was concluded that the sample volumes did not affect peak shape. Thus, all samples should be reconstituted with 50:50 H_2O:ACN, separated using the shorter run time with a sample injection of 50 µL.

3.3.4. Blanks & Carryover

Each sample was derivatized individually so that all product ions could be unambiguously identified and the daughter ion-extracted channels observed. For example a solution of PUT was derivatized following the optimized protocol, then it was analyzed to verify that there was little to no signal produced from the other daughter ion fragments (cross-interferences). In other words only the ion-extracted channel with a transition of *m/z* 297.1→ 176.1 from PUT and no other compound would have an abundant peak, the other transitions or ion-extracted channels would show little or no peaks. This was investigated for all the internal standards, solvent system, and the derivatizing reagent. Appendix C.2 shows the chromatogram of the ion-extracted channel for each analyte and

internal standard. The chromatograms demonstrated that there were no cross-interferences between the PAs.

In some assays analytes were carried over from one injection to another due to sample contamination of the HPLC injector; this is known as sample carryover. To ensure sample carryover was not occurring, injection of sample standards and blanks were alternated. Blank samples consisted of a 50:50 mixture of mobile phase A and B. Figure 3.13 are the total ion chromatograms of: (A) blank sample, (B) derivatized fruit fly sample, and (C) blank sample that were consecutively analyzed. From these we concluded that no sample carryover took place.

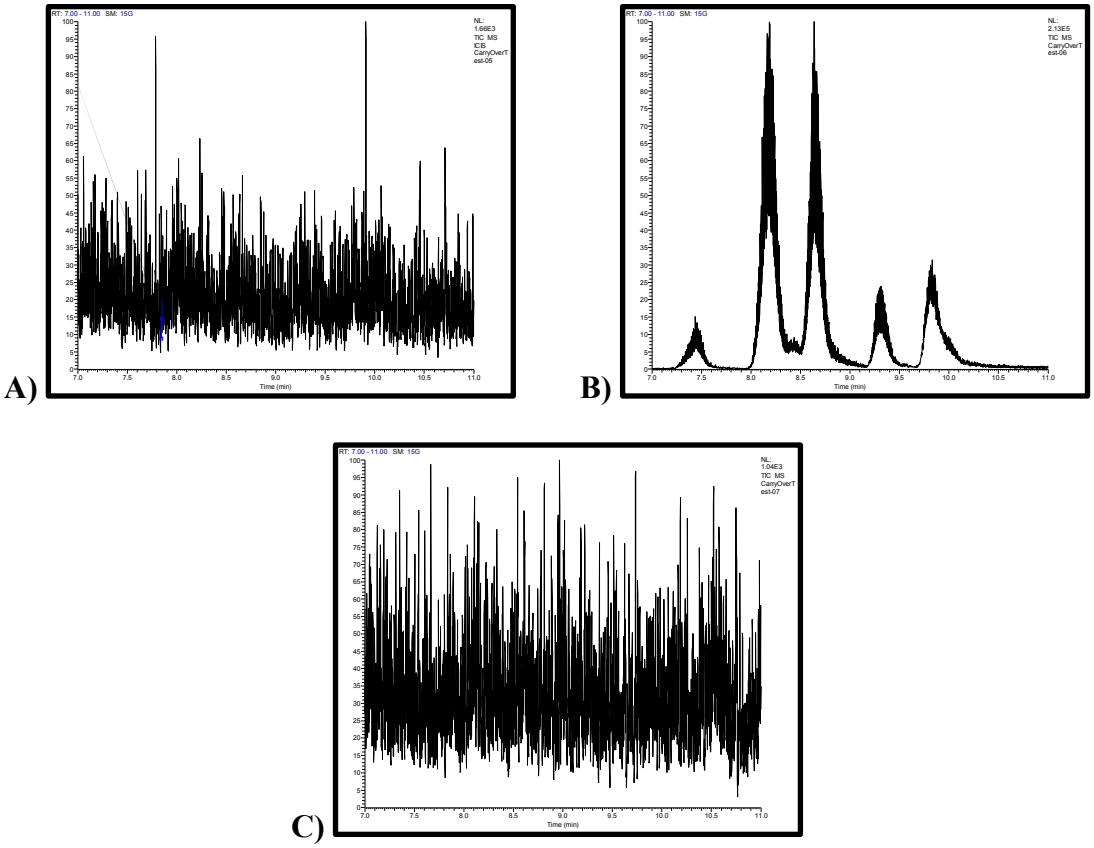

Figure 3.13. Total ion chromatogram from MS/MS data of 3 consecutive runs: A) blank sample, B) 50-µL injection of derivatized fly sample, and C) blank sample.

3.4. Optimization of Mass Spectrometer Parameters

For each compound: the fragmentation pattern was established, the optimal collision energy was determined, and the sensitivity of the signals using formic acid and acetic acid were compared. In the last section an in-depth investigation and explanation of the collision energies for the isotopic internal standards is presented.

3.4.1. Fragmentation and Collision Energy Optimization of PAs and Internal Standards

Each standard and internal standard was individually derivatized to their corresponding amides and analyzed to confirm product ion masses. The mass spectra of the standards confirmed that each amine moiety reacted with one equivalent of benzoyl chloride. Figure 3.14 and Figure 3.15 show the structures of the derivatized PAs and the internal standards, respectively. The blue arrow depicts the fragmentation of the confirming ion and the red arrow depicts the fragmentation of the quantifying ion.

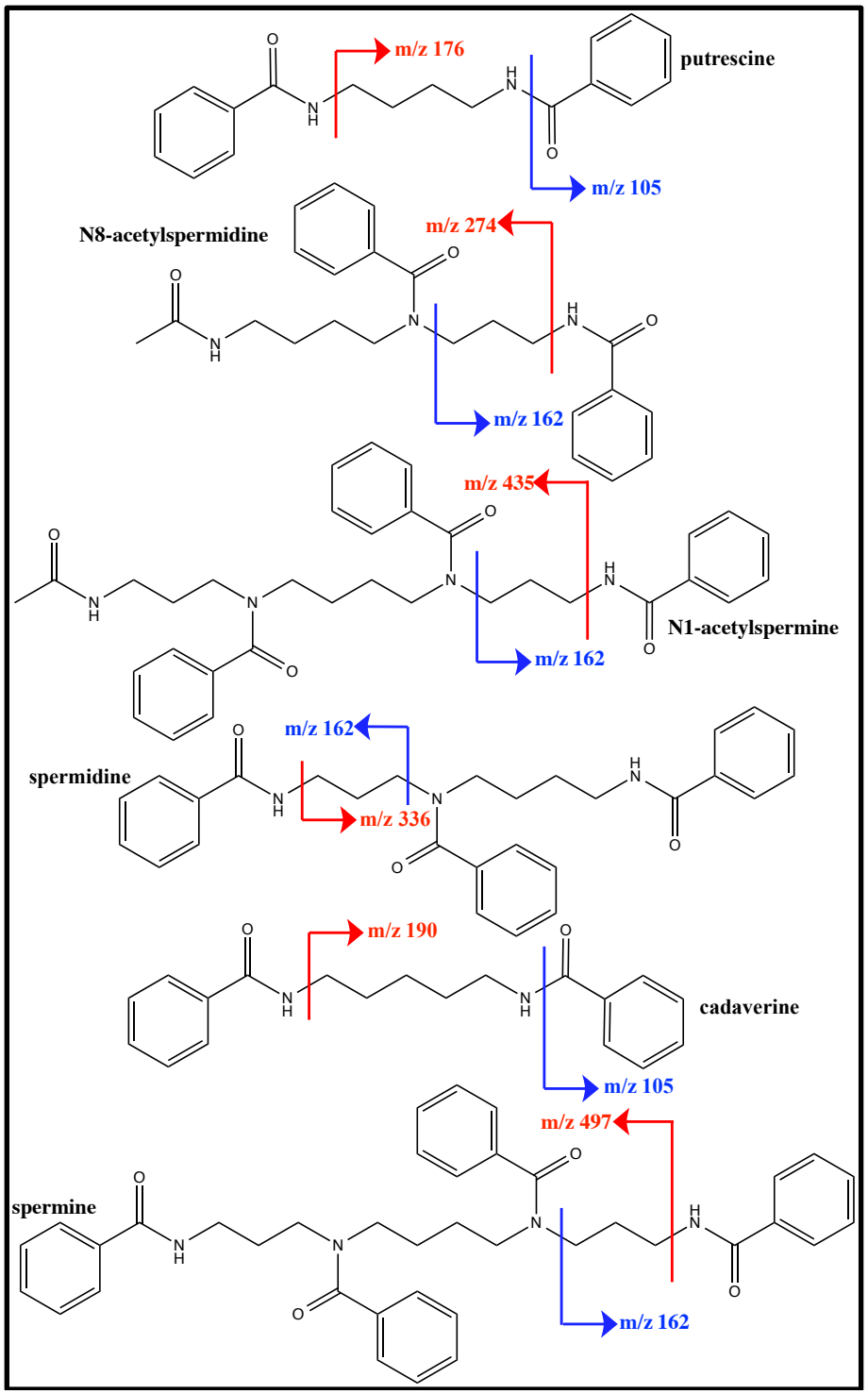

*Blue arrows depict the fragmentation for the qualifying ion, the red arrows depict the fragmentation of the quantifying ion

Figure 3.14. Structures of derivatized PAs and their corresponding MS/MS fragmentations.*

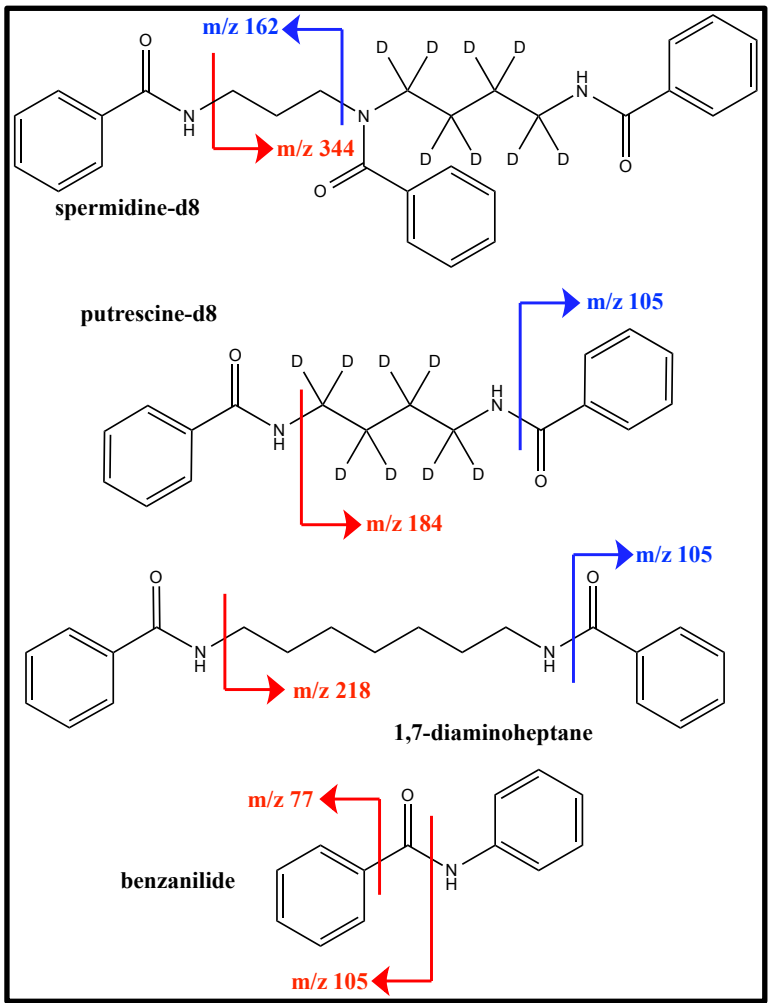

*Blue arrows depict the fragmentation for the qualifying ion, the red arrows depict the fragmentation of the quantifying ion

Figure 3.15. Structures of internal standards and their corresponding MS/MS fragmentations.

Collision energy was varied and the intensities of the fragment ions were observed. The collision energy was optimized for each compound to give the best sensitivity. The MS/MS spectrum of each compound (compiled in Appendix D) contained the protonated molecular ion and multiple fragment ions. The final collision energy determined for each compound was based on the best intensity of the base peak

(quantifying ion) with a visible but small presence of the protonated molecular ion. The most intense fragment was used for quantification and the second most intense fragment was used as a qualifying ion. The final collision energies used for each compound were shown in Table 2.2.

3.4.2. Formic Acid versus Acetic Acid

Acetic (AA) and formic acid (FA) were often used interchangeably in the protonation of analytes for positive ESI-MS. The recommended concentrations was 0.1% (v/v) of either acids.[35] A comparison was carried out to determine whether one acid resulted in better sensitivity than the other. The peak area of each analyte and internal standard are shown in Table 3.8. The conclusion was that formic acid provided about twice the sensitivity for all the analytes.

Table 3.8. Peak area of analytes using either acetic acid (AA) or formic acid (FA).

Sample	PUT	N8-ASPD	N1-ASPM	SPD	CAD	SPM
AA	4,724,889	2,159,536	1,080,670	3,390,417	6,773,368	2,012,227
FA	8,037,364	5,942,708	1,889,597	6,170,507	14,452,841	2,696,499

3.4.3. Optimization of Collision Energy (CE) for Isotopic Internal Standards (PUT-d8 and SPD-d8)

The collision energies used for PUT-d8 and SPD-d8 were carefully studied to determine if they corresponded to values optimized for their non-deuterated counterparts. Present and past published works usually used the same collision energy for the analyte and the isotopic analog internal standard because of the assumption that the

fragmentation pattern and intensity were the same. Even if fragmentation was different it was rarely clarified whether a RF was calculated or a factor of 1.00 was used.[8,36,37]

The experiment was carried out by preparing 2 solutions; one solution contained a mixture of PUT and PUT-d8 at concentrations of 37.4 ng/mL and 36.6 ng/mL, respectively, and the second solution contained a mixture of SPD and SPD-d8 at concentrations of 39.1 ng/mL and 39.5 ng/mL, respectively. Both solutions were derivatized using the optimized derivatization procedure and separated using the shorter gradient profile. If the RFs were equal to 1.00, the integrated peak areas of equal concentrations of the pairs PUT:PUT-d8 and SPD:SPD-d8 should be identical. The sensitivity for PUT-d8 and SPD-d8 were first optimized by varying the collision energy and observing the area count (signal). It was concluded that 17 and 18 volts for PUT-d8 and SPD-d8, respectively, showed the best sensitivity. The same type of experiment using PUT and SPD demonstrated that 20 and 23 volts, respectively, showed the best sensitivity. The results for these two measurements are shown in Table 3.9. The conclusion of this experiment was that different collision energies for the isotopic internal standard and the analyte were needed to yield accurate concentrations. The next experiment completed was to compare the accuracy of these voltages versus the voltages used for the non-deuterated compounds. When the same voltage was applied for both the analyte and the isotopic internal standard, the error was very high. Table 3.9 shows the results of different CE used (Appendix E).

Table 3.9. Results from CE experiment comparing the CE used for accuracy comparison.

Expected RF	
P/d8*	**S/d8†**
0.991	1.02

CE (volts)		Observed RF		CE (volts)		Observed RF	
PUT	**PUT-d8**	**P/d8***	**% Error**	**SPD**	**SPD-d8**	**S/d8†**	**% Error**
20	20	1.68	70	23	23	1.38	35
		1.51	53			1.38	35
		1.54	56			1.45	42
	17	0.936	5.5		18	1.00	1.9
		0.957	3.4			1.04	1.8
		0.924	6.8			1.00	1.9

*P/d8 – the RF of PUT to PUT-d8
†S/d8 – the RF of SPD to SPD-d8

An explanation as to why isotopic compounds behaved differently than their non-deuterated counterparts with CE could be explained in terms of zero-point vibrational energies (ZPVE). ZPVE is the ground or lowest energy level of a system where lighter atoms or molecules vibrate at higher frequencies and heavier atoms or molecules vibrate at lower frequencies. The smaller the frequency, the lower the ZPVE, hence the higher the energy required to break a covalent bond in the molecule. This means that PUT-d8 and SPD-d8 would require larger CEs than their non-deuterated analogs.[38,39] However, this was not observed. According to Whalley's paper, this difference could be due to change in ZPVE upon collision.[38]

The dissociation of the bonds requires more energy for isotopically labeled molecules. This is known as a kinetic isotope effect (KIE). Primary KIE are defined as

the bond dissociation at the site of the isotope. Secondary effects are where the bond cleavage is in a position near the isotope's location. Since the location of the bond dissociation in fragmentation of PUT-d8 and SPD-d8 in MS/MS were not at the site of the isotope, secondary KIE could explain why there was a difference in CE.

3.5. Matrix Effect

In the previous sections optimization of the reaction and analysis was carried out and completed with solutions of chemical standards. The developed method was applied to fruit fly samples. Translation of the method from standards to real samples required a careful examination of potential matrix effects that could affect method accuracy. It has become a necessary part of method development and validation procedures to study and reduce matrix effects even when the method used an isotopic internal standard.[40-43]

The most common matrix effect was due to lipids, which are found in all biological samples. Glycerophospholipids are the most abundant class of lipids in cellular membranes.[44] Within this class of lipids there are glycerophosphocholines and lysoglycerophosphocholines, which have been investigated and shown to be the main source of matrix effects in LC-MS analyses.[45,46] Matrix effect studies of phospholipids have been difficult for many reasons: 1) they are present in biologically samples at high concentrations relative to analytes of interest; 2) there is high diversity even within a class of lipids that makes elimination of phospholipids almost impossible; 3) the detergent properties - a polar head group and a non-polar tail makes removal by solvent extraction a challenge; and 4) they undergo oxidation which produces other sources of contaminant compounds.[44,46,47]

There are presently no protocols or universally accepted method to test for or to remove matrix effects. Several manufacturers produce proprietary solid phase chromatographic products that claim to remove phospholipids from some biological samples.[48] Here we employ classical methods of infrared spectroscopy and mass spectrometry experiments to help identify and quantify what compound classes were present in fly samples that might either enhance or suppress the signal of the analyte or internal standard of this project.

3.5.1. Filtered Versus Unfiltered Homogenized Flies

A simple technique was developed to remove the bulk of lipids present in samples before derivatization. It was not important to preserve any lipids; therefore a strong acid was used to hydrolyze and digest the lipids followed by filtration. The acid hydrolysis broke down the glycerophospholipids into its glycerol, fatty acid, phosphate, and amino alcohol components.[49,50] This also freed any PAs that were trapped between the spaces of lipid aggregates that were not exposed to the aqueous environment.[44]

Batches of fruit flies (~20 flies) were homogenized with a mortar and pestle in 1.0 M perchloric acid. One batch was gravity filtered twice with Whatman Q5 grade filter paper and the other batch was not. Each aliquot was mixed with equal volumes of methylene chloride. Visually the methylene chloride extracts of each aliquot looked very different. The unfiltered flies had visible oily masses on the side of the glassware while the filtered flies were clear, the oily components remained on the filter paper.

The CH_2Cl_2 extracts from each were dried down for analysis with infrared (IR) spectroscopy. As a reference compound, a whole butter sample, was also analyzed.

Figure 3.16 shows the IR spectrum for: A) whole butter lipid sample, B) unfiltered homogenized flies, and C) filtered homogenized flies.

In Figure 3.16 a red and blue rectangle is used to highlight the biggest difference amongst the three spectra. The red rectangle showed that the filtered flies had no evidence of a peak at about 1720 - 1750 cm^{-1}. This was indicative of a carbon-oxygen double bond (C=O) that could be from an aldehyde, carboxylic acid, and or ester; these functional groups were found on different classes of lipids and related compounds. The other observation was a cluster of peaks between 1000 – 1400 cm^{-1}, which were predominant in the reference compound (whole butter). These bands were indicative of: carbon nitrogen bonds (C-N, an amine); carbon oxygen single bonds (C-O) from an ester, ether, carboxylic acid, or alcohol; or phosphorous oxygen bonds (P-O) from phosphates. The desired analytes do have C=O, C-O, and C-N but in an infrared sample lipids would be responsible for the signal observed because they were present in greater quantities.

In conclusion, comparison of all three spectra indicated that the bulk of the unfiltered fraction consisted of lipids, whereas the filtered fraction had little to no evidence of lipids. The residual lipids could interfere with the analysis because they would be extracted into the methylene chloride fractions. The filtration step was successfully in the removal of the bulk of the lipids from the sample.

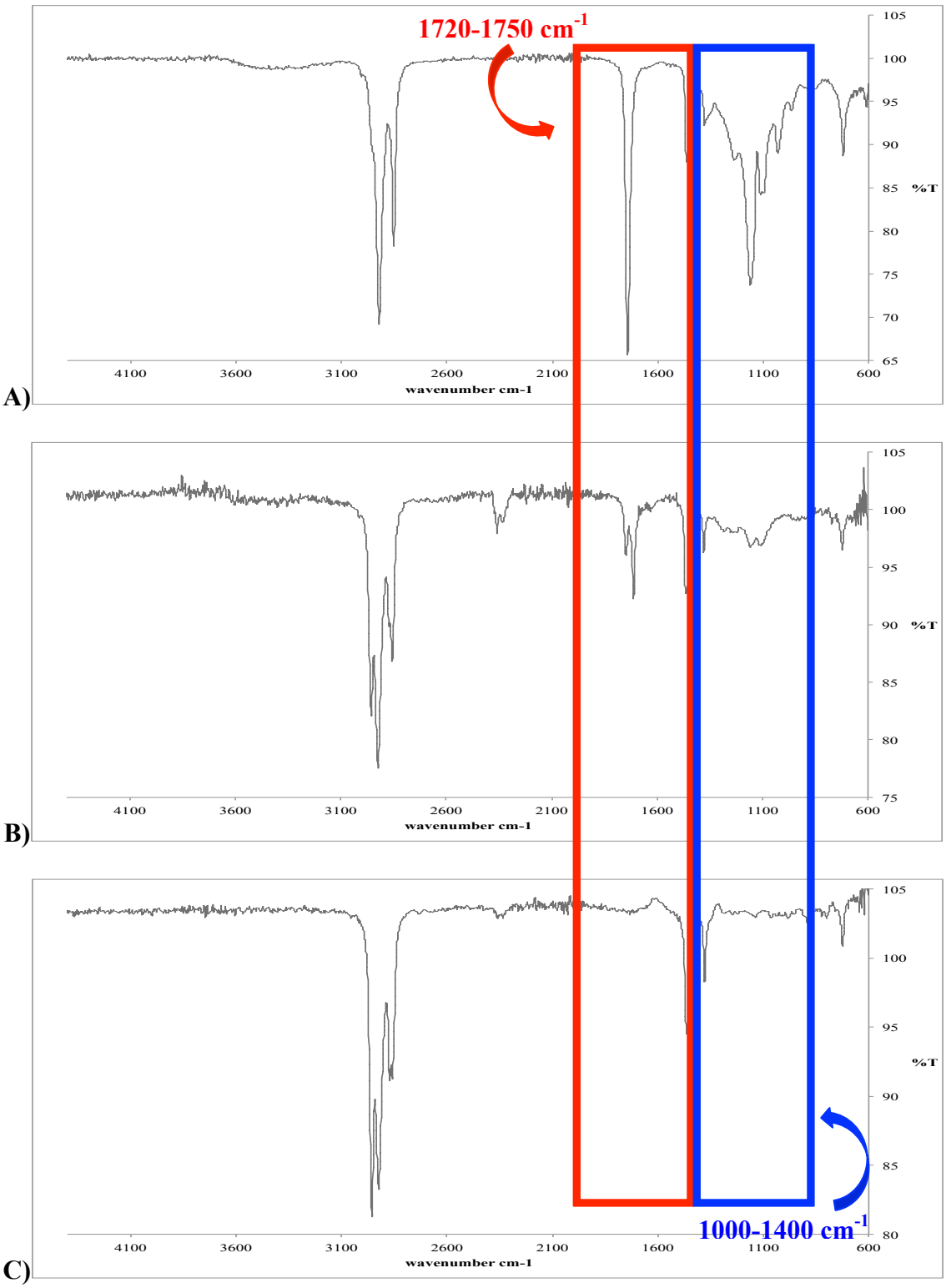

Figure 3.16. IR of A) whole butter lipid sample, B) unfiltered homogenized flies, and C) filtered homogenized flies.

3.5.2. Full Scan and Single Reaction Monitoring for Phospholipids

As mentioned earlier in this thesis phospholipids were the main causes of matrix effects when it comes to the analysis of biological samples by ESI-MS. This was thought to be from their detergent properties, which interfere with formation of ions in electrospray ionization. The prevailing theory of ESI was that whatever ions were on the surface of the charged droplets become observable ions, either suppressing or enhancing ion formation of other compounds that were present in the solution.

Glycerophosphocholines and lysoglycerophosphocholines specifically have been the focus of matrix effect studies. Both class of lipids fragment under ESI conditions to form a very intense peak at *m/z* 184 ion (Figure 3.17). This ion resists further fragmentation and survives MS/MS analysis even at high collision energies.[45,46,51] The PAs in this project were not affected by this *m/z*, however the presence of these classes of phospholipids could suppress the signal of interest if they co-eluted with any of the PAs or internal standards. Additionally PUT-d8 has a quantifying ion of *m/z* 184, which lead to the possibility of enhancing the internal standard's signal, thereby causing inaccurate results. This puts to question whether *m/z* 184 from PUT-d8 was the best ion for quantification.

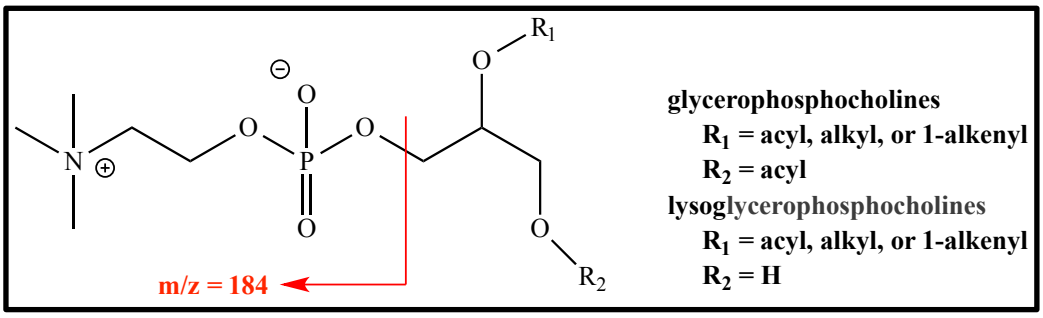

Figure 3.17. Structure of two classes of phospholipids that have a fragmentation that interferes with putrescine-d8.[45,51]

Although in the previous section most of the phospholipids have been removed via filtration, any small amount that remains may still cause significant signal enhancement or suppression, therefore further investigation was carried out.

The purpose of the next experiment determined if the *m/z* 184 ion from glycerophosphocholines and lysoglycerophosphocholines interfered with the analytical measurement method. The whole fly homogenate was first gravity filtered through Q5 filter paper and a split sample was treated three different ways (Figure 3.18). In treatment (A) the aliquot was derivatized as specified in the experimental section of this thesis; treatment (B) was an aliquot of the filtered fly sample and it was not derivatized; and treatment (C) was an aliquot of the filtered fly sample which was not derivatized but extra cleanup steps were carried out.

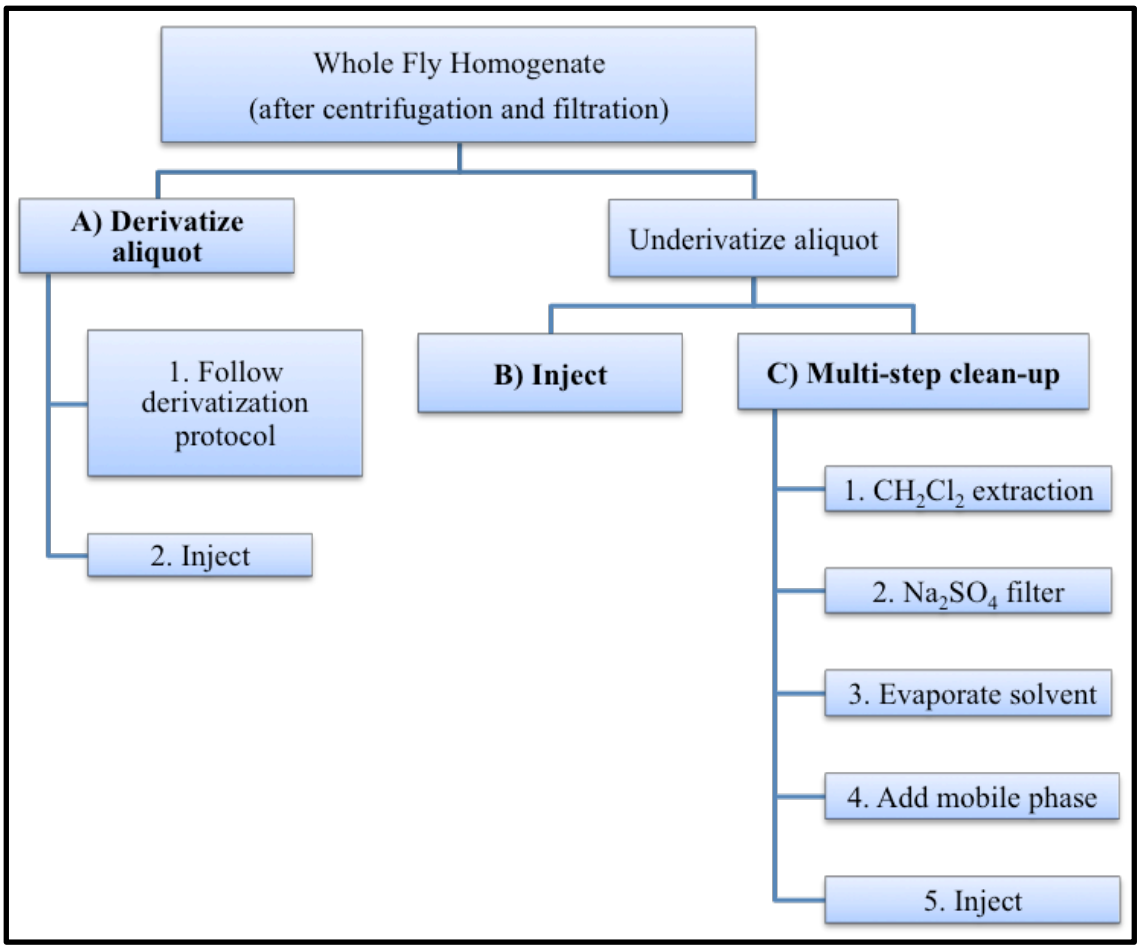

Figure 3.18. Flow chart of the three types of fly samples injected for the matrix effect experiment. The items in bold are the three types of samples.

A full scan of all 3 samples (matrices) were first analyzed to see if there were any artifacts that could affect the signal of the PAs of the internal standards. Over a scan range of 150 – 1000 da, there was no evidence of interferents (Appendix F).

All 3 matrices were further analyzed by MS/MS to determine if *m/z* 184 appeared at the same retention times of the PAs or internal standards. As shown in Figure 3.19 there were no peaks for *m/z* 184 at a retention time corresponding to any of the analytes. There was a very small peak at about 12.7 minutes (red dashed line in chromatograms),

but it did not interfere with the analysis. This observation was consistent with published works reporting that in reversed phase liquid chromatography phospholipids eluted late in an LC chromatographic program (high organic solvent content).[51]

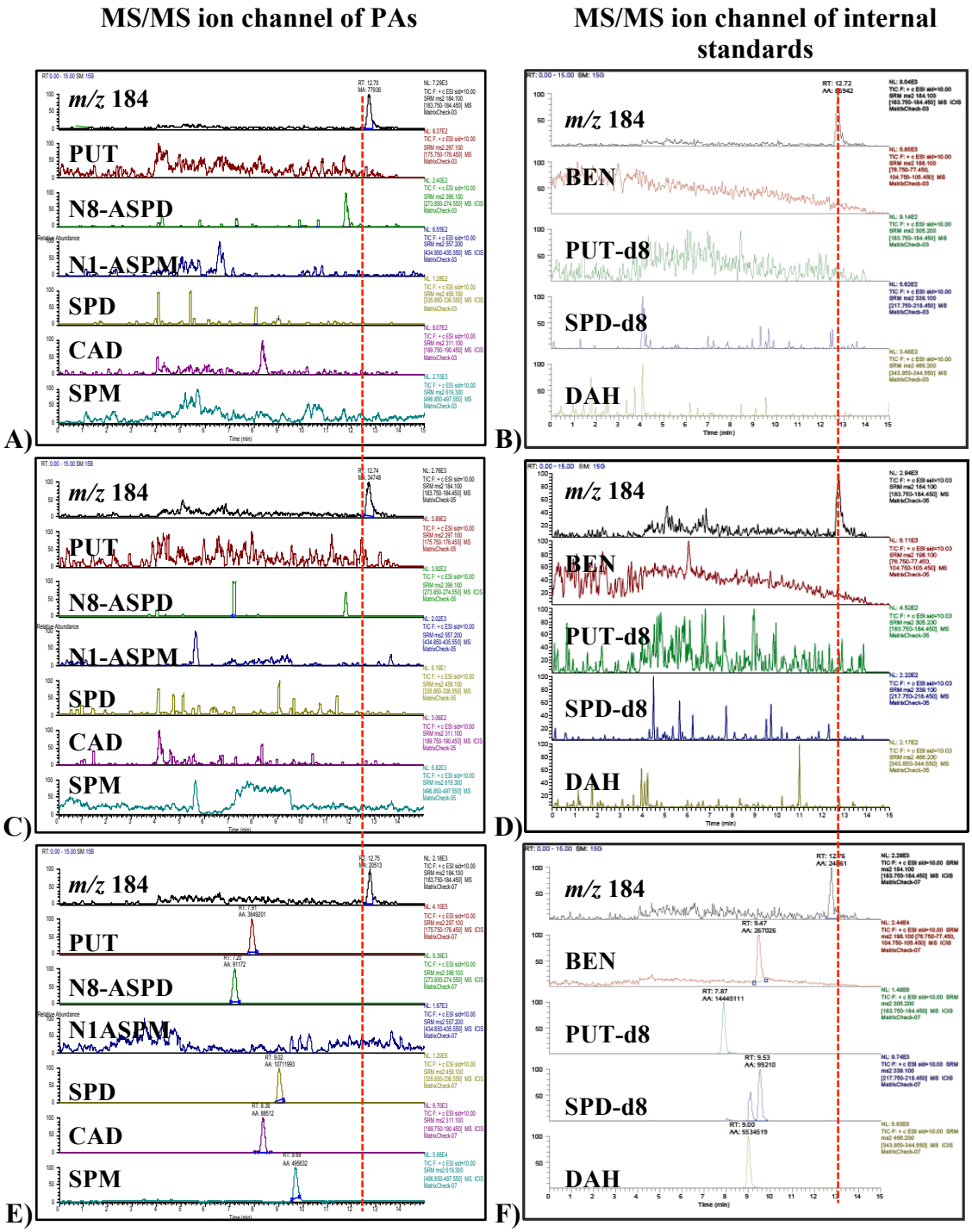

Figure 3.19. MS/MS ion channels of all PAs to show if *m/z* 184 is an interferent (A,C, & E) internal standards (B, D, & F) and the phospholipid *m/z* 184 ion channel (first ion channel of each figure). A) & B) chromatogram of the matrix with a multi-step cleanup underivatized; C) & D) chromatogram of underivatized matrix without cleanup; E) & F) chromatogram of derivatized flies.

The final and more definitive matrix effect experiment was conducted called the post-column infusion method first described by King et al.[52] The concept was to infuse a mixture of all analytes and internal standards into the MS at a constant rate using a syringe pump, which produced a constant signal response at the detector for all fragment ions shown in Table 2.2. Then a derivatized sample was injected into the HPLC and analyzed using standard operating conditions. An example of this was from a published method and is shown in Figure 3.20. A, B, and C were ion-extracted channels of the targeted analyte. Channel A was of the target analyte in the infusion solution with no injection of matrix. Channel B and C were of the same infusion solution with an injection of sample that was prepared two different ways. Signal suppressions were indicted by the "dips" in the otherwise constant signal response, shown with red arrows in Figure 3.20.

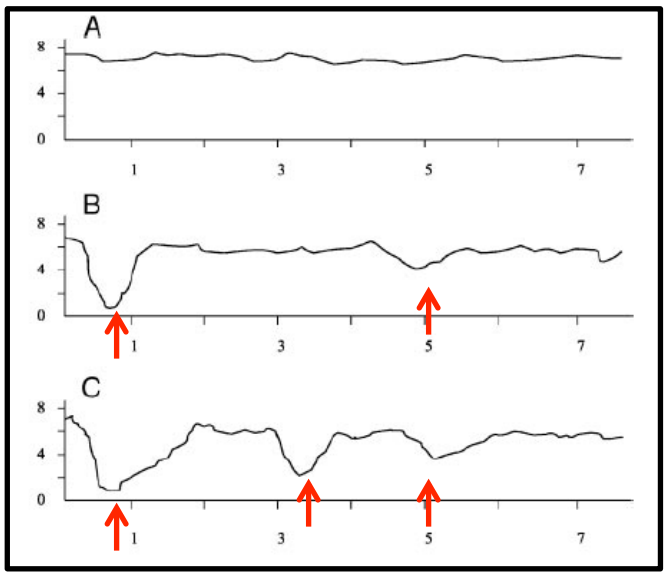

Figure 3.20. Infusion experiment result of a published method. A is of the infusion solution they investigated , B and C are of the same matrices treated two different ways. Permission to reproduce this figure was authorized. [53]

Figure 3.21 depicts how our HPLC-MS/MS instrument was configured for the post-column infusion experiment. A solution of derivatized standards and internal standards, approximately 80 ng/mL each were infused at 5 µL/min post column with a syringe pump through a T-connector. Each of the three samples, described in Figure 3.18, were injected via the autosampler (AS), separated on the HPLC column, passed through the divert valve and then mixed with the infusion solution just before entering the MS.

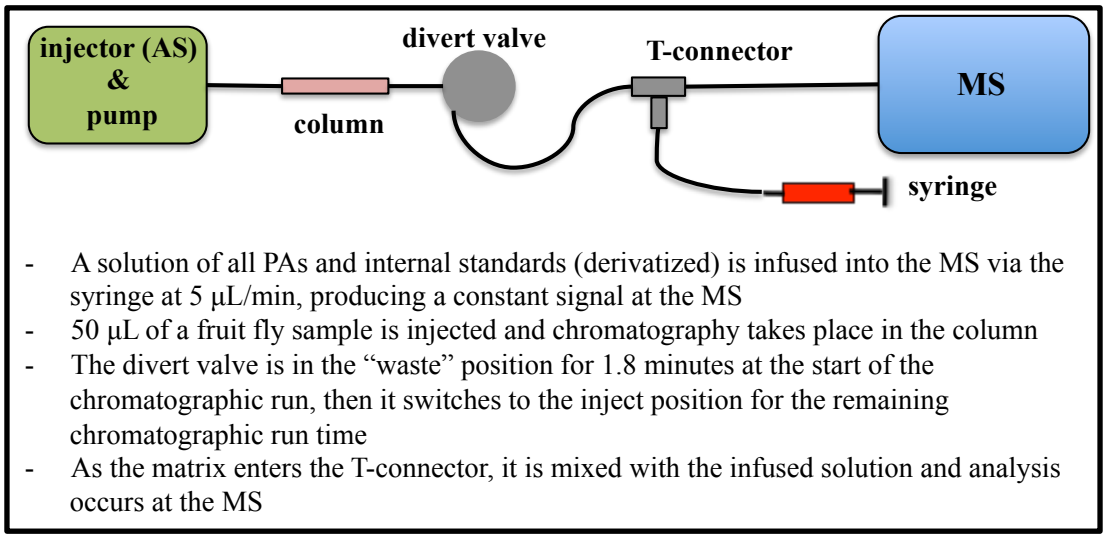

Figure 3.21. Post-column infusion set-up for the matrix effect experiment.

In determining matrix effects, all possible ways that the sample components could interfere with the measurement of the analytes should be tested. With this in mind derivatized and underivatized fly sample extracts (Figure 3.18) were tested. Figure 3.22 compared the infusion result of 1) the infusion solution with no sample injected, 2) infusion solution with matrix B (filtered- underivatized fly sample) injected, and 3) infusion solution with matrix C (filtered-cleaned-underivatized fly sample) injected.

All the chromatograms showed no difference implying that the sample matrix had no observable affects on the signals from the derivatized products. Also, all the chromatograms in Figure 3.22 demonstrated that the amide derivatives were not in the native samples to begin with.

Infusion solution only

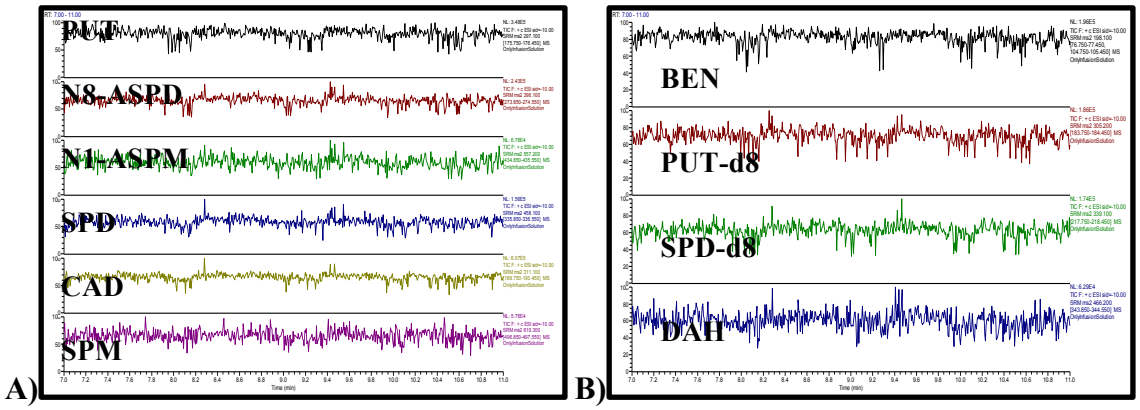

Underivatized fruit flies without cleanup – Sample B

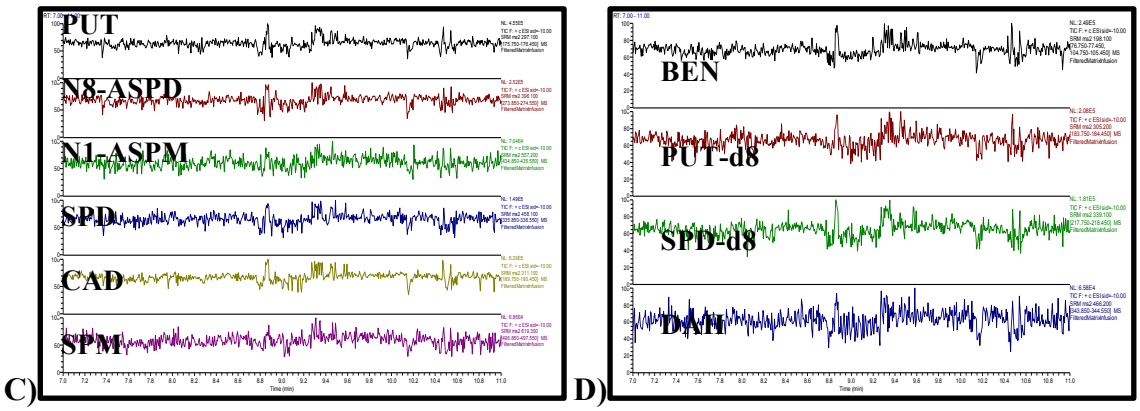

Underivatized fruit flies with cleanup – Sample C

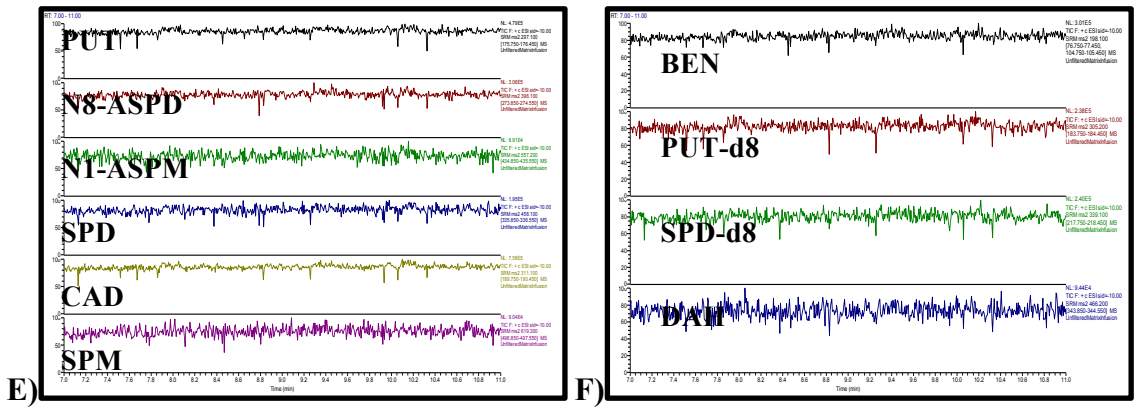

Figure 3.22. Infusion experiment of 6 PAs (A, C, & E); 4 internal standards (B, D & F). Figure A & B is only the infusion solution; figure C & D is underivatized flies without cleanup; figure E & F underivatized flies without.

The next post-column infusion experiment using the same sample configuration shown in Figure 3.21 tested derivatized fly samples. This was accomplished by injection of derivatized flies in the post-column infusion experiment. This experiment truly represented a realistic test of the matrix because analytes in fruit flies were not separated before it was derivatized, and other compounds in the matrix could also react with benzoyl chloride. Figure 3.23 shows the results from the post column experiment, it demonstrated that there was no observable presence of signal interference, and no "dip" in signal at the retention times of where the analytes eluted was observed.

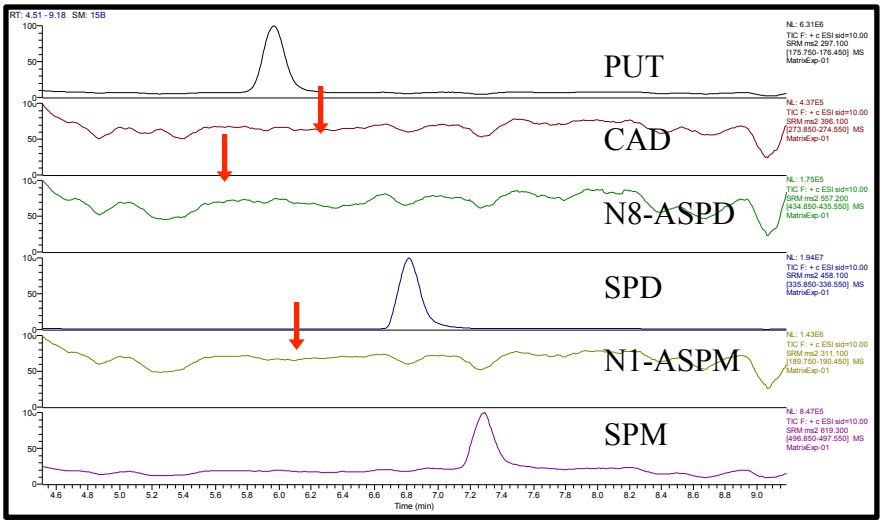

Figure 3.23. Chromatogram of matrix effect using a post-column infusion set-up. A derivatized sample was injected. Red arrows indicate where the analyte of the respective ion channel should be.

In conclusion all the matrix experiments carried out in this thesis showed that there was no observable evidence of interferences and signal suppression from other compounds that were present in the extracts from derivatized fruit fly samples.

3.6. Method Validation

Additional tests were run for method validation were carried out to: 1) determine linearity, accuracy and precision of the procedure and instrument; 2) the limit of detection (LOD); 3) the limit of quantification (LOQ); 4) and ruggedness (stability). In our data, isotope dilution have been shown to be more accurate than using an internal standard method, therefore this method was only validated for PUT and SPD compounds for which isotopic standards were available. In the event that isotopic standards become available, the methods described here could be extended to those compounds as well. However, raw data was still reported for optimization experiments found in Appendix B of this thesis for all PAs and internal standards studied. Without further work the data for N1-ASPM, N8-ASPD, CAD, and SPM had to be considered qualitative.

3.6.1. Linearity

Calibration solutions were serially diluted then individually derivatized. The final concentrations of PUT, SPD, and their respective isotopic internal standards are shown in Table 3.10. Results from these test, shown in Table 3.11, demonstrated excellent linearity for both PUT and SPD within the range of the calibration solutions. The correlation coefficient (R^2) for PUT and SPD were 1.00. These results demonstrated the linearity of the HPLC-MS instrument and the derivatization procedures over a very wide concentration range. All the concentrations, R^2 values, and calibration curves of all PAs and internal standards are also found in Appendix G.

Table 3.10. Concentration of calibration solutions.*

	Concentration (ng/mL)							
Analyte	**L 1**	**L 2**	**L 3**	**L 4**	**L 5**	**L 6**	**L 7**	**L 8**
PUT	505	241	79.2	31.7	6.19	3.39	0.402	0
SPD	528	252	82.8	33.1	6.48	3.55	0.420	0

*The concentrations of internal standards used were 45.5 ng/mL and 48.7 ng/mL for SPD-d8 and PUT-d8, respectively.

Table 3.11. R^2 of each PA using PUT-d8 and SPD-d8 as an internal standard.

	PUT	**N8ASPD**	**N1ASPM**	**SPD**	**CAD**	**SPM**
PUT-D8	1.00	0.987	0.978	0.989	0.998	0.959
SPD-D8	0.949	1.00	0.998	1.00	0.921	0.984

3.6.2. Accuracy and Precision

Accuracy, a measurement of how close the experimental value was to the true value, and precision, a measurement of closeness within multiple measurements, was determined for the derivatization method and instrument response.

3.6.2.1 Derivatization method accuracy and precision

High, medium, and low levels of PUT and SPD standards were prepared and derivatized in triplicate and then analyzed in triplicate on the same day (n=3). In the results of this experiment, shown in Table 3.12, accuracy was expressed as percent error and precision was expressed in terms of relative standard deviation (RSD). PUT exhibited very good precision, less than 10% RSD, and good accuracy with less than 15% error. SPD had slightly lower precision and accuracy compared to PUT especially for the low level, but the percent RSD and percent error was below 15%, which was within the acceptable range for precision and accuracy.[54,55]

Table 3.12. Accuracy and precision of derivatization method. Each level was derivatized in triplicate (n=3).

	Level	expected (ng/mL)	observed (ng/mL)	accuracy % error	precision % RSD
PUT	High	77.9	68.2 ± 2	12	3.1
	Medium	11.9	10.2 ± 0.2	14	2.2
	Low	1.47	1.42 ± 0.1	3.2	8.5
SPD	High	81.4	76.1 ± 2	6.5	2.7
	Medium	12.5	11.3 ± 0.4	9.1	3.6
	Low	1.54	1.32 ± 0.1	14	13

3.6.2.2 Instrument accuracy and precision

In a separate experiment high, medium, and low levels of PUT and SPD were prepared and analyzed in 5 replicates (n=5) for intra-day experiments. The same three levels were analyzed in triplicate on three different days spanning a period of over a week (n=9) for inter-day experiments. Accuracy was expressed as percent error and precision was expressed in terms of RSD. Values for instrument accuracy and precision were calculated from raw data found in Appendix H, and the data for PUT and SPD are summarized in Table 3.13. The accuracy and precision was good for both PUT and SPD except for SPD at the lowest level for both inter and intra day experiments. This indicated that analysis of SPD at levels of ≤1 ng/mL or lower should be carefully analyzed due to its lower accuracy, and larger injection volumes and more replicates could decrease the percent error, if necessary. However, since SPD was the most abundant PA in eukaryotes[56,57] it was unlikely that low levels would be found that reached lower levels of detection.

Table 3.13. Results from 3 levels of PUT and SPD for intra-day and inter-day experiments.*

	Level	expected (ng/mL)	Intra-Day (n=5) observed (ng/mL)	% error	% RSD	Inter-Day (n=9) observed (ng/mL)	% error	% RSD
PUT	High	77.9	68.2 ± 2	12	3.1	66.3 ± 2	15	3.3
	Medium	11.9	10.3 ± 0.2	14	2.4	10.1 ± 0.4	15	3.5
	Low	1.47	1.30 ± 0.1	12	7.9	1.33 ± 0.1	9.3	8.1
SPD	High	81.4	76.9 ± 2	5.5	2.3	75.6 ± 3	7.1	3.7
	Medium	12.5	11.7 ± 0.4	6.3	3.0	11.8 ± 0.5	5.6	3.8
	Low	1.54	1.12 ± 0.2	27	19	1.19 ± 0.2	22	14

*This table is a summery of the data from Appendix H

3.6.3. Limit of Detection (LOD) and Limit of Quantitation (LOQ)

Limit of detection (LOD) was defined as the lowest concentration of the analyte likely to be dependably distinguished from a blank.[58] The LOD was also commonly determined by reporting concentrations with a signal to noise of at least 3. The limit of quantification (LOQ) was defined as the concentration at which analytes could be reliably quantified[59]. It was an acceptable procedure to determine LOD and LOQ based from standards and not actual samples. The LOD was calculated from a 10-µL on-column injection, and the LOQ was from a 50-µL on-column injection (Table 3.14). The difference in injection volume was due to a change to a more efficient HPLC pump in the instrumentation set-up midway through this project. Signal to noise (S/N) was also listed on Table 3.14 to show that the signal of the peak was greatly distinguishable from the noise

Table 3.14. LOD and LOQ for the method developed.

	LOD*		LOQ†	
Analyte	**S/N‡**	**pg**	**S/N‡**	**pg**
Putrescine	107	2.80	22,724	20.1
Spermidine	119	2.93	15,871	21.1

*LOD was determined from an injection volume of 10 µL
†LOQ was determined from an injection volume of 50 µL
‡S/N – signal to noise ratio values were generated by XCalibur software

The LOD and LOQ reported in this study exceeded values that have been published. Table 3.15 shows a compilation of the best detection limits found in the literature from the four most common analytical methods for PUT and SPD. The best reported results for benzoyl chloride derivatives from other authors were also included. The reported LOD for each method was based on the acceptable signal to noise ratio of at least 3. The LOQ for this study was one or more order of magnitude lower than the LOD of the compared methods.

Table 3.15. LOD of 4 published methods.

	LOD of Various Published Works (ng)				
	Ion Pair*	**Dansyl Derivatives†**	**O-phthaldialdehyde Derivatives‡**	**Benzoyl Derivatives§**	**This work (ng)**
PUT	0.168	1.763	0.009	0.02	0.00280
SPD	0.198	29.05	1.162	0.1	0.00293

*PUT and SPD were not derivatized in this work, LOD was determined from plant extracts, and method of detection was by ESI-MS/MS[3]
†LOD was determined from standards, and method of detection was by TurboIonSpray-MS/MS[1]
‡LOD was determined from water samples, and method of detection was by fluorescence[2]
§LOD was determined from standards, and method of detection was by Quadrupole-Time of Flight (Q-TOF) – MS[6]

3.6.4. Stability and Storage (Ruggedness)

Stability and storage were important components of a validated analytical method. PUT and SPD were separately derivatized to have a final concentration of about 11 ng/mL. The products were prepared stored in either, 50:50 H_2O:ACN or 100% acetonitrile, then each set was split into three groups and stored under 3 conditions: 1) room temperature in the dark, 2) room temperature exposed to room light, 3) and in the dark at -10^{o}C. These standards were analyzed in triplicate on 4 different days that spanned over a period of 22 days.

The raw data from the analysis of these samples are found in Appendix I, and Table 3.16 and Table 3.17 show a summary of the accuracy, represented by percent error, for PUT and SPD under different storage conditions and days. The data showed that products were still detectable over a period of about 3 weeks, but degradation occurred and it was faster when the products were stored in 50:50 H_2O:ACN. The accuracy also fluctuated when products were stored in the 50:50 H_2O:ACN solution. With the exception of spermidine stored in the dark at room temperature, the results demonstrated that products should be stored in 100% acetonitrile for at most three weeks and have an acceptable percent error of under 20%. However, the length of time the products were stored not the storage conditions appeared to be the major factor of degradation.

Table 3.16. Calculated concentrations of PUT on different days, with different treatments. One set was stored in 50:50 ACN:H_2O and the other set stored in 100% acetonitrile. The expected concentration was 11.9 ng/mL.

Day	Condition	50:50 (ACN:H_2O) Calculated ng/mL	50:50 (ACN:H_2O) % Error	Acetonitrile Calculated ng/mL	Acetonitrile % Error
1*	Light Room Temp	11.7 ± 0.4	2.1	11.2 ± 0.4	10
	Dark Room Temp	11.3 ± 0.4	4.7	10.5 ± 0.3	16
	Dark Freezer	11.2 ± 0.1	5.7	9.88 ± 0.3	21
8	Light Room Temp	10.5 ± 0.3	12	11.1 ± 0.4	11
	Dark Room Temp	11.0 ± 0.1	7.9	11.3 ± 0.6	9.3
	Dark Freezer	10.7 ± 0.2	9.9	12.0 ± 0.4	3.6
15	Light Room Temp	10.4 ± 0.1	13	11.7 ± 0.2	6.1
	Dark Room Temp	10.4 ± 0.1	13	11.3 ± 0.5	9.7
	Dark Freezer	10.3 ± 0.1	13	11.2 ± 0.4	10
22	Light Room Temp	9.07 ± 0.3	24	12.3 ± 0.4	0.9
	Dark Room Temp	8.80 ± 0.02	26	12.2 ± 0.1	1.8
	Dark Freezer	8.73 ± 0.2	27	11.9 ± 0.2	4.1

*Day 1 – is the same day in which the sample preparation was complete

Table 3.17. Calculated concentrations of SPD on different days, with different treatments. One set was stored in 50:50 ACN:H_2O and the other set stored in 100% acetonitrile. The expected concentration was 12.4 ng/mL.

Day	Condition	50:50 (ACN:H_2O) Calculated ng/mL	50:50 (ACN:H_2O) % Error	Acetonitrile Calculated ng/mL	Acetonitrile % Error
1*	Light Room Temp	13.2 ± 0.8	6.0	10.2 ± 0.4	14
	Dark Room Temp	11.8 ± 0.2	5.0	11.1 ± 0.1	6.9
	Dark Freezer	11.3 ± 0.2	9.6	11.1 ± 0.2	7.1
8	Light Room Temp	10.4 ± 0.7	16	10.7 ± 0.2	10
	Dark Room Temp	9.66 ± 0.2	22	11.1 ± 0.2	6.7
	Dark Freezer	9.61 ± 0.1	23	11.1 ± 0.2	6.5
15	Light Room Temp	12.4 ± 0.2	0.1	10.8 ± 0.4	9.6
	Dark Room Temp	12.0 ± 0.3	3.8	10.7 ± 0.4	10
	Dark Freezer	12.5 ± 0.5	0.6	10.4 ± 0.2	13
22	Light Room Temp	10.2 ± 0.2	18	10.2 ± 0.4	14
	Dark Room Temp	7.95 ± 0.08	36	9.59 ± 0.2	20
	Dark Freezer	8.86 ± 1	29	9.17 ± 0.2	23

*Day 1 – is the same day in which the sample preparation was complete

One reason to explain why degradation of the products occurred when stored in 50:50 ACN:H_2O was due to the presence of water. As stated in Zahn's paper, in the presence of water there were low concentrations of hydronium ion (H_3O^+) and hydroxide ion (OH^-) that could cause hydrolysis of the amide bond.[60] The proposed mechanism of amide hydrolysis in water was proposed by Zahn and is shown in Figure 3.24. Since the amide hydrolysis produced benzoic acid as a byproduct, we could not confirm this hypothesis for reasons described in Section 3.2.3.

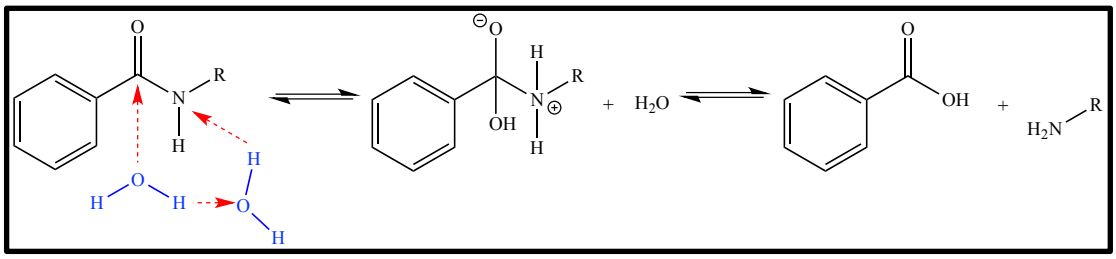

Figure 3.24. Proposed mechanism of amide hydrolysis in water.[60]

3.7. Fly Samples

The studies on matrix effect was investigated in great lengths to show that the signal for all analytes were not suppressed or enhanced in fruit fly sample derivatives. This was especially important for PUT and SPD since these two analytes were quantified with isotopic internal standards.

The validated analytical method described in this thesis was applied to the analysis of PUT and SPD in fruit flies Kim Finley of the SDSU Bioscience Center. In order to determine if the method was accurate, two concentrations of internal standards were used to demonstrate that the concentrations of PUT and SPD were independent of the amount of internal standard added. First the amount of PUT and SPD present had to be estimated in order to add the appropriate amount of internal standard, PUT-d8 and SPD-d8. From the matrix effect experiments it was established that about 20 fruit flies would result in a signal that was within linearity of the instrument and method. A solution that contained 400 flies in a total volume of 2 mL of perchloric acid was prepared; therefor 100 µL contained approximately 20 flies. For the comparison of 2 different concentrations of internal standard added, 50 µL aliquots of fruit fly homogenate was used, and the amount of internal standard added was no more than 10 times more than the

expected concentration of PUT and SPD. The final concentrations of internal standards used at two different levels is found in Table 3.18. Each sample was prepared in triplicate and analyzed in triplicate.

Table 3.18 shows the results from analyses of these two types of samples using the high and low isotopic internal standards. From this data, the concentration of PUT and SPD was about 13 and 113 ng/mL, respectively. The variance was calculated by determining the percent difference of the two values. This experiment also demonstrated that the amount of isotopic compound added was not important as it yielded results with little variance, which were 5.6% and 5.2% for PUT and SPD, respectively.

Table 3.18. Results from two levels of isotopic internal standards.

Sample	PUT-d8*	PUT†	%RSD	% difference‡
	ng/mL			
Low ISTD	45.8	12.8 ± 0.2	1.2	5.6
High ISTD	91.6	13.5 ± 0.7	4.9	
Sample	**SPD-d8***	**SPD†**	**%RSD**	**% difference‡**
	ng/mL			
Low ISTD	304	110 ± 1	1.2	5.2
High ISTD	608	116 ± 1	0.79	

*Final low and high concentrations of PUT-d8 and SPD-d8.
†Calculated concentrations for each sample with the addition of the low or high concentration of internal standard added.
‡Calculated from the average calculated concentration of PUT and SPD from the low and high internal standard addition.

To further confirm that isotopic internal standards yielded accurate results a final experiment was executed with two different quantities of fruit flies. Flies from the same batch were divided into 100 µL and 20 µL aliquots, then derivatized in triplicate and analyzed in triplicate with 100 µL and 20 µL aliquots. The results summarized in Table 3.19 and Table 3.20 were calculated from the all the data that was collected and presented

in Appendix J. A ratio of 5 was expected because of the aliquot 100 µL vs. 20 µL. The result of PUT was acceptable with an observed ratio of approximately 4.5, whereas SPD was more accurate with an observed ratio of 5. The levels of accuracy were not surprising since the concentration of SPD was ten times higher then PUT. The precision was very good for both PUT and SPD, both PA were within ±5% RSD. This showed that the method was suitable for whole fruit fly homogenate. If there were any matrix effects, they did not interfere with the accuracy of the measurements.

Table 3.19. Concentration of PUT in fruit fly homogenate in a 100 µL aliquot and 20 µL aliquot of the same sample (n=3).

	PUT				
	100 µL aliquot		20 µL aliquot		Observed Ratio
	ng/mL	% RSD	ng/mL	% RSD	
Replicate 1	25.1 ± 1	4.9	5.69 ± 0.2	2.8	4.4
Replicate 2	26.2 ± 0.5	1.8	5.72 ± 0.2	2.7	4.6
Replicate 3	25.2 ± 0.6	2.4	5.82 ± 0.1	1.9	4.3

Table 3.20. Concentration of SPD in fruit fly homogenate in a 100 µL aliquot and 20 µL aliquot of the same sample (n=3).

	SPD				
	100 µL aliquot		20 µL aliquot		Observed Ratio
	ng/mL	% RSD	ng/mL	% RSD	
Replicate 1	211 ± 4	2.1	42.6 ± 0.3	0.73	5.0
Replicate 2	215 ± 1	0.82	44.3 ± 0.7	1.5	4.9
Replicate 3	217 ± 0.1	0.05	44.6 ± 0.3	0.65	4.9

3.8. Rat Liver Cell Lysate

Along with fruit flies, rat liver was another type of sample matrix that Dr. Kim Prisk at the SDSU Bioscience Center group wanted to know the concentrations of PAs.

Although this method was not developed and validated for rat liver matrix, the method was applied without modification to rat liver cell lysates. No additional steps to validate the analytical method were planned.

The SDSU Bioscience center provided rat liver cell lysate from two different age groups. Two samples were from 5½-month old rats, and the other two samples were from 22-month old rats, for a total of 4 different sample. The samples were analyzed for all 6 analytes but only PUT and SPD was quantified.

The same experiment comparing the quantification values of two aliquots, described in Section 3.7, were carried out for rat liver cell lysate. Before PUT and SPD were quantified, an estimation of PUT and SPD concentration was determined by taking a 50 µL aliquot of the old and young sets of rat liver cell lysates, adding internal standard, followed by the standard derivatization procedure. Since the appropriate amount of internal standard was not known, a concentration of about 100 ng/mL was added as a reference. The area counts for PUT, SPD, PUT-d8, and SPD-d8 and amount of internal standard added is found in Appendix K. By comparing the area counts it was concluded that 50 µL was the right volume to use because the approximate concentration would be within linearity of the method and instrument detection.

Two volumes of sample were used to help identify if there were any unforeseen contaminants present that affected the measurement of PUT and SPD. Three sets each of 10 and 50 µL aliquots were subjected to the standard derivatization procedure and then analyzed in triplicate. In the data obtained, shown in Table 3.21 and Table 3.22, the 50-µL aliquots should have results that were 5 times higher than the 10-µL aliquots, but that was not observed. The observed ratio was much lower than 5 for PUT but closer to 5 for

SPD. This was the same trend we observed in the fly data in Section 3.7 but much larger. What could be misleading from the data was the precision of the replicates. From this data it was not determined if the lack of accuracy in PUT was due to sample losses or a matrix effect. This data also demonstrated that there was little variability in the formation and yield of the derivatized products from sample to sample (low RSD's) but further investigation would be required to determine accuracy from this different type of cell type. Since matrix effect studies were not carried out for rat liver cell lysate, there may be some interferences that caused the variability in this set of data. One observation was that the sample, before derivatization was carried out, was not homogenous; this in itself would cause variability in results of the same sample. This was an example of where applying a validated method to another matrix was not straightforward.

If values were to be reported the results from the 50 and 10 μL aliquots for putrescine would be acceptable and the 10 μL aliquot for spermidine would be used because the values were within the working range of the calibration solutions. The values are labeled with an asterisk on Table 3.21 and Table 3.22. The range of linearity for putrescine as mentioned in the linearity section was between 0.402-505 ng/mL, and 0.426-528 ng/mL for spermidine. Since it was shown that there were some discrepancies in the result of the two aliquots further experiments must be carried out if rat liver cell lysate data were to be confidently reported.

Table 3.21. Concentration of PUT in rat liver cell lysate in a 50 µL aliquot and 10 µL aliquot of the same sample (n=3).

	PUT				
	50 µL aliquot*		10 µL aliquot		Observed
	ng/mL	% RSD	ng/mL	% RSD	Ratio
young set 1†	11.2 ± 0.2	1.7	3.06 ± 0.1	3.6	3.7
young set 2†	8.43 ± 1	13	3.02 ± 0.3	9.1	2.8
old set 1†	4.74 ± 0.01	0.29	1.77 ± 0.2	11	2.7
old set 2†	14.6 ± 0.9	5.9	3.96 ± 0.4	9.3	3.7

*indicates the volume of sample that should analyzed if values were to be reported
†young rat liver cell lysate were from two different rats, set 1 and set 2
‡old rat liver cell lysate were from two different rats, set 1 and set 2

Table 3.22. Concentration of SPD in rat liver cell lysate in a 50 µL aliquot and 10 µL aliquot of the same sample (n=3).

	SPD				
	50 µL aliquot		10 µL aliquot*		Observed
	ng/mL	% RSD	ng/mL	% RSD	Ratio
young set 1†	2740 ± 100	3.5	598 ± 30	4.6	4.6
young set 2†	2.00×10^3 ± 200	11	480. ± 30	6.4	4.2
old set 1‡	866 ± 20	2.5	192 ± 9	4.5	4.5
old set 2‡	2350 ± 200	7.2	503 ± 20	4.2	4.7

*indicates the volume of sample that should analyzed if values were to be reported
†young rat liver cell lysate were from two different rats, set 1 and set 2
‡old rat liver cell lysate were from two different rats, set 1 and set 2

Since it was known that phospholipids were the major cause of affecting quantification of biological samples, this could be the reason for imprecise measurements within different volumes of rat liver cell lysate. Matrix effect studies were not studied for rat liver cell lysate therefore it was not confirmed if artifacts in the matrix caused the imprecision.

References

1 Ducros, V.; Ruffieux, D.; Belva-Besnet, H.; de, F. F.; Berger, F.; Favier, A. *Analytical Biochemistry* 2009, *390*, 46.

2 Padovan, G. J.; Leme, I. A.; Fassini, P. G.; Iucif, N.; Marchini, J. S. *Journal of Chromatography & Separation Techniques* 2014, *5*, 1000223/1.

3 Sanchez-Lopez, J.; Camanes, G.; Flors, V.; Vicent, C.; Pastor, V.; Vicedo, B.; Cerezo, M.; Garcia-Agustin, P. *Plant Physiology and Biochemistry* 2009, *47*, 592.

4 Oezdestan, O.; Ueren, A. *Talanta* 2009, *78*, 1321.

5 Jia, S.; Ryu, Y.; Kwon, S. W.; Lee, J. *Journal of Chromatography A* 2013, *1282*, 1.

6 Liu, R.; Bi, K.; Jia, Y.; Wang, Q.; Yin, R.; Li, Q. *Journal Mass Spectrometry* 2012, *47*, 1341.

7 Liu, R.; Jia, Y.; Cheng, W.; Ling, J.; Liu, L.; Bi, K.; Li, Q. *Talanta* 2011, *83*, 751.

8 Mayr, C. M.; Schieberle, P. *Journal of Agricultural and Food Chemistry* 2012, *60*, 3026.

9 Bomke, S.; Seiwert, B.; Dudek, L.; Effkemann, S.; Karst, U. *Analytical and Bioanalytical Chemistry* 2009, *393*, 247.

10 Salazar, C.; Armenta, J. M.; Cortes, D. F.; Shulaev, V. *Methods in Molecular Biology* 2012, *828*, 13.

11 Stevens, A. P.; Dettmer, K.; Kirovski, G.; Samejima, K.; Hellerbrand, C.; Bosserhoff, A. K.; Oefner, P. J. *Journal of Chromatography A* 2010, *1217*, 3282.

12 Zoerner, A. A.; Heusser, K.; Gutzki, F. M.; Mitschke, A.; Tank, J.; Stichtenoth, D. O.; Jordan, J.; Tsikas, D. *Journal of Chromatography B* 2011, *879*, 1444.

13 Liu, S.; Ruan, H. *Chemistry and Physics of Lipids* 2013, *166*, 18.

14 Davison, A.; Milan, A.; Dutton, J. *Annals of Clinical Biochemistry* 2013, *50*, 274.

15 Roberts, D. R.; Walker, M. A.; Dumbroff, E. B. *Phytochemistry* 1985, *24*, 1089.

16 Verkoelen, C. F.; Romijn, J. C.; Schroeder, F. H.; Van, S. W. P.; Splinter, T. A. W. *Journal of Chromatography* 1988, *426*, 41.

17 Taibi, G.; Schiavo, M. R. *Journal of Chromatography* 1993, *614*, 153.

18 Mei, Y. H. *Journal of Liquid Chromatography* 1994, *17*, 2413.

19 Schenkel, E.; Berlaimont, V.; Dubois, J.; Helson-Cambier, M.; Hanocq, M. *Journal of Chromatography B: Biomedical Applications* 1995, *668*, 189.

20 Morgan, D. M. L. *Methods in Molecular Biology* 1998, *79*, 111.

21 Sethi, R.; Chava, S. R.; Bashir, S.; Castro, M. E. *American Journal of Analytical Chemistry* 2011, *2*, 456.

22 Aflaki, F.; Ghoulipour, V.; Saemian, N.; Salahinejad, M. *Analytical Methods* 2014, *6*, 1482.

23 Alsouz, M. A. *Chemistry and Materials Research* 2015, *7*, 47.

24 Yegin, S.; Uren, A. *Food Chemistry* 2008, *111*, 983.

25 Gao, S.; Wilson, D. M.; Edinboro, L. E.; McGuire, G. M.; Williams, S. G. P.; Thomas, K. H. *Journal of Liquid Chromatography & Related Technologies* 2003, *26*, 3413.

26 Taibi, G.; Schiavo, M. R.; Gueli, M. C.; Calanni, R. P.; Muratore, R.; Nicotra, C. M. A. *Journal of Chromatography B* 2000, *745*, 431.

27 Wongyai, S.; Oefner, P.; Bonn, G. *Biomedical Chromatography* 1988, *2*, 254.

28 Hockl, P. F.; Thyssen, S. M.; Libertun, C. *Journal of Liquid Chromatography & Related Technologies* 2000, *23*, 693.

29 Watanabe, S.; Saito, T.; Sato, S.; Nagase, S.; Ueda, S.; Tomita, M. *Journal of Chromatography* 1990, *518*, 264.

30 Wang, Z. In *Comprehensive Organic Name Reactions and Reagents*; John Wiley & Sons, Inc.: 2010.

31 Piwowar, A. M.; Lockyer, N. P.; Vickerman, J. C. *Analytical Chemistry* 2009, *81*, 1040.

32 Constantopoulos, T. L.; Jackson, G. S.; Enke, C. G. *Journal of the American Society for Mass Spectrometry* 1999, *10*, 625.

33 Harris, D. C. *Quantitative Chemical Analysis*; W. H. Freeman, 2010.

34 Reichenbächer, M.; Einax, J. W. *Challenges in Analytical Quality Assurance*; Springer, 2011.

35 Fluka Analytical. *LC-MS Mobile Phase Additives - Tips & Tricks*, 2012.

36 Means, J. C.; Olsen, P. D.; Schoffers, E. *Journal of the American Society for Mass Spectrometry* 2003, *14*, 1057.

37 Maunsell, Z.; Wright, D. J.; Rainbow, S. J. *Clinical Chemistry* 2005, *51*, 1683.

38 Whalley, E. *Transactions of the Faraday Society* 1958, *54*, 1613.

39 Scheiner, S.; Čuma, M. *Journal of the American Chemical Society* 1996, *118*, 1511.

40 Taylor, P. J. *Clinical Biochemistry* 2005, *38*, 328.

41 Wang, S.; Cyronak, M.; Yang, E. *Journal of Pharmaceutical and Biomedical Analysis* 2007, *43*, 701.

42 Chambers, E.; Wagrowski-Diehl, D. M.; Lu, Z.; Mazzeo, J. R. *Journal of Chromatography B* 2007, *852*, 22.

43 Matuszewski, B. K.; Constanzer, M. L.; Chavez-Eng, C. M. *Analytical Chemistry* 1998, *70*, 882.

44 Voet, D.; Voet, J. G.; Pratt, C. W. *Fundamentals of Biochemistry: Life at the Molecular Level*; Wiley, 2006.

45 Ismaiel, O. A.; Halquist, M. S.; Elmamly, M. Y.; Shalaby, A.; Thomas Karnes, H. *Journal of Chromatography B* 2008, *875*, 333.

46 Pulfer, M.; Murphy, R. C. *Mass Spectrometry Review* 2003, *22*, 332.

47 Guo, X.; Lankmayr, E. *Bioanalysis* 2011, *3*, 349.

48 Ahmad, S.; Kalra, H.; Gupta, A.; Raut, B.; Hussain, A.; Rahman, M. A. *Journal of Pharmacy & Bioallied Sciences* 2012, *4*, 267.

49 Akoh, C. C.; Min, D. B. *Food Lipids: Chemistry, Nutrition, and Biotechnology, Third Edition*; Taylor & Francis, 2008.

50 Cevc, G. *Phospholipids Handbook*; Taylor & Francis, 1993.

51 Little, J. L.; Wempe, M. F.; Buchanan, C. M. *Journal of Chromatography B* 2006, *833*, 219.

52 Bonfiglio, R.; King, R. C.; Olah, T. V.; Merkle, K. *Rapid Communications in Mass Spectrometry* 1999, *13*, 1175.

53 Annesley, T. M. *Clinical Chemistry* 2003, *49*, 1041.

54 United Nations Office on Drugs and Crime. *Guidance for the Validation of Analytical Methodology and Calibration of Equipment used for Testing of Illicit Drugs in Seized Materials and Biological Specimens*, 2009.

55 Smith, G. *Bioanalysis* 2012, *4*, 865.

56 Minois, N.; Rockenfeller, P.; Smith, T. K.; Carmona-Gutierrez, D. *PLoS ONE* 2014, *9*, e102435.

57 Minois, N.; Carmona-Gutierrez, D.; Bauer, M. A.; Rockenfeller, P.; Eisenberg, T.; Brandhorst, S.; Sigrist, S. J.; Kroemer, G.; Madeo, F. *Cell Death and Disease* 2012, *3*, e401.

58 Armbruster, D. A.; Pry, T. *The Clinical Biochemist Reviews* 2008, *29*, S49.

59 Armbruster, D. A.; Tillman, M. D.; Hubbs, L. M. *Clinical Chemistry* 1994, *40*, 1233.

60 Zahn, D. *European Journal of Organic Chemistry* 2004, *2004*, 4020.

CHAPTER 4. CONCLUSION

The PAs putrescine (PUT), cadaverine (CAD), spermidine (SPD), spermine (SPM), n8-acetylspermidine (N8-ASPD), and n1-acetylspermine (N1-ASPM) are a group of very important biological compounds whose roles in cell regulation are not fully understood. PAs are abundant in all species and vary over a wide range of concentrations depending on the state of the cells and their environment; therefore it was important to detect all analytes of interest at the lowest concentration possible. The panel of PAs investigated, the sample clean up, matrix effect studies, and limits of quantification and detection in standards achieved have not been reported specifically to whole fruit flies.

Development and validation of an analytical method to detect PAs by derivatization with benzoyl chloride was completed. The derivatization conditions were optimized for all PAs, and method validation was completed for putrescine (PUT) and spermidine (SPD). The method exhibited: high accuracy (<15% error) and precision (< 10% RSD); stability of products for 22 days; linearity within concentration ranges of 0.402-505 ng/mL for PUT and 0.420-528 ng/mL for SPD; levels of detection (LOD) of 2.80 and 2.39 picograms (pg) for PUT and SPD respectively; and levels of quantitation (LOQ) of 20.1 and 21.1 pg for PUT and SPD respectively.

Quantification methods using a derivatization process may introduce interferents from reaction by-products. The method developed included an incubation step, which removed most of the by-products. However, other interferences could be present when applying the reaction to biological samples. Phospholipids are abundant in biological samples and can suppress or enhance detection signals; therefore matrix effect experiments were executed to check for interferences. It was concluded that signal

enhancement and suppression was not observed, once filtration and acid digestion/hydrolysis of biological samples removed most of the lipids that affect the solubility and extraction of derivatized products.

This analytical method reported improvements in the detection limits over literature values, and good linearity over a wide concentration range for all Pas. Accuracy was only achieved when isotope dilution methods were used on PUT and SPD. Part of the project focused on the comparison of 3 different types of internal standards: DAH, a derivatizable and BEN, a non-derivatizable standard; and PUT-d8 and SPD-d8, isotopically enriched forms of PUT and SPD, respectively. The use of DAH and BEN constituted an internal standard method, and PUT-d8 and SPD-d8 would be referred to as an isotope dilution method. The results from this comparison showed that isotope dilution demonstrated the best accuracy and precision, whereas the internal standard method showed poor accuracy but reasonable precision. The problems from the internal standard method may be due to different yields of DAH and the analyte of interest, or other interferences that were not determined.

This work also demonstrated the importance of internal standard selection and treatment for accurate analysis. Matrix effects and interferences were additionally studied and proved that interferences were minimized. A few published works quantified PAs using isotope dilution but it was not shown why it worked better than internal standards as it has been shown in this project. Furthermore, it was common practice to use the same collision energy in MS/MS for isotope as in the analyte itself; but this work showed that it was very important to optimize the collision energy for each internal standard independently before using it for quantification. The collision energy used for PUT and

PUT-d8 was 20 and 17 volts respectively, and for SPD and SPD-d8 the CE used was 23 and 18 volts respectively. The difference in voltage was very large and this project demonstrated that high error could be observed if the voltages were not properly investigated.

The validated method demonstrated specificity, accuracy and precision at different concentration levels, product stability for up to 3 weeks, and good LOD and LOQ. This method demonstrated that all 6 PAs could be derivatized and detected by HPLC-MS/MS, however quantitation would only be advised with the use of an isotope for each PA. Although the objective of developing and validating the method of all 6 PAs was not achieved, it was only accomplished for PUT and SPD. Better detection limits were achieved for PUT and SPD compared to recent published methods. The chromatographic run time of 6 minutes was also much shorter than most published methods. Analysis time is always an important factor, especially when high throughput is of concern. While analysis time was short, the derivatization process was much more time consuming, but could be applied to large sample batches at one time. Since derivatization conditions and analysis parameters were optimized for all PAs, this assay could be applied to quantify all 6 PAs if isotopic internal standards were available.

This developed and validated method exceeds the LOD of PUT and SPD of past and recent published methods with isotopic internal standards, which was used to accurately analyze PUT and SPD in fruit flies. We also demonstrated that this method could be applied to another matrix, or sample type with limitations. Detection and quantitation of PUT and SPD was accomplished for rat liver cell lysate, however the data collected suggested there may be matrix effects due to the inconsistent data; but, without

an extensive matrix study, it could not be confirmed if this was the problem. Having an "analyte-free matrix" to study signal suppression and enhancements would be ideal, but since one is rarely available, experiments using a specific type of matrix is recommended.

Part 1, in full, will be used to prepare a manuscript that will be submitted for publication. I was the primary researcher and will be the first author on this paper. Van, Jenny K.; Chatfield, Dale A. "Method Development for the Analysis of Polyamines by Derivatives with Benzoyl Chloride by HPLC Tandem Mass Spectrometry" *Manuscript in preparation.*

Appendix

A. Comparison of Four Internal Standards Investigated

The compiled data in this appendix shows 3 derivatized levels of PUT and SPD and the observed concentrations calculated using each internal standard. Within each level for PUT and SPD the expected concentration, observed concentration, and accuracy in terms of percent error is shown.

Table. A.1. Accuracy calculated for SPD and PUT using all 4 internal standards to show that DAH and BEN are not suitable internal standards.

			d8		DAH	
	Level	**expected (ng/mL)**	**observed (ng/mL)**	**% error**	**observed (ng/mL)**	**% error**
PUT	High	77.9	68.2 ± 2	12	55.6 ± 4	29
	Med	11.9	10.3 ± 0.2	14	11.5 ± 0.7	3.7
	Low	1.47	1.30 ± 0.1	12	1.10 ± 0.1	25
SPD	High	81.4	76.9 ± 2	5.5	13.0 ± 1	84
	Med	12.5	11.7 ± 0.4	6.3	0.84 ± 0.09	93
	Low	1.54	1.12 ± 0.2	27	0.0025 ± 0.0002	100

			BEN-77		BEN-105	
	Level	**expected (ng/mL)**	**observed (ng/mL)**	**% error**	**observed (ng/mL)**	**% error**
PUT	High	77.9	833 ± 100	970	104 ± 20	770
	Med	11.9	21.6 ± 6	1400	17.2 ± 5	1100
	Low	1.47	138 ± 30	1100	649 ± 100	734
SPD	High	81.4	267 ± 50	230	208 ± 40	160
	Med	12.5	27.5 ± 4	12	20.7 ± 3	66
	Low	1.54	1.85 ± 0.5	20	1.47 ± 0.4	4.4

B. Raw Data Collected from Optimization Experiments

The following tables are the raw data collected for the optimization of the benzoyl chloride derivation reaction experiments. The optimization parameters investigated were solvent type for preparation of benzoyl chloride reagent, ratio of benzoyl chloride, time, and temperature. Each run was analyzed in triplicate and the area counts are of all 6 PAs and 4 internal standards are shown. The chromatograms at the end of this appendix show the results of each extraction. Each fraction was analyzed to demonstrate a maximum of 5 methylene chloride extractions was sufficient to remove all products formed.

B.1. Raw Data of Different Treatments of Benzoyl Chloride

The different treatments of benzoyl chloride were: 1) 5 µL pure liquid, 2) 25 µL, 3) diluted with acetonitrile (ACN), 4) diluted with methylene chloride (CH_2Cl_2), and 5) diluted with diethyl ether (ether). The area counts of each PA and internal standard is shown in

Table. B.1. Reagent Amount Experiment – Peak area of 6 polyamines prepared with 5µL pure benzoyl chloride, 25 µL pure benzoyl chloride, benzoyl chloride prepared in acetonitrile (ACN), methylene chloride (CH_2Cl_2), and diethyl ether (Ether).

Sample	PUT	N8-ASPD	N1-ASPM	SPD	CAD	SPM
5µL-01	2,292,326	789,267	324,568	1,221,838	4,873,868	640,765
5µL-02	2,978,658	900,833	326,660	1,588,153	6,040,923	739,534
5µL-03	3,146,902	1,116,526	415,494	1,546,303	6,116,706	777,813
25µL-01	5,421,404	1,966,493	855,587	1,459,793	8,770,817	1,542,939
25µL-02	5,664,510	1,965,294	994,997	2,986,616	10,041,664	1,737,333
25µL-03	5,525,933	2,200,641	577,448	3,090,991	9,665,375	1,768,963
ACN-01	2,537	1,215	1,224	7,492	8,795	673
ACN-02	1,229	3,658	249	1,556	16,009	129
ACN-03	609	1,165	897	2,156	8,260	1,496
CH_2Cl_2-01	3,251,471	411,220	33,730	752,374	10,008,575	173,942
CH_2Cl_2-02	3,567,946	382,981	72,509	788,043	10,012,753	182,676
CH_2Cl_2-03	3,500,666	414,260	65,216	782,241	9,895,830	158,763
Ether-01	214,800	22,335	2,706	19,718	720,964	5,364
Ether-02	213,700	24,105	4,496	57,374	705,572	14,325
Ether-03	203,517	21,901	938	45,309	762,541	8,765

Table. B.2. Reagent Amount Experiment – Peak area of 4 internal standards prepared with 5µL pure benzoyl chloride, 25 µL pure benzoyl chloride, benzoyl chloride prepared in acetonitrile (ACN), methylene chloride (CH_2Cl_2), and diethyl ether (Ether).

Sample	PUT-d8	SPD-d8	1,7-DAH	BEN-77	BEN-105
5µL-01	2,322,331	879,807	6,010,949	648,950	762,255
5µL-02	2,847,650	1,162,187	7,181,675	773,811	901,313
5µL-03	2,896,253	1,081,765	6,957,764	554,975	1,152,652
25µL-01	206,482	13,265	11,409,272	1,104,628	1,479,368
25µL-02	238,189	10,054	11,115,166	1,195,923	1,616,865
25µL-03	197,818	5,139	11,698,372	1,416,673	1,925,931
ACN-01	10,131	70	5,957	1,578,940	2,127,698
ACN-02	376	192	4,819	1,803,194	2,243,221
ACN-03	1,989	58	4,995	951,163	2,334,399
CH_2Cl_2-01	5,084,208	1,090,474	16,837,105	1,965,868	2,318,634
CH_2Cl_2-02	5,222,392	1,149,738	17,167,697	1,957,473	2,732,079
CH_2Cl_2-03	5,730,264	1,150,275	16,876,504	1,861,232	2,626,432
Ether-01	358,415	58,376	2,722,239	2,261,989	3,127,720
Ether-02	377,773	68,427	2,548,986	2,349,637	3,155,782
Ether-03	426,582	22,117	2,787,335	2,636,569	3,445,962

B.2. Raw Data of Optimized Ratio of Benzoyl Chloride to Each PA

After concluding the best treatment for benzoyl chloride, the ratio of benzoyl chloride to each PA was investigated.

Table. B.3. Reagent Mole Ratio Experiment - Peak area of 6 PAs prepared in ratio moles of benzoyl chloride to total amines. Benzoyl chloride reagent was prepared in methylene chloride.

Sample	PUT	N8-ASPD	N1-ASPM	SPD	CAD	SPM
10:1-01	6,313,372	383,896	42,867	397,026	22,928,257	99,330
10:1-02	6,499,840	406,702	33,575	324,722	21,022,483	59,829
10:1-03	6,886,169	407,137	26,831	416,233	22,638,241	67,682
20:1-01	13,253,024	3,261,581	426,359	2,480,570	22,127,964	758,617
20:1-02	12,812,393	3,235,913	429,299	2,531,536	21,614,884	844,698
20:1-03	13,461,834	3,544,736	468,151	2,527,364	22,932,926	760,531
50:1-01	14,298,744	4,726,159	913,926	4,928,772	24,502,470	1,727,366
50:1-02	14,749,514	4,796,685	863,988	5,263,936	24,434,109	1,678,451
50:1-03	14,395,643	5,019,017	883,238	5,376,380	25,089,377	1,730,059
100:1-01	13,361,391	4,931,978	1,193,032	6,198,225	21,925,447	2,033,661
100:1-02	13,563,523	4,796,358	1,212,195	6,197,941	21,911,937	2,069,182
100:1-03	13,322,393	4,879,880	1,201,801	6,690,648	22,909,468	2,316,258
200:1-01	14,418,670	4,995,985	1,993,538	6,676,837	24,692,454	3,784,907
200:1-02	14,169,912	5,001,859	1,959,051	5,975,859	23,923,364	3,373,773
200:1-03	13,980,635	4,815,788	1,966,570	6,637,760	24,576,066	3,638,739

Table. B.4. Reagent Mole Ratio Experiment - Peak area of 4 internal standards prepared in ratio moles of benzoyl chloride to total amines. Benzoyl chloride reagent was prepared in methylene chloride.

Sample	PUT-d8	SPD-d8	1,7-DAH	BEN-77	BEN-105
10:1-01	6,002,480	435,162	24,218,383	2,537,955	3,155,513
10:1-02	6,435,044	324,635	20,665,309	2,236,585	3,002,114
10:1-03	6,802,666	388,922	19,578,283	2,840,664	3,982,076
20:1-01	13,905,769	2,318,706	17,256,843	2,693,624	3,464,915
20:1-02	13,667,827	2,285,096	19,601,709	2,764,046	3,582,765
20:1-03	14,511,558	2,346,067	19,605,029	2,943,270	3,885,768
50:1-01	15,271,322	4,917,806	20,597,883	4,250,764	4,918,432
50:1-02	15,415,056	5,061,124	20,722,715	3,977,665	5,081,056
50:1-03	15,583,452	5,359,957	19,266,365	4,034,502	4,890,102
100:1-01	13,715,889	6,187,420	17,381,239	4,712,460	5,922,403
100:1-02	13,997,891	6,101,689	17,212,112	3,358,685	4,243,139
100:1-03	13,945,070	6,781,660	18,870,710	4,107,551	5,398,799
200:1-01	15,921,348	6,604,669	19,803,424	3,069,028	4,638,719
200:1-02	15,367,266	6,032,424	20,495,651	3,726,091	4,525,988
200:1-03	15,477,047	6,757,473	21,484,724	4,895,499	5,884,420

B.3. Raw Data of Optimization of Reaction Time and Temperature

The following tables are the raw data of the different time and temperatures used to optimize the reaction conditions.

Table. B.5. Derivatization Time Experiment - Peak area of 6 PAs derivatized with different reaction times. One set prepared at room temperature and a second set was prepared at 30°C.

Sample	PUT	N8-ASPD	N1-ASPM	SPD	CAD	SPM
20-min-01	368,789	57,498	12,642	101,865	726,399	21,451
20-min-02	421,380	62,276	12,452	117,499	925,212	20,559
20-min-03	558,683	76,881	17,385	127,887	1,008,598	24,859
60-min-01	759,003	121,723	18,999	187,387	1,178,900	22,657
60-min-02	820,204	144,815	32,084	189,220	1,198,034	13,949
60-min-03	663,067	126,300	23,739	186,776	1,211,252	27,979
3-hr-01	1,031,694	206,185	46,211	252,445	1,494,833	46,576
3-hr-02	750,617	187,435	46,971	185,020	1,021,640	30,947
3-hr-03	774,687	192,621	41,068	190,408	1,068,566	39,432
overnight-01	700,512	166,731	38,907	144,804	963,812	25,047
overnight-02	764,244	186,484	40,993	177,268	1,090,010	48,903
overnight-03	786,457	206,037	45,206	178,642	1,106,160	45,596
30°C-20min-01	687,818	113,990	21,267	91,593	1,329,721	22,802
30°C-20min-02	754,523	109,212	28,268	104,641	1,527,716	26,604
30°C-20min-03	837,479	116,972	28,057	105,878	1,600,961	21,794
30°C-60min-01	860,127	104,617	35,022	96,620	1,723,855	18,400
30°C-60min-02	865,902	88,777	22,239	105,762	1,789,527	18,907
30°C-60min-03	858,789	98,089	27,116	91,384	1,694,811	22,652
30°C-3hr-01	585,972	80,749	8,918	52,051	1,507,486	17,572
30°C-3hr-02	650,757	80,243	10,527	62,968	1,818,955	10,888
30°C-3hr-03	534,490	67,817	9,880	45,906	1,522,290	15,004
30°C-overnight-01	719,709	121,491	16,383	99,608	1,642,046	24,291
30°C-overnight-02	682,771	98,966	15,934	88,326	1,587,404	23,796
30°C-overnight-03	723,358	113,801	17,639	105,678	1,672,065	25,180

Table. B.6. Derivatization Time Experiment - Peak area of 4 internal standards derivatized with different reaction times. One set prepared at room temperature and a second set was prepared at 30°C.

Sample	PUT-d8	SPD-d8	1,7-DAH	BEN-77	BEN-105
20-min-01	945,217	230,792	4,038,510	1,772,059	2,192,124
20-min-02	1,193,412	280,590	3,339,284	1,126,044	1,433,118
20-min-03	1,416,903	318,112	4,028,772	1,652,319	2,136,811
60-min-01	2,136,086	444,566	3,675,496	987,172	1,297,406
60-min-02	2,245,913	430,191	4,172,633	1,235,692	1,704,765
60-min-03	2,036,007	453,871	4,239,091	1,535,689	1,980,785
3-hr-01	3,047,220	631,919	4,427,353	1,628,547	2,385,951
3-hr-02	2,121,069	462,776	3,432,409	1,317,512	1,788,116
3-hr-03	2,250,969	465,485	3,475,175	1,272,784	1,913,870
overnight-01	2,089,528	394,242	2,882,703	2,312,047	3,803,749
overnight-02	2,314,318	449,491	4,030,651	1,930,403	2,835,364
overnight-03	2,371,459	471,628	3,615,052	4,203,397	5,914,283
30°C-20min-01	1,923,485	256,773	5,004,111	2,400,318	3,403,662
30°C-20min-02	2,084,995	291,022	5,232,924	2,630,066	3,787,532
30°C-20min-03	2,236,908	296,147	5,726,535	2,736,930	3,810,977
30°C-60min-01	2,341,486	306,477	5,780,362	3,067,655	4,582,401
30°C-60min-02	2,324,658	299,549	6,046,341	3,495,307	5,077,296
30°C-60min-03	2,334,047	301,887	5,719,189	3,245,914	4,602,518
30°C-3hr-01	1,565,354	163,789	6,146,651	3,505,740	5,189,340
30°C-3hr-02	1,704,945	189,780	5,841,074	3,810,942	5,503,442
30°C-3hr-03	1,480,236	143,758	5,423,858	3,641,393	5,507,725
30°C-overnight-01	2,073,662	250,695	5,252,057	3,515,390	5,420,934
30°C-overnight-02	1,971,892	253,705	5,155,548	4,806,808	6,687,244
30°C-overnight-03	2,015,538	278,933	5,612,136	5,519,510	8,342,605

B.4. Methylene Chloride Extracts of Products

The chromatograms shown in this section are the analysis of each fraction of methylene chloride extract. This was to demonstrate how many extractions were needed to completely remove all products.

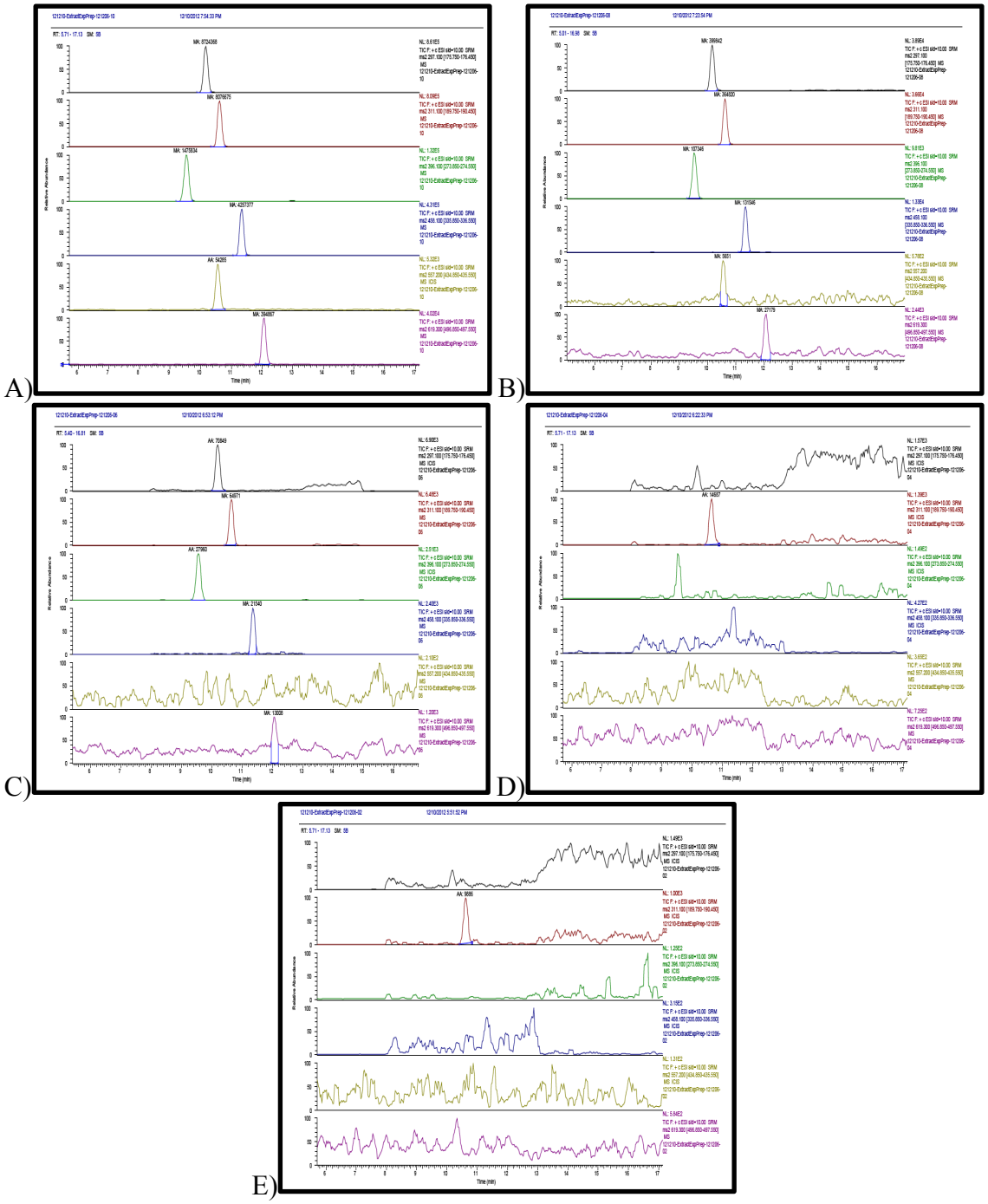

Figure. B.1. Chromatogram of the A) first extraction, B) second extraction, C) third extraction, D) fourth extraction, and E) fifth extraction.

C. Chromatograms of Liquid Chromatography Experiments

The first set of 4 chromatograms compared 4 different compositions of solvents used to reconstitute the final derivatized products.

The remaining chromatograms in Appendix C shows the results of each PA or internal standard derivatized. Each chromatogram shows the ion-extracted channel for all the PAs and internal standard. Within each chromatogram there is only one channel that shows the largest area counts, which corresponds to the standard or internal standard that was derivatized.

C.1. Chromatograms of Solvent Ratio Reconstitution of Samples

Four identical samples were prepared and different ratios of acetonitrile to water were added and the peak shapes were observed.

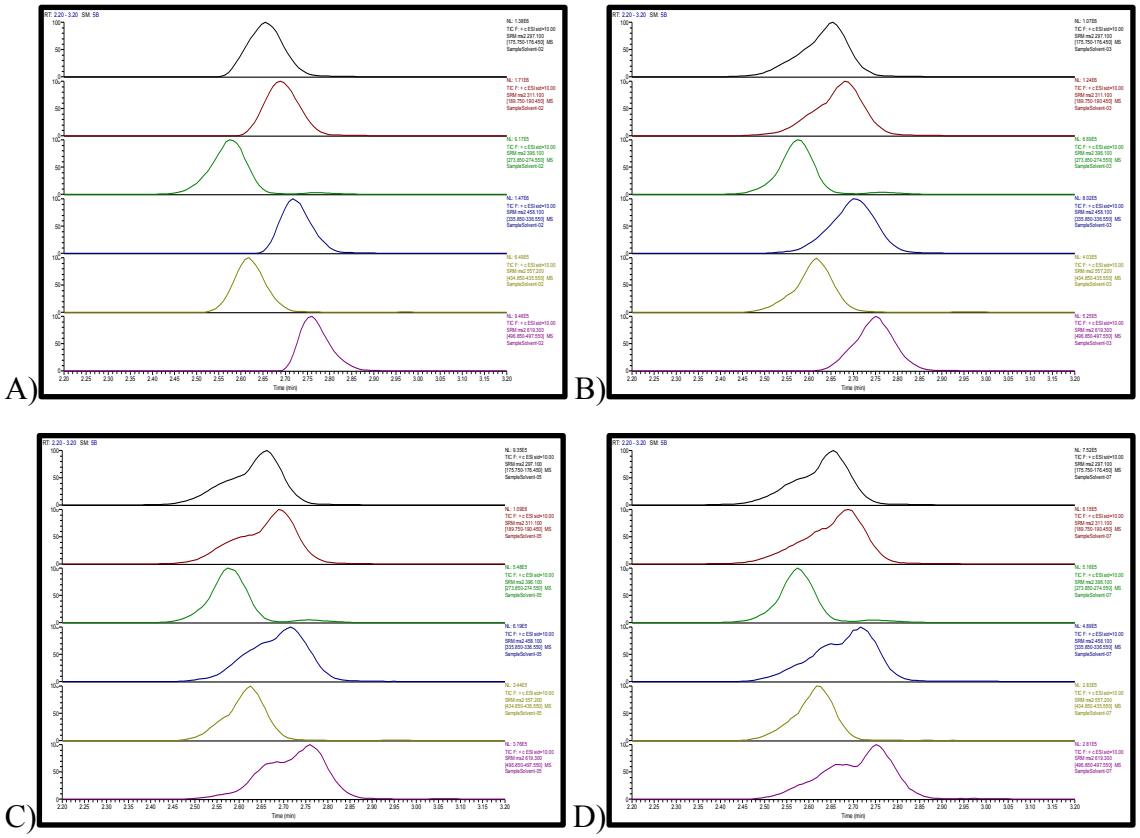

Figure. C.1. Chromatogram of analytes reconstituted with: A) 50:50 ACN:H_2O, B) 40:60 ACN:H_2O, C) 30:70 ACN:H_2O, D) 30:70 ACN:H_2O.

C.2. Chromatograms of Individually Prepared PAs and Internal Standards

Each PA and internal standard was prepared individually and analyzed to show that there was no other compound present. The chromatograms show the ion-extracted channel for all PAs and internal standard.

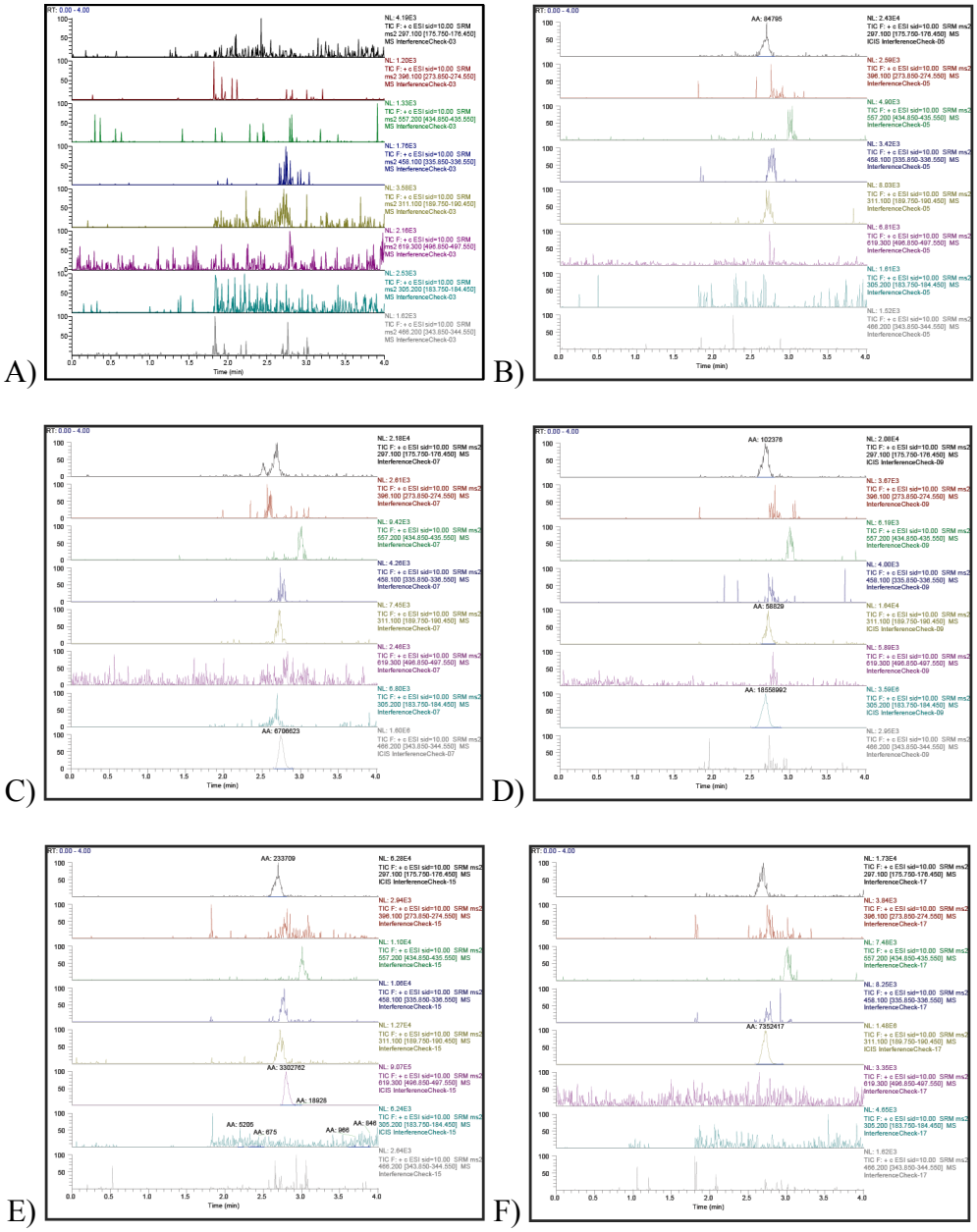

Figure. C.2. Chromatogram of each standard individually prepared. A) blank-no reagent added, B) blank-benzoyl chloride added, C) SPD-d8, D) PUT-d8, E) SPM, F) CAD, G) SPD, H) N1-ASPM, I) N8-ASPD, and J) PUT.

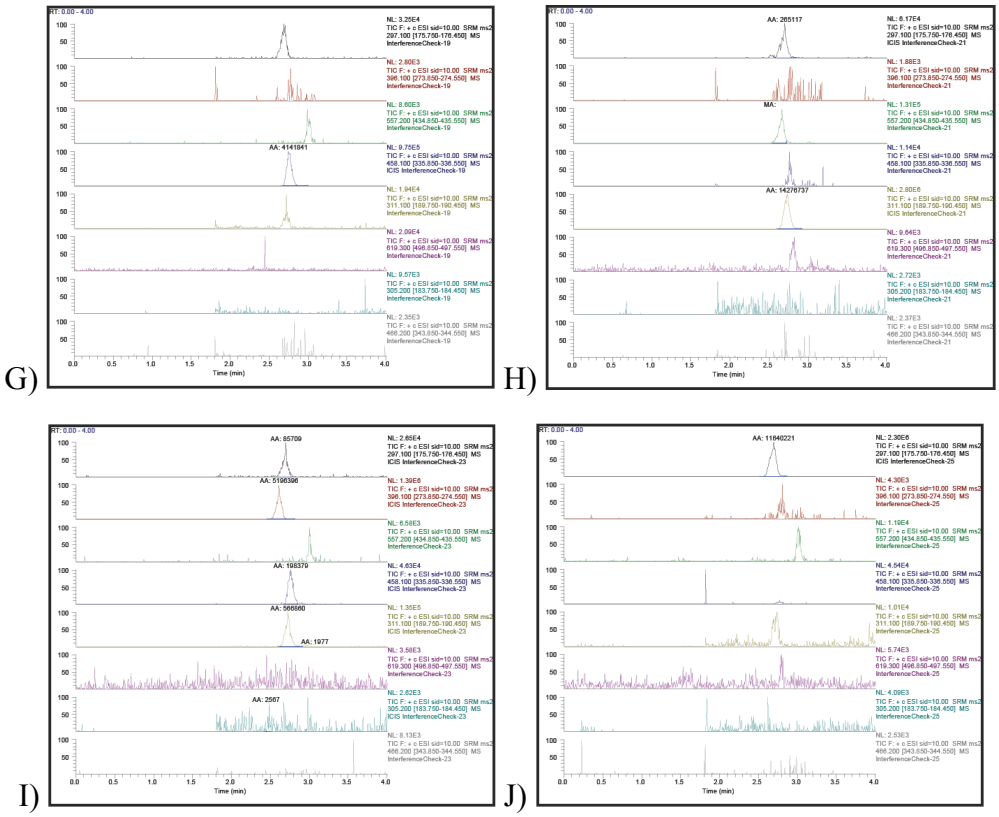

Figure. C.2. Chromatogram of each standard individually prepared. A) blank-no reagent added, B) blank-benzoyl chloride added, C) SPD-d8, D) PUT-d8, E) SPM, F) CAD, G) SPD, H) N1-ASPM, I) N8-ASPD, and J) PUT, continued.

D. Mass Spectra and Raw Data from Collision Energy Optimization Experiments

Each derivatized PA and internal standard was analyzed by MS/MS and monitored in full scan mode. This appendix shows all the fragments that would result from collision-induced dissociation in Q2. The chromatogram shown was of the experiment that resulted in the best sensitivity of the base peak, quantifying fragment ion, with a small intensity of the protonated molecular ion, this was also used to determine the best collision energy.

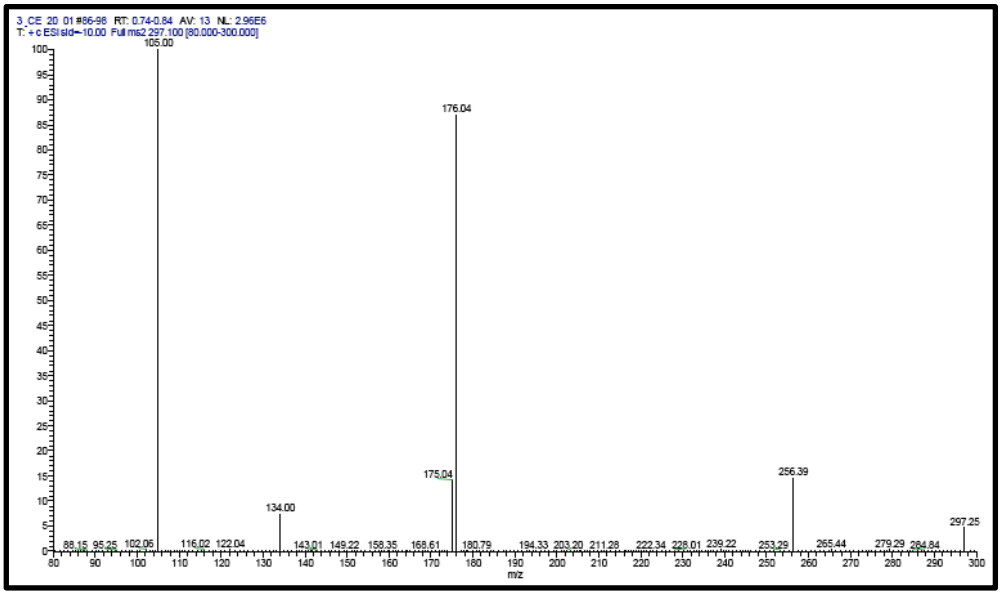

Figure. D.1. MS/MS full scan spectrum of PUT with optimized CE of 20 volts showing *m/z* 297 (parent ion), 176 (quantifying ion), and 105 (confirming ion).

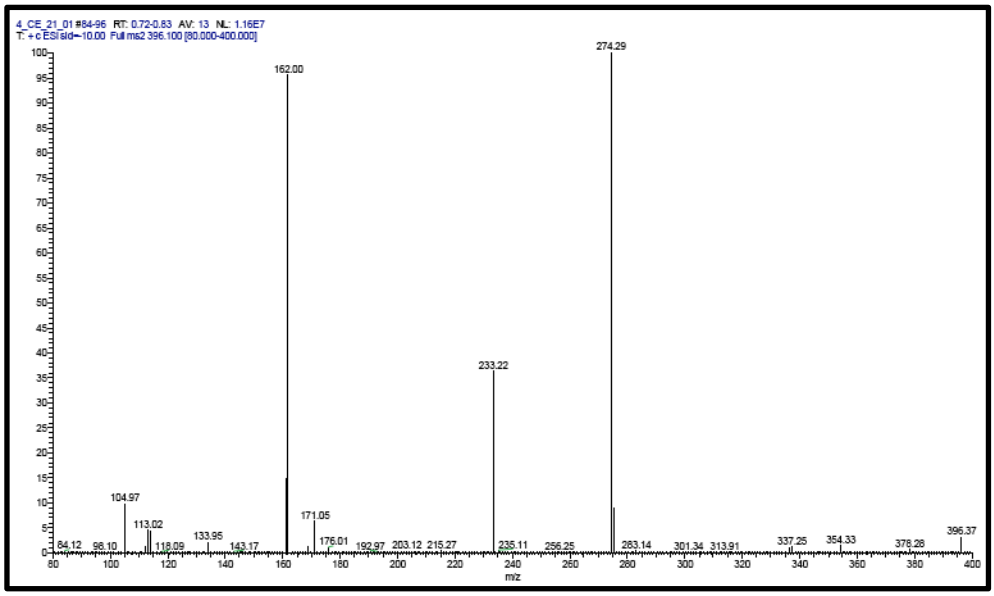

Figure. D.2. MS/MS full scan spectrum of N8-ASPD with optimized CE of 21 volts showing *m/z* 396 (parent ion), 274 (quantifying ion), and 162 (confirming ion).

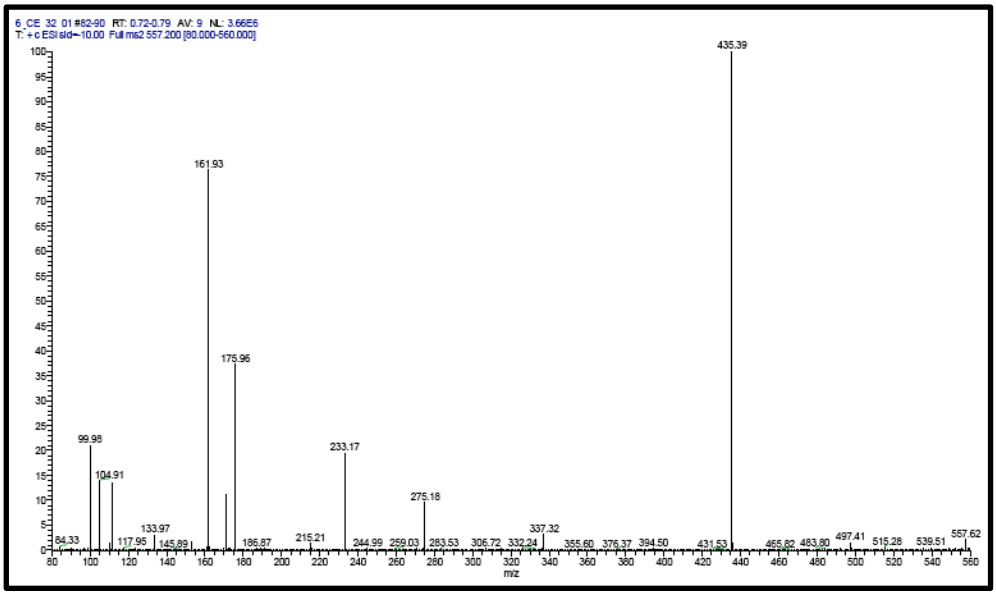

Figure. D.3. MS/MS full scan spectrum of N1-ASPM with optimized CE of 32 volts showing *m/z* 557 (parent ion), 435 (quantifying ion), and 161 (confirming ion).

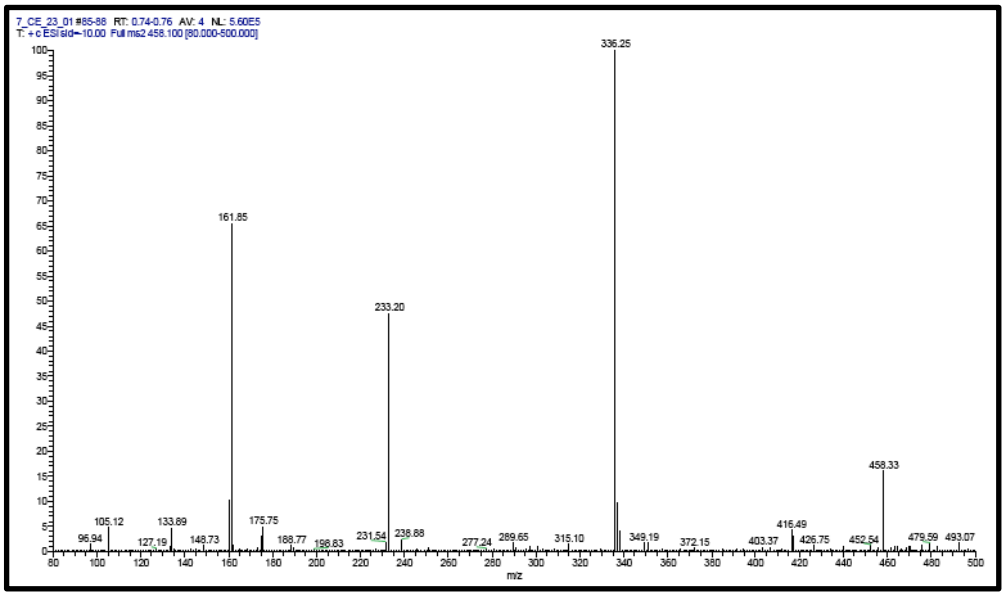

Figure. D.4. MS/MS full scan spectrum of SPD with optimized CE of 23 volts showing *m/z* 458 (parent ion), 36 (quantifying ion), and 162 (confirming ion).

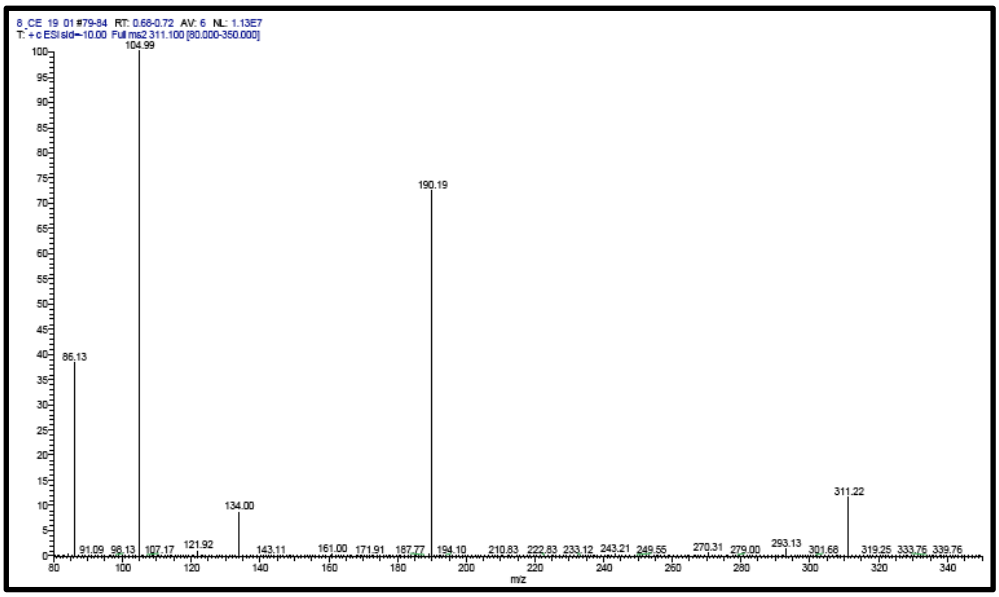

Figure. D.5. MS/MS full scan spectrum of CAD with optimized CE of 19 volts showing *m/z* 311 (parent ion), 190 (quantifying ion), and 105 (confirming ion).

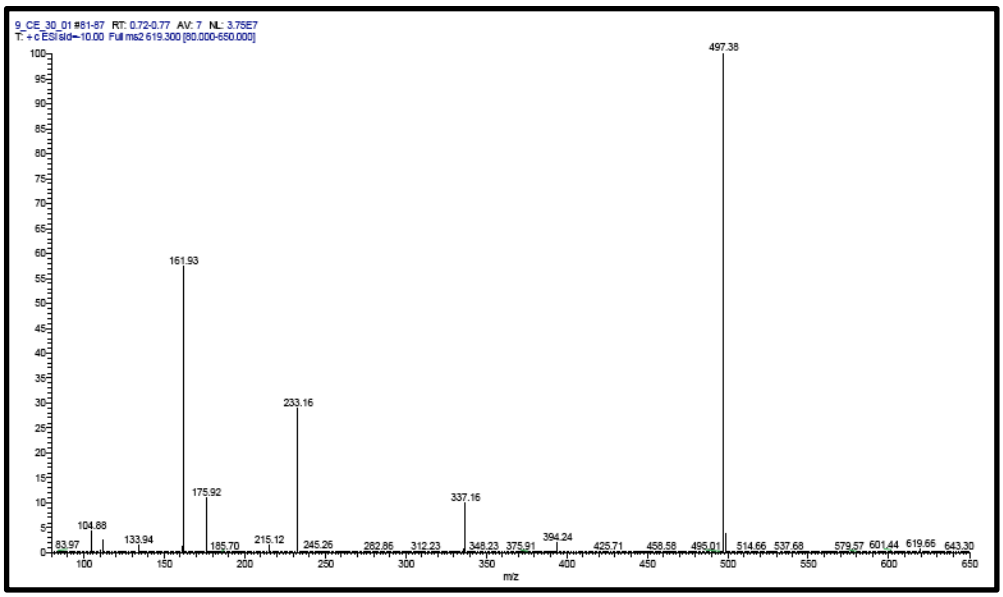

Figure. D.6. MS/MS full scan spectrum of SPM with optimized CE of 30 volts showing *m/z* 619 (parent ion), 497 (quantifying ion), and 162 (confirming ion).

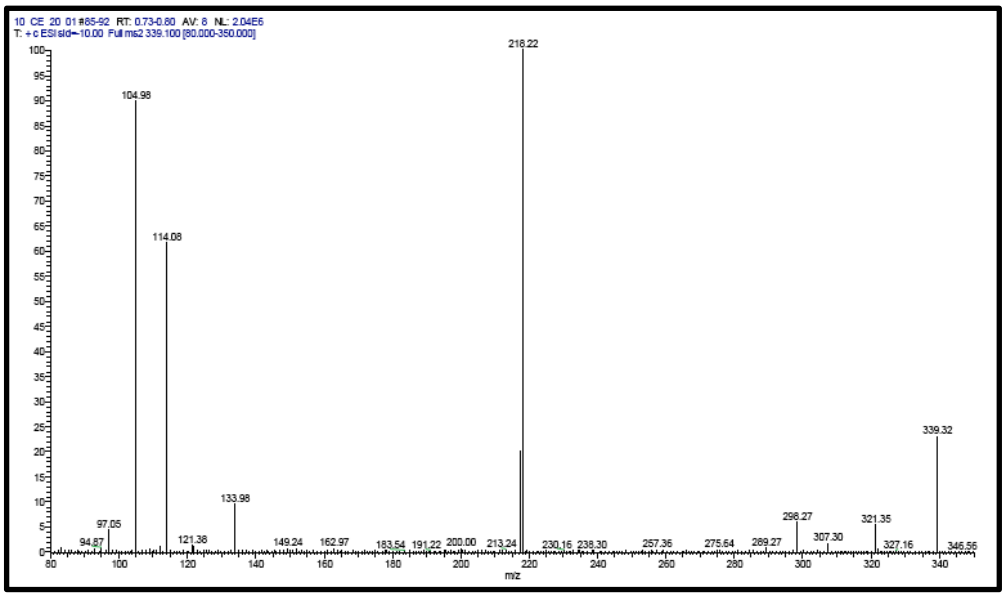

Figure. D.7. MS/MS full scan spectrum of DAH with optimized CE of 20 volts showing *m/z* 339 (parent ion), 218 (quantifying ion), and 105 (confirming ion).

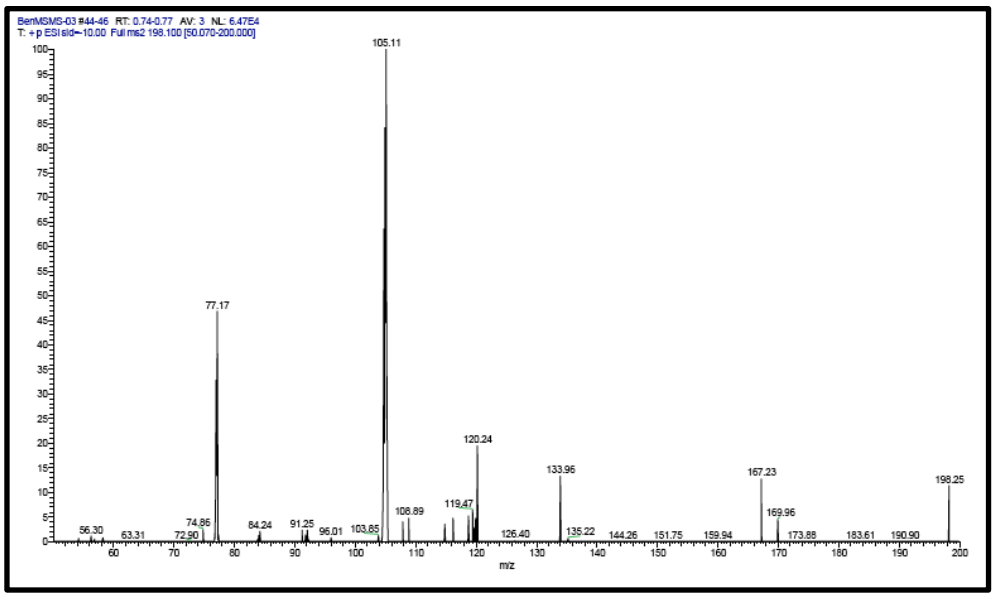

Figure. D.8. MS/MS full scan spectrum of BEN with optimized CE of 27 volts showing *m/z* 198 (parent ion), 77 and 105 (both can be the quantifying ion).

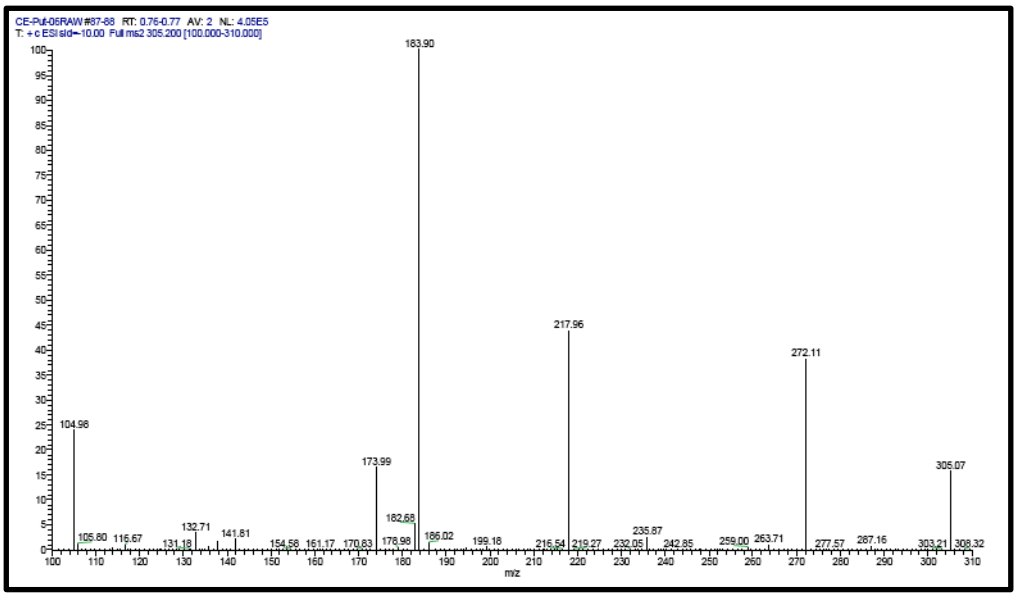

Figure. D.9. MS/MS spectrum of PUT-d8 with optimized CE of 17 volts showing *m/z* 305 (parent ion), 184 (quantifying ion), and 105 (confirming ion).

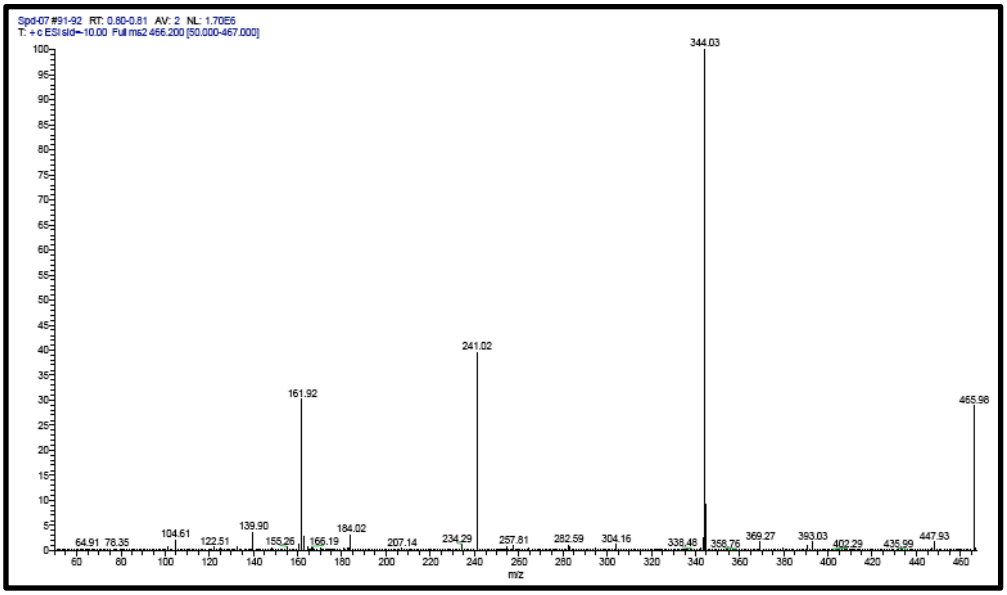

Figure. D.10. MS/MS spectrum of SPD-d8 with optimized CE of 18 volts showing *m/z* 297 (parent ion), 344 (quantifying ion), and 162 (confirming ion).

E. Raw Data of Collision Energy Experiments of PUT and SPD

PUT-d8 and SPD-d8 were the only isotopic labeled internal standard available. Collision energy was established for PUT and SPD. The data in Table. E.1 are the results of using the same and different collision energy for each compound and its isotope.

Table. E.1. Peak area of PUT, SPM and its isotopic internal standards comparing CE used for quantification.

Sample	CE PUT/SPD (volts)	CE PUT-d8/ SPD-d8 (volts)	PUT	SPD	PUT-d8	SPD-d8
Same-CE-01	20/23	20/23	1,418,843	402,649	844,298	291,950
Same-CE-02	20/23	20/23	1,546,543	454,174	1,021,813	328,401
Same-CE-03	20/23	20/23	1,619,678	439,692	1,051,103	303,583
Diff-CE-01	20/23	17/18	14,298,744	4,928,772	15,271,322	4,917,806
Diff-CE-02	20/23	17/18	14,749,514	5,263,936	15,415,056	5,061,124
Diff-CE-03	20/23	17/18	14,395,643	5,376,380	15,583,452	5,359,957

F. Full scan spectra from matrix effect experiments

The chromatograms shown in Figure. F.1 are of fruit fly matrix treated 3 different ways. Within each chromatogram the ion-extracted channel of *m/z* 184 and the total ion current is shown for each matrix treatment. The details of each matrix treatment is found in Figure 3.18.

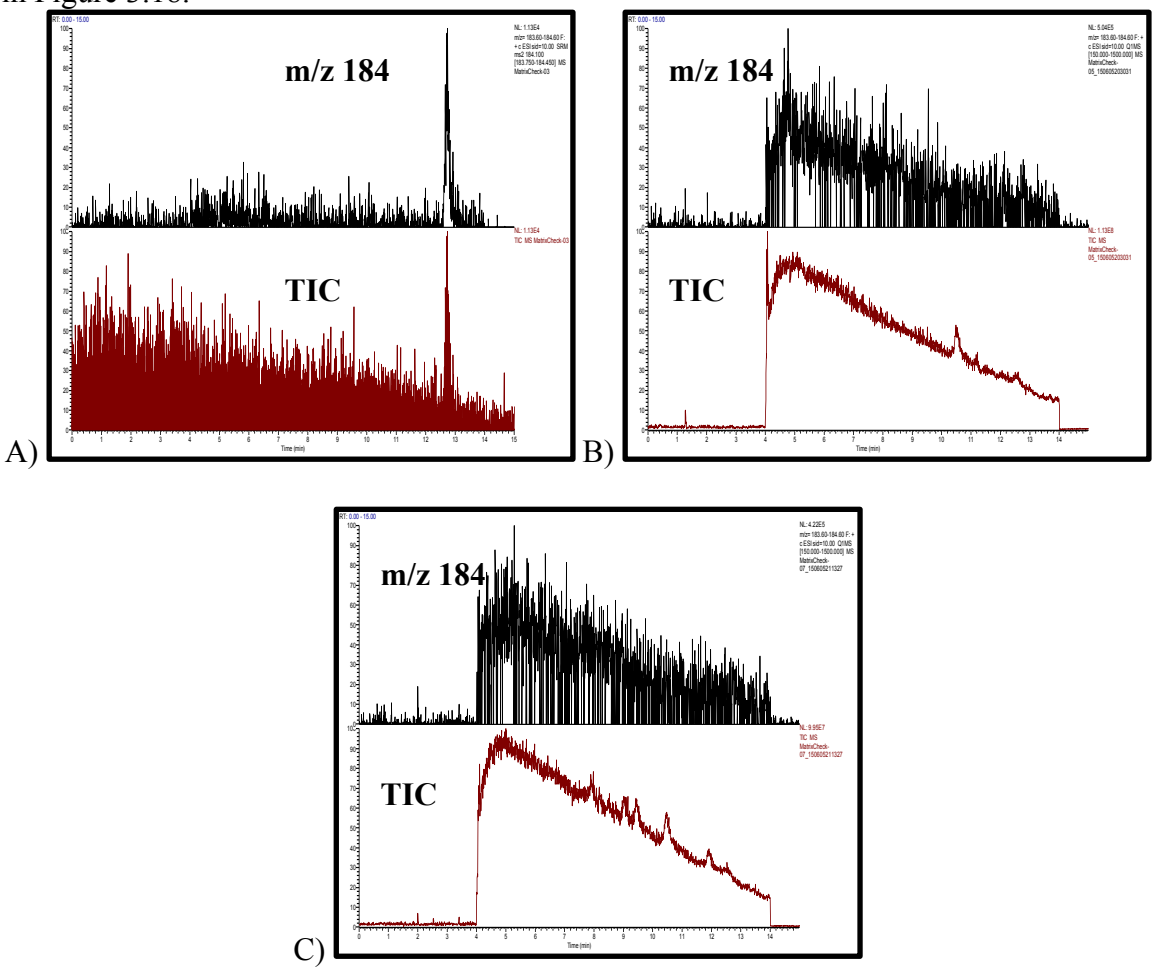

Figure. F.1. Full scan of A) filtered & cleaned fly matrix, B) filtered fly matrix, and C) derivatized fly matrix.

G. Calibration Curve of Each Analyte Relative to an Internal Standard

Only the data for PUT and SPD were reported in the body of thesis. In this appendix the concentrations of PAs and internal standards used for linearity experiments are compiled in a table. A table with all the R^2 values for each analyte and the internal standard used is also reported.

Table. G.1. Concentration of calibration solutions.

	Concentration (ng/mL)							
Analyte	**L 1**	**L 2**	**L 3**	**L 4**	**L 5**	**L 6**	**L 7**	**L 8**
PUT	505	241	79.2	31.7	6.19	3.39	0.402	0
N8ASPD	633	302	99.3	39.7	7.76	4.25	0.504	0
N1ASPM	639	305	100.	40.0	7.82	4.29	0.508	0
SPD	528	252	82.8	33.1	6.48	3.55	0.420	0
CAD	924	441	145	58.0	11.3	6.21	0.735	0
SPM	538	257	84.4	33.8	6.60	3.61	0.428	0

Table. G.2. Concentration of internal standards used in calibration solutions.

Compound	Concentration (ng/mL)	Compound	Concentration (ng/mL)
1,7-DAH	49.9	SPD-d8	45.5
BEN	44.6	PUT-d8	48.7

Table. G.3. Correlation coefficient (R^2) of each analyte relative to an internal standard. * Indicates a value below the accepted value of 0.96.

	PUT	**N8ASPD**	**N1ASPM**	**SPD**	**CAD**	**SPM**
PUT-D8	1.00	0.987	0.978	0.989	0.998	0.959
SPD-D8	0.949	1.00	0.998	1.00	0.921	0.984
DAH	0.998	0.991	0.984	0.993	0.992	0.965
BEN-77	*0.935	0.998	0.996	0.999	*0.904	0.989
BEN-105	*0.933	0.999	0.999	0.998	*0.901	0.988

Figure. G.1. Calibration curve of each amine with PUT-d8 or SPD-d8 as the internal standard.

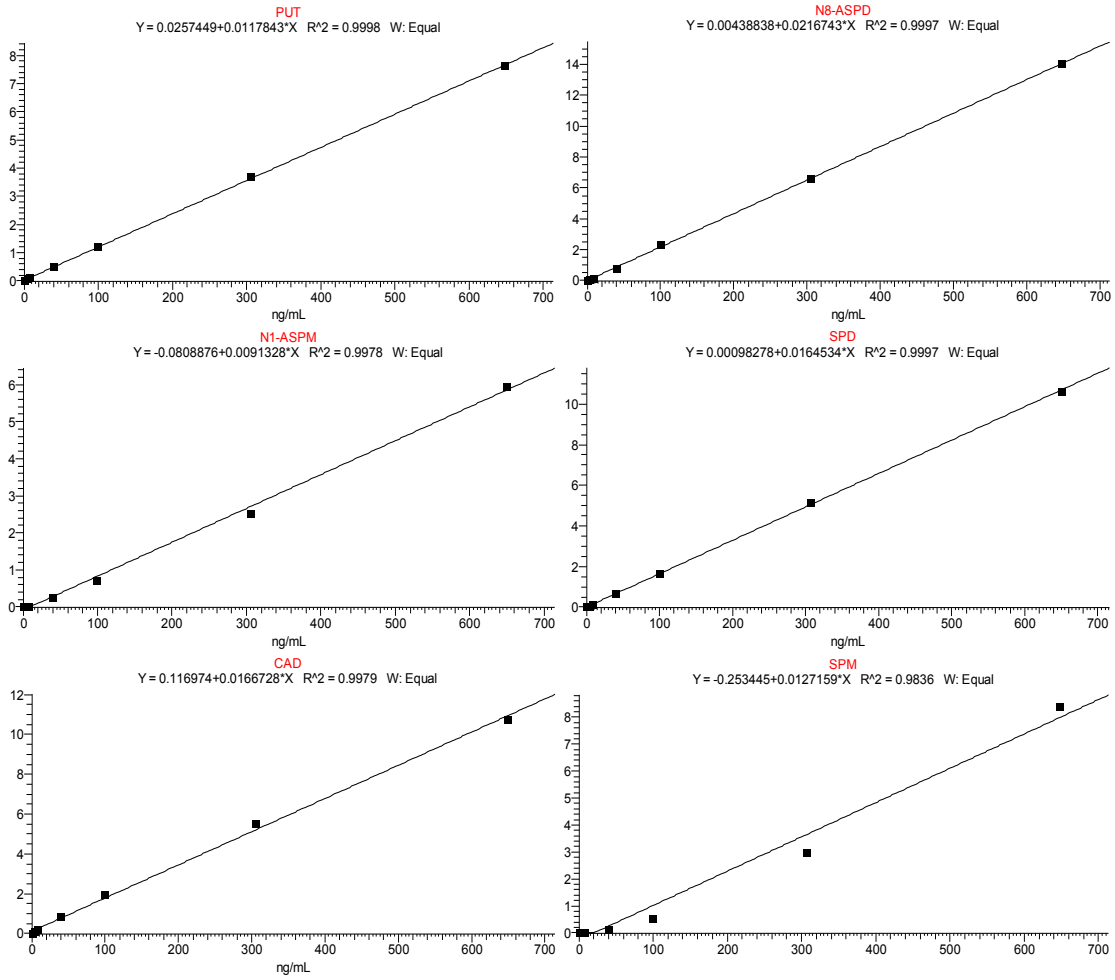

Figure. G.2. Calibration curve of each amine with DAH as the internal standard.

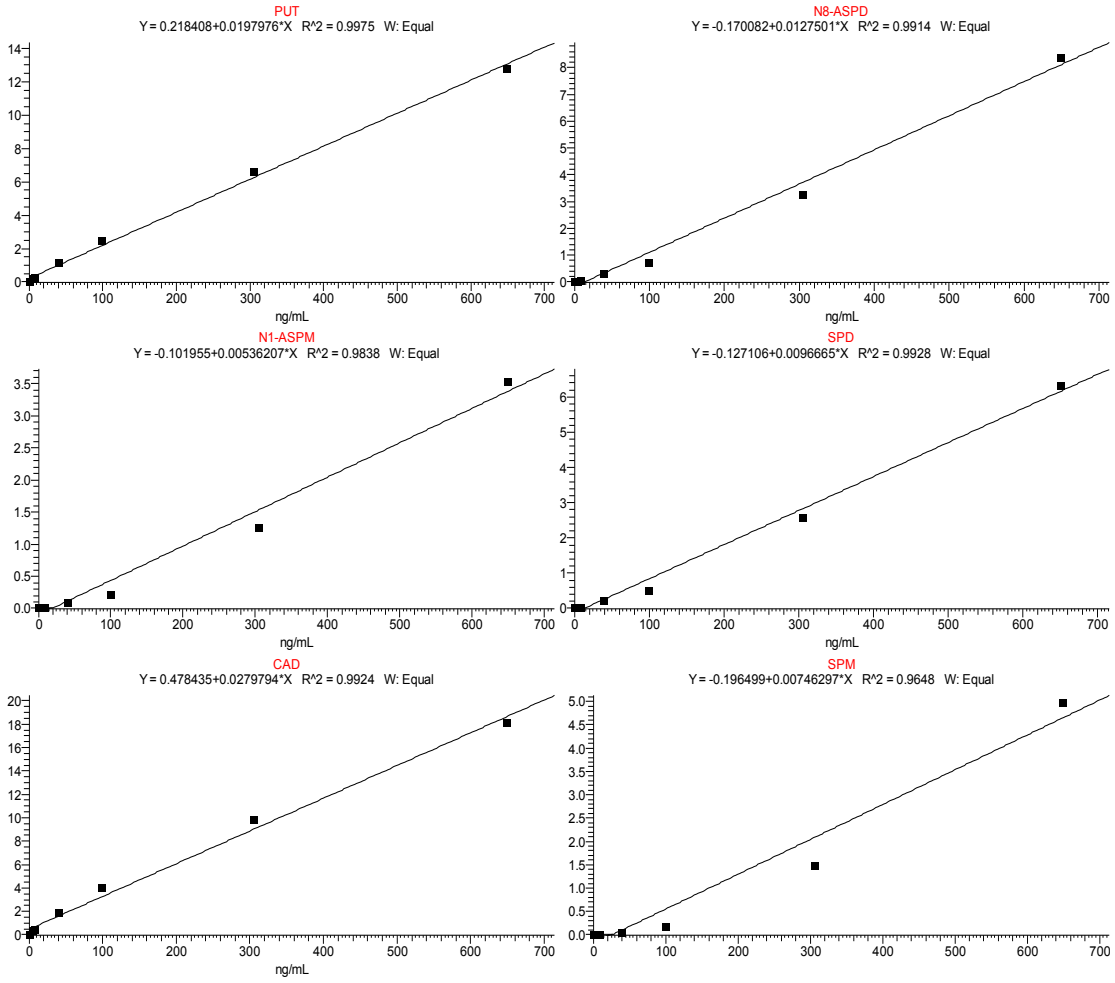

Figure. G.3. Calibration curve of each amine with BEN-77 as the internal standard.

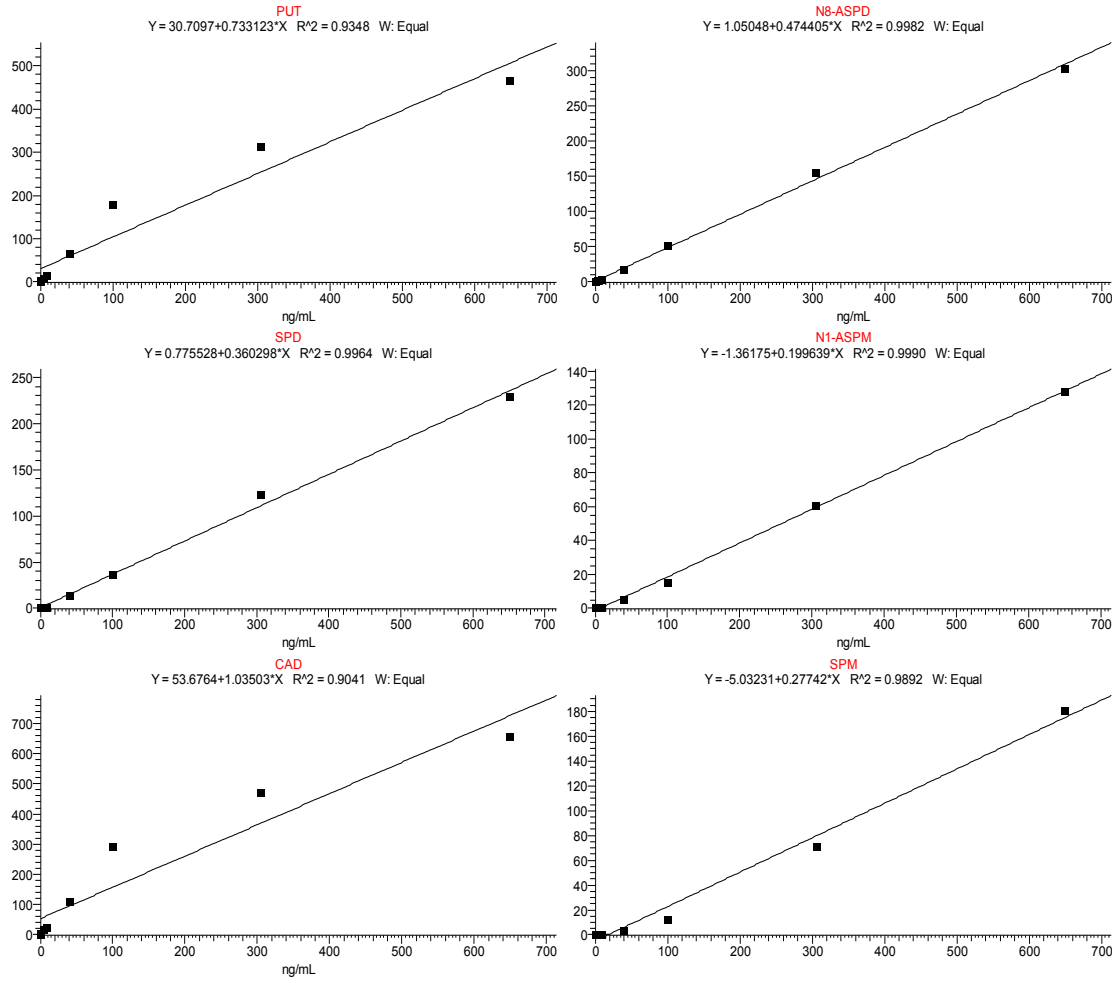

Figure. G.4. Calibration curve of each amine with BEN-105 as the internal standard.

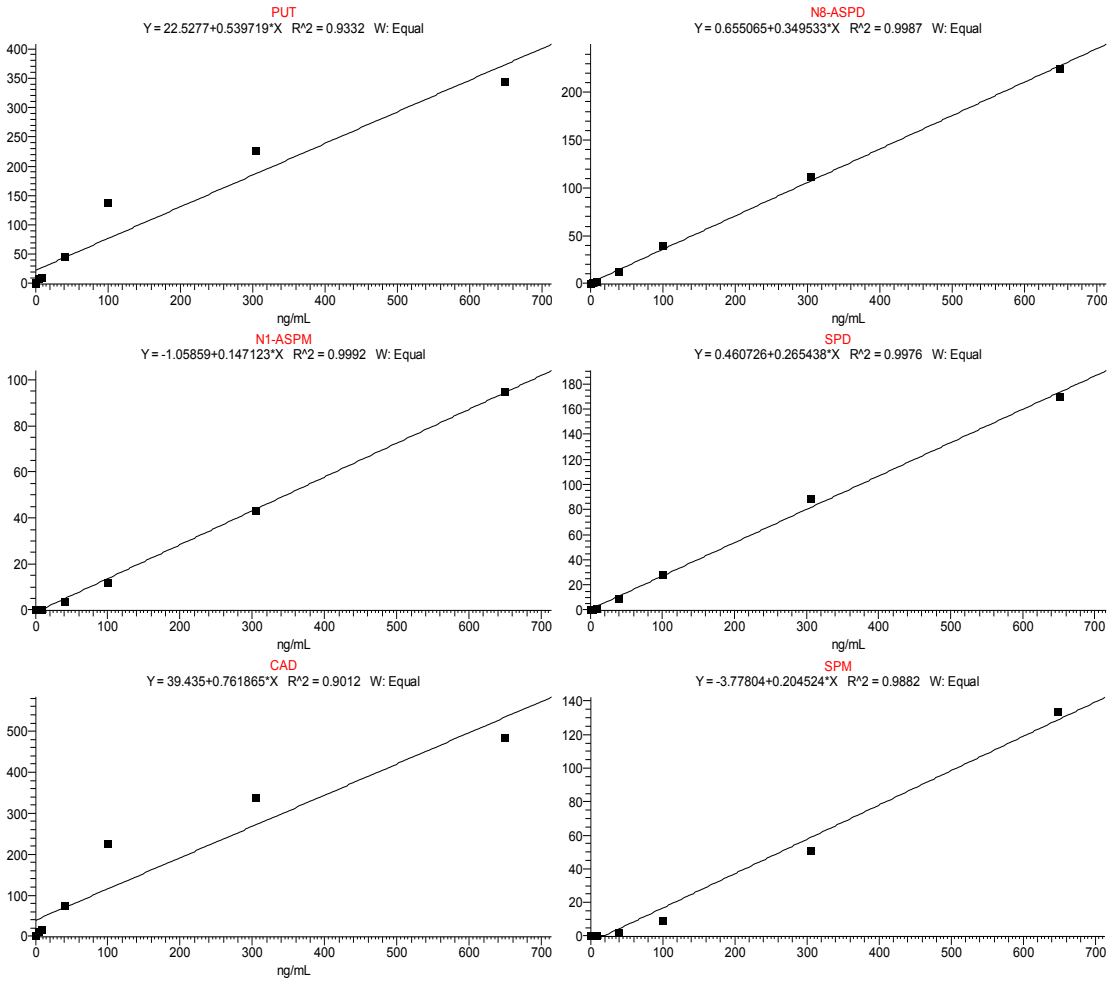

H. Raw Data from Intra-day and Inter-day Experiments

Table. H.1. Peak areas of PUT, SPD, PUT-d8, and SPD-d8 for intra-day experiment.

Sample	PUT	SPD	PUT-d8	SPD-d8
Low-1-01	344,021	30,888	305,971	28,335
Low-1-02	352,866	30,127	322,282	24,848
Low-1-03	400,136	30,820	313,100	29,086
Low-1-04	217,704	18,020	206,064	18,959
Low-1-05	214,868	20,692	176,582	29,684
Med-1-01	3,375,402	652,148	4,853,816	831,042
Med-1-02	3,909,233	758,187	5,716,769	964,664
Med-1-03	3,691,569	695,744	5,442,333	952,554
Med-1-04	3,143,491	675,002	4,745,382	881,089
Med-1-05	2,964,788	625,438	4,517,132	807,019
High-1-01	7,519,778	2,550,812	3,497,255	993,023
High-1-02	7,865,828	2,304,360	3,460,620	882,075
High-1-03	8,699,999	2,761,994	3,833,141	1,102,397
High-1-04	8,844,068	2,895,954	4,068,670	1,173,965
High-1-05	9,671,075	3,152,306	4,184,987	1,259,731

Table. H.1. Peak areas of PUT, SPD, PUT-d8, and SPD-d8 for inter-day experiment results.

Sample	PUT	SPD	PUT-d8	SPD-d8
Day-1-Low-01	344,021	30,888	305,971	28,335
Day-1-Low-02	352,866	30,127	322,282	24,848
Day-1-Low-03	400,136	30,820	313,100	29,086
Day-4-Low-01	240,337	26,470	196,857	21,131
Day-4-Low-02	286,846	21,329	278,023	22,509
Day-4-Low-03	349,301	24,603	269,627	27,970
Day-7-Low-01	341,156	41,398	267,773	33,372
Day-7-Low-02	416,220	50,965	374,031	49,716
Day-7-Low-03	447,206	42,883	360,972	49,420
Day-1-Med-01	3,375,402	652,148	4,853,816	831,042
Day-1-Med-02	3,909,233	758,187	5,716,769	964,664
Day-1-Med-03	3,691,569	695,744	5,442,333	952,554
Day-4-Med-01	2,579,148	500,893	4,047,338	684,086
Day-4-Med-02	2,333,512	487,552	3,650,154	637,523
Day-4-Med-03	2,405,014	532,454	3,640,207	666,472
Day-7-Med-01	3,549,826	884,687	5,559,351	1,078,827
Day-7-Med-02	3,488,942	1,004,909	5,472,901	1,321,446
Day-7-Med-03	3,692,086	1,042,726	5,472,262	1,328,290
Day-1-High-01	19,064,194	2,550,812	8,262,161	993,023
Day-1-High-02	15,805,821	2,304,360	7,061,255	882,075
Day-1-High-03	15,448,366	2,761,994	7,275,653	1,102,397
Day-4-High-01	12,487,947	4,015,314	5,896,215	1,594,792
Day-4-High-02	13,102,063	3,765,853	6,239,922	1,562,515
Day-4-High-03	13,168,037	3,748,328	6,242,115	1,509,740
Day-7-High-01	20,205,811	6,709,162	9,045,591	2,776,887
Day-7-High-02	20,558,070	7,308,193	9,517,034	3,153,548
Day-7-High-03	21,012,094	7,612,379	9,682,431	2,980,932

I. Raw Data from Stability Experiments

Table. I.1. Stability Experiment Day 22 - Peak area of 6 PAs derivatized and stored in 50:50 ACN:H_2O. One set stored at room temperature exposed to light, one set stored at room temperature not exposed to light, and a third set stored in the freezer not exposed to light.

Sample	PUT	N8-ASPD	N1-ASPM	SPD	CAD	SPM
Lt-RT-01	8,802,022	957,646	148,225	1,371,824	15,257,797	215,292
Lt-RT-02	9,208,412	1,003,635	173,003	1,313,795	15,898,800	207,493
Lt-RT-03	9,506,724	1,011,859	162,449	1,400,814	16,299,175	217,120
Dk-RT-01	8,301,851	933,031	157,284	1,131,186	14,881,375	196,863
Dk-RT-02	8,563,400	952,919	171,616	1,176,263	16,340,716	197,052
Dk-RT-03	8,587,808	999,319	169,011	1,175,946	15,830,121	205,840
Dk-Cold-01	8,667,058	890,533	153,212	1,125,035	15,443,464	214,851
Dk-Cold-02	8,910,579	813,265	143,804	1,179,654	15,626,838	201,124
Dk-Cold-03	8,304,126	834,593	155,905	1,124,262	13,575,668	215,098

Table. I.2. Stability Experiment Day 22 - Peak area of 4 internal standards derivatized and stored in 50:50 ACN:H_2O. One set stored at room temperature exposed to light, one set stored at room temperature not exposed to light, and a third set stored in the freezer not exposed to light.

Sample	PUT-d8	SPD-d8	1,7-DAH	BEN-77	BEN-105
Lt-RT-01	28,798,447	3,333,333	49,033,500	4,107,968	5,239,001
Lt-RT-02	31,009,765	3,328,057	41,325,714	4,000,730	4,776,375
Lt-RT-03	32,898,721	3,555,036	42,112,985	4,091,852	4,955,234
Dk-RT-01	28,830,825	2,929,129	43,197,810	4,296,080	5,418,694
Dk-RT-02	29,703,198	3,257,975	46,671,071	4,475,958	5,524,775
Dk-RT-03	29,801,023	3,270,002	44,561,155	4,553,090	5,512,494
Dk-Cold-01	30,836,361	3,340,912	37,723,761	4,468,633	4,884,053
Dk-Cold-02	31,352,053	3,383,649	40,245,954	4,042,207	4,978,743
Dk-Cold-03	28,403,863	3,057,410	29,788,171	3,396,232	3,806,460

Table. I.3. Stability Experiment Day 22 - Peak area of 6 PAs derivatized and stored in 100% ACN. One set stored at room temperature exposed to light, one set stored at room temperature not exposed to light, and a third set stored in the freezer not exposed to light.

Sample	PUT	N8-ASPD	N1-ASPM	SPD	CAD	SPM
Lt-RT-01	10,915,787	1,363,231	161,976	1,593,899	15,917,972	188,067
Lt-RT-02	10,660,955	1,477,630	155,139	1,432,404	14,750,784	160,443
Lt-RT-03	11,132,768	1,704,172	190,571	1,679,564	15,899,253	182,677
Dk-RT-01	11,126,782	1,257,881	194,294	1,674,395	16,469,416	210,376
Dk-RT-02	11,916,733	1,402,014	216,397	1,658,641	17,199,042	237,295
Dk-RT-03	11,421,075	1,481,679	210,987	1,752,034	17,389,541	236,398
Dk-Cold-01	9,450,840	1,341,015	178,538	1,272,301	13,641,823	166,512
Dk-Cold-02	8,882,733	1,302,916	165,389	1,198,833	12,783,118	179,144
Dk-Cold-03	8,711,825	1,373,483	156,018	1,245,879	12,632,085	163,575

Table. I.4. Stability Experiment Day 22 - Peak area of 4 internal standards derivatized and stored in 100% ACN. One set stored at room temperature exposed to light, one set stored at room temperature not exposed to light, and a third set stored in the freezer not exposed to light.

Sample	PUT-d8	SPD-d8	1,7-DAH	BEN-77	BEN-105
Lt-RT-01	31,377,135	3,790,434	41,599,863	4,227,240	5,017,558
Lt-RT-02	31,883,198	3,601,492	40,038,213	3,563,439	4,441,814
Lt-RT-03	34,635,630	4,197,295	39,438,175	3,805,005	4,820,214
Dk-RT-01	34,556,633	4,189,479	47,689,345	4,435,974	5,651,082
Dk-RT-02	37,985,897	4,067,735	48,654,039	4,606,739	6,139,134
Dk-RT-03	37,189,168	4,374,806	47,755,236	4,040,985	5,149,624
Dk-Cold-01	30,882,257	3,235,695	31,120,721	3,410,342	4,327,573
Dk-Cold-02	29,332,632	3,109,147	29,273,120	3,513,779	4,238,761
Dk-Cold-03	29,840,871	3,114,189	30,149,400	3,430,713	4,348,588

Table. I.5. Stability Experiment Day 15 - Peak area of 6 PAs derivatized and stored in 50:50 ACN:H_2O. One set stored at room temperature exposed to light, one set stored at room temperature not exposed to light, and a third set stored in the freezer not exposed to light.

Sample	PUT	N8-ASPD	N1-ASPM	SPD	CAD	SPM
Lt-RT-01	6,436,716	613,566	144,156	831,909	9,581,561	186,474
Lt-RT-02	6,275,647	592,755	157,049	750,312	9,377,422	188,847
Lt-RT-03	6,704,463	644,144	171,817	835,253	9,552,054	218,605
Dk-RT-01	5,336,433	629,335	134,015	688,326	8,460,466	162,733
Dk-RT-02	5,514,283	634,697	145,035	705,141	8,765,406	184,896
Dk-RT-03	5,890,011	656,077	158,504	746,591	9,455,260	193,784
Dk-Cold-01	6,086,652	607,931	132,361	754,407	9,626,654	206,265
Dk-Cold-02	6,091,554	578,871	139,210	758,928	9,239,646	206,561
Dk-Cold-03	5,755,375	646,235	156,878	800,694	8,104,111	201,692

Table. I.6. Stability Experiment Day 15 - Peak area of 4 internal standards derivatized and stored in 50:50 ACN:H_2O. One set stored at room temperature exposed to light, one set stored at room temperature not exposed to light, and a third set stored in the freezer not exposed to light.

Sample	PUT-d8	SPD-d8	1,7-DAH	BEN-77	BEN-105
Lt-RT-01	18,790,879	2,024,126	28,179,610	2,462,274	3,425,838
Lt-RT-02	18,524,686	1,811,271	25,908,499	2,811,909	3,726,852
Lt-RT-03	19,618,017	2,072,231	27,829,855	2,835,877	3,745,307
Dk-RT-01	15,545,808	1,789,241	28,387,310	2,845,557	3,955,051
Dk-RT-02	16,279,834	1,774,990	29,810,409	3,020,381	4,072,957
Dk-RT-03	17,263,542	1,861,780	27,922,741	3,035,357	4,279,348
Dk-Cold-01	18,214,545	1,820,926	28,734,156	3,206,872	4,473,447
Dk-Cold-02	17,962,451	1,920,493	28,020,866	3,399,802	4,620,516
Dk-Cold-03	16,778,313	1,874,901	23,742,672	3,513,081	4,503,189

Table. I.7. Stability Experiment Day 15 - Peak area of 6 PAs derivatized and stored in 100% ACN. One set stored at room temperature exposed to light, one set stored at room temperature not exposed to light, and a third set stored in the freezer not exposed to light.

Sample	PUT	N8-ASPD	N1-ASPM	SPD	CAD	SPM
Lt-RT-01	5,895,872	1,122,827	156,914	1,283,840	11,371,039	153,850
Lt-RT-02	5,796,437	1,161,407	156,748	1,335,825	10,962,770	205,301
Lt-RT-03	4,999,964	1,046,346	141,614	959,600	9,358,730	147,750
Dk-RT-01	5,862,763	938,055	171,564	1,142,587	10,954,178	220,246
Dk-RT-02	5,466,481	962,623	173,708	1,219,589	10,719,587	193,226
Dk-RT-03	6,194,639	910,867	168,791	1,144,193	11,608,128	211,316
Dk-Cold-01	6,794,113	886,950	162,991	1,269,951	11,950,014	207,732
Dk-Cold-02	4,911,036	853,430	162,944	997,895	9,185,387	199,734
Dk-Cold-03	5,870,122	853,003	169,868	956,221	10,301,164	167,725

Table. I.8. Stability Experiment Day 15 - Peak area of 4 internal standards derivatized and stored in 100% ACN. One set stored at room temperature exposed to light, one set stored at room temperature not exposed to light, and a third set stored in the freezer not exposed to light.

Sample	PUT-d8	SPD-d8	1,7-DAH	BEN-77	BEN-105
Lt-RT-01	16,103,023	3,298,503	19,825,407	2,508,060	2,077,656
Lt-RT-02	16,650,618	3,460,725	20,720,200	3,001,269	2,443,124
Lt-RT-03	14,502,576	2,526,576	17,703,561	2,850,350	2,850,684
Dk-RT-01	16,017,491	2,940,159	19,582,501	2,464,526	1,878,529
Dk-RT-02	16,070,033	3,370,076	22,240,316	3,425,662	2,961,301
Dk-RT-03	17,858,389	3,180,349	22,891,333	3,094,641	2,611,672
Dk-Cold-01	19,639,160	3,308,152	25,822,972	2,265,205	2,174,994
Dk-Cold-02	14,461,824	2,785,688	18,509,443	2,417,902	2,149,441
Dk-Cold-03	17,475,051	2,659,723	16,797,746	2,788,875	2,443,384

Table. I.9. Stability Experiment Day 8 - Peak area of 6 PAs derivatized and stored in 50:50 ACN:H_2O. One set stored at room temperature exposed to light, one set stored at room temperature not exposed to light, and a third set stored in the freezer not exposed to light.

Sample	PUT	N8-ASPD	N1-ASPM	SPD	CAD	SPM
Lt-RT-01	5,351,453	742,533	158,877	932,892	11,113,922	182,413
Lt-RT-02	5,129,041	735,915	179,098	866,448	10,627,289	170,670
Lt-RT-03	5,381,333	729,809	156,672	843,613	11,646,794	169,022
Dk-RT-01	5,283,190	713,090	166,811	802,559	11,798,482	177,280
Dk-RT-02	4,829,435	694,909	149,276	693,274	11,116,876	168,518
Dk-RT-03	5,038,370	737,393	184,858	773,958	11,495,222	205,328
Dk-Cold-01	5,214,610	512,055	130,893	671,787	11,455,088	185,217
Dk-Cold-02	5,046,946	495,381	107,678	710,289	11,547,233	178,383
Dk-Cold-03	4,748,238	495,138	115,850	636,050	10,187,432	151,749

Table. I.10. Stability Experiment Day 15 - Peak area of 4 internal standards derivatized and stored in 50:50 ACN:H_2O. One set stored at room temperature exposed to light, one set stored at room temperature not exposed to light, and a third set stored in the freezer not exposed to light.

Sample	PUT-d8	SPD-d8	1,7-DAH	BEN-77	BEN-105
Lt-RT-01	15,690,290	2,571,025	22,511,053	3,133,011	2,605,963
Lt-RT-02	15,224,340	2,476,464	20,476,903	2,393,573	2,001,779
Lt-RT-03	15,266,829	2,652,027	22,803,722	2,280,915	2,155,838
Dk-RT-01	14,540,331	2,527,230	25,122,545	2,628,903	2,356,517
Dk-RT-02	13,613,959	2,214,392	21,995,760	2,749,089	2,380,833
Dk-RT-03	13,985,670	2,394,218	22,623,631	2,937,544	2,469,407
Dk-Cold-01	14,604,924	2,123,014	20,269,136	2,999,057	2,460,494
Dk-Cold-02	14,215,390	2,217,948	20,850,762	2,929,876	2,490,042
Dk-Cold-03	13,824,552	2,039,786	16,984,996	2,530,339	2,287,117

Table. I.11. Stability Experiment Day 8 - Peak area of 6 PAs derivatized and stored in 100% ACN. One set stored at room temperature exposed to light, one set stored at room temperature not exposed to light, and a third set stored in the freezer not exposed to light.

Sample	PUT	N8-ASPD	N1-ASPM	SPD	CAD	SPM
Lt-RT-01	7,065,865	736,783	1,529	975,465	8,689,431	125,220
Lt-RT-02	6,456,772	531,790	87,581	943,528	8,928,888	96,617
Lt-RT-03	7,169,082	600,413	104,043	1,050,247	9,629,337	133,739
Dk-RT-01	5,120,819	417,033	80,365	702,484	7,489,779	129,338
Dk-RT-02	5,390,283	441,405	82,972	756,198	7,615,559	85,031
Dk-RT-03	5,344,772	451,128	74,644	697,147	7,436,125	89,748
Dk-Cold-01	6,064,871	508,794	81,101	882,977	8,485,329	122,077
Dk-Cold-02	5,536,037	462,189	82,186	776,963	7,260,526	87,956
Dk-Cold-03	7,152,870	535,175	97,596	1,008,298	10,129,569	118,318

Table. I.12. Stability Experiment Day 8 - Peak area of 4 internal standards derivatized and stored in 100% ACN. One set stored at room temperature exposed to light, one set stored at room temperature not exposed to light, and a third set stored in the freezer not exposed to light.

Sample	PUT-d8	SPD-d8	1,7-DAH	BEN-77	BEN-105
Lt-RT-01	20,499,876	2,710,064	34,329,538	1,575,474	1,961,500
Lt-RT-02	18,479,433	2,485,722	37,442,168	1,063,906	1,284,385
Lt-RT-03	19,947,632	2,944,631	35,884,547	819,155	972,565
Dk-RT-01	14,447,635	1,988,509	27,666,997	861,844	1,023,188
Dk-RT-02	14,768,514	1,940,416	31,890,064	792,428	972,019
Dk-RT-03	14,301,552	1,874,305	29,895,156	747,559	970,800
Dk-Cold-01	16,952,688	2,165,158	33,497,199	764,221	920,341
Dk-Cold-02	14,832,156	1,956,582	23,020,853	741,921	946,673
Dk-Cold-03	19,648,496	2,647,268	35,231,637	958,500	1,244,697

Table. I.13. Stability Experiment Day 1 - Peak area of 6 PAs derivatized and stored in 50:50 ACN:H_2O. One set stored at room temperature exposed to light, one set stored at room temperature not exposed to light, and a third set stored in the freezer not exposed to light.

Sample	PUT	N8-ASPD	N1-ASPM	SPD	CAD	SPM
Lt-RT-01	4,570,192	418,838	89,475	513,839	6,621,422	84,546
Lt-RT-02	4,988,465	666,691	110,607	550,149	6,882,557	88,027
Lt-RT-03	5,081,079	449,126	100,371	462,001	6,608,156	87,648
Dk-RT-01	4,727,397	615,183	100,436	436,618	6,532,797	89,382
Dk-RT-02	4,262,296	588,069	112,947	388,942	5,767,813	89,206
Dk-RT-03	5,033,124	634,734	120,331	467,324	6,866,592	99,082
Dk-Cold-01	4,825,892	527,548	104,948	452,076	6,374,337	111,899
Dk-Cold-02	5,316,471	490,146	106,894	460,662	7,275,363	125,268
Dk-Cold-03	4,844,632	479,609	105,903	400,533	6,668,115	95,370

Table. I.14. Stability Experiment Day 1 - Peak area of 4 internal standards derivatized and stored in 50:50 ACN:H_2O. One set stored at room temperature exposed to light, one set stored at room temperature not exposed to light, and a third set stored in the freezer not exposed to light.

Sample	PUT-d8	SPD-d8	1,7-DAH	BEN-77	BEN-105
Lt-RT-01	11,634,678	1,200,949	17,154,492	1,857,343	2,464,657
Lt-RT-02	13,563,496	1,187,224	19,249,969	1,540,041	1,963,649
Lt-RT-03	13,182,526	1,122,017	16,948,070	1,629,843	2,220,540
Dk-RT-01	12,179,091	1,119,671	18,125,342	1,937,805	2,632,636
Dk-RT-02	11,648,741	987,504	16,780,368	2,023,298	2,643,624
Dk-RT-03	13,907,296	1,216,340	19,645,068	1,882,044	2,649,510
Dk-Cold-01	13,014,655	1,215,569	20,679,393	2,230,820	2,858,648
Dk-Cold-02	14,398,546	1,221,913	20,674,751	2,105,175	2,796,664
Dk-Cold-03	13,302,066	1,103,224	17,064,168	1,975,381	2,788,477

Table. I.15. Stability Experiment Day 1 - Peak area of 6 PAs derivatized and stored in 100% ACN. One set stored at room temperature exposed to light, one set stored at room temperature not exposed to light, and a third set stored in the freezer not exposed to light.

Sample	PUT	N8-ASPD	N1-ASPM	SPD	CAD	SPM
Lt-RT-01	2,240,468	295,230	53,583	421,755	2,833,105	65,249
Lt-RT-02	2,693,766	382,631	80,590	515,010	3,444,240	98,056
Lt-RT-03	2,839,559	392,772	94,368	498,313	3,564,466	109,175
Dk-RT-01	2,755,629	301,832	98,185	416,492	3,677,111	117,528
Dk-RT-02	2,733,019	358,615	109,943	442,078	3,685,192	122,707
Dk-RT-03	2,686,452	365,398	108,559	397,503	3,560,071	122,388
Dk-Cold-01	2,478,641	330,343	94,140	389,534	3,487,574	112,123
Dk-Cold-02	2,645,033	307,127	94,233	379,560	3,746,331	140,528
Dk-Cold-03	2,784,193	289,725	95,787	370,567	3,755,613	137,014

Table. I.16. Stability Experiment Day 1 - Peak area of 4 internal standards derivatized and stored in 100% ACN. One set stored at room temperature exposed to light, one set stored at room temperature not exposed to light, and a third set stored in the freezer not exposed to light.

Sample	PUT-d8	SPD-d8	1,7-DAH	BEN-77	BEN-105
Lt-RT-01	6,825,792	1,145,599	9,908,986	899,792	993,101
Lt-RT-02	8,237,240	1,353,148	10,099,538	1,099,975	1,258,098
Lt-RT-03	8,117,173	1,394,224	10,794,268	1,431,447	1,717,066
Dk-RT-01	7,695,614	1,219,925	10,344,185	1,678,554	2,046,629
Dk-RT-02	7,462,166	1,236,970	10,172,355	1,457,133	1,912,691
Dk-RT-03	7,340,890	1,183,099	9,859,543	1,582,851	1,923,278
Dk-Cold-01	6,937,652	1,166,727	9,328,775	1,484,428	1,893,610
Dk-Cold-02	7,165,037	1,195,877	9,745,632	1,802,622	2,193,436
Dk-Cold-03	7,701,561	1,142,114	9,504,573	1,990,089	2,587,560

J. Raw Data from Analysis of Fruit Flies

Table. J.1. Raw data of two whole fruit fly homogenate with a high and low amount of internal standard added.

Sample	PUT	PUT-d8	SPD	SPD-d8
low-1-01	1,400,734	4,965,456	4,509,085	12,130,475
low-1-02	1,565,929	5,592,384	4,459,407	12,284,865
low-1-03	1,759,761	6,337,260	3,785,696	10,483,953
low-2-01	1,246,448	4,524,614	3,856,911	10,705,043
low-2-02	1,256,657	4,384,012	3,899,876	10,570,507
low-2-03	1,250,221	4,463,255	3,827,868	10,552,196
low-3-01	892,792	3,188,224	3,563,533	9,913,278
low-3-02	995,151	3,611,074	3,100,167	8,474,691
low-3-03	1,118,241	3,994,792	3,032,075	8,451,300
high-1-01	1,907,217	12,928,584	3,999,876	21,008,883
high-1-02	1,799,330	13,008,025	3,933,730	20,624,485
high-1-03	2,100,301	13,323,940	4,009,085	20,847,902
high-2-01	1,524,066	10,327,488	3,927,868	20,765,561
high-2-02	1,437,853	10,390,946	3,975,169	20,903,003
high-2-03	1,598,361	10,573,303	3,935,417	20,436,239
high-3-01	1,928,463	12,766,104	3,609,790	18,675,702
high-3-02	1,819,374	12,844,547	3,451,528	17,842,642
high-3-03	2,023,698	12,856,492	3,804,016	19,923,706

Table. J.2. Raw data of two aliquot volumes studied for whole fruit fly homogenate.

Sample	PUT	PUT-d8	SPD	SPD-d8
100µL-1-01	3,601,906	6,829,852	9,530,903	13,434,044
100µL-1-02	4,086,436	7,066,880	10,775,063	15,507,032
100µL-1-03	3,840,455	7,123,317	10,198,758	14,988,564
100µL-2-01	4,201,458	7,214,141	11,164,956	15,879,435
100µL-2-02	4,129,214	7,253,971	11,396,002	15,951,887
100µL-2-03	3,925,490	6,975,788	9,368,047	13,263,873
100µL-3-01	3,905,642	6,975,788	9,854,719	13,780,292
100µL-3-02	3,748,442	6,995,606	10,167,145	14,204,072
100µL-3-03	4,018,657	7,212,240	9,340,891	13,053,840
20µL-1-01	905,171	2,384,845	2,117,202	6,075,509
20µL-1-02	952,538	2,515,893	2,333,841	6,601,650
20µL-1-03	904,672	2,504,362	2,206,877	6,300,477
20µL-2-01	976,612	2,557,236	2,227,984	6,120,522
20µL-2-02	1,006,994	2,661,017	2,462,894	6,656,084
20µL-2-03	972,778	2,678,262	2,234,034	6,215,559
20µL-3-01	987,538	2,642,746	2,701,062	7,422,412
20µL-3-02	993,495	2,588,506	2,680,243	7,305,997
20µL-3-03	1,011,884	2,611,857	2,713,778	7,362,131

K. Raw Data from Analysis of Rat Liver Cell Lysates

Initial analysis of rat liver cell lysate to approximate how much internal standard to use.

Table. K.1. Raw data of peak area of PUT and SPD for old and young rat liver cell lysates.

Sample	PUT	PUT-d8
Old-01	482,276	3,233,244
Old-02	447,995	3,132,342
Old-03	528,922	3,467,400
Young-01	1,404,497	4,579,641
Young-02	1,290,248	4,273,866
Young-03	1,387,551	4,461,339

Sample	SPD	SPD-d8
Old-01	19,778,192	740,921
Old-02	20,056,307	739,513
Old-03	23,397,602	831,313
Young-01	51,080,550	610,213
Young-02	52,139,291	652,309
Young-03	56,646,077	711,226

Table. K.2. Raw data of peak area of two aliquot volumes for rat liver cell lysate.

Sample	PUT	PUT-d8	SPD	SPD-d8
10µL-young-1-01	156,815	9,250,603	5,515,150	1,608,162
10µL-young-1-02	186,339	10,857,949	7,344,455	2,347,842
10µL-young-1-03	227,134	14,160,988	9,886,784	3,010,512
10µL-young-2-01	195,547	13,066,951	7,302,667	2,962,904
10µL-young-2-02	223,157	13,498,725	8,191,205	2,926,222
10µL-young-2-03	267,054	14,852,273	8,368,372	3,177,193
10µL-old-1-01	151,290	13,933,061	3,492,376	3,163,623
10µL-old-1-02	142,949	15,466,770	3,187,360	3,147,715
10µL-old-1-03	128,286	14,482,488	3,045,403	2,942,408
10µL-old-2-01	301,692	15,302,347	8,019,043	3,001,032
10µL-old-2-02	341,220	15,868,749	8,292,385	3,050,181
10µL-old-2-03	396,693	16,718,184	9,071,677	3,139,246
50µL-young-1-01	905,672	14,515,425	25,995,958	1,775,050
50µL-young-1-02	795,172	13,175,467	24,199,586	1,546,944
50µL-young-1-03	776,179	12,674,189	23,337,759	1,573,879
50µL-young-2-01	772,994	15,656,375	18,425,958	1,696,244
50µL-young-2-02	632,088	16,127,474	20,009,972	2,043,123
50µL-young-2-03	840,150	16,976,646	18,469,538	1,511,589
50µL-old-1-01	1,087,360	17,602,826	10,681,918	2,186,250
50µL-old-1-02	470,815	18,145,476	12,499,297	2,667,691
50µL-old-1-03	458,101	17,727,715	13,405,235	2,866,006
50µL-old-2-01	1,349,642	17,340,221	29,854,027	2,313,499
50µL-old-2-02	1,352,178	17,809,212	31,897,293	2,667,947
50µL-old-2-03	1,485,446	17,514,029	32,281,463	2,338,056

PART 2: DETECTION OF VOLATILE ORGANIC COMPOUND TRACERS IN HUMAN BREATH

CHAPTER 5. INTRODUCTION

Analytical and biological monitoring for metabolites and environmental exposures in humans were limited to urine, blood, nail clippings, hair, and skin swabs, which could be very invasive and/or uncomfortable. Breath component analysis (BCA) is an ideal noninvasive method that has emerged in the past few decades and has become more attractive in many research fields for several reasons. There is little to no physical discomfort and emotional distress to the subject, and many samples can be collected without comprising a subject's health.[1,2] It is also a much simpler matrix to analyze compared to other biological matrices, especially with gas chromatography mass spectrometry (GC-MS) because it is an excellent detection method.[3]

There have been greater than 200 volatile organic compounds (VOCs) detected in breath[4,5] that can provide an abundance of information from biomarkers for disease diagnoses (metabolomics) to environmental hazard exposures. VOCs detected in breath are from both endogenous and exogenous sources. Endogenous compounds found in breath results from metabolic processes within the body, whereas exogenous compounds in the breath are from environmental exposures.

Breath analysis dates back as far as the Roman and ancient Greek times, where the sweet odor of a person's breath was indicative of diabetes[5-7], which is known now due to the presence of acetone. This was one of the many documented ways in which BCA was used as diagnostic tool in medicine. Recently, the measurement of endogenous compounds have become a widely accepted routine metabolomic technique used in many research laboratories by physicians, and researchers, and forensic labs to probe for potential biomarkers of early disease states and or illnesses.[6-8]

Presently there are very few practiced and trusted BCA methods.[9] One common BCA procedure is practiced in medicine to test for the bacteria *Helicobacter pylori* to identify infections in the gastrointestinal tract that can cause ulcers. Another BCA method was for the detection of NO as a diagnosis for inflammation of the airways.[10-12] Lipid peroxidation of n-3 and n-6 polyunsaturated fatty acids resulted in ethane and pentane by-products, respectively, that have been reported in over 400 papers.

Measurements of exogenous compounds have been the main focus of environmental and toxicological exposure studies for many decades.[2,3,13-17] Exogenous VOCs in breath are a direct measure of exposure to toxicants from environmental, household, and workplace exposures to chemicals.[18-21] Exposures to VOCs often result in retention by body tissue through modes of ingestion, inhalation and or skin contact[22], and residence times in vivo may range from minutes to weeks depending upon the tissues in which they reside.[11,19,21] The most recognized breath analysis of exogenous VOC that is used worldwide is the measurement of ethanol to estimate the blood alcohol concentration from breath samples.[23-27] Public health professionals routinely assess risk by measuring exposure to VOCs in the workplace using dosimeters or by testing blood and urine. Dosimeters are a convenient way to measure exposure, but they don't provide data about the levels of VOCs that remain in the breath. Direct measurements of VOCs in breath have not been in common practice because it requires more advanced techniques in sample collection and analysis.

There are many other potential applications for BCA that one can list that are yet to be explored. One of these, a potential forensic application, is the subject of this thesis. An example would be to determine by BCA if a subject has been in a particular room in the

last 24 hours. If a cocktail of VOC were introduced into room air in some inconspicuous way such as an air freshener device, traces of these specific compounds would remain in the breath of occupants. Subsequent analysis of a subject's breath could reveal these compounds in proportions that mirror those placed in the air freshener mixture. Rooms where this might be used would include sensitive document rooms, restricted access areas, safe deposit vaults, etc.

5.1. Review of Literature

Although it is a relatively new and progressing technique, BCA has been studied and in great depths by various research groups for over 40 years.[28] Breath samples are a simpler matrix than other biological sample types, but there are major hurdles that must be overcome in BCA for it to be a quantifiable measure. Many published works have investigated topics specific to BCA including: types of breath samples, methods for standardization of breath collection, normalization of data, differentiating exogenous from endogenous compounds, and how to achieve a proper blank. These topics are reviewed in the following sections.

5.1.1. Breath Sample Types for BCA

BCA could be carried out by collecting tidal breath, alveolar breath, mixed expired breath, and or breath condensate (exhaled breath condensate, EBC).[14,16] Tidal breath is the breath that is exhaled in the natural rhythm of breathing or resting breathing. In some literature the tidal breath was also referred to as dead air space because it is the air that is in the mouth, trachea, and bronchi.[29] Alveolar breath, sometimes referred to as end-tidal breath, is the expired breath that represents the gas exchanged between the

blood and alveoli structures.[1] Mixed expired breath is alveolar breath diluted by tidal breath.[14]

Exhaled breath condensate (EBC) is tidal and or alveolar breath cooled and condensed. EBC contains mainly water, carbon dioxide, volatile and non-volatile compounds in the form of gases and aerosols that are condensed at subzero temperatures.[7,16,30,31] The detection limits are controlled by the time of sampling and efficiency in which the vapor can be collected.

5.1.2. Standardization of Sample Collection

Standardization of breath sample collection is more difficult with BCA than with blood, or urine. The average person has a lung capacity of about 6 - 10 liters with a respiratory rate of 10-20 breaths a minute. [29,32,33] With such a large range in volume and breathing rate, it has been proven to be a challenge to precisely collect samples from subject to subject and even multiple samples from the same subject. BCA is a valuable qualitative diagnostic tool, but to be a quantitative technique, methods for standardization of breath collection is needed and, more importantly, normalization of data based on the biometrics of the subject is required for inter-comparison of data between subjects.

Breath samples are commonly collected in electropolished stainless steel canisters or Tedlar gas sampling bags that come in different volumes. Using a container with a fixed volume can standardize the amount of breath collected, but it is difficult to determine the fractions of tidal to alveolar breath collected. Carbon dioxide (CO_2), which is present in pure alveolar breath at 5.5%, can be simultaneously monitored to ensure that alveolar breath is collected, but this method presents additional factors to consider. For

example, the respiration rate and concentration of CO_2 would increase if a person holds their breath or if they were not in a resting state.[18,34,35] Also, if nose clamps were not used during sampling, external air would dilute the sample.

5.1.3. Normalization of Data

High variations in BCA concentrations were reported due to the lack of a uniform method for data normalization.[36] Quantification of compounds in BCA is related to the standardization of breath sample collection but similar problems are encountered. To have a diagnostic value, a quantitative measure of EBC is desired to have units such as ng/min or ng/kg of body mass per minute in resting state as two examples. However, numerous factors are present that make this difficult. Dilution of compounds due to air temperature, respiration rate, and lung capacity are among the many factors that change the concentration of VOCs in breath and EBC.[16] In the previous section it was mentioned that CO_2 concentration measurements to standardize breath collection found little use because of the other variables involved in collection and variations among subjects. Since alveolar breath correlated best with blood gas VOC concentrations. It has been suggested that all data be normalized to 5.5% CO_2 concentrations. However, normalization of the data using CO_2 concentrations makes breath collection a complicated non-portable tool. In addition, there are other factors that need to be addressed, as it has been reported that the breathing rate and environment effects the concentration of CO_2 even from the same subject within two consecutive samples were not the same.[19,36,37]

Some authors have also utilized modeling methods, data manipulation, and different types of calibrants to precisely and accurately analyze BCA.[38-40] A recent

review summarized and tabulated all the compounds, analysis techniques, and statistical approaches studied over the past few decades.[41] In summary, despite efforts in many published works have been made to increase normalization and standardization of BCA data, they are still presently the most difficult issues that limits BCA as a diagnostic tool.

5.1.4. 'Background' Sample

The lack of methods to differentiate exogenous from endogenous VOCs makes BAC a difficult tool to use for any study. To identify VOCs, it was very important to quantify exogenous compounds are present in breath. The problem was compounded by the fact that many endogenous compounds were also found in the air we breathe, being metabolites with biological origins. There are many pitfalls in analyzing exogenous and endogenous compounds in breath. For example it is difficult to determine if acetone in a breath sample was due to an environmental exposure or if it was a product of the decarboxylation of ketones from an anabolic process.[39] Therefore a 'background' sample was usually collected.

'Background' samples are air or breath samples collected in an attempt to identify exogenous VOCs from endogenous VOCs. Pliel et al. and other authors have reviewed three techniques to differentiate VOC types: 1) subtracting a sample of the air from a subject's breath sample (alveolar gradient), 2) simultaneously measuring the environment air and the subject's air, and 3) defining a metabolic pathway in which the particular VOC(s) were produced.[18,39,42] Even with the aforementioned techniques there lies a larger problem in that some or even all chemicals have a residence time in breath after exposure, this would most likely occur if the subject was exposed to the same VOCs in

their daily routine.[19,21] For example, benzene in urban air was detected in breath samples days after exposure. Therefore flushing the breath with clean air does not remove this problem. Treatments of exogenous VOCs are a great problem for the measurement of endogenous VOCs and long-term studies of environmental exposures.

Reports of the measurement of BCA of some exogenous compounds have only been for short (i.e. several hours) periods. Nonetheless, re-exposure to the same VOC(s) and chemicals residing within the tissues were another problem of BCA, especially at ultratrace concentrations (sub ppb range). The National Institute for Occupational Safety and Health has set forth exposure limits for many toxic VOCs, but there was still a concern about the chronic effects of low concentration exposures.[15,43]

5.2. Objectives

The objective of this project was to develop and validate analytical methods for BCA measurement at the ppb to ppt range to detect the presence of endogenous compounds that remained in the breath for at least 72 hours post exposure. Having such a sensitive analytical method capable of measuring compounds at low concentration would provide a tool that is not yet available for compounds that are of interest, like gas anesthetics. Since we were only interested in whether or not specific VOCs were retained for long periods of time, the problems of high variability in breath collection and the difficulty in differentiating exogenous and endogenous compounds were only of secondary interest to this study.

Secondly, we envisioned this study as a proof of concept that this method could be a possible tool in forensics in the form of physical evidence to link suspects or victims

to a crime scene. Forensic scientists are increasingly relying upon collecting physical evidence using techniques with greater sensitivity, improved discrimination power, simplicity of application, and minimal sample analysis time. Since subject(s) retain VOCs in their breath then it may be possible to use unique, non-native compounds as tracers that could be measured by GC-MS. For example, this may lead to a simple test to determine whether suspect(s) were present in a high security or limited access room, or if a victim was removed from the actual crime scene.

Our main objective was to investigate and use non-native compound(s) that were not commonly found in the environment, workplace, or home and use it as a "tracer VOC". To test this hypothesis, subjects were exposed to low (1-2 parts per million (ppm)) concentrations of the compound(s) in a controlled environment for a fixed amount of time. EBC breath samples were collected at timed intervals to determine if the compound was present after this single exposure. Sampling of breath continued until they were no longer detectable.

References

1 Ligor, T. *Critical Reviews in Analytical Chemistry* 2009, *39*, 2.

2 Lindstrom, A. B.; Pleil, J. D. *Biomarkers* 2002, *7*, 189.

3 Amorim, L. C. A.; de L. Cardeal, Z. *Journal of Chromatography B* 2007, *853*, 1.

4 Chen, X.; Xu, F.; Wang, Y.; Pan, Y.; Lu, D.; Wang, P.; Ying, K.; Chen, E.; Zhang, W. *Cancer* 2007, *110*, 835.

5 Hill, D.; Binions, R. *International Journal on Smart Sensing and Intelligent Systems* 2012, *5*, 401.

6 Dent, A. G.; Sutedja, T. G.; Zimmerman, P. V. *Journal of thoracic disease* 2013, *5 Suppl 5*, S540.

7 Kim, K. H.; Jahan, S. A.; Kabir, E. *Trends in Analytical Chemistry* 2012, *33*, 1.

8 Di Francesco, F.; Fuoco, R.; Trivella, M. G.; Ceccarini, A. *Microchemical Journal* 2005, *79*, 405.

9 van Mastrigt, E.; de Jongste, J. C.; Pijnenburg, M. W. *Clinical & Experimental Allergy* 2015, *45*, 1170.

10 Klein, P. D.; Malaty, H. M.; Martin, R. F.; Graham, K. S.; Genta, R. M.; Graham, D. Y. *Am J Gastroenterol* 1996, *91*, 690.

11 Cao, W.; Duan, Y. *Clinical Chemistry (Washington, DC, United States)* 2006, *52*, 800.

12 Cikach, F. S.; Dweik, R. A. *Progress in Cardiovascular Diseases* 2012, *55*, 34.

13 Perbellini, L.; Faccini, G. B.; Pasini, F.; Cazzoli, F.; Pistoia, S.; Rosellini, R.; Valsecchi, M.; Brugnone, F. *British Journal of Industrial Medicine* 1988, *45*, 345.

14 Wilson, H. K. *Scandinavian Journal of Work, Environment & Health* 1986, *12*, 174.

15 Tanko, B.; Molnar, L.; Fulesdi, B.; Molnar, C. *Journal of Anesthesia & Clincal Research* 2014, *5*, 426/1.

16 Corradi, M.; Mutti, A. *Acta Bio Medica : Atenei Parmensis* 2005, *76*, 20.

17 Cone, J. E.; Shusterman, D. *Environmental Health Perspectives* 1991, *95*, 53.

18 Lourenço, C.; Turner, C. *Metabolites* 2014, *4*, 465.

19 Beauchamp, J. *Journal of Breath Research* 2011, *5*, 037103/1.

20 Veres, P. R.; Faber, P.; Drewnick, F.; Lelieveld, J.; Williams, J. *Atmospheric Environment* 2013, *77*, 1052.

21 Wallace, L.; Buckley, T.; Pellizzari, E.; Gordon, S. *Environmental Health Perspectives* 1996, *104*, 861.

22 Jo, W. K.; Weisel, C. P.; Lioy, P. J. *Risk Analysis* 1990, *10*, 575.

23 Andersson, A.; Wirehn, A.-B.; Olvander, C.; Ekman, D. S.; Bendtsen, P. *BioMed Central Public Health* 2009, *9*, 229.

24 Barquin, J.; Luna, J. d. D.; Hernandez, A. F. *Forensic Science International* 2008, *177*, 140.

25 Harding, P.; Field, P. H. *Journal of Forensic Sciences* 1987, *32*, 1235.

26 Jones, A. W.; Andersson, L. *Forensic Science International* 2003, *132*, 18.

27 Flanagan, N.; Dillingham, S. D.; Whitcomb, D.; Ross, G. *Alcohol Toxicology for Prosecutors Targeting Hardcare Imparied Drivers*, 2003.

28 Dweik, R. A.; Amann, A. *Journal of Breath Research* 2008, *2*, 030301.

29 Alonso, M.; Sanchez, J. M. *Trends in Analytical Chemistry* 2013, *44*, 78.

30 Risby, T. H.; Solga, S. F. *Applied Physics B Lasers and Optics* 2006, *85*, 421.

31 Horvath, I.; Hunt, J.; Barnes, P. J.; Alving, K.; Antczak, A.; Baraldi, E.; Becher, G.; van Beurden, W. J. C.; Corradi, M.; Dekhuijzen, R.; Dweik, R. A.; Dwyer, T.; Effros, R.; Erzurum, S.; Gaston, B.; Gessner, C.; Greening, A.; Ho, L. P.; Hohlfeld, J.; Jobsis, Q.; Laskowski, D.; Loukides, S.; Marlin, D.; Montuschi, P.; Olin, A. C.; Redington, A. E.; Reinhold, P.; van Rensen, E. L. J.; Rubinstein, I.; Silkoff, P.; Toren, K.; Vass, G.; Vogelberg, C.; Wirtz, H. *European Respiratory Journal* 2005, *26*, 523.

32 Yuan, G.; Drost, N. A.; Mclvor, R. A. *McMaster University Medical Journal* 2013, *10*, 23.

33 Pleil, J. D.; Lindstrom, A. B. *American Journal of Industrial Medicine* 1995, *28*, 109.

34 Cope, K. A.; Watson, M. T.; Foster, W. M.; Sehnert, S. S.; Risby, T. H. *Journal of Applied Physiology* 2004, *96*, 1371.

35 Levitt, M. D.; Ellis, C.; Furne, J. *Dig Dis Sci* 1998, *43*, 1938.

36 Miekisch, W.; Schubert, J. K.; Noeldge-Schomburg, G. F. E. *Clinica Chimica Acta* 2004, *347*, 25.

37 Thekedar, B.; Oeh, U.; Szymczak, W.; Hoeschen, C.; Paretzke, H. G. *Journal of Breath Research* 2011, *5*, 016001.

38 Pleil, J. D.; Lindstrom, A. B. *Clinical Chemistry (Washington, DC, United States)* 1997, *43*, 723.

39 Pleil, J. D.; Stiegel, M. A.; Risby, T. H. *Journal of Breath Research* 2013, *7*, 017107/1.

40 Luczak, S. E.; Rosen, I. G. *Alcoholism: Clinical and Experimental Research* 2014, *38*, 2243.

41 Pereira, J.; Porto-Figueira, P.; Cavaco, C.; Taunk, K.; Rapole, S.; Dhakne, R.; Nagarajaram, H.; Câmara, J. S. *Metabolites* 2015, *5*, 3.

42 Phillips, M. *Analytical Biochemistry* 1997, *247*, 272.

43 Bierbaum, P. J.; Dement, J. M.; Geraci, C. L., Jr. *DHEW (NIOSH) Publication (United States)* 1977, *77-140*, 194 pp.

CHAPTER 6. EXPERIMENTAL

6.1. Subject(s) Recruitment Protocol

Institutional Review Board (IRB) approval was confirmed before any outside subject(s) were asked for their participation, a copy of the approval is found in Appendix A. The approval was contingent on the use of only the 4 of the 6 analytes of interest and at concentrations below 2 parts per million each. Data from this proof of concept study were collected from breath samples of the principal investigator, Dale Chatfield, and myself. No other subjects participated in this study.

For future collections from other subject(s) the following protocol would be followed. Subject(s) would be given the information required by the IRB, and a consent form would be provided to all subjects willing to participate. Following a screening process to eliminate subject(s) who are pregnant, or have health concerns subject(s) would be informed of the protocol regarding either breath samples or EBC collection, then each subject would be exposed to one or a combination and concentration of the tracer chemical(s) within the concentration limits approved by the IRB. Subject(s) would wear an exposure mask that was attached to a tank containing a gas mixture that contained the tracer chemical(s) to administer them to the subject in a controlled environment. The duration of exposure will be 45 minutes. Following exposure a breath sample or EBC would be collected. During follow-up visits to the lab additional samples would be collected in varying time intervals until the tracer(s) would be no longer detected. All participants would be allowed to withdraw from the study at any time for any reason.

6.2. Chemicals, Materials, and Instruments

Internal standards were prepared with a mixture of benzene-d6 (BEN-d6, CAS# 1076-43-3), toluene-d8 (TOL-d8, CAS# 2037-26-5), and ρ-xylene-d10 (XYL-d10, CAS# 41051-88-1) (Cambridge Isotope Laboratories, Tewksbury, MA). Chemicals used for exposure were: α,α,α-trifluorotoluene (TFT, CAS# 98-08-8) (Sigma-Aldrich, Saint Louis, MO), 1,1,1,3,3,3-hexafluoro-2-(fluoromethoxy)propane (sevoflurane, SEV, CAS# 28523-86-6) (Matrix Scientific, Columbia, SC), 3-fluorobenzotrifluoride (3-FBT, CAS# 401-80-9) (Oakwood Products Inc., West Columbia, SC), 4-chlorobenzotrifluoride (4-CBT, CAS# 98-56-6), 2,2-dichloro-1,1-difluoroethyl methyl ether (methoxyflurane, MET, CAS# 76-38-0), and 2-chloro-1-(difluoromethoxy)-1,1,2-trifluoroethane (enflurane, ENF, CAS# 13838-16-9) (Alfa Aesar, Ward Hill, MA).

Zero air (hydrocarbon free air, HCF, CAS# 132259-10-0) was used to purge the breath collector apparatus. For EBC samples, liquid nitrogen (CAS# 7727-37-9) was used to trap the breath condensate, 4.8-grade nitrogen gas (CAS# 7727-37-9) was used during the desorption step, nitrogen gas was also used in the canister cleaning apparatus, and 5.0-grade helium gas (CAS# 7440-59-7) was used for the gas chromatograph and mass spectrometer. All gases and liquid nitrogen was purchased from Praxair (Danbury, CT). The adsorbent traps were packed with Tenax® TA mesh size 35/60 (Sigma-Aldrich, Fluka, St. Louis, MO, CAS# 24938-68-9), and Carbopack™ B mesh size 60/80 (Supelco, Bellefonte, PA, CAS# 1333-86-4).

All traps were prepared in-house using stainless tubes and Swagelok® fittings purchased from San Diego Fluid System Technologies (San Diego, CA). 1.0 liter TO-Can Air Sampling Canisters were purchased from Restek (Bellefonte, PA). Chemical

tracers and internal standards were prepared in 2.2 L and 0.870 L steel cylinder tanks, respectively. The tanks were Scott specialty gas tanks that were cleaned and re-purposed. Each subject used a disposable PulmoGuard II mouthpiece (SDI Diagnostics, Easton, MA) for breath collections. The breath collection apparatus and canister cleaning apparatus were built in-house with stainless steel and Teflon parts that were available in the laboratory. Breath condensate was collected on a glass subliminator (Ace Glass, Vineland, NJ).

Samples collected in canisters and traps for GC-MS analysis were first concentrated with a Tekmar Dohrmann 3100 (Teledyne Tekmar, Mason, OH). Samples were desorbed onto a .1.6 mm (O.D.) U-shaped cryogenic trap made from Silico steel tubing (Restek, Bellefonte, PA) mounted inside the GC oven. The outlet of the trap was connected to a low volume Swagelok® "T" fitting San Diego Fluid System Technologies San Diego, CA), with the GC column attached to the second port, and the third port fitted with a Swagelok® cap. The samples were separated on a DB-5 60 m x 0.250 μm (I.D.), 0.5 μm column (Agilent J&W Scientific, Santa Clara, CA). Sample concentrator and GC-MS set-up is shown in Figure 6.1. Analysis of samples was carried out on a GC-MS system that was a modified Hewlett-Packard 5890 gas chromatograph (Hewlett-Packard, Wilmington, DE) coupled to a Mass Selective Detector 5973 (Agilent Technologies, Santa Clara, CA). Data acquisition and processing were accomplished by using Agilent Technologies' Enhanced ChemStation software. Spectral matches were carried out with the NIST Mass Spectral Search Program software version 2.0 with a database provided by the Standard Reference Data Program of the National Institute of Standards and Technology (Gaithersburg, MD).

Figure 6.1. Analysis set-up. Left to right: Agilent 5973 mass spectrometer, HP 5890 gas chromatograph, and Tekmar Sample Concentrator.

6.3. Preparation of Internal Standards

A clean 0.870 L cylinder was used to prepare internal standard gases by adding by syringe pure liquid samples of benzene-d6 (BEN-d6), toluene-d8 (TOL-d8), and ρ-xylene-d10 (XYL-d10) (Figure 6.2), followed by pressurization to 687 kPa (100 psi), and then heated thoroughly to mix the chemicals in a gas phase. The cylinder was allowed to cool to room temperature and connected to the breath collection apparatus.

Two different internal standard cylinders were prepared. For breath collection in canisters, the internal standard cylinder (0.870 liter cleaned Scott cylinder) was injected with 3.0 μL each of BEN-d6, TOL-d8, and XYL-d10 and then pressurized to 687 kPa with 4.8-grade nitrogen gas resulting in a final concentration of 31.0 parts per million (ppm) (1.08 ng/mL), 26.0 ppm (1.08 ng/mL), and 22.6 ppm (1.08 ng/mL), respectively. For adsorbent traps, the internal standard cylinder had a final concentration of 1180 parts per billion (ppb) (41.0 ng/mL), 992 ppb (41.0 ng/mL), and 861 ppb (41.3 ng/mL) for

BEN-d6, TOL-d8, and XYL-d10, respectively. Concentrations in terms of ppm or ppb of each compound was calculated from the equation:

$$\text{ppm} = 10^6 \frac{moles\ of\ x}{moles\ of\ N_2} \quad (2.1)$$

$$\text{ppb} = 10^9 \frac{moles\ of\ x}{moles\ of\ N_2} \quad (2.2)$$

Where moles of x is the moles of compound, and moles of N_2 is the moles of gas used to pressurize the cylinder from vacuum to 687 kPa.

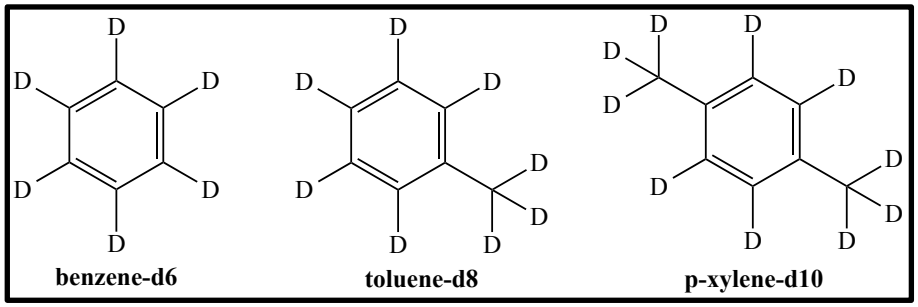

Figure 6.2. Structure of internal standards.

6.4. Preparation of Chemical Tracers in Exposure Device

The exposure device was assembled in our laboratory with available parts. Figure 6.3.A shows a schematic of the device and its parts, and Figure 6.3.B is a picture of the assembled device. A 2.2-liter empty clean evacuated Scotty cylinder was used to prepare the gases. A pressure gauge, pressure regulator, and flow controller was attached between the tank and the mask. A pressure regulator controlled the pressure to a flow controller, which provided accurate low flow rates. With this arrangement, a low constant flow of 20 mL/min at 20 psi was achieved. A flexible Teflon tube extended from the flow controller to a modified sleep apnea mask.

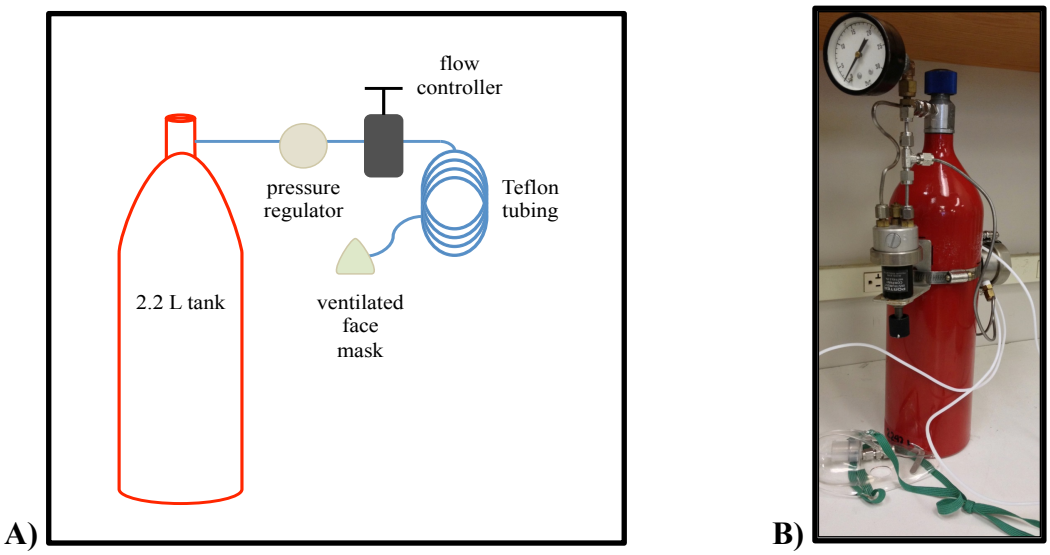

Figure 6.3. Scotty tank used for preparing analytes at varying concentrations. A) Schematic of the tank, B) Picture of the tank used.

The tank was injected with pure solutions of enflurane (ENF), sevoflurane (SEV), methoxyflurane (MET), α,α,α-trifluorotoluene (TFT), 3-fluorobenzotrifluoride (3-FBT), and 4-chlorobenzotrifluoride (4-CBT) (Figure 6.4) to attain a concentration of 500 parts per million (ppm) each of any one or combination of chemicals. The concentrations of ppm were calculated with Equation 2.1. The cylinder was pressurized to 412 kPa (60 psi) with HCF air. The mask contained holes to allow room air to enter the mask and blend with the gasses flowing from the tank. The final concentrations of the tank resulted in a maximum exposure of 2 ppm of each compound within a 45-minute time period.

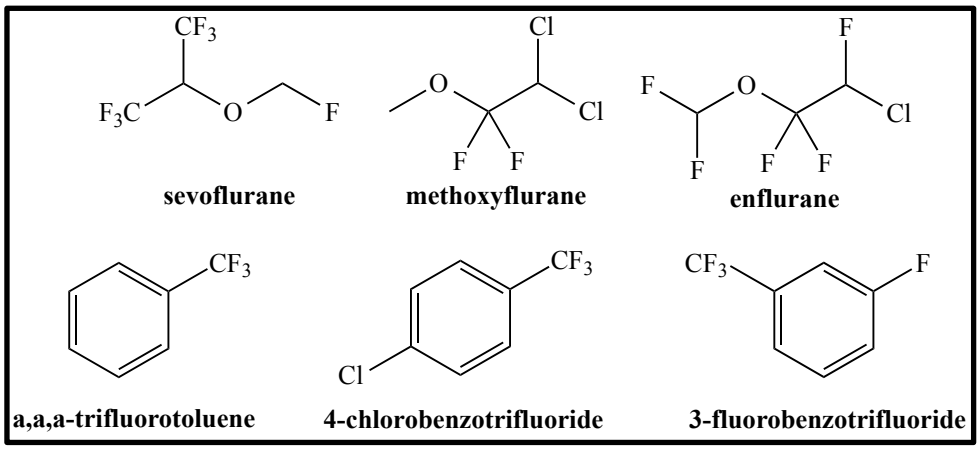

Figure 6.4. Structure of chemical tracers.

6.5. Canister Cleaning Apparatus and Protocol

Proper canister cleaning was required to ensure that trace levels of any of the investigated compounds were not present. The canister cleanup steps were adapted from the California Environmental Protection Agency Air Resources Board standard operating procedures.[1] A vacuum line was fabricated from 1.27 cm O.D. seamless stainless steel tubing and stainless steel Swagelok® fittings shown in Figure 6.5. All canisters were cleaned with a process that used 3 full cleaning and venting cycles before each use. Each canister full cleaning cycle was carried out in an oven set to 80^{o}C and consisted of the following steps: 1) ventilation to atmospheric pressure, 2) pressurization to 206 kPa (30 psi) with humidified N_2 gas, 3) equilibration time of 10 minutes, 4) evacuation of cylinder to 1.0 x 10^{-1} torr, and 5) pressurization to 206 kPa with humidified N_2 gas. Steps 1-5 were repeated two more times and the final step was evacuation of the cylinder to 1.0 x 10^{-1} torr. As shown in Figure 6.5, 1-4 canisters could be attached to the apparatus through stainless steel Swagelok® fittings inside the oven.

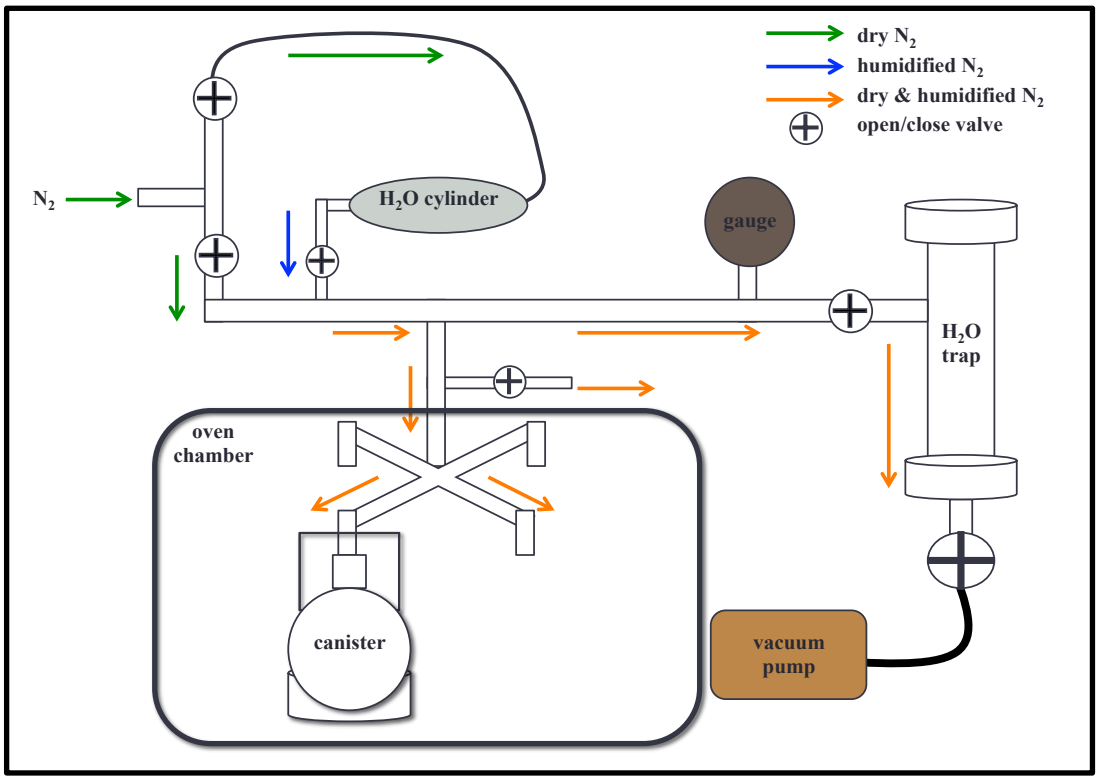

Figure 6.5. Canister cleaning apparatus.

6.6. Breath and Exhaled Breath Condensate (EBC) Collection Apparatus

The apparatus was setup to collect breath samples in canisters or EBC in the breath condensate collector. It was similar to an IRB approved design used in prior works carried out in our lab.[2] Each subject used a personal disposable mouthpiece that was attached to apparatus shown in Figure 6.6. Subjects were asked to inhale and exhale only through the mouth, a nose clamp was provided. Hydrocarbon free (HCF) air was used in lieu of breathing grade air to ensure that external VOCs would not contaminate breath samples. The air reservoir tube acted as a HCF air supply so that the subject would not feel any discomfort as experienced with a scuba-type rebreather apparatus. The HCF air supply was humidified by passing it through a cylinder lying on its side that was partially

filled with water. With inhalation, rebreather valve 2 (RB2) opened and rebreather valve 1 (RB1) closed; with exhalation RB2 closed and RB1 opened. The purpose of RB1 and RB2 was to allow unidirectional flow of inhalation and exhalation; the valves opened and closed automatically by gravity. Samples were collected by one of the three ways: 1) breath condensate collector, 2) gas canisters, or 3) adsorbent traps. EBC was collected with the breath condensate collector, and breath samples were collected by opening the solenoid valve for the duration of the exhalation. All critical Teflon and stainless tubes and fittings were heated to 40^{o}C ensure no condensation contamination or carryover of analyte or internal standards occurred. Although quantification of the tracers was not an objective of this project, the apparatus was also setup to precisely add known amounts of internal standards to canisters or adsorbent traps.

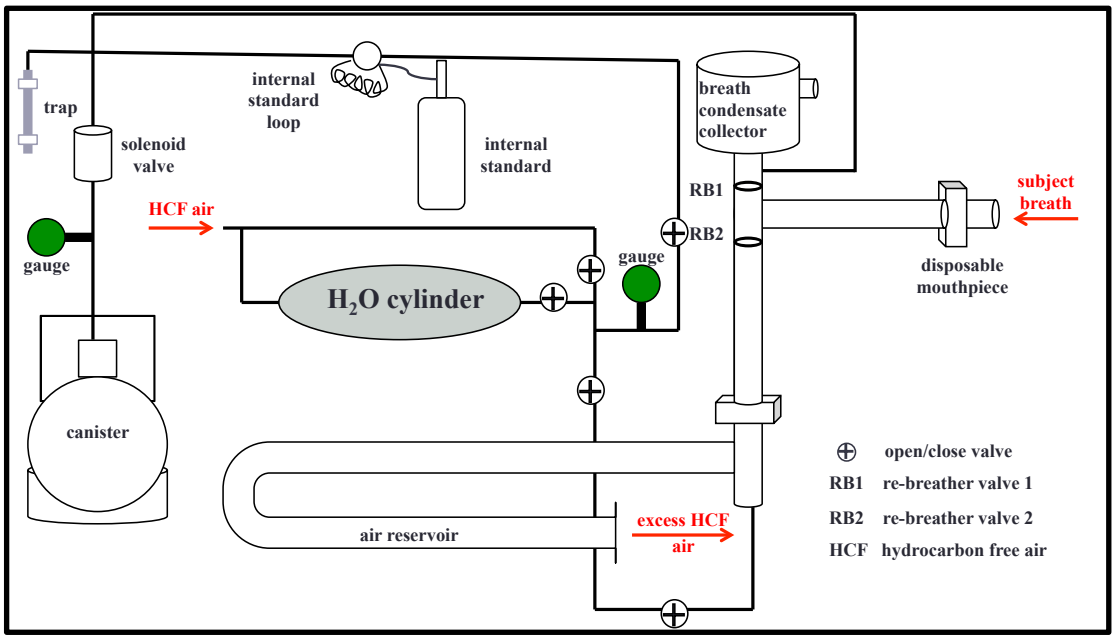

Figure 6.6. Breath and EBC collection apparatus.

6.6.1. Breath Sample Collection (Canisters) Protocol

Canisters were cleaned and evacuated to 1.0 x 10^{-1} torr using the procedure outlined in Section 6.5 before breath samples were collected. Subjects were seated in front of the breath collection apparatus that was placed at bench height, and then asked to breath only through the mouthpiece. When the subject was ready to have a breath sample collected, they were asked to flip a toggle to open the solenoid valve in Figure 6.6 until the end of their exhalation. Breath was drawn by vacuum into in the canister. Breath collection continued with the same process until the canister was full (0 mm Hg gauge pressure), which was approximately 5-8 breaths. Then 250 µL of the gaseous internal standard sample containing 26.9, 26.9, and 27.1 ng of BEN-d6, TOL-d8, and XYL-d10, respectively was added using the apparatus shown in Figure 6.6. Canisters were

pressurized to 206 kPa with HCF air, heated to 80^{o}C for 30 minutes, and then cooled to room temperature before analysis.

6.6.2. EBC Collection

For exhaled breath condensate collection, the condensate was desorbed onto an adsorbent trap in preparation for analysis. The next section will explain the adsorbent trap preparation steps followed by a section describing the EBC collection protocol.

6.6.2.1 Preparation of adsorbent traps

Traps were prepared with 9.5 cm long, 0.35 mm O.D. stainless steel tubing and Swagelok® fittings. Traps were packed with Tenax® and Carbopack™ B, and glass wool was added between each packing material and at the ends of the trap. The weaker adsorbent material was Tenax®, a 2,6-diphenylene oxide polymer resin, and the stronger adsorbent was Carbopack™ B, a graphitized carbon black. Tenax® was good for adsorbing and desorbing compounds with approximately 6-27 carbon atoms, and Carbopack™ B was suitable for compounds with 2-5 carbon atoms of higher volatility such as acetone. Approximately 0.23 g Tenax® and 0.17 g Carbopack™ B were loosely packed, resulting in trap lengths for Tenax® and Carbopack™ B of 50 cm and 35 cm respectively (Figure 6.7). Traps were then conditioned by passing N_2 gas at 20 mL/min at 220^{o}C for 4 hours before use.

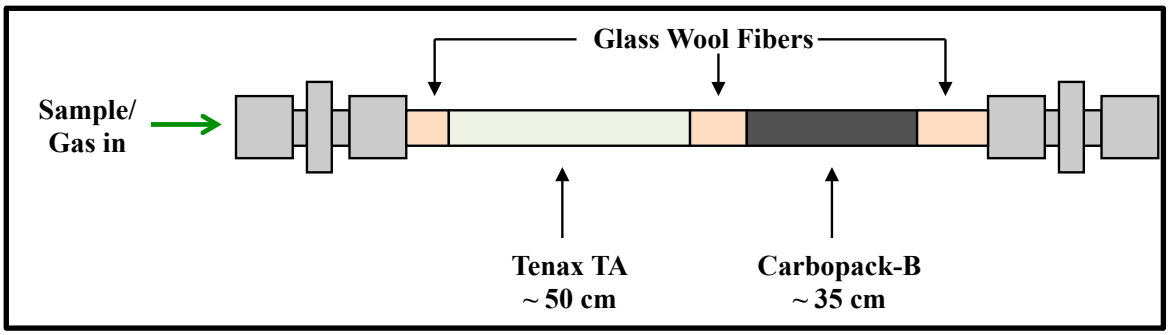

Figure 6.7. Adsorbent trap and approximate length of each adsorbent material.

6.6.2.2 EBC collection protocol

Liquid nitrogen was added into the cavity of the breath condensate collector (subliminator) shown in Figure 6.6. Subjects were seated in the same manner as described for the breath collection protocol and asked to breathe in the same normal manner as before and provide the same number of breaths in every sample, which was 25-30 breaths. Once the collection was complete, the subliminator was removed from the apparatus and connected to an adsorbent trap and the condensate was thermally desorbed onto the adsorbent trap (Figure 6.8). The purging gas, N_2 was set at a flow rate of 75 mL/min and the subliminator was directly heated with a heat gun for duration of approximately 10 minutes. The trap was then removed and connected to the apparatus shown in Figure 6.6 so that 1.02, 1.02, and 1.03 ng of BEN-d6, TOL-d8, and XYL-d10, respectively were precisely added via the gas sampling loop. Finally, the trap was removed and connected to the Tekmar sample concentrator for analysis.

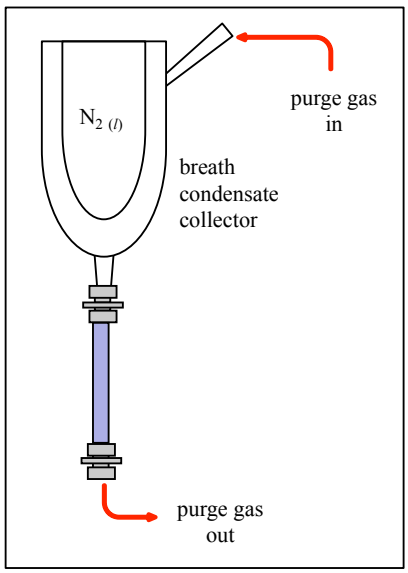

Figure 6.8. Subliminator device for EBC collection, gas flow direction for the desorption of EBC onto an adsorbent trap.

6.6.3. Sample Concentration

Samples collected in the canisters or adsorbent traps were concentrated twice by first desorbing the sample into the Tekmar sample concentrator and then onto a cryogenic trap inside the GC oven. Due to the water content, sample volumes from canisters were limited to 200-250 cm^3. The adsorbent traps were purged for 6.0 minutes while being heated to 180^oC. The purging step concentrated the sample onto the internal trap within the Tekmar sample concentrator. The second step was a 3.0-minute dry purge, where dry nitrogen gas was set to flow through the internal trap of the Tekmar sample concentrator, which removed as much water as possible. The last step was to desorb the sample into the liquid N_2 cooled trap inside the gas chromatograph for 2.5 minutes. The steps and direction of gas flow are shown in Figure 6.9.

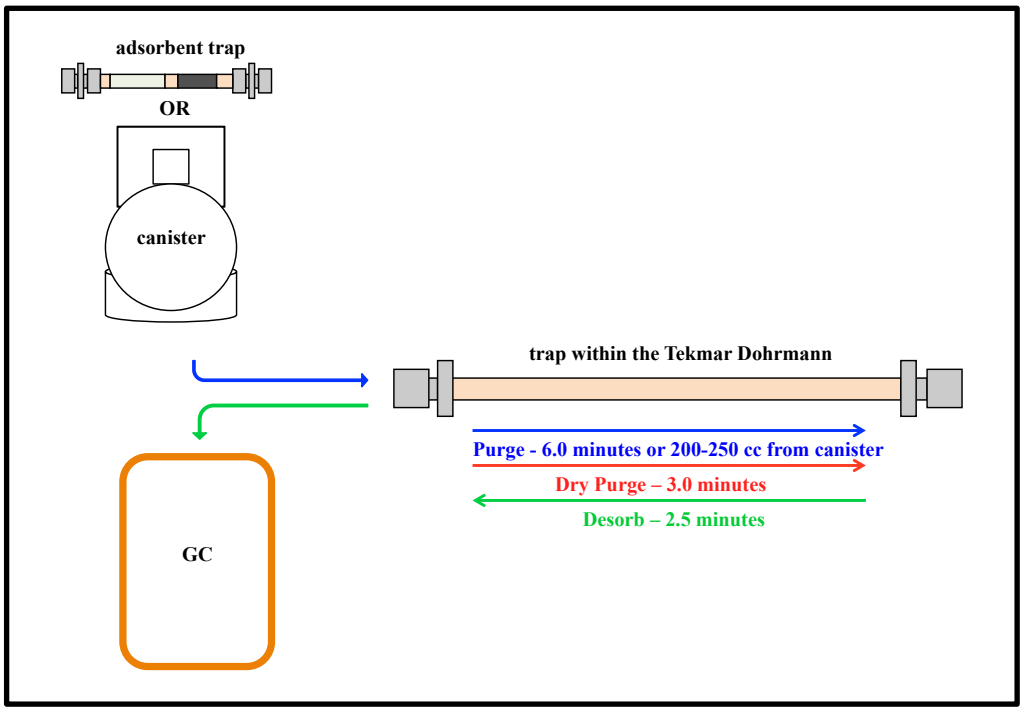

Figure 6.9. Sample concentration steps on a trap carried out inside the Tekmar sample concentrator.

6.7. Gas Chromatography

Once samples were concentrated in the Tekmar sample concentrator, they were desorbed onto the liquid N_2 cooled trap inside the gas chromatograph, which is shown in Figure 6.10. The capped branch of the "T" fitting was removed and the sample was trapped at a flow rate of 60 mL/min. The purpose of the trap was to focus the sample into a small volume before injecting onto the GC column. Once the sample was transferred, the cap was replaced on the "T" fitting, the liquid N_2 was removed and the trap was submerged into hot water for 5 seconds to thaw the sample. The door of the GC oven was then closed and the GC temperature program started.

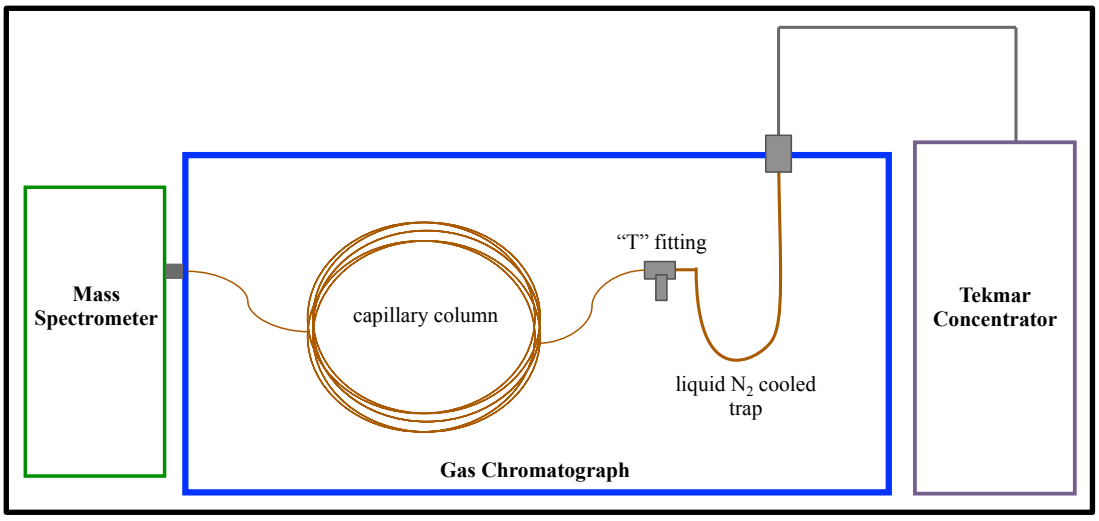

Figure 6.10. Schematic of the Tekmar concentrator, modified gas chromatograph and mass spectrometer.

The helium carrier gas was set at 10 psi with a flow of 20 mL/min. Separation was achieved by using a temperature program listed in Table 6.1.

Table 6.1. GC temperature program used for separation.

	Hold time (min)	Temperature (^{o}C)	Rate (^{o}C/min)
Initial	3.0	35	0.0
Ramp 1	0.0	35-95	20.0
Ramp 2	0.0	95-220	10.0
Final	0.5	220	0.0

6.8. Mass Spectrometry

The detector was set to scan 5.0 minutes after the GC was started with a total run-time of 17.0 minutes. The analysis was a full scan between 50-300 Da. Data analysis was carried out on an Agilent Enhanced ChemStation software using the ions and corresponding retention times found in Table 6.2. For each analyte and internal standard,

the retention time and the most abundant ion (base peak) and second most abundant ion were identified. The base peak was used for quantification (quantifying ion), and the second ion was used as a qualifying ion. BEN-d6 and MET did not have a qualifying ion because the intensities were large enough to confidently distinguish from noise. The MS was calibrated daily to ensure mass accuracy and consistency in sensitivity.

Table 6.2. Compounds with its corresponding quantifying ion and qualifying ion, with observed retention times.

Compound	Molecular Ion (*m/z*)	Quantifying Ion (*m/z*)	Confirming Ion (*m/z*)	Retention Time (min)
SEV	200.1	131.1	181.1	5.7
ENF	-	51.0	117.1	6.3
BEN-d6[§]	84.0	84.0	-	9.0
3-FBT	164	164.1	145.1	9.3
TFT	146	146.1	127.1	9.8
MET	-	81.0	-	10.0
TOL-d8[§]	100	98.0	100.0	11.0
4-CBT	180.5	180.1	145.1	12.5
XYL-d10[§]	116	98.0	116.0	13.0

[*] Molecular Ion – heaviest ion in the mass spectrum
[†] Quantifying Ion – most intense ion in the mass spectrum, base peak
[‡] Confirming Ion – second most intense fragment ion, for some compounds it is also the same as the molecular ion
[§] Internal Standard

References

1 **Air Resources Board.** ***Standard Operating Procedure for Cleaning 6-Liter Summa Polished Canisters*****, 2002.**

2 **Roman, B. I., San Diego State University, 2003.**

CHAPTER 7. RESULTS AND DISCUSSION

7.1. Tracer Compound Selection

Many compounds, especially natural products could be found in common household products, such as air fresheners and deodorizers.[1] These same compounds would also be detected in breath.[2] In prior work, our laboratory observed that exposure to exogenous chemicals prior to breath collection was detected. For example, in one study chemicals present in a tire store waiting room were detectable in breath over 24 hours post exposure.[3] This gave us the idea that unique compounds might be useful as a marker or tracer in our breath that could later be detected in breath days after exposure. We first investigated many natural compounds like: limonene, p-cymene, carene, terpinenes, and pinenes because they are known to be "safe", but differentiating them from background environment levels proved to be difficult.[4,5] These natural compounds are found in plants, common household products, toiletries and foods, so estimating background concentrations was futile. Another problem with natural products was that they were metabolized within the gut, which was confirmed in published works.[4,6] This lead us to the investigation of patented chemicals used in the food and flavor industry. Most of these chemicals appeared to be compounds readily metabolized if ingested, so we did not pursue this avenue further. One class of VOCs that were proven to be nontoxic and have no known metabolites were the commonly used gas anesthetics and other fluorine-containing compounds.

7.1.1. Gas Anesthetics

Gas anesthetics were man-made chemicals that are usually found in hospitals, dentist clinics, and other medical facilities used to temporarily induce a state of amnesia, unconsciousness, or paralysis. Ideal gas anesthetics are slightly lipophilic, non-toxic, stable, not metabolized by the body, and easily eliminated via the respiratory system.[7-9] As a starting point we were interested in compounds with similar properties to be used as tracers.

Among its ideal properties, gas anesthetics always contained halogenated functionalities, particularly fluorines that made them unique. Research showed that the addition of fluorine would greatly change properties of a compound. As an example many pharmaceuticals contained a fluorine atom to increase bioavailability.[10-12] Fluorines are unique in that very few naturally occurring volatile compounds contain them.[13] Fluorinated compounds are not only used in pharmaceuticals, they are present as refrigerants and also used for medical imaging (positron emission tomography or PET scans), tagging objects for security purposes, and in earlier published studies as a blood substitute.[14-16] Along with gas anesthetics we wanted to study other fluorinated compounds with similar properties since a less volatile compound would be easier to capture and analyze by GC-MS. We used three common gas anesthetics: enflurane (ENF), sevoflurane (SEV), and methoxyflurane (MET). All three compounds contained fluorines and toxicological data has been reported so we were aware what concentrations would be safe to be used for our studies.[17]

7.1.2. Fluorinated Compounds

Along with the three selected gas anesthetics α,α,α-trifluorotoluene (TFT), 3-fluorobenzotrifluoride (3-FBT), and 4-chlorobenzotrifluoride (4-CBT) were also studied. TFT was commonly found used as an internal standard in gas chromatography analyses because it was not found in nature. We decided TFT would be a good candidate because it was a volatile fluorinated compound that had little to no known health and safety issues that would harm subjects. TFT was the most ideal candidate also due to its simple and unique mass spectrum, and it was readily available. 3-FBT and 4-CBT were selected because of its similar structure to TFT. To detect compounds in breath for extended periods of time, the compound should be unique and not metabolized by the body. These fluorinated chemicals looked like excellent candidates because they were volatile, stable, and not known to be found in the environment, households, or workplaces.

There was data published on the properties of gas anesthetics, but there was little to no data reported on how TFT, 3-FBT, and 4-CBT behaved in the body. Table 7.1 lists the properties, in which we hypothesized to be important when choosing a suitable compound for this study. The molecular weight and boiling point provided information on how well it would chromatograph, while the blood to gas partition coefficient ($\lambda_{b/g}$) and partition coefficient in octanol and water (log P) provided information relating to its lipophilic properties. High log P values indicated the compound's high solubility in octanol compared to its solubility in water, and a high $\lambda_{b/g}$ value indicated a higher solubility in blood than in the gas phase. We decided to use three gas anesthetics with very different $\lambda_{b/g}$ to determine if there were any correlations between $\boldsymbol{\lambda_{b/g}}$ and residence

times. We predicted that methoxyflurane would be retained in the breath the longest of the anesthetics because its $\lambda_{b/g}$ was very high.

Since there were no $\lambda_{b/g}$ values available for TFT, 3-FBT, and 4-CBT, the log P values were compared, and the $\lambda_{b/g}$ values of benzene, toluene, and xylene were also compared. The log P values were collected from the database in PerkinElmer's software ChemBioDraw. By looking at the values there were not any obvious reasons why one fluorinated compound would work better than the other, but our preliminary experimental data showed that TFT was a very promising candidate. This led to the hypothesis that compounds with a log P of about 3, a boiling point approximately 100^{o}C, and contained mainly fluorines as a halogen would be ideal. Another piece of data that could be used to select other compounds was the $\lambda_{b/g}$ values of benzene, toluene, and xylene. Since TFT was the most ideal candidate this showed that compounds similar in structure to toluene or toluene's $\lambda_{b/g}$ value would also work. Data supporting this hypothesis would be helpful and may lead to a whole group or class of compounds that could be used as a continuation of this study.

Table 7.1. Properties of the 6 prospective compounds (tracers) studied, and three comparative compounds.

Compound	M.W.*	B.P. (°C)†	$\lambda_{b/g}$‡	log P§
SEV¶	200.1	58.6	0.6[17]	2.24
ENF¶	184.5	56.5	1.9[17]	2.44
MET¶	165	104.8	11[17]	2.03
TFT	146.1	102	-----	2.96
3-FBT	164.1	101-102	-----	2.68
4-CBT	180.6	136-138	-----	3.51
Toluene◊	92.1	113	6-9[18]	2.52
Benzene◊	78.1	85	8-16[18]	2.03
Xylene◊	106.2	141	42.1[18]	3.01

*M.W. – molecular weight of compound (g/mol)
†B.P. – boiling point
‡$\lambda_{b/g}$ – blood to gas partition coefficient, larger the value higher its solubility in blood
§log P – octanol to water partition coefficient, larger the value higher its solubility in octanol
¶compounds used as gas anesthetics
◊common VOC in environment air that are detected in breath

7.2. Gas Chromatography

The final temperature program, which was a modification of the Environmental Protection Agency's Toxic Organic method (TO-15)[19] was used, and the resulting chromatogram of the target compounds is shown in Figure 7.1. Table 7.2 lists the name of each compound, type, and retention time from the highlighted peaks in Figure 7.1, which was the Standard Sample L5. The concentrations of each compound are found in Table 7.7 and Table 7.8.

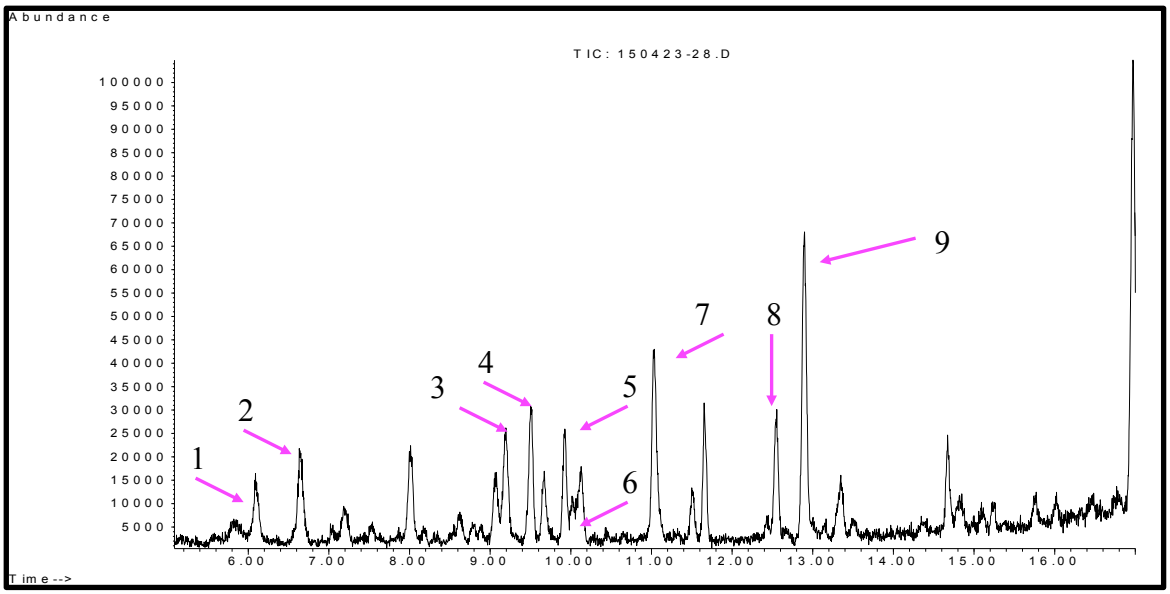

1) SEV, 2) ENF, 3) BEN-d6, 4) 3-FBT, 5) TFT, 6) MET, 7) TOL-d8, 8) XYL-d10, 9) 4-CBT

Figure 7.1. Chromatogram of the L5 (lowest level standard), concentrations found in Table 7.7 and Table 7.8, standard solution with all analytes and internal standards present.

Table 7.2. Retention time of each compound from the previous chromatogram.

#*	Compound	Type of Compound	Retention Time (~min)†
1	SEV	Analyte	6.1
2	ENF	Analyte	6.7
3	BEN-d6	Internal Standard	9.2
4	3-FBT	Analyte	9.3
5	TFT	Analyte	10.0
6	MET	Analyte	10.1
7	TOL-d8	Internal Standard	11.0
8	XYL-d10	Analyte	12.5
9	4-CBT	Internal Standard	13.0

*number corresponds to the labeling of peaks in Figure 7.1
†retention time reported was an approximation due to retention time shifts

7.3. Mass Spectrometry

Separation was achieved for each analyte and internal standard (Figure 7.1). For each compound the mass spectrum was compared to library database to ensure that the peak corresponded to the correct compound. Appendix B shows the results from a software match for each compound with the NIST library. Table 7.3 shows the calculated 'fit' values of the match, reverse match, and percent probability of the identification of the compound from the NIST search program. The match values scored how well the sample spectrum matched the library's spectrum, the reverse match value scored how well the library's spectrum matched the sample's spectrum; a score of 100 is a perfect match. The percent probability in which the compound was what the library identified it to be was also reported in the table. The probability was low for many of compounds because the software included fragmentation peaks above and below the scan range used in this project. Thus, we used the match, reverse match scores, and we looked at the spectrum to confirm the identity of the peaks.

Table 7.3. NIST library search 'fit' values to confirm the spectrum comparisons.

Compound	Match*	Reverse Match†	Probability‡
SEV	786	917	97.5
ENF	862	864	96.8
BEN-d6	820	830	61.1
3-FBT	805	884	46.4
TFT	838	853	77.8
MET	716	824	77.2
TOL-d8	862	880	94.6
XYL-d10	823	831	39.7
4-CBT	874	878	96.0

*Match – scores how well the sample's spectrum matches the library's spectrum
†Revers Match – scores how well the library's spectrum matches the sample's spectrum
‡Probability – probability in which the compound is what the library indicates it is

7.4. Blanks

This project aimed to detect compounds at very low concentrations; hence, attaining clean blank results was paramount. Experiments were first carried out to determine the quality of blanks from canisters, adsorbent traps, the breath collection apparatus, and the GC-MS system. We also wanted to prove that sample carryover from subject to subject did not occur. The studies on blanks were focused on TFT because it was retained in breath samples the longest among all the analytes and most likely to be adsorbed on surfaces.

7.4.1. Canister Blanks

Most of the initial work on this project was carried out with gas canisters, so proper canister cleaning protocols were first developed. Initially canisters were cleaned with dry gas using the same protocol described in the above section 6.5. Since the canisters were made from electropolished stainless we assumed, based on the product use

guidelines[20] it was completely inert and VOCs would not be retained just as long as cleaning was carried out at high temperatures between 75–150^{o}C. However, we were having much difficulty in achieving a proper canister blank sample; this initially resulted in a very big problem since this interfered with our goal of detecting compounds below ppb levels.

Figure 7.2.A shows a chromatogram of a cylinder that was used to collect breath samples that was subsequently cleaned with three cycles of dry heated gas. This demonstrated that the initial method of canister cleaning was incomplete (the peaks present were internal standards used in this study). Following this, the canister was cleaned using humidified air, and a clean chromatogram was achieved, as shown in Figure 7.2.B. The presence of water vapor, which has an affinity for the metallic surface, outcompetes hydrocarbons for the surface of the canisters.[21]

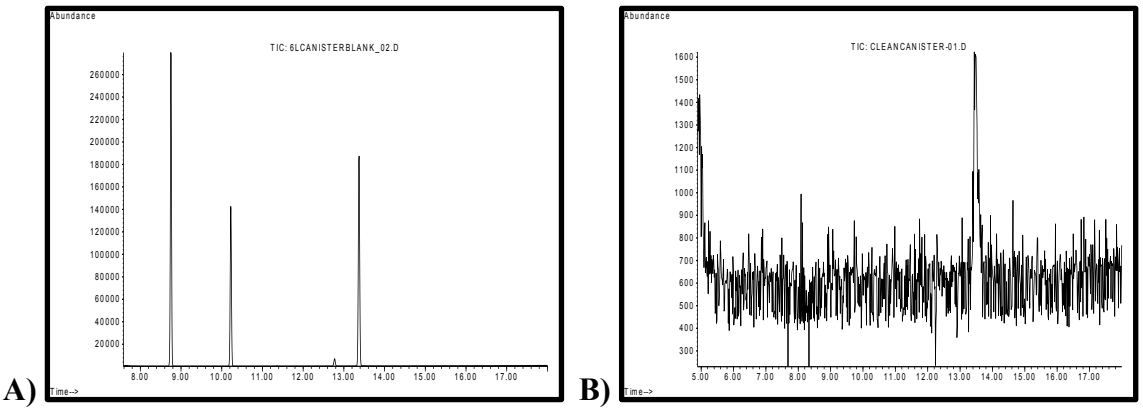

Figure 7.2. A) Chromatogram of a canister cleaned with dry gas. Contaminant peaks can be observed. B) Chromatogram of the same canister after the application of proper cleaning cycles.

The key step in cleaning canisters was canister flushing with humidified air or nitrogen. The stainless steel canisters were electropolished to: 1) increase its resistance to

corrosion, 2) smooth the surface of crevices and burrs that could potentially retain contaminants, and 3) remove impurities.[21-23] However, it was shown that the dry surfaces still retained compounds at the ppb level even after several cleaning cycles.

One gas canister that was used for breath collection was tested through one full cleaning cycle. Figure 7.3.A shows the chromatogram of the canister after breath collection with an estimated concentration of 15, 17, and 20 parts per trillion (ppt) of BEN-d6, TOL-d8, and XYL-d10 respectively. Figure 7.3.B shows the results after 3 cleaning cycles with peaks that were not distinguishable from noise. It was determined that three cycles of the cleaning process with humidified air was sufficient to attain a clean canister for sampling.

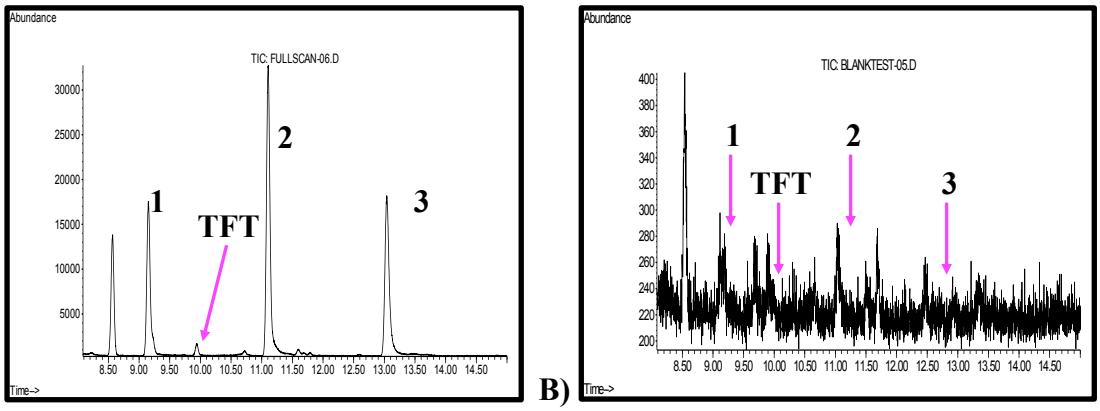

A) **B)**

*1) BEN-d6, 2) TOL-d8, and 3) XYL-d10.

Figure 7.3. A) Chromatogram shows a breath sample after TFT exposure, B) Chromatogram shows the same canister after 3 cleaning cycles.

The process of cleaning canisters was a time consuming task, so we determined if clean evacuated canisters could be stored for future use. A used canister was cleaned following the canister cleaning protocol, sealed with a stainless steel cap, and stored at

ambient temperature for 30 days. Figure 7.4 shows the results for the stored canister (chromatogram A) compared to an identical canister that was cleaned and analyzed the same day (chromatogram B). There were some contaminant peaks, but they were not of the analytes and internal standard, and did not interfere with the signals. A library search of the peaks at 8.5, 9.7-9.8, and 12.5 minutes resulted in β-alanine, and the peaks at 10.6-10.7 and 11.5 minutes resulted in 2-hydroxyaminoheptanoic acid, but the 'fit' values were very low. These peaks did not interfere with detection of the compounds in this study. However, it was no advisable to store clean evacuated canisters for long periods of time.

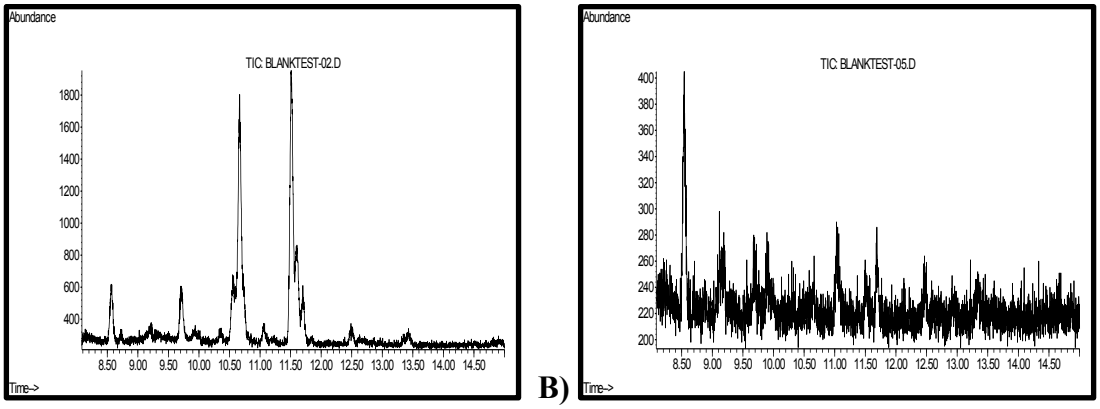

Figure 7.4. A) Chromatogram of a cleaned canister that was stored for 30 days. B) Chromatogram of canister that was cleaned and analyzed on the same day.

7.4.2. Adsorbent Traps

Adsorbent traps were ideal due to their compact size, portability, and ease of use. However, complete desorption of VOCs needed to be achieved in order to eliminate cross contamination. The following experiment carried out was collection of an EBC sample, transfer of the sample to an adsorbent trap, and desorption at 180^{o}C onto the Tekmar

sample concentrator. We wanted to determine if 180°C was a suitable temperature for desorption from the trap to the sample concentrator. 180°C was used tested because this temperature was well above the highest boiling point among all the compounds, and the manufacturer recommended it. Figure 7.5.A shows the results of an adsorbent trap with a breath sample collected after a 6-minute purging time at 180°C. Chromatogram B was the same trap reanalyzed without being removed from the concentrator. The peak at about 11.9 minutes was identified as a polydimethylsiloxane (PDMS), which was due to GC column degradation (column bleed) not carryover from the previous analysis. This peak also appeared with about the same intensity as seen in Figure 7.5.A. The source of contamination as the GC column itself was confirmed by running the GC-MS program without a trap desorption step. This result confirmed that complete desorption at 180°C was accomplished which eliminated the need of any extra cleaning steps between uses. It also demonstrated that there were no sample carryover in-between analyses occurring within the Tekmar sample concentrator, GC, or MS.

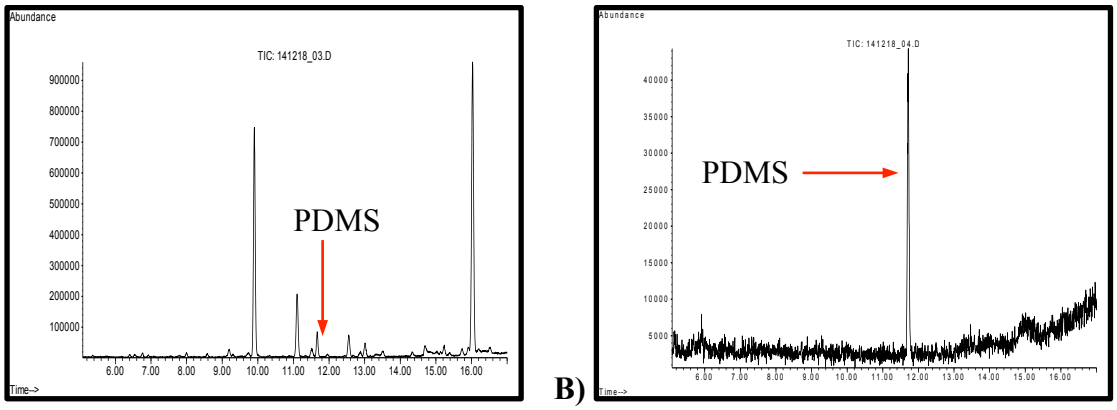

Figure 7.5. A) Chromatogram of a breath sample analyzed from a trap. B) Chromatogram of the same trap.

7.4.2.1 Breakthrough experiments of adsorbent traps

Many manufacturers reported breakthrough volumes of adsorbent material. Breakthrough volumes indicate the maximum volume and moles of sample that could be adsorbed onto the adsorbent material per unit mass of adsorbent. Although the breakthrough volumes of Tenax® and Carbopack™ were published, they were only recommended guidelines as it varied batch to batch and somewhat dependent upon the compound type, volatility, and flow rate of adsorption used. Thus it was important to test each system to ensure that no breakthrough occurred with the flow rates and the amount of adsorbent material used.

Two traps were prepared with the same approximate amounts of Tenax® and Carbopack™ B, 0.23 g and 0.17 g, respectively. Two cleaned adsorbent traps were connected in series with the outlet end of the first trap connected to the inlet of the second trap as shown in Figure 7.6 and Figure 7.7. Then, one μL of the Standard Solutions L2 solution, concentrations of compounds are found in Table 7.7 and Table 7.8, was injected onto the inlet of the first adsorbent trap. Nitrogen gas at a flow of 75 mL/min, which was the highest flow the adsorbent traps could possibly be subjected to, was flushed through the traps for 20 minutes. The contents of both traps were then separately analyzed by GC-MS. According to the manufacturers specifications, we expected that the first trap (TRAP A) would retain all of the compounds injected, while the second trap (TRAP B) would show no peaks from any of the compounds injected. Figure 7.6 shows the set-up and results of the experiment. The chromatogram from TRAP A showed what was expected, with all the compounds in the L2 solution detected. TRAP B did not show any of the L2 solution components. The peak at about 7 minutes in the chromatogram for TRAP B was

confirmed by mass spectrometry to be methylene chloride (CH_2Cl_2), and the second peak at 11.6 minutes was column bleed, or degradation of the capillary column. Methylene chloride was a solvent used in our laboratory.

This experiment was carried out a second time by switching the order of TRAP A and TRAP B to demonstrate that both traps behaved identically despite not containing the exact the amount of adsorbent material. Figure 7.7 shows the results of the second experiment, which again demonstrated that no breakthrough of sample was observed.

Thus, it was shown that adsorbent traps packed with 0.23 g of Tenax® and 0.17 g Carbopack™ B was sufficient for this study, and a total flow rate used for traps should not exceed 75 mL/min for 20 minutes to minimize the occurrence of breakthrough.

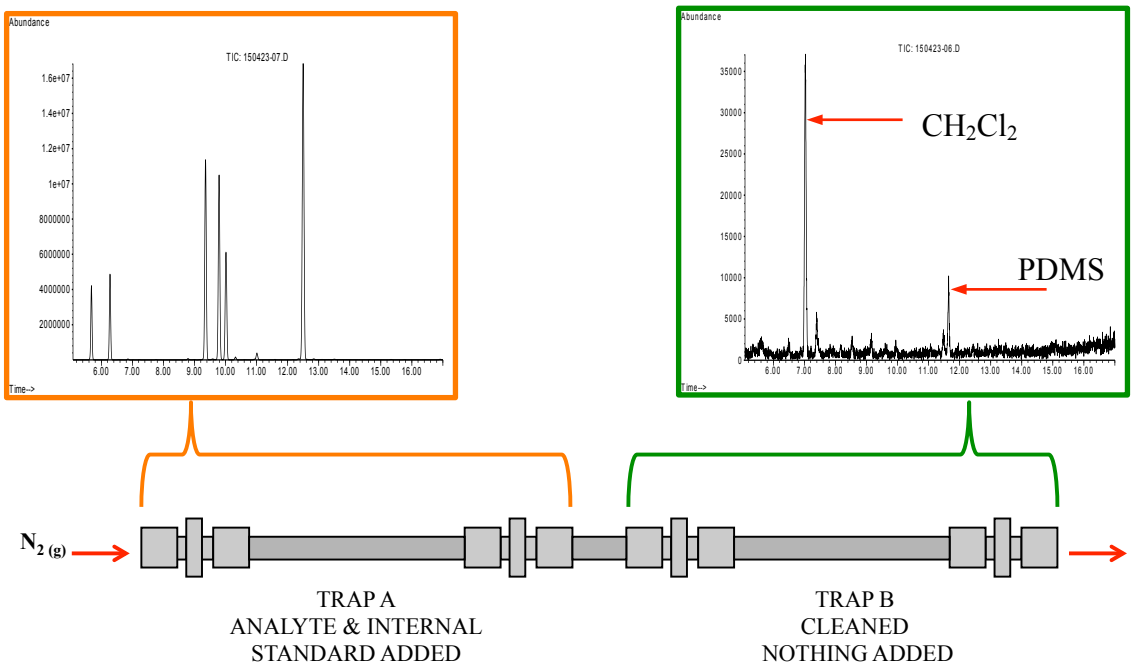

Figure 7.6. Breakthrough experiment with resulting chromatogram from each trap.

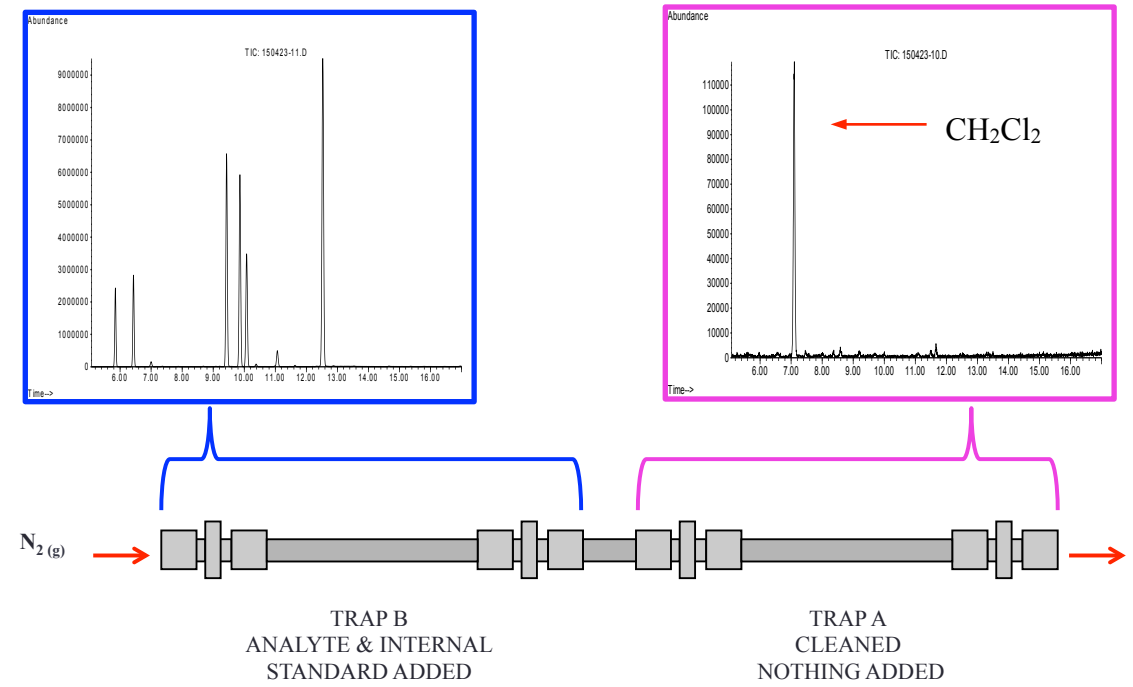

Figure 7.7. Breakthrough experiment with resulting chromatogram from each trap.

7.4.3. Carryover From Subject to Subject

A problem that many authors have encountered with BCA was the presence of endogenous compounds. Sources of endogenous compounds were usually from the environment, workplace, and home. However, one question we had was, would a person's exhalant be considered exogenous if it was detected in the breath of another person? In other words we wanted to demonstrate that one subject's exhalant would not be inhaled and detected in another person's breath.

Three different subjects were used for this experiment with the single tracer TFT because it was detected in the breath from a single subject for several days. EBC samples were collected from: 1) subject X, who was exposed to 1 ppm of TFT for 45 minutes; 2) subject Y, who was in the same work environment as subject X; and 3) subject Z who was in close living quarters with subject X for at least 12 hours per day but was never in contact or exposed to TFT otherwise (Table 7.4). EBC samples of all subjects were collected after 4 days after the initial exposure of TFT to subject X. What we expected was that TFT would only be detected in subject X's data, and there would be little to no presence of TFT in either of subject Y's or subject Z's EBC.

Figure 7.8 show the chromatograms of the extracted ion channels of TFT from each subject 4 days after the initial exposure; the specific peak for TFT was labeled with a red oval. In subject X the EBC contained approximately 100 ppt of TFT, subject Y had a low signal for TFT, which was estimated to be less than 1.0 ppt, and subject Z showed a signal that was too small to quantify. The conclusion was that there was no evidence that subject X's exhalant would expose subject Y and or Z to TFT. The low signal found in

subject Y was most likely due to the fact that subject Y worked in the same environment where a bottle of TFT was occasionally opened to prepare standard solutions.

Table 7.4. Table of 3 three subjects.

Subject	Subject Type	Figure
Subject X	Exposed to 1 ppm TFT	Figure 7.8.A
Subject Y	Works in same environment Subject X	Figure 7.8.B
Subject Z	Lives in close quarters with Subject X	Figure 7.8.C

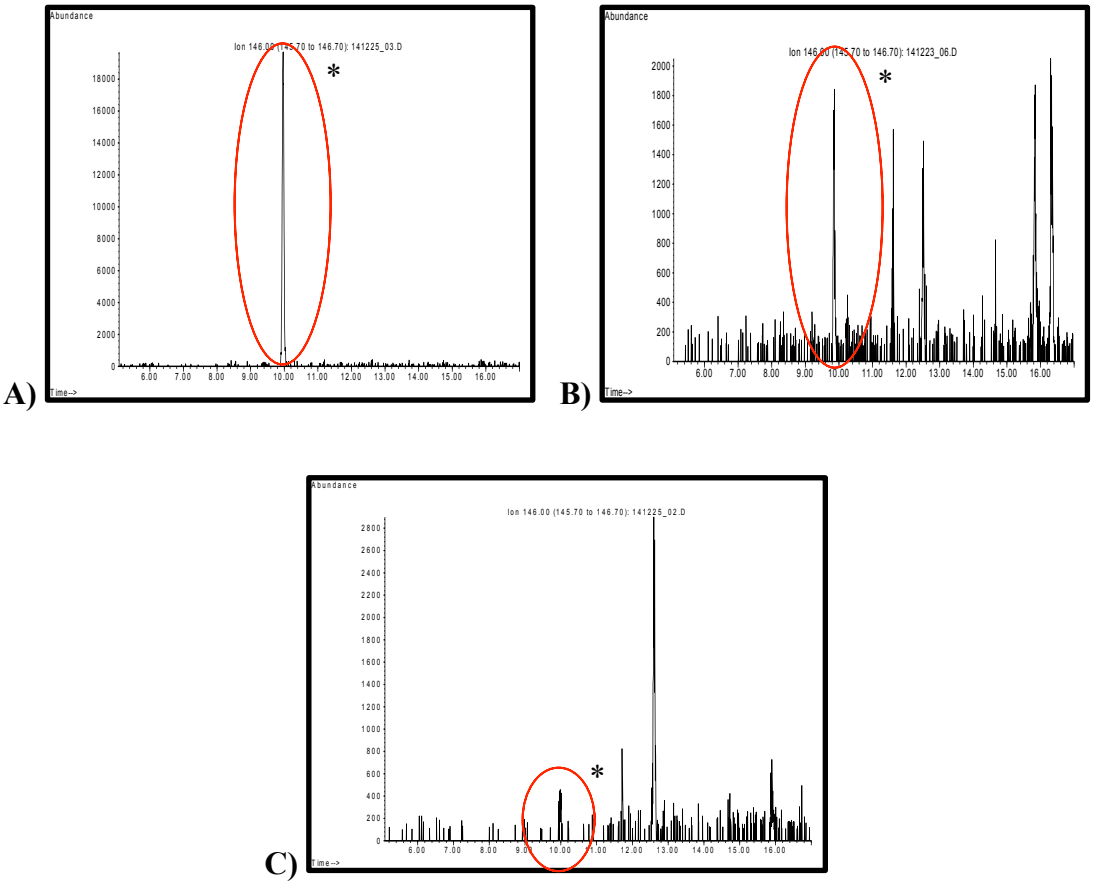

A) Subject X, B) Subject Y, C) Subject Z
* red circles indicate the peak for TFT

Figure 7.8. Ion extracted chromatograms of TFT for three different samples.

7.5. Reproducibility of Results from Canisters and Adsorbent Traps

It has been stated that there were issues with BCA due to the lack of standardization in sample collection and data normalization. However, we were only indirectly limited to those problems since we were not aiming to quantify compounds in breath, but rather track relative changes in concentration changes for a particular subject for as long as possible. A single subject, with instructions on how to breathe during testing, may provide the most consistent results. Beyond this, it was important to ensure that canisters and adsorbent traps yielded reproducible results under well-controlled conditions.

7.5.1. Reproducibility of Internal Standards with Canisters

For the next experiment a clean canister was spiked with 26.9, 26.9, and 27.1 ng of BEN-d6, TOL-d8, and XYL-d10, respectively, using the breath collection apparatus in Figure 6.6. After pressurization and equilibration, canisters were then connected to the Tekmar sample concentrator and 200 cm^3 of sample was analyzed. This procedure was repeated twice with two other clean canisters, for a total of 3 analyses. The area counts for peaks from all 3 internal standards are shown in Table 7.5. It was apparent from this experiment that there was a lack of run-to-run precision in area counts. This was encountered throughout these experiments, the origins of which have not been clearly identified. Despite the inconsistency, the percent RSD in the ratios of components in each analysis were remarkably the same. Thus, this experiment demonstrated that the canister sampling technique and method in which internal standard was added was precise.

Table 7.5. Results from reproducibility experiments of canisters.

	Area Counts			Area Count Ratios		
Trial #	**A***	**B†**	**C‡**	**A/B§**	**B/C¶**	**A/C#**
1	703,667	664,535	420,475	1.06	1.58	1.67
2	810,527	709,380	552,341	1.14	1.28	1.47
3	540,833	492,952	349,713	1.10	1.41	1.55
			%RSD**	3.81	10.43	6.65

*A – area count for BEN-d6
†B – area count for TOL-d8
‡C – area count for XYL-d10
§BEN-d6/TOL-d8 – area count ratio of BEN-d6 to TOL-d8
¶TOL-d8/XYL-d10 – area count ratio of TOL-d8 to XYL-d10
#BEN-d6/XYL-d10 – area count ratio of BEN-d6 to XYL-d10
**%RSD – relative standard deviation of the ratios within 3 trials

7.5.2. Reproducibility of Internal Standards with Adsorbent Traps

A similar experiment to the one in Section 7.5.1 was carried out with adsorbent traps. A cleaned trap was spiked with 1.02, 1.02, and 1.03 ng of BEN-d6, TOL-d8, and XYL-d10, respectively, using the breath collection apparatus in Figure 6.6. What could be deduced from the results of this experiment, shown in Table 7.6, was that adsorbent traps provided reproducible data if the same amount of sample was collected. By comparing the percent RSD of canisters versus adsorbent traps, the latter produced better precision when used with internal standards.

Table 7.6. Area counts of internal standards for each trial of the experiment carried out for adsorbent traps.

	Area Counts			Area Count Ratios		
Trial #	**A***	**B†**	**C‡**	**A/B§**	**B/C¶**	**A/C#**
1	1,715,836	2,275,855	1,619,934	0.75	1.40	1.06
2	2,317,092	2,826,843	1,941,906	0.82	1.46	1.19
3	1,218,325	1,572,915	1,099,287	0.77	1.43	1.11
			%RSD**	4.30	1.78	6.05

*A – area count for BEN-d6
†B – area count for TOL-d8
‡C – area count for XYL-d10
§BEN-d6/TOL-d8 – area count ratio of BEN-d6 to TOL-d8
¶TOL-d8/XYL-d10 – area count ratio of TOL-d8 to XYL-d10
#BEN-d6/XYL-d10 – area count ratio of BEN-d6 to XYL-d10
**%RSD – relative standard deviation of the ratios within 3 trials

7.6. Sensitivity of Canisters versus Adsorbent Traps

It was very important to have the most sensitive method possible for this project because we wanted to be able to identify compounds for as long a time as possible. First we needed to determine if canisters or adsorbent traps worked better for this purpose. Canisters were limited by volume (about 6-8 breaths), whereas as adsorbent traps could collect 30 breaths without undue stress on the subject. Although some experiments were carried out using both canisters and adsorbent traps, the final EBC experiments were completed for this project with adsorbent traps only due to its superior sensitivity.

7.7. Linearity of Instrument

The linearity of the entire GC-MS system was checked by analyzing adsorbent traps that were spiked with known amounts of standards. Five concentration levels of standards were prepared with a fixed amount of internal standards (Table 7.7 and Table 7.8) prepared in methanol. For each concentration level a clean adsorbent trap was

injected with 1±0.1 μL of the solution by 10-μL syringe that was quickly inserted into the glass wool plug in front of the trap. It was recognized that there would be losses of volatile compounds in this method of introducing sample into the traps. However, the data does not seem to be adversely affected by this method. Following analysis of the traps with the GC-MS, calibration curves were generated to check the linearity of the instrumental setup.

Table 7.7. Concentration levels of each analyte used for the calibration curve.

	Concentration (μg/mL)				
Analyte	**L1**	**L2**	**L3**	**L4**	**L5**
SEV	71.6	4.44	0.276	0.0170	0.00105
ENF	78.3	4.85	0.301	0.0186	0.00115
3-FBT	75.6	4.68	0.291	0.0180	0.00111
TFT	77.6	4.81	0.299	0.0185	0.00114
MET	83.1	5.15	0.320	0.0198	0.00122
4-CBT	71.4	4.04	0.251	0.0155	0.00096

Table 7.8. Concentration of internal standards.

Internal Standard	Concentration (μg/mL)
ρ-xylene-d10	1.29
toluene-d8	1.28
benzene-d6	1.28

In the results shown in Table 7.9, the regression values for levels 2-5 (representing over 3 orders of magnitude) demonstrated good linearity ($R^2 > 0.97$) with the exception of ENF with a regression value of 0.950. The most important conclusion that could be drawn from this experiment was that the calibration curves were linear to concentrations of about 1 ppt from the adsorption traps.

Table 7.9. The R^2 value of the regression line for each analyte and the corresponding internal standards. Table A) represents the concentration levels 2-5 and Table B) represents all concentration levels.

	A Level 2-5			B Level 1-5		
Analyte	**BEN-d6**	**TOL-d8**	**XYL-d10**	**BEN-d6**	**TOL-d8**	**XYL-d10**
SEV	0.989	0.987	0.979	0.994	0.993	0.999
ENF	0.975	0.971	0.950	0.987	0.985	0.975
3-FBT	0.994	0.992	0.987	0.993	0.991	0.991
TFT	0.992	0.990	0.985	0.992	0.991	0.990
MET	0.996	0.996	0.994	0.991	0.990	0.992
4-CBT	0.994	0.994	0.998	0.982	0.980	0.988

7.8. Normalization of Data

As described in section 5.1.3, one of the major difficulties in BCA was normalization of data. Several published works have used CO_2 concentrations in breath or different methods of collecting 'background' samples to normalize data. In one popular method, called the Alveolar Gradient method, an ambient air sample was collected to represent the 'blank' at the same time an EBC sample was drawn.[24] The GC-MS data from the blank was digitally subtracted from EBC sample data. This method presupposes that the exogenous chemicals that the subject was exposed to during the last 12-24 hours was the same as the air collected as a blank at the time of EBC sample collection. In light of the findings of this research, this was not a sound assumption. Nevertheless, the issues involving blanks and sample normalization have not been resolved. In this project we used several different ways of data normalization to explore methods that have been reported.

It was well accepted that the best way to quantify any analyte was with the use of an internal standard that was chemically identical to the analytes that was added prior to

any sample preparation or handling. However, with breath samples, it was difficult to accurately quantify any analyte because collection methods are too imprecise. It has been reported in medical texts that the average respiration rates vary between 12-20 breaths per minute.[25] Thus, in this study we had to rely upon the subject to breathe in a consistent fashion during each sampling period while in a resting state. Since the duration a compound resides in breath that is measured by the GC-MS was the primary goal and not the quantification, observation of a logical decay of the analyte concentrations in the breath was observed by using three data analysis approaches: 1) measuring the ratio of tracer to internal standard; 2) using the peak area of the tracer compound alone; and 3) using the ratio of the tracer to an exogenous compound assumed to be constant in the breath.

7.8.1. Quantifying Results Using Ratios of Tracer Compound to Internal Standard

These experiments were conducted with canisters because, although it was not the most sensitive technique, it allowed for a more precise way to collect a consistent amount of exhalant. In this experiment, a subject was exposed to approximately 1.0 ppm of TFT, MET, and SEV for 45 minutes. After exposure, the subject's breath was collected with canisters following the protocol detailed in the earlier section. In a 1.0-L canister about 6-9 breaths were collected, and the internal standard was added to the canister after breath samples were collected. Samples were collected at least once per day until the all of the compounds were no longer detectable in the breath samples.

With the use of a canister only 200-250 cm^3 of gas was analyzed at one time. This was because the water content in breath would exceed the sampling capacity of the

sample concentrator; at some point water condenses and forms a blockage in one of the gas lines. Despite this limitation, the sensitivity of the assay was adequate to measure the analytes to a concentration of approximately 0.5 ppt, which was sufficient to measure TFT for 170 hours (~7 days) and 45 hours (~1.8 days) for MET and SEV, as shown in Graph 7.1.A. This data proved that internal standard added after breath collection in a precise manner could be used to observe the decay of the analyte. This approach may be used either with canisters or adsorbent traps. A kinetic graph of the concentrations versus time is shown in Graph 7.1.B. The graph indicated that the decay of concentration might follow a one-compartment model, which obeyed first order kinetics (to be discussed in the following section).

Graph 7.1. Ratio of analyte to internal standard: A) Decay of TFT (green), MET (blue), and SEV (red) vs. time. B) First order kinetics of the decay of the same compounds.

A) 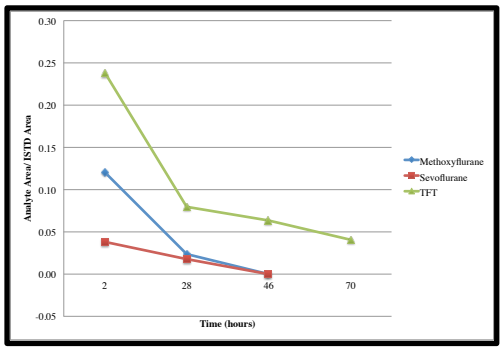

B) 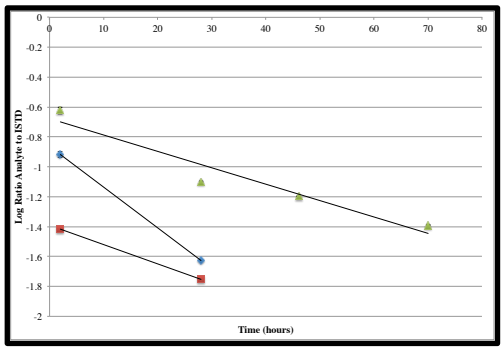

7.8.1.1 Pharmacokinetic modeling

In pharmacokinetic studies, elimination of drugs after exposure via inhalation, injection, and or ingestion is mathematically modeled with compartmental models. The simplest models were a one or two-compartment model. A one-compartment model suggested that the drug or compound of interest was eliminated in the same way it was

introduced due to its rapid equilibration once it entered the body. A two-compartment model proposed that the compound entered the body (compartment 1), then was diffused to fatty tissues, organs etc. (compartment 2) then exited the body via the lungs. Figure 7.9 depicts a subject's elimination of an environmental exposure via a one or two compartment model.

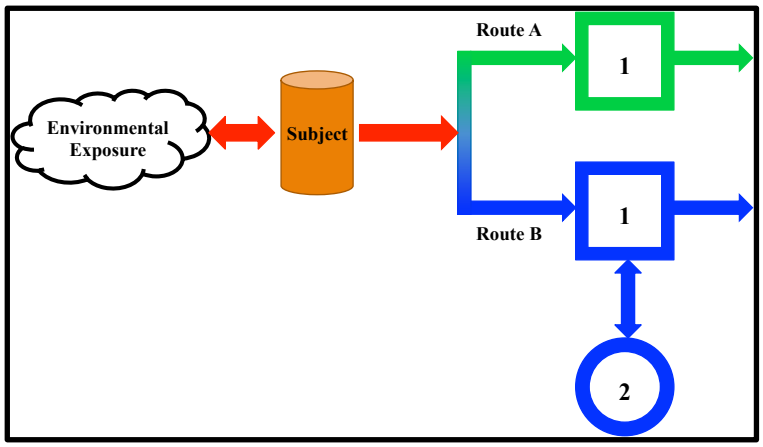

Figure 7.9. Models for one compartment model (route A), and a two compartment model (route B).

The pharmacokinetic model for inhaled volatile exposures was assumed to follow a one compartment model.[26] According to American Conference of Governmental Industrial Hygienists (ACGIH) if the levels in which subjects were breathing in the compounds were well below the accepted levels allowed in the workplace, the elimination followed first-order kinetics.[26] Using an internal standard the concentrations coulld be calculated with the half-life rate equation (3.1), and integrated first order rate law equation (3.2) :

$$\ln 2/_{k} = t_{1/2} \qquad (3.1)$$

$$ln[A]_t = -kt + \ln [A]_0 \quad (3.2)$$

The first order rate constant (k) represents the rate of elimination of analyte from breath, and $t_{1/2}$ is the time where the concentration of the analyte is one-half of its initial concentration (A_0), which is the first data point collected. A_t represents the concentration of the compound in the breath at any time point on the graph.

Although the initial concentration in which subjects were exposed to was known, it was difficult to accurately determine how much was truly present in the first breath exhaled. In these experiments, the first breath collected occurred within 30 minutes. But, with a more accurate way to quantify the compounds in breath, the concentrations at a particular time could be calculated and be used as a powerful tool in correlating initial time of exposure to breath collection time.

7.8.2. Quantifying Results Using Only Peak Area of Tracer Compound

The second approach simply used the area of the analyte and no internal standard. If the subject was giving the same amount of breaths per collection there should be a logical observation of elimination of TFT through time. Graph 7.2.A is from breath samples collected from a subject who was exposed to approximately 1.0 ppm of TFT for 45 minutes after exposure. The subject was asked to give 30 breaths at a normal breathing rate every time sample was collected; this was an attempt to normalize breath collection volume. Samples were collected at least once a day until TFT was no longer detected.

We were able to observe that the use of only area counts in a kinetics graph showed a first order decay (Graph 7.2.B), but there was a small observation that suggested that it followed a two-compartment model. It looked like there was a faster

elimination rate at the earlier time periods and a slower elimination rate at the later time periods as seen in Graph 7.2.A. However, time was not available to collect additional data to confirm this. In summary, the key to this method of data normalization was sample volume consistency.

Graph 7.2. A) Decay of TFT B) First order kinetics of the decay.

A) 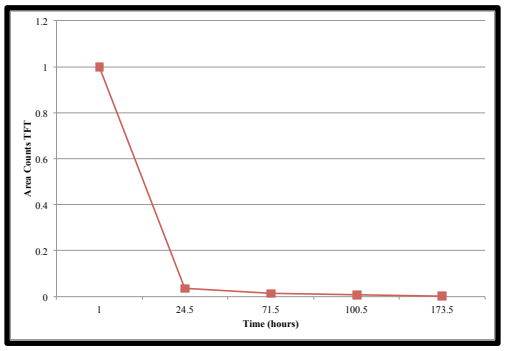

B) 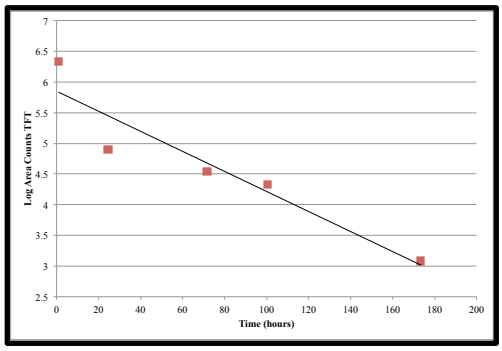

7.8.3. Quantifying Results Using Ratios of Tracer Compound and a Compound that was Assumed to be Constant in Breath

The last data analysis method we tried was to rely upon the observation that certain exogenous chemicals are present in a relatively constant concentration. We hypothesize that if a person has a set daily routine, such as going to work at the same location at the same time of day, and the ambient temperature, relative humidity, etc. were the same, the compounds he or she were exposed to remained relatively constant. Living in an urban environment with emissions from various types of vehicles and the abundance of gas stations, the concentrations of benzene, toluene, ethylbenzene, and xylenes (BTEX) met this criteria.[27] With this known we assumed that if the amounts of breath samples collected were the same, the concentrations of toluene in breath should be the same from sample to sample. Benzene was not used because it eluted too early on the

GC-MS chromatogram and we were not sure if the higher volatility of benzene would be a problem in the breath. We chose toluene because it was relatively easy to measure with our apparatus. We were able to accurately predict the retention time of toluene because in our method we used toluene-d8 as an internal standard.

The following data was collected from a subject that was exposed to TFT at 1.0 ppm for 45 minutes. EBC samples of standard 30 breaths were collected and transferred to adsorbent traps for analysis. Samples were collected periodically until TFT was no longer detected, and the results are shown in Graph 7.3.A. This data agreed with an exponential decay curve relatively well. Since we detected TFT in the breath for up to 350 hours post exposure, it supported the idea that it was not necessary to immediately obtain a sample after exposure to get reliable kinetic data.

More data points have been collected in this study to determine if a two-compartment model was observed. In Graph 7.3.A, there was evidence of a long distribution phase before the elimination which indicated a two-compartment model; however, when graph of the log of ratio area of TFT to toluene was generated (Graph 7.3.B) it was clear that it obeyed a one-compartment model.

Graph 7.3. Ratio of area of TFT to toluene: A) Decay of TFT B) First order kinetics of the decay.

A) 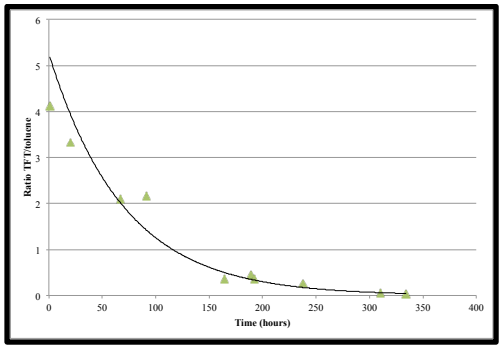

B) 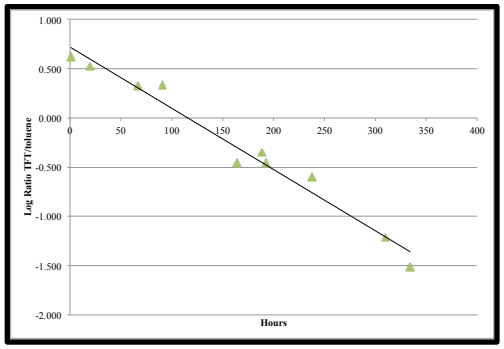

7.9. Decay of Compounds in Breath Samples

Our data demonstrates that all three methods of data analysis yielded kinetic data on the loss of the tracer(s) from EBC. However, we chose to collect EBCs and analyze them via adsorbent traps with the addition of an internal standard for two reasons: 1) EBC was more sensitive than canisters, and 2) the addition of internal standard allowed for possible quantification and normalization of data.

In the next experiment, the principal investigator (subject 1) and myself (subject 2) were exposed to a combination of ENF, SEV, MET, 4-CBT, 3-FBT, and TFT at a concentration of 1.0 ppm of each compound. The concentration exposed to the subject in the breathing mask was estimated using the following equation:

$$\text{ppm exposure} = \text{x ppm in cylinder } X \frac{0.02L\ cylinder\ gas}{breathing\ rate\ in\ L} \div breathing\ rate\ in\ L \quad (3.3)$$

Where "x ppm in cylinder" was the concentration of tracer compound(s) that was prepared in the 2.2-L cylinder, which was 500 ppm; 0.02 L/min was the flow rate of the exposure device; and the breathing rate would range between 6 – 10 L/min. Specifically

for this study the exposure was calculated as to be 1 ppm at a breathing rate of 10 L/min (Equation 3.4).

$$1\ ppm = \ 500\ \text{ppm}\ X\ \frac{0.02L}{min} \div \frac{10L}{min} \tag{3.4}$$

After a single exposure, 30 breaths were collected as EBC for each analysis. Then the sample was thermally desorbed onto the adsorbent trap, and internal standard was added using the apparatus shown in Figure 6.6. EBC was collected for as long as the compounds were detected in the breath. Each compound was compared to all three of the internal standards used and the elimination and kinetic graphs for each compound was generated and is found in Appendix F. The graphs in the appendix showed the decay of each compound relative to all three internal standards used. Among all the compounds, ENF exhibited data that does not correlate with a logical elimination from breath. This was due to an artifact that co-eluted with ENF. The spectrum of the artifact was also very similar to ENF.

Aside from kinetic information, the graphs in Appendix F provided data from multiple tests from two subjects. Within both subjects ENF, MET, and SEV was each used 4 times ; 4-CBT and 3-FBT was each used 3 times; and TFT was used 7 times total. Exhaled breath condensate were collected and a bar graph of the longest time each compound was detected is found on Figure 7.10. On the bar graphs one data set of breath samples collected in canisters was included; this was done to demonstrate the sensitivity of exhaled breath condensate compared to breath samples.

The three gas anesthetics examined were (longest number of days detected in breath): SEV (1.2), ENF (7.7), and MET (1.2) (Figure 7.10.A). The large deviation of ENF was due to the co-elution of an artifact. Although, the compounds were not detected

in breath for longer than one day for SEV and MET, this information indicated that gas anesthetics in breath were not eliminated fully even after a few hours at such a low concentration, especially MET since its $\lambda_{b/g}$ value was 11. SEV also followed the prediction that it would not be a good candidate due to its low $\lambda_{b/g}$ value. 4-CBT, and 3-FBT was retained for at most 7.2 and 1.2 days, respectively. Between both subjects TFT was detected the longest compared to the other compounds. TFT was detected in the breath 8 and 13 days for subject 1 and subject 2, respectively (Figure 7.10.B). This concluded that MET, TFT, 4-CBT, and 3-FBT would be ideal candidates to carry out further studies with a pool of subjects. However, due to the IRB limited approval to MET and TFT, 4-CBT and 3-FBT would be investigated upon permission.

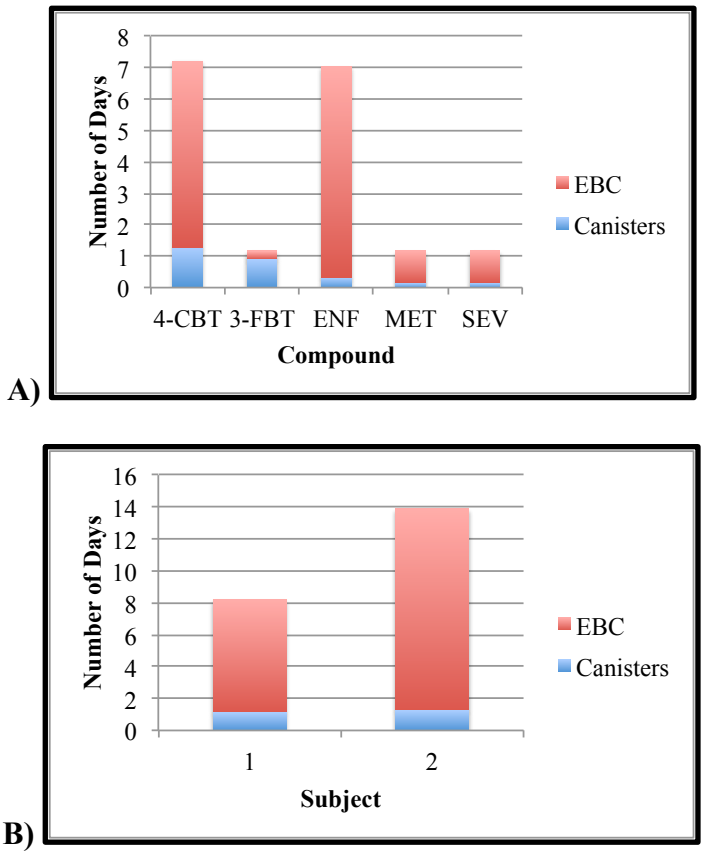

Figure 7.10. Compiled data of decay of tracers: A) SEV, ENF, and MET (n=4), B) 4-CBT and 3-FBT (n=3), and C) TFT for subject 1 (principal investigator, n=3) and subject 2 (myself, n=4).

There was high variability within the two subjects, and there was also high variability within the same subject. This demonstrated that there was a considerable variation in results even under conditions where sample collection was relatively well controlled and the concentration and duration of exposure were held constant. This was further confirmed by looking at the rate constants (rate of elimination of the specific compound) within the same subject, which is shown in Table 7.10. One subject was exposed to 1ppm of all six tracer compounds for 45 minutes, and exhaled breath

condensate was collected and analyzed at varying time intervals until all of the compounds were no longer detected. This experiment was carried out in triplicate. High variability was observed from the precision of each analysis (%RSD); even within the same subject who was exposed to the same concentration and time the data exhibited high variability.

Table 7.10. Rate constants from the 1st order kinetic graphs of subject 2's EBC sample (n=3).

Compound	Rate constant (hr^{-1})	%RSD
SEV	0.39 ± 0.2	51
ENF	0.0048 ± 0.01	284
3-FBT	0.064 ± 0.02	25
TFT	0.044 ± 0.02	38
MET	0.23 ± 0.2	107
4-CBT	0.012 ± 0.003	29

As mentioned previously in Section 5.1.2 and 5.1.3, standardization of breath collection and normalization of remains a primary challenge in EBC analysis. However, in this proof of concept study, our objective to detect tracer compounds in breath for 72 hours or longer have been met for three of the compounds: TFT, ENF and 4-CBT. The data collected showed promise that this could be expanded into a larger study with larger cohorts and combinations of compounds at different concentrations.

References

1 Cengage, G. *Air Freshener*, 2002.

2 Phillips, M.; Gleeson, K.; Hughes, J. M. B.; Greenberg, J.; Cataneo, R. N.; Baker, L.; McVay, W. P. *Journal of Chromatography B* 1999, *353*, 1930.

3 Roman, B. I., San Diego State University, 2003.

4 Gambliel, H.; Croteau, R. *Journal of Biological Chemistry* 1982, *257*, 2335.

5 Kotzias, D.; Sparta, C.; Duane, M. *Naturwissenschaften* 1992, *79*, 24.

6 Hardcastle, I. R.; Rowlands, M. G.; Barber, A. M.; Grimshaw, R. M.; Mohan, M. K.; Nutley, B. P.; Jarman, M. *Biochemical Pharmacology* 1999, *57*, 801.

7 Lee, L., Pharmacology - Inhalant Anesthetics.

8 Eger, E. I. *American Journal of Health-System Pharmacy* 2004, *61*, S3.

9 Mason, A. *Pharmacology of Inhalation Anaesthetic Drugs*, Department of Anaesthesia, Hope Hospital, Salford.

10 Boehm, H.-J.; Banner, D.; Bendels, S.; Kansy, M.; Kuhn, B.; Mueller, K.; Obst-Sander, U.; Stahl, M. *ChemBioChem* 2004, *5*, 637.

11 Filler, R.; Saha, R. *Future Medicinal Chemistry* 2009, *1*, 1370.

12 Tsagogiorgas, C.; Krebs, J.; Pukelsheim, M.; Beck, G.; Yard, B.; Theisinger, B.; Quintel, M.; Luecke, T. *European Journal of Pharmaceutics and Biopharmaceutics* 2010, *76*, 75.

13 Thayer, A. M. *Chemical & Engineering News* 2006, *84*, 15.

14 Spahn, D. R. *Critical Care* 1999, *3*, R93.

15 Le Bars, D. *Journal of Fluorine Chemistry* 2006, *127*, 1488.

16 Park, B. K.; Kitteringham, N. R.; O'Neill, P. M. *Annual Review of Pharmacology and Toxicology* 2001, *41*, 443.

17 Torri, G. *Minerva anestesiologica* 2010, *76*, 215.

18 Dart, R. C. *Medical Toxicology*; Lippincott, Williams & Wilkins, 2004.

19 McClenny, W. A.; Holdren, M. W. *Compendium of Methods for the Determination of Toxic Organic Compounds in Ambient Air, Second Edition*, 1999.

20 Restek Corporation. *TO-Can Canister with RAVE Valve*, 2014.

21 Entech Instruments INC. *SUMMA Canisters And How They Differ From Silonite Canisters And Other TO-15 Canisters*, 2015.

22 Lee, S.-J.; Lai, J.-J. *Journal of Materials Processing Technology* 2003, *140*, 206.

23 Ziemniak, S. E.; Hanson, M.; Sander, P. C. *Corrosion Science* 2008, *50*, 2465.

24 Phillips, M. *Analytical Biochemistry* 1997, *247*, 272.

25 Yuan, G.; Drost, N. A.; Mclvor, R. A. *McMaster University Medical Journal* 2013, *10*, 23.

26 *Topics in Biological Monitoring A Compendium of Essays by Members of the ACGIH Biological Exposure Indices Committee*; American Conference of Governmental Industrial Hygienists: Cincinnati, Ohio, 1995.

27 Leusch, F. *A short primer on benzene, toluene, ethylbenzene and xylenes (BTEX) in the environment and in hydraulic fracturing fluids*, 2010.

CHAPTER 8. CONCLUSION

This objective of this study was to: 1) develop a technique that allowed for tracer compound(s) to be introduced to subject(s) in a controlled manner; 2) refine a sensitive EBC collection and analysis method; 3) develop proper protocols for sample collection, cleaning, and handling; 4) select specific compounds to be used as tracer(s) in breath; and 5) detect the selected tracer(s) for an extended period of time after a single exposure. All five objectives were met.

Breath analysis is a non-invasive method that can be used for many applications. The analysis is simple yet complicated due to the nature of the VOCs that are detected. Endogenous VOCs in breath that are of interest, which were also found in the environment, introduced difficulties in measurement when ultratrace concentrations (sub ppb) were involved. Challenges in measurement include sample carryover, sample preparation, and GC-MS blanks. Much of the work carried out in this study was to determine what compounds or compound class would be unique, nontoxic, and retained in breath for an extended period. Fluorine-containing structures were the most logical and applicable property of compounds that we were interested in, which resulted in the selection of the following VOCs: MET, ENF, SEV, TFT, 4-CBT, and 3-FBT. They were selected based on: volatility, log P, fluorine-containing structure, safety, and its minimal to no presence in nature. These compounds were introduced to subjects in a controlled manner with a device built in our laboratory; due to IRB limitations and safety precautions the exposure concentration was 1-2 ppm for a maximum of 45 minutes.

Blanks are the most important sample to collect and most difficult sample to attain due to the aforementioned problems. Moreover, at such low exposure

concentrations, the levels at which these compounds would be detected in breath were estimated to be in the sub ppb to ppt levels; thus, it was important to ensure proper blanks were collected.

Blanks of canisters and adsorbent traps were investigated. Canister cleaning was carried out on a fabricated system. The apparatus allowed for two important components in the cleaning process: 1) use of humidified N_2 gas for pressurization, and 2) constant heating of canisters 80^{o}C. Humidified N_2 was the most important component, because water was required to out-compete other VOCs for the surface of the canisters. Heating was necessary to keep all compounds in a gaseous state and it also increased the collision of water molecules and surface of the canisters aiding in the cleaning process.

We showed that the adsorption traps did not have sample carryover or loss of sample from breakthrough. Both the temperature and longer desorption time ensured that the traps did not carryover sample and produced clean blanks. We also demonstrated that the adsorbent traps did not shown breakthrough at the flow rates used.

We showed that canisters and adsorbent traps were equally suitable for this study. However, there were advantages and disadvantages for both methods and the summary of these are shown in Table 8.1.

Table 8.1. Comparison of sample collection with canisters and adsorbent traps.

	Comparison of Two Collection Methods	Canisters	Adsorbent Traps
1	Volumes of breath collected known, thus absolute concentrations obtained	Good	Poor
2	Length of time tracers can be measured in breath samples (related to sensitivity)	Fair	Better
3	Replicate analysis of same sample	Yes	No
4	Sample storage	Possibly	Yes
5	Portability; field sampling possible	Yes	No
6	Option to increase sample size	No	Yes
7	Sensitivity	Fair	Good
8	Ease of cleaning	Fair	Good

The number of breaths collected in either canisters or adsorbent traps could be standardized, but the number of breaths did not always equate to the same EBC volume; this was why canisters would be better if absolute concentrations were needed. It was difficult to determine the volume collected using adsorbent traps. Other advantages of canisters compared to adsorbent traps were the option for replicate analysis of the same sample, and portability. Portability, which was one of the main goals of many studies with BCA, was a benefit. While, in this study a complicated apparatus was used to collect breath samples, in theory the evacuated canisters could be carried out into the field and samples could be collected without extra equipment because the compounds investigated were not present in ambient air. For this specific study we were only interested in the length in which compounds were present in breath; therefore, EBC samples collected on adsorbent traps was the best option despite the disadvantages it has compared to canisters. Since the lack of standardization of sample collection was not an issue for this work, the ability to calculate absolute concentrations would not benefit this study; however, this would be desired if future work were to correlate time and concentration.

This study demonstrated that VOCs can be retained within a subject for a long period of time after a single exposure. The chemicals tested and the duration they were detectable in a subject's breath (longest number of days) were methoxyflurane (1.2), enflurane (7.7), sevoflurane (1.2), α,α,α-trifluorotoluene (14), 4-chlorobenzotrifluoride (7.2), and 3-fluorobenzo-trifluoride (1.2). The data showed high variability of days in which the VOCs were retained within two subjects; yet, this was not a problem for this study because we wanted to be able to detect VOCs for as long as it was present in breath.

TFT exhibited the best retention in breath, and it was detected in one data set for 14 days. TFT's properties could provide valuable information in selecting more compounds to extend this study since it was retained in the breath for 2 weeks.

We see that this study's proof of concept results could be valuable in forensics and occupational exposure assessments. In forensics, it could be used to determine if a suspect was present in a secured area. Another forensics application could be correlating a breath sample to a location. Since the method developed in this study could measure VOCs down to the sub ppt level, it could be possible to correlate the location in where a victim's body was last found by looking at profiles of VOCs within their breath.

This study could also be used to determine if and how chronic exposures to gas anesthetics were affecting health care providers. There have been studies carried out but measuring trace and ultratrace levels of waste gas anesthetics in breath as a tool to study long-term occupational exposure could be a powerful tool. We showed that gas anesthetics were detected for longer than a day after a low exposure, but at higher concentrations it may be retained longer.

This was a proof of concept study, which prompts further studies and parallel projects within breath work. Future works may be carried out like: testing more compounds similar in properties to those studied in this thesis; correlating high and low concentrations of tracers with length of time; increasing the number of subjects; using subjects of different weights and ages; and using a room for tracer exposure instead of a respirator mask. Expanding the types of studies with tracer compounds may also lead to more data that can lead to the development standardization of breath collection and normalization of data.

Part 2 contains material, which will be prepared for submission of publication. I was the primary researcher and will be the first author on this paper. Van, Jenny K.; Chatfield, Dale A. "Detection of Volatile Organic Compound Tracers in Human Breath" *Manuscript in preparation.*

Appendix

A. Institutional Review Board (IRB) Approval For Outside Subject(s)

Graduate and Research Affairs
Division of Research Affairs
San Diego State University
5250 Campanile Drive
San Diego CA 92182-1933
Phone: 619-594-5938
Fax: 619-594-4109

Expedited Approval

Reg: 46.110(9) – ROP for continuing, minimal risk
Submit Report of Progress by: September 6, 2015

October 6, 2014

Faculty Researcher: Dr. Dale Chatfield
Department: Chemistry
Contract/grant number: pending
vIRB Number: 364062

Re: *Detection of Volatile Organic Compound Tracers in Human Breath for Development of a New Forensic Technique*

Dear Dr. Chatfield

The SDSU Institutional Review Board approved the project referenced for continuation on October 6, 2014, in accordance with SDSU's Assurance and federal requirements pertaining to human subjects protections within the Code of Federal Regulations (45 CFR 46). This approval applies to the recruitment of human subjects and collection/analysis of data based on procedures described in your protocol and the information you provided within your report of progress. Approval carries with it the understanding that you will contact the IRB to obtain authorization to implement any proposed changes to the protocols, to document a change in your affiliation with SDSU (student, faculty or staff), and/or to report the completion of study recruitment, data collection and data analysis.

Project approval expires October 6, 2015

The following consent document(s) have been modified, stamped and uploaded to your protocol file within the vIRB system, within the Supporting Documents section:

Chatfield_364062_ICF_v12-2013_Approved_10-6-14.pdf

For questions related to this correspondence, please contact the IRB office ((619) 594-6622 or e-mail irb@mail.sdsu.edu). To access IRB review application materials, SDSU's Assurance, the 45 CFR 46, the Belmont Report, and/or any other relevant policies and guidelines related to the involvement of human subjects in research, please visit the IRB web site at http://gra.sdsu.edu/research.php.

Sincerely,

Ramona Pérez

B. Spectra of Analytes and Internal Standards

This appendix shows NIST MS Search Program's library spectrum matched with a spectrum from a standard solution that was prepared and analyzed. Figure. B.1 shows the chromatogram of all the compounds while Figure. B.2 through Figure. B.10 shows the (B) prepared standards spectrum.

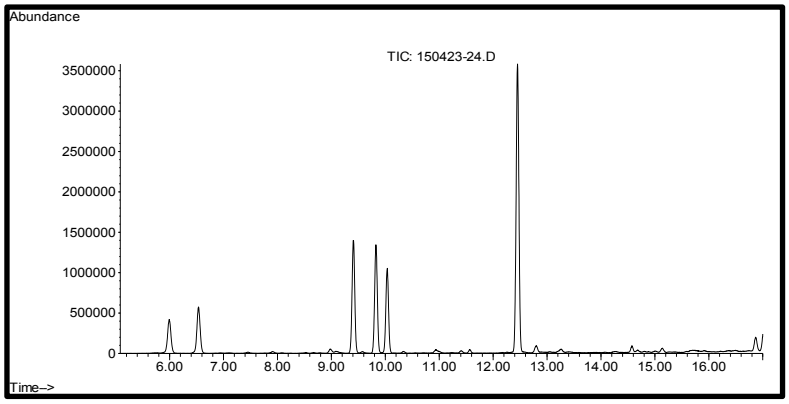

Figure. B.1. Chromatogram of standards and internal standards.

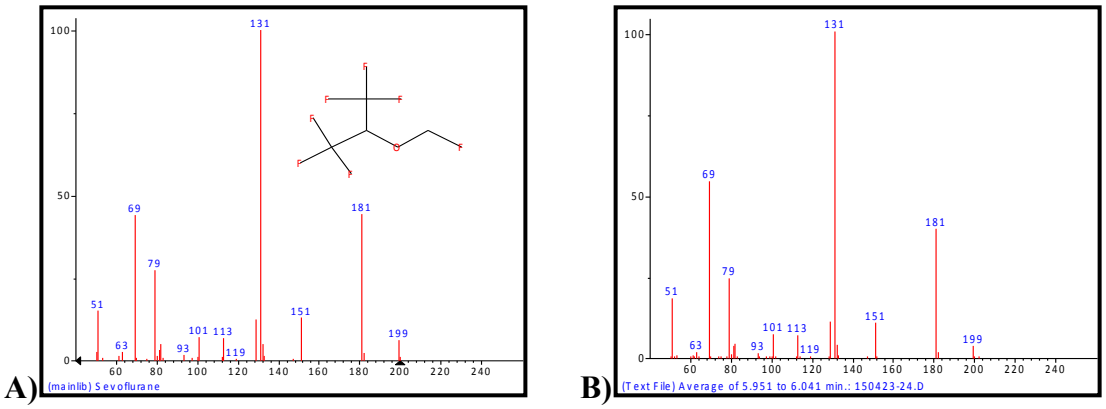

Figure. B.2. A) Spectrum of SEV from the NIST MS Search Program, and B) spectrum from a sample standard of SEV at a retention time of ~6.0 minutes.

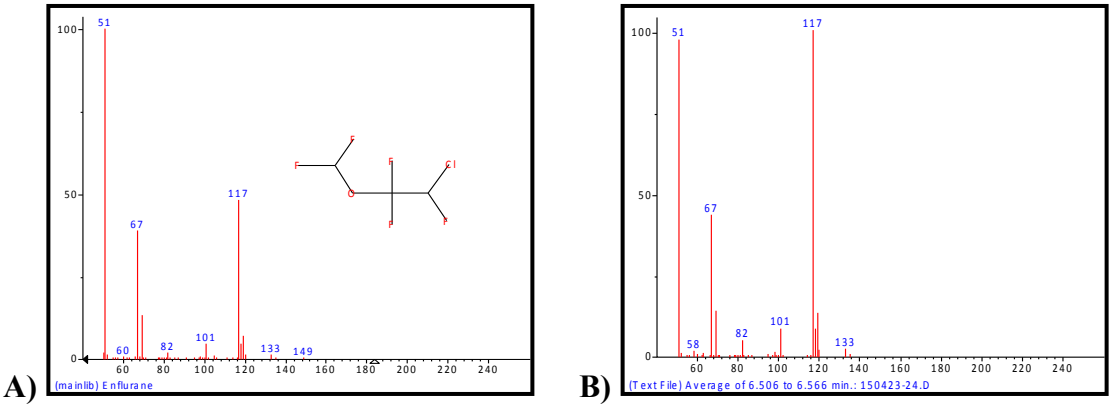

Figure. B.3. A) Spectrum of ENF from the NIST MS Search Program, and B) spectrum from a sample standard of ENF at a retention time of ~6.5 minutes.

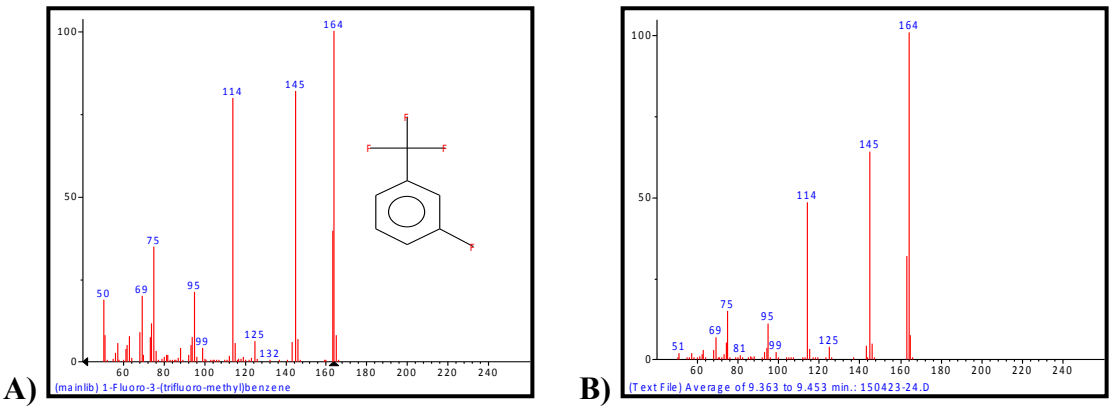

Figure. B.4. A) Spectrum of 3-FBT from the NIST MS Search Program, and B) spectrum from a sample standard of 3-FBT at a retention time of ~9.4 minutes.

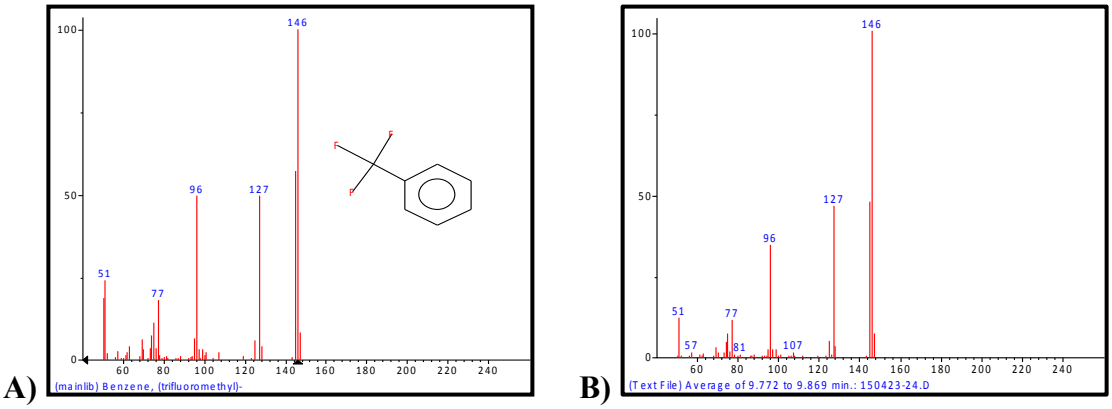

Figure. B.5. A) Spectrum of TFT from the NIST MS Search Program, and B) spectrum from a sample standard of TFT at a retention time of ~9.8 minutes.

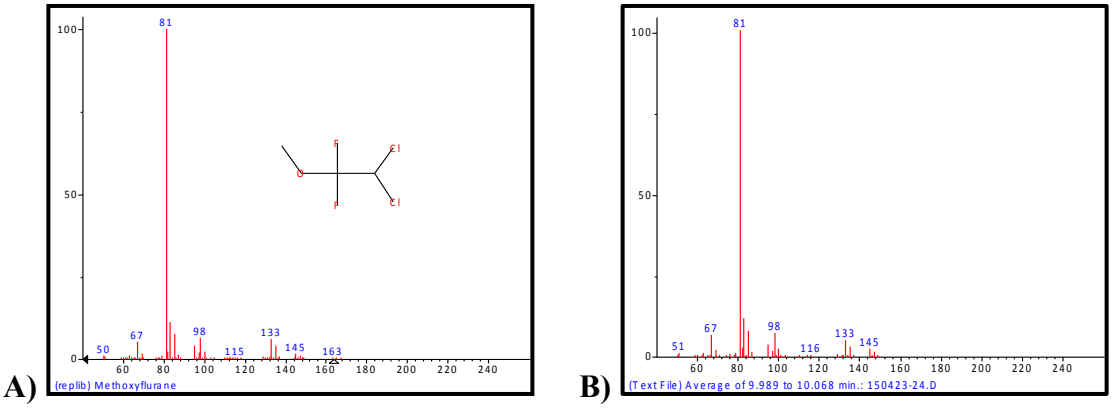

Figure. B.6. A) Spectrum of MET from the NIST MS Search Program, and B) spectrum from a sample standard of MET at a retention time of ~10.0 minutes.

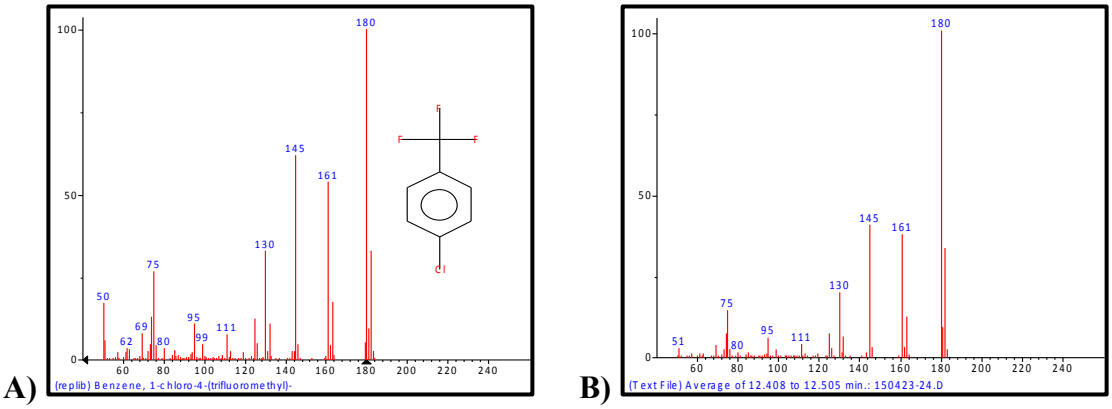

Figure. B.7. A) Spectrum of 4-CBT from the NIST MS Search Program, and B) spectrum from a sample standard of 4-CBT at a retention time of ~12.5 minutes.

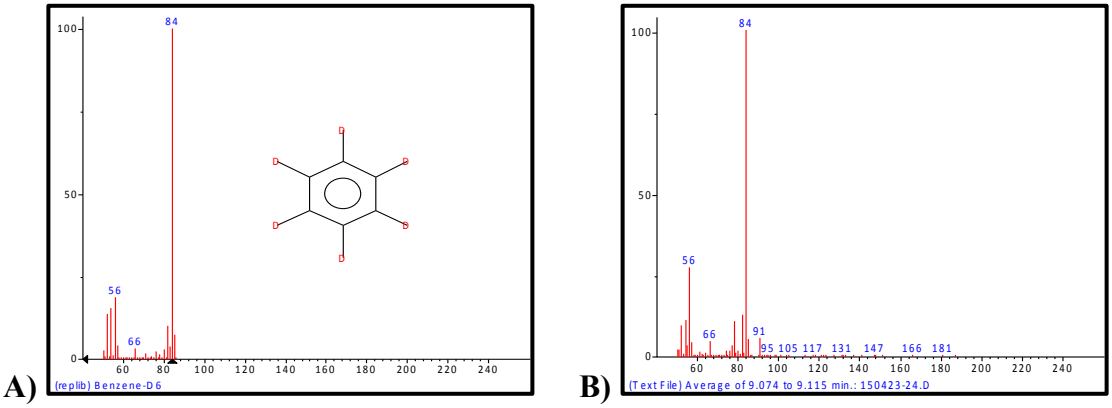

Figure. B.8. A) Spectrum of BEN-d6 from the NIST MS Search Program, and B) spectrum from a sample standard of BEN-d6 at a retention time of ~9.1 minutes.

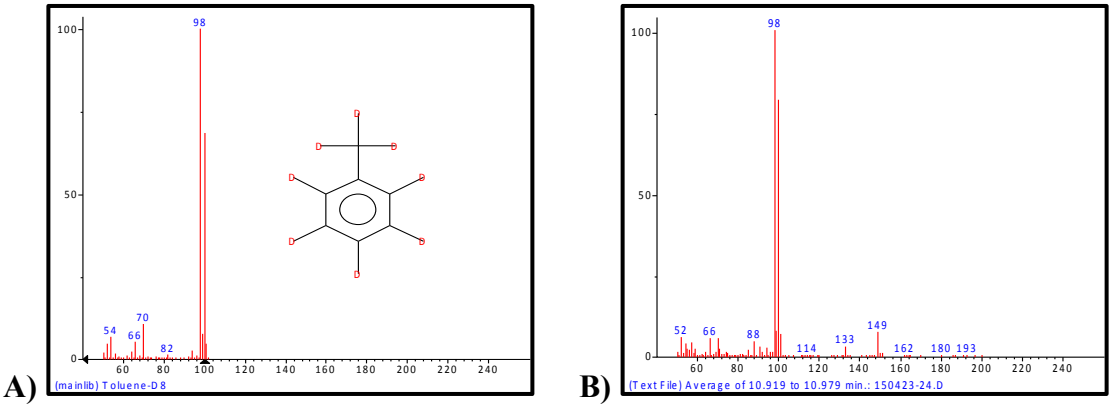

Figure. B.9. A) Spectrum of TOL-d8 from the NIST MS Search Program, and B) spectrum from a sample standard of TOL-d8 at a retention time of ~10.9 minutes.

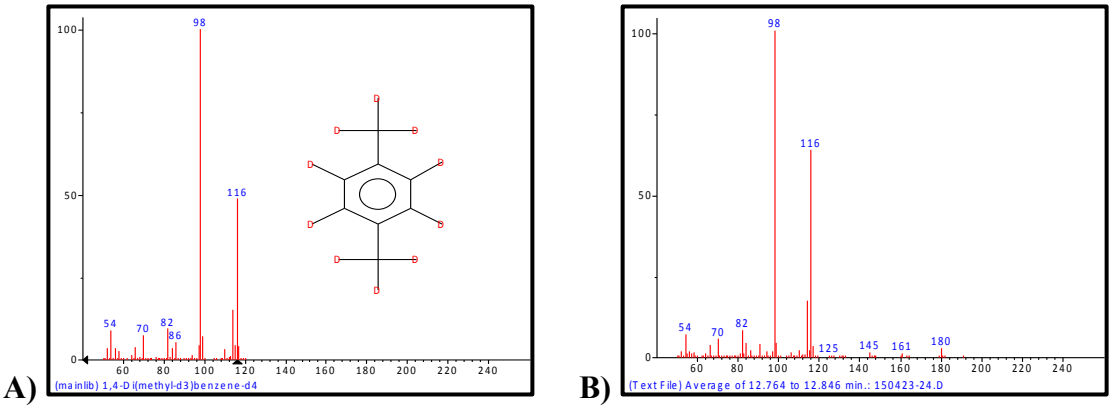

Figure. B.10. A) Spectrum of XYL-d10 from the NIST MS Search Program, and B) spectrum from a sample standard of XYL-d10.

C. Canister Cleaning Cycle Raw Data

The results for canister cleaning cycles are found in the following chromatograms. A used canister was first analyzed to show that there were compounds present. Then the same canister was cleaned following the canister cleaning protocol described in section 0Three full cleaning cycles were required to properly clean the canisters. We wanted to show why at least three cycles were needed. After each cleaning cycle, the canister was pressurized with clean gas and analyzed to demonstrate how much of the compounds are remained.

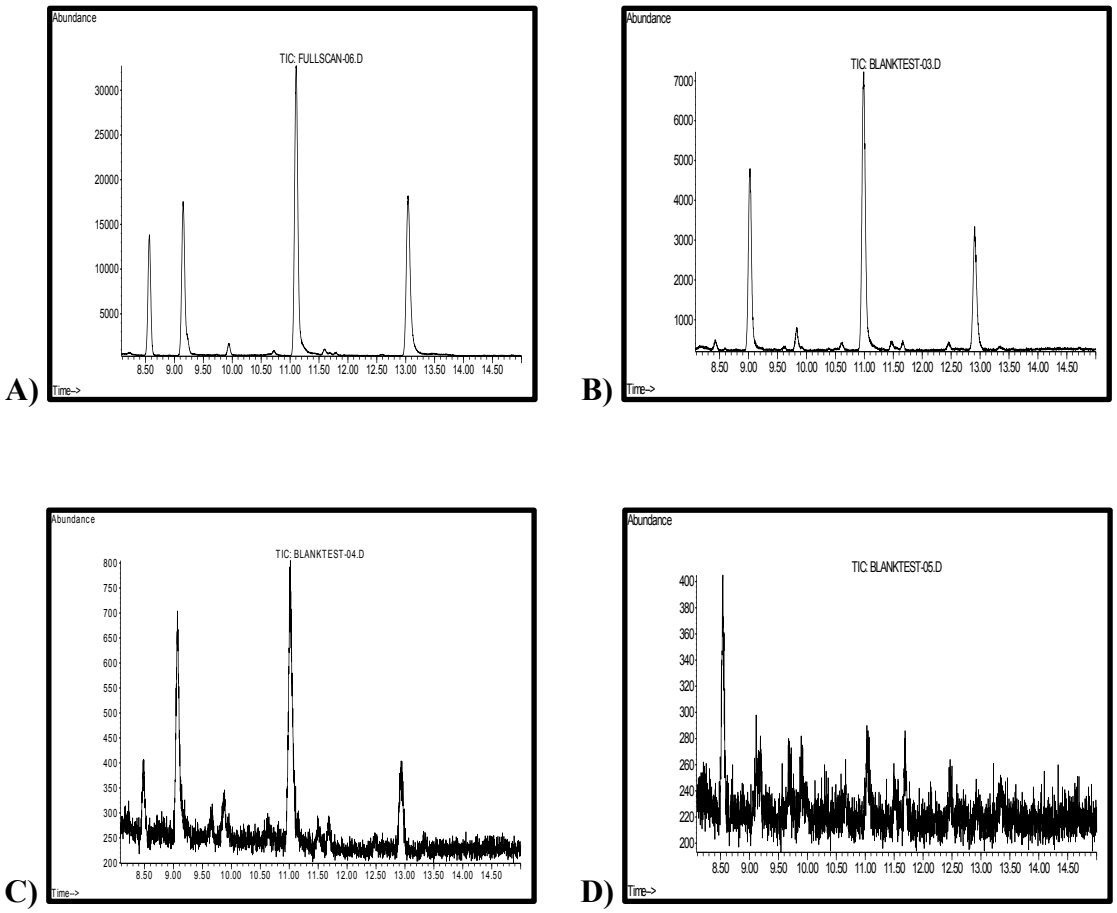

Figure. C.1. A) Chromatogram of a canister with a sample collected, B) chromatogram of the same canister after 1 cleaning cycle, C) chromatogram of the same canister after 2 cleaning cycles, and D) chromatogram after 3 cleaning cycles.

D. Data of Reproducibility Experiments from Canisters and Adsorbent Traps

The chromatograms and data shown in this appendix are results from reproducibility experiments of canisters and adsorbent traps. For canisters and traps, internal standards were added, sample concentration and analysis was carried out in triplicate. This experiment was executed to demonstrate that results are reproducible in both canisters and adsorbent traps.

D.1. Reproducibility of Canisters

The following chromatograms are of three separate analyses of internal standards in canisters. The area counts for each replicate and internal standard were compiled in Table. D.1. The ratios of internal standards in Table. D.2 was also compared to demonstrate low variability from analysis to analysis of the same sample. By simply looking at the area counts it was difficult to determine if the canister data was reproducible therefore the ratios were used because it normalizes the data for comparison.

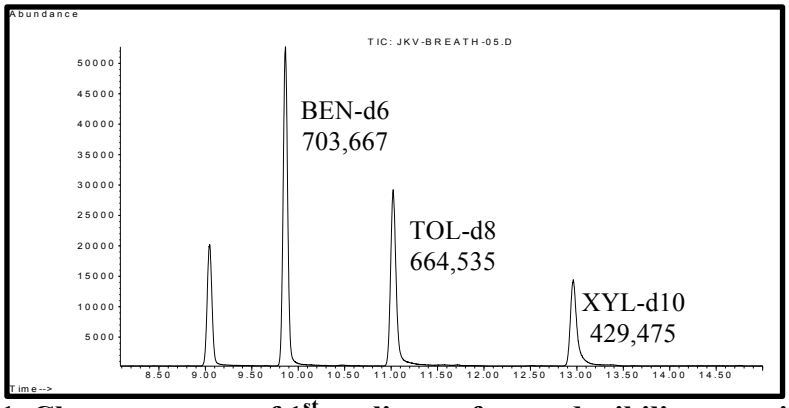

Figure. D.1. Chromatogram of 1st replicate of reproducibility experiment with canisters.

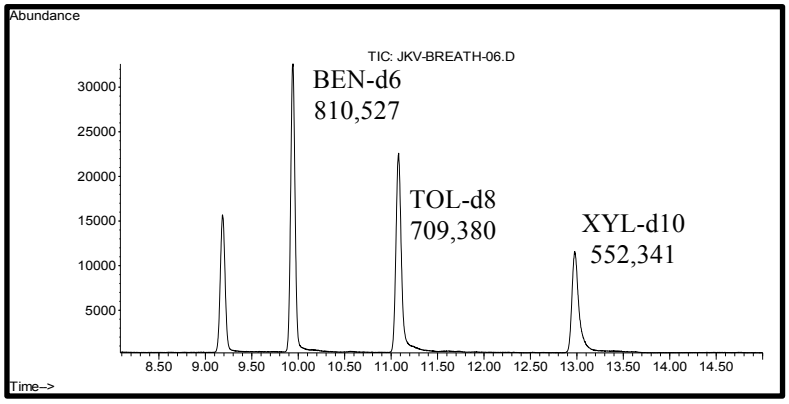

Figure. D.2. Chromatogram of 2nd replicate of reproducibility experiment with canisters.

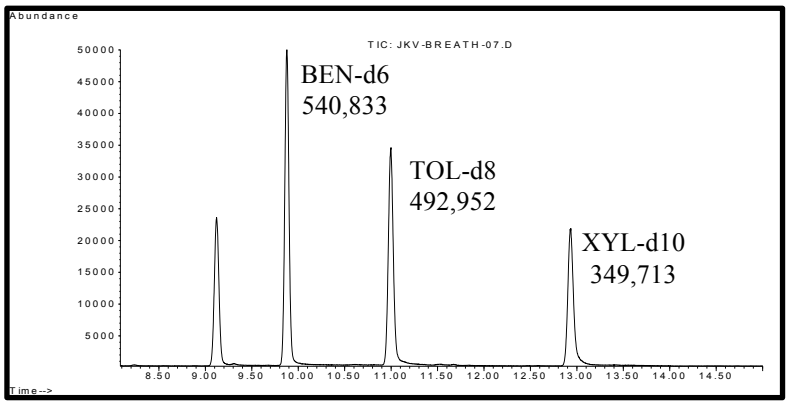

Figure. D.3. Chromatogram of 3rd replicate of reproducibility experiment with canisters.

Table. D.1. Compiled peak areas of each internal standard from the chromatograms shown above.

	Area Counts		
Trial #	**BEN-d6**	**TOL-d8**	**XYL-d10**
1	703,667	664,535	420,475
2	810,527	709,380	552,341
3	540,833	492,952	349,713

Table. D.2. Ratios of internal standards for each trial. The mean and standard deviation, and % RSD for each ratio.

	Ratio of Area Counts		
Trial #	**BEN-d6 / TOL-d8***	**TOL-d8 / XYL-d10***	**BEN-d6 / XYL-d10***
1	0.7539	1.4049	1.0592
2	0.8197	1.4557	1.1932
3	0.7746	1.4309	1.1083
x + s†	1.0995 ± 0.0419	1.4248 ± 0.1486	1.5625 ± 0.104
%RSD	3.8108	10.43283415	6.6534

*Ratios of one internal standard to another, arbitrarily selected

† x + s – expresses the mean and standard deviation of the ratios of all three trials

D.2. Reproducibility of Adsorbent Traps

The following chromatograms are of three separate analyses of internal standards in adsorbent traps. The area counts for each replicate and internal standard were compiled in Table. D.3. The ratios of internal standards in Table. D.4 was also compared to demonstrate low variability from analysis to analysis of the same sample. The reasoning in which we compared ratios of internal standards was the same as mentioned in section D.1 of Appendix D

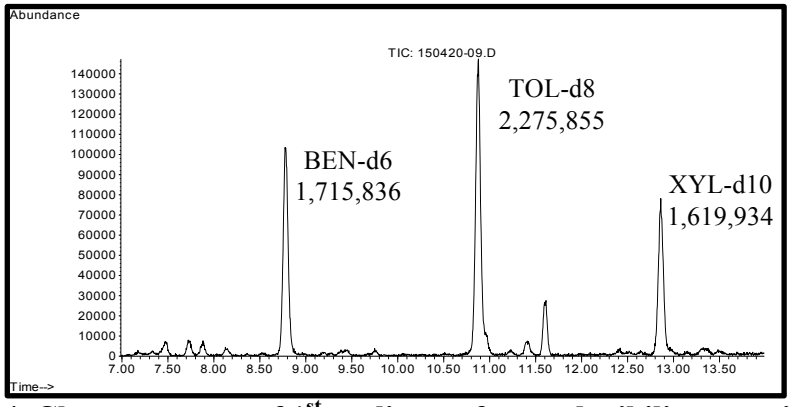

Figure. D.4. Chromatogram of 1st replicate of reproducibility experiment with adsorbent traps.

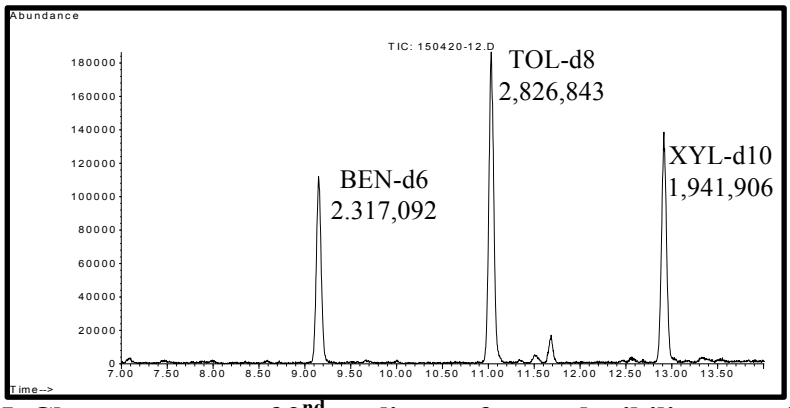

Figure. D.5. Chromatogram of 2nd replicate of reproducibility experiment with adsorbent traps.

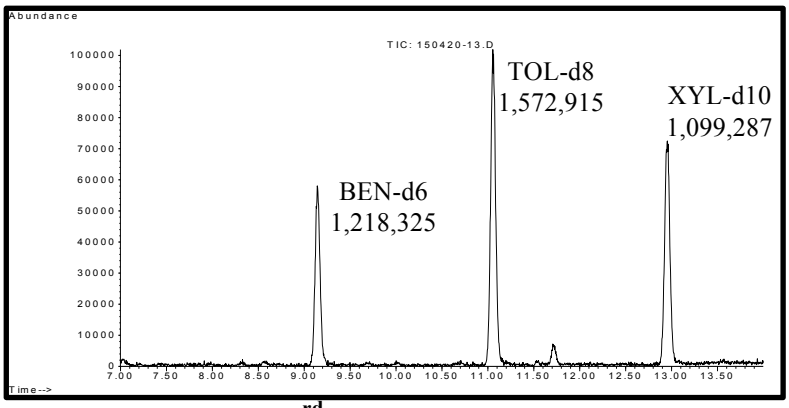

Figure. D.6. Chromatogram of 3rd replicate of reproducibility experiment with adsorbent traps.

Table. D.3. Compiled area counts of each internal standard from the chromatograms shown above.

	Area Counts		
Trial #	**BEN-d6**	**TOL-d8**	**XYL-d10**
1	1,715,836	2,275,855	1,619,934
2	2,317,092	2,826,843	1,941,906
3	1,218,325	1,572,915	1,099,287

Table. D.4. Ratios of internal standards for each trial. The mean and standard deviation, and % RSD for each ratio.

	Ratio of Area Counts		
Trial #	**BEN-d6 / TOL-d8***	**TOL-d8 / XYL-d10***	**BEN-d6 / XYL-d10***
1	0.7539	1.4049	1.0592
2	0.8197	1.4557	1.1932
3	0.7746	1.4309	1.1083
x + s†	0.7827 ± 0.0336	1.4305 ± 0.0254	1.1202 ± 0.0678
%RSD	4.2956	1.7757	6.0519

*Ratios of one internal standard to another, arbitrarily selected

† x + s – expresses the mean and standard deviation of the ratios of all three trials

E. Linearity graphs

Graph. E.1.Calibration curve of all 6 analytes and benzene-d6 as the internal standard. Levels 2-5 represented in the graph (concentrations listed in Table 7.7).*

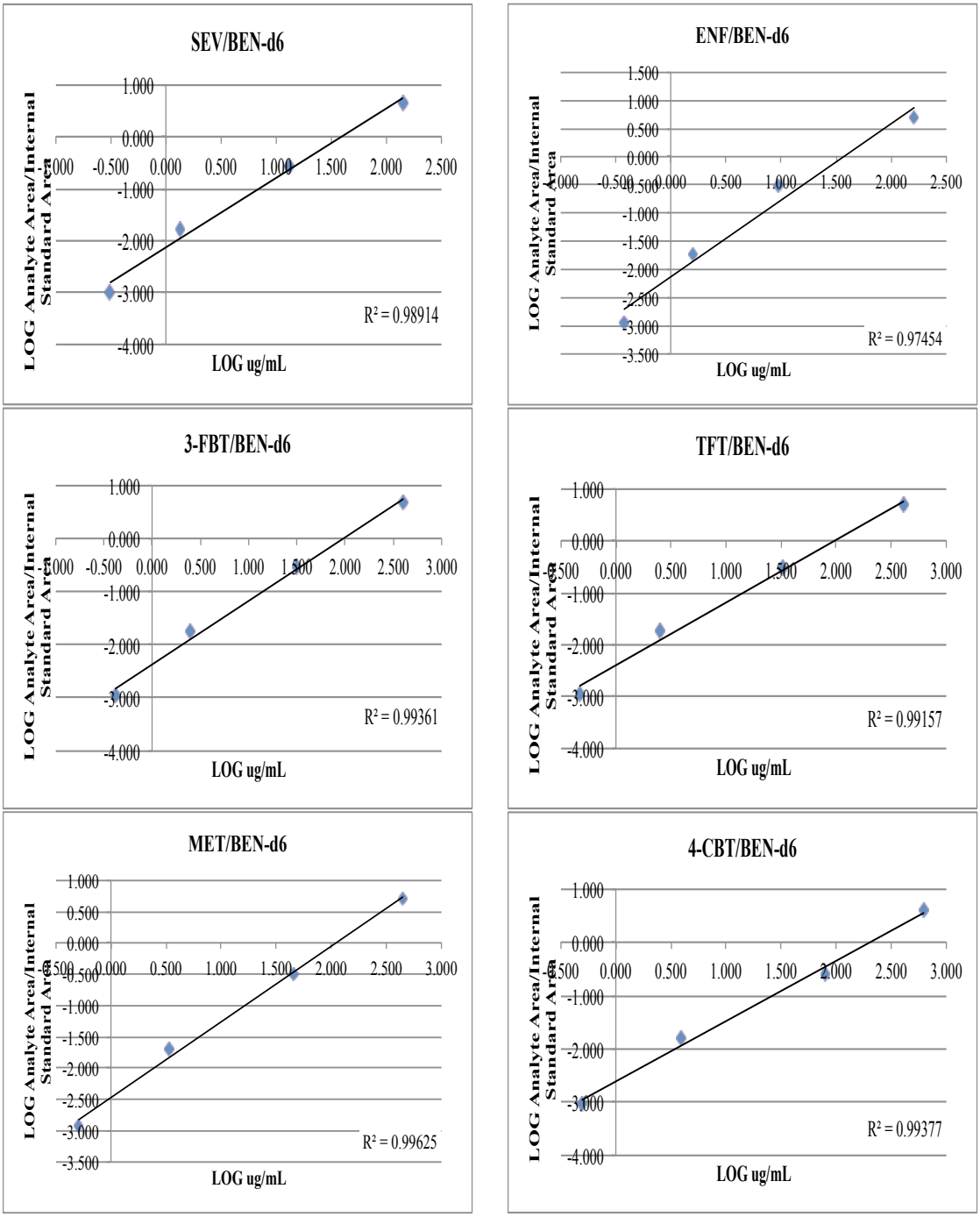

*The title for each graph signifies the graph generated for the tracer compound versus the internal standard.

Graph. E.2. Calibration curve of all 6 analytes and toluene-d8 as the internal standard. Levels 2-5 represented in the graph (concentrations listed in Table 7.7).*

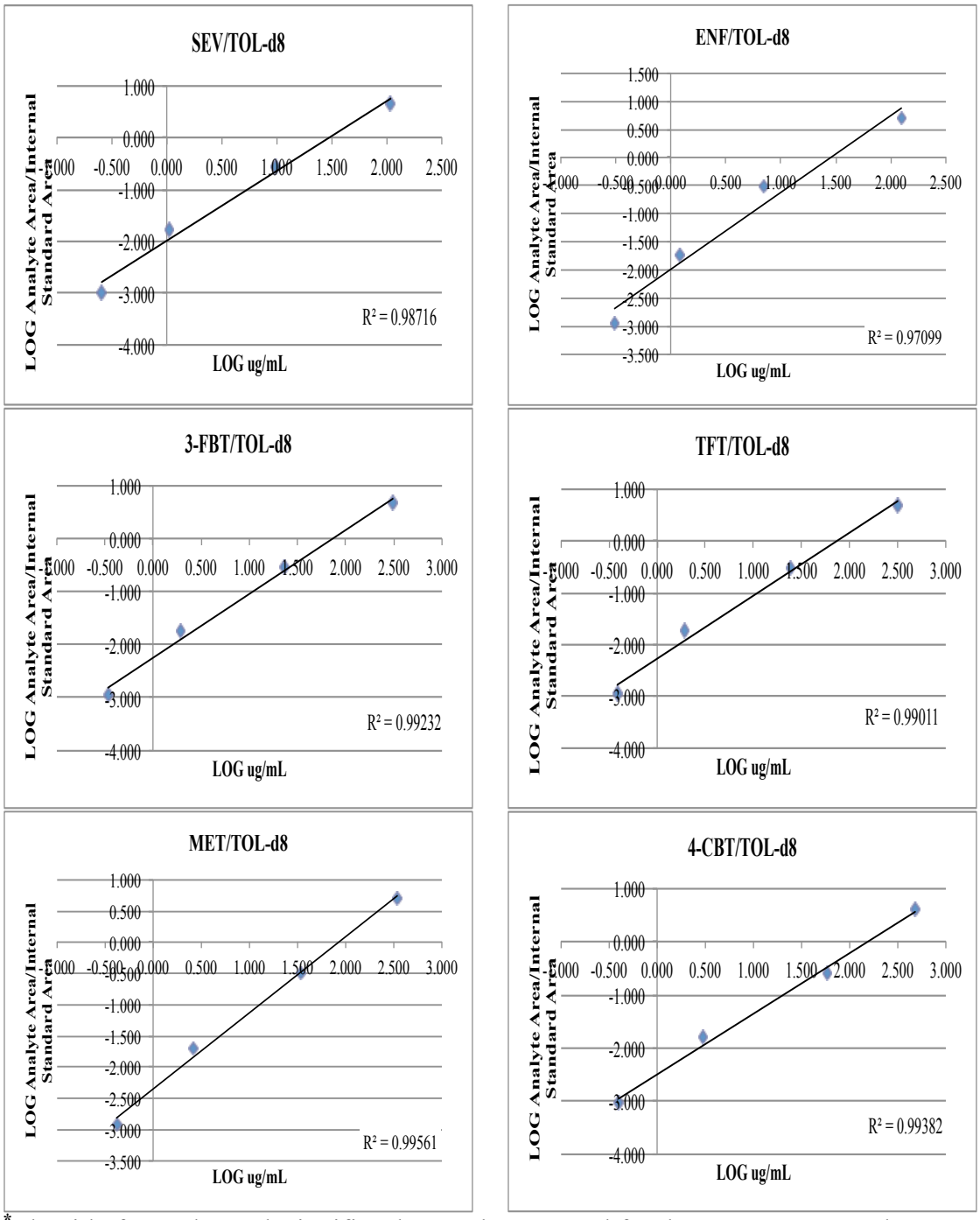

*The title for each graph signifies the graph generated for the tracer compound versus the internal standard.

Graph. E.3. Calibration curve of all 6 analytes and ρ-xylene-d10 as the internal standard. Levels 2-5 represented in the graph (concentrations listed in Table 7.7).*

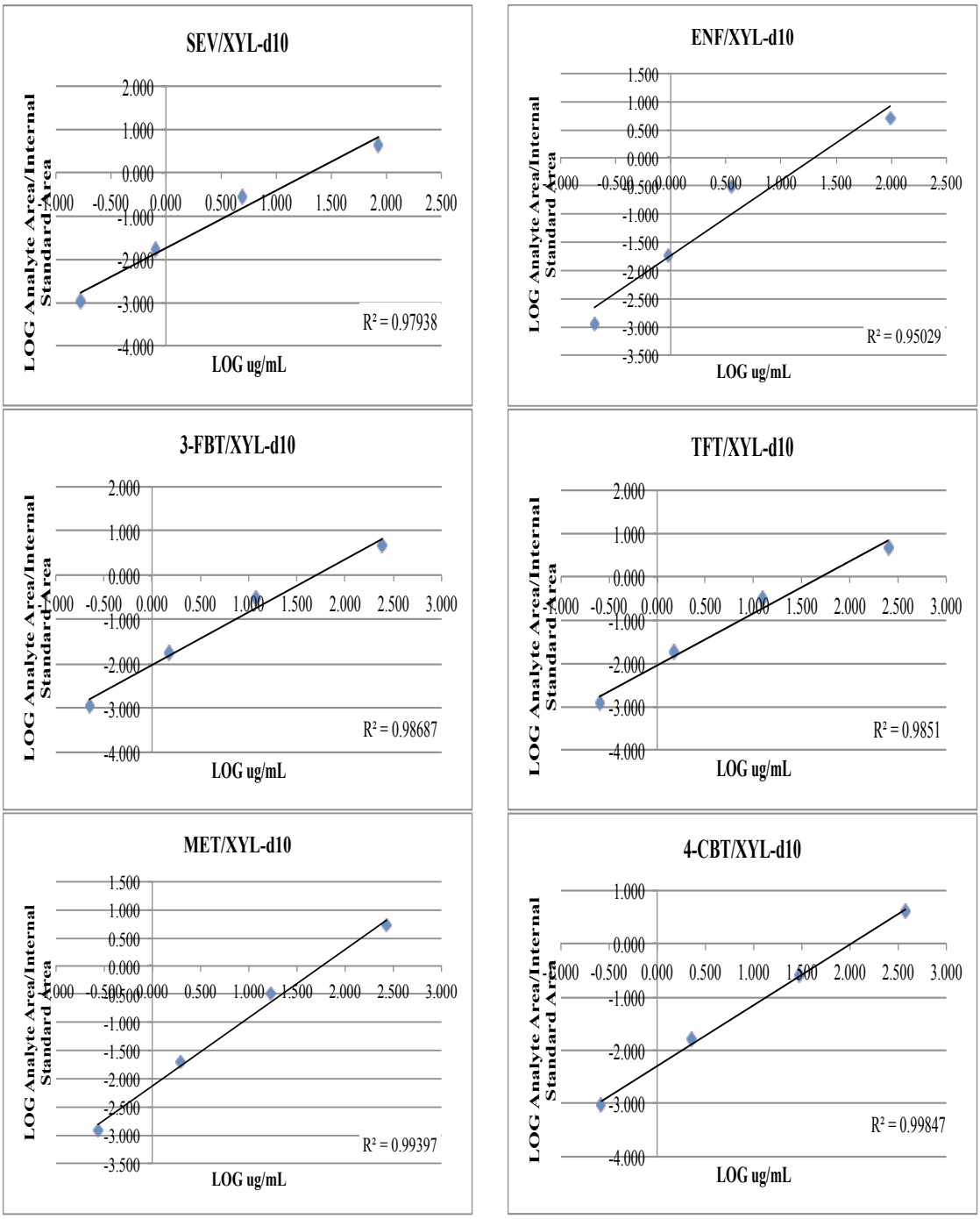

*The title for each graph signifies the graph generated for the tracer compound versus the internal standard.

Graph. E.4. Calibration curve of all 6 analytes and benzene-d6 as the internal standard. Levels 1-5 represented in the graph (concentrations listed in Table 7.7).*

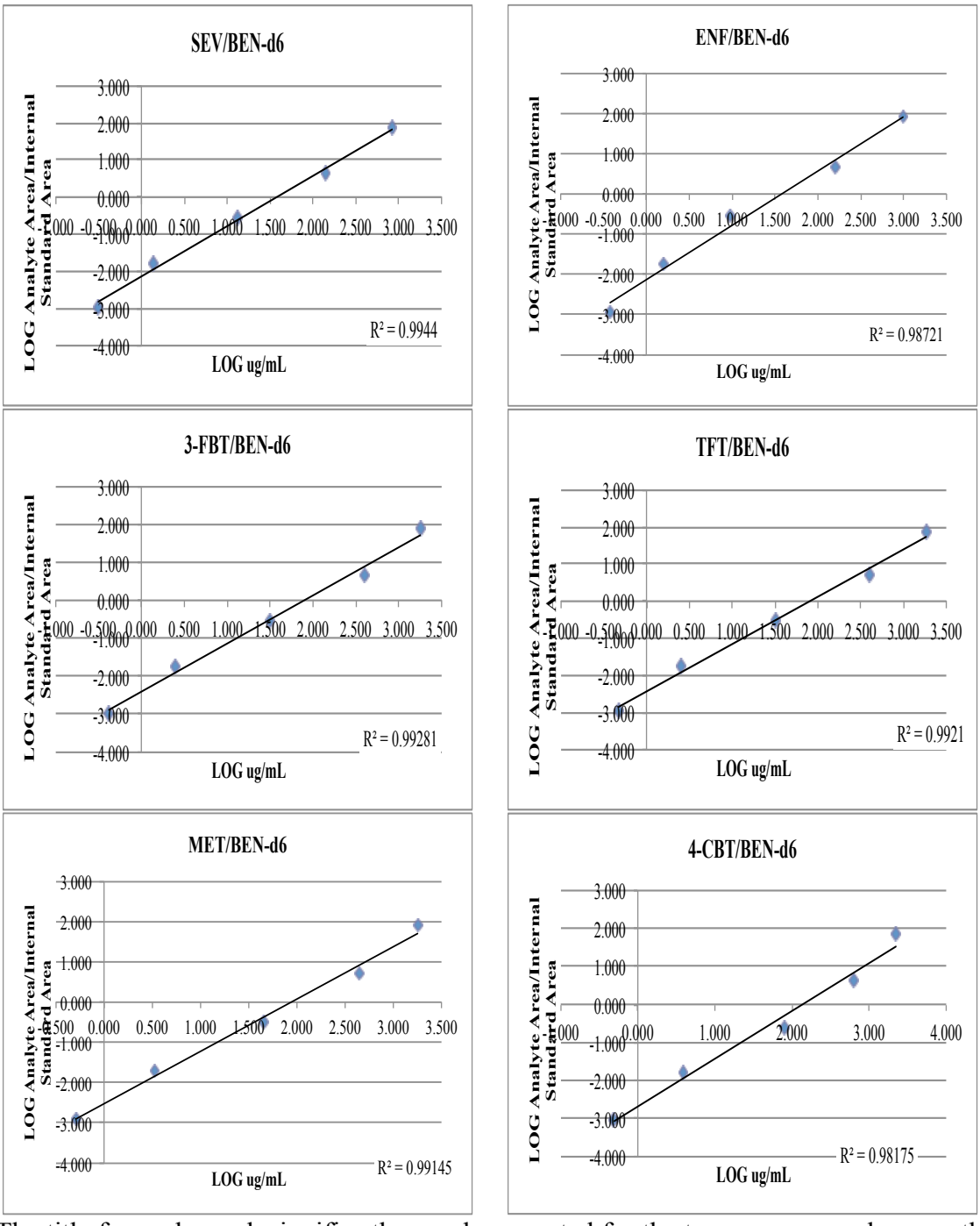

*The title for each graph signifies the graph generated for the tracer compound versus the internal standard.

Graph. E.5. Calibration curve of all 6 analytes and toluene-d8 as the internal standard. Levels 1-5 represented in the graph (concentrations listed in Table 7.7).*

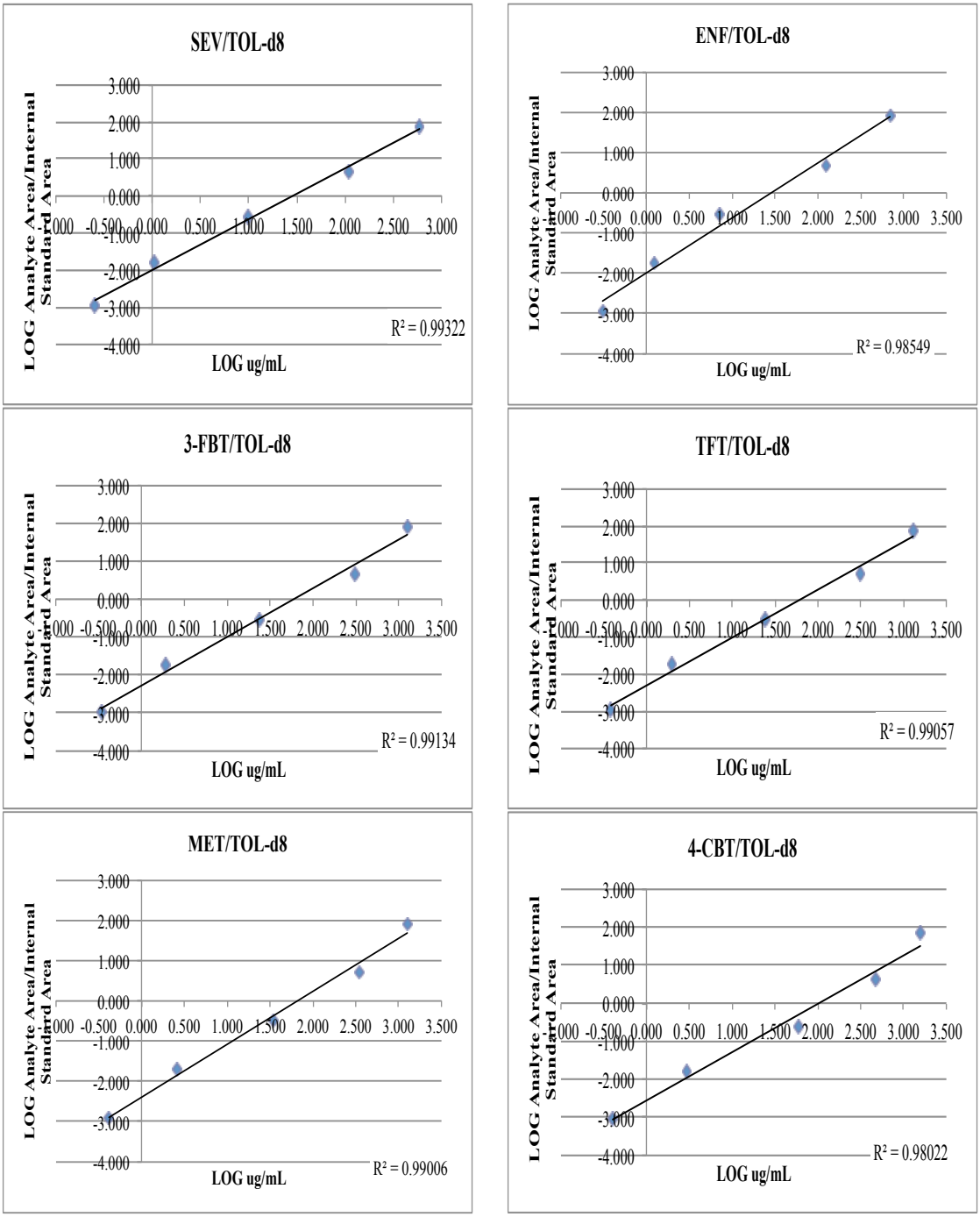

*The title for each graph signifies the graph generated for the tracer compound versus the internal standard.

Graph. E.6. Calibration curve of all 6 analytes and ρ-xylene-d10 as the internal standard. Levels 1-5 represented in the graph (concentrations listed in Table 7.7).*

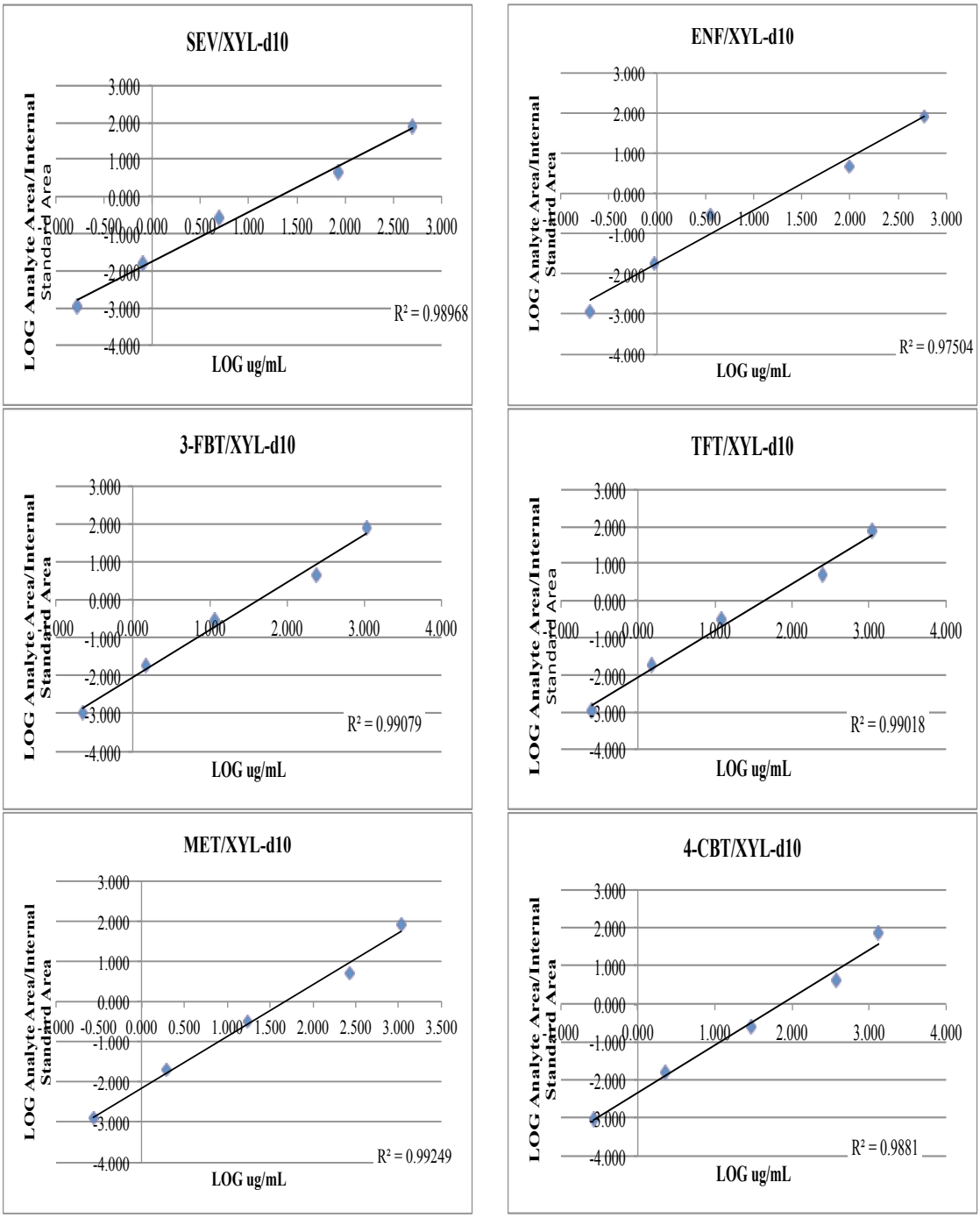

*The title for each graph signifies the graph generated for the tracer compound versus the internal standard.

F. Elimination Graphs of EBC from Subject 1 and Subject 2

The following graphs in this appendix were generated from data collected from EBC and canister samples after a single exposure. The number of days was compiled from both subjects for each compound and a bar graph was generated and found in Section 7.9 (Figure 7.10) of this thesis. Graph. F.6 - Graph. F.8 shows data that used all three internal standards for each tracer compound. This was carried to demonstrate that all 3 internal standards will have the same elimination trend.

Graph. F.1. Elimination graph of tracer compound from subject 2's breath, who was exposed to 1 ppm of TFT.

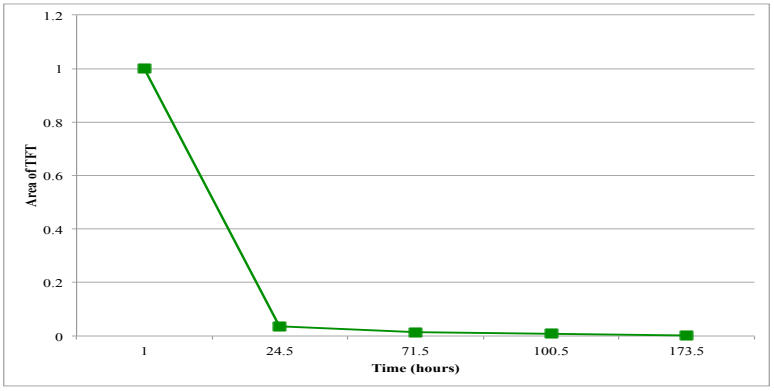

Graph. F.2. Elimination graph of tracer compounds from 1's breath, who was exposed to 1 ppm each of A) MET, SEV, and TFT; and B) ENF.

A)

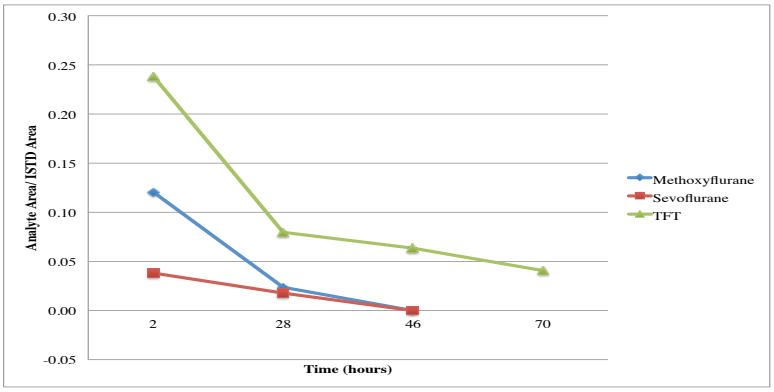

B)

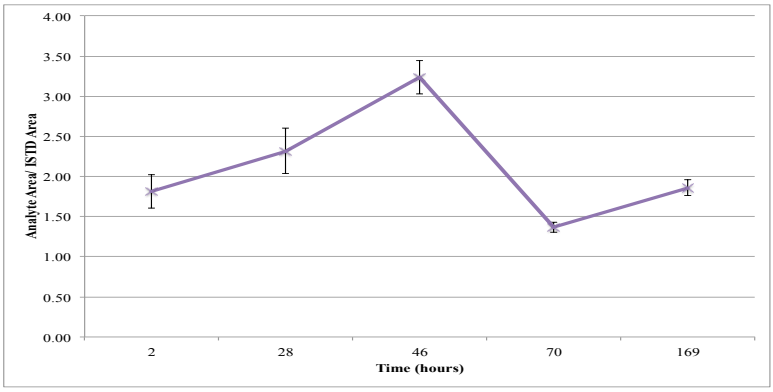

Graph. F.3. Elimination graph of tracer compound from subject 2's breath, who was exposed to 1 ppm of TFT.

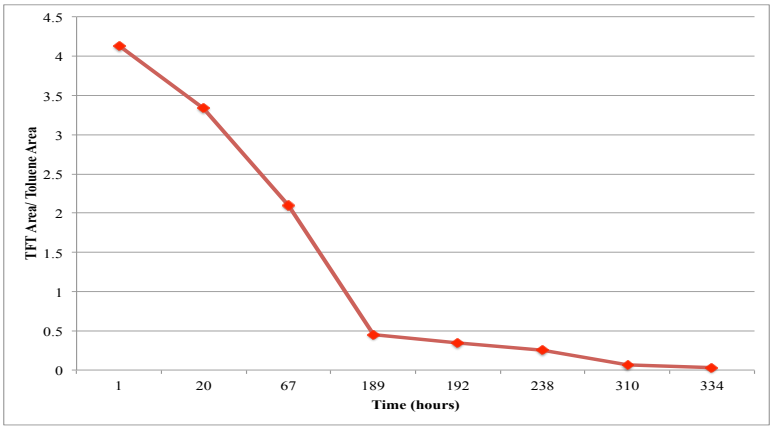

Graph. F.4. Elimination graph of tracer compound from subject 1's breath, who was exposed to 1 ppm of TFT.

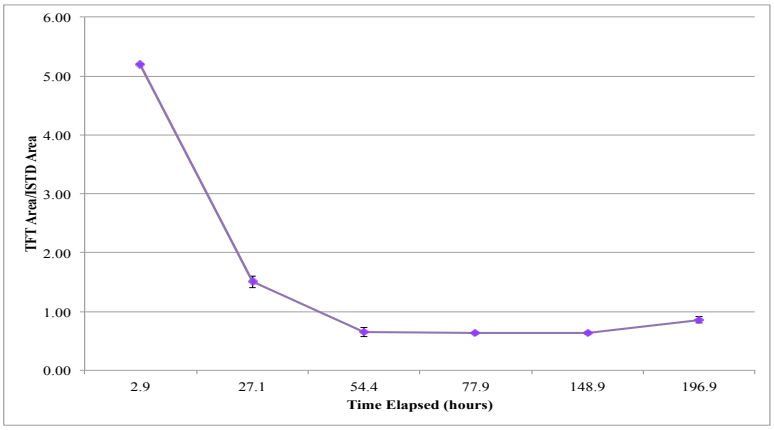

Graph. F.5. Elimination graph of tracer compound from subject 1's breath, who was exposed to 1 ppm of TFT.

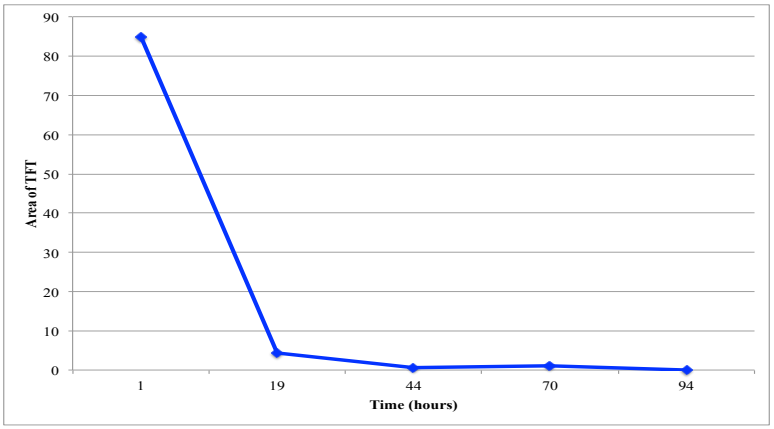

Graph. F.6. Elimination of MET, SEV, ENF, 4-CBT, 3-FBT, and TFT from EBC of subject 2, trial 1.*

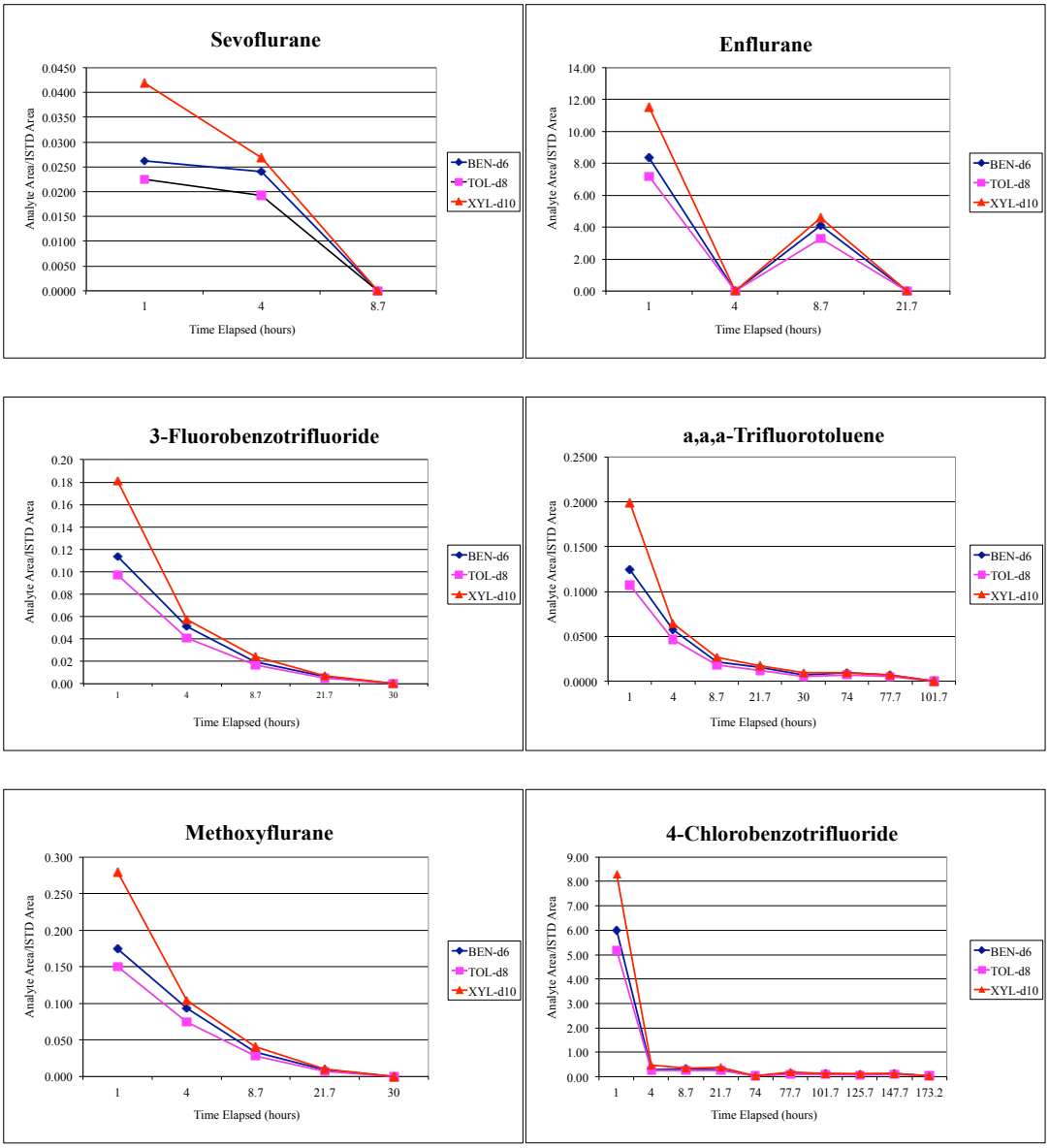

*Each graph contains data points in which the area of the compound was normalized by calculating and graphing ratios of tracer and internal standard vs. time. All 3 internal standards were used and the data points are defined by the legend.

Graph. F.7. Elimination of MET, SEV, ENF, 4-CBT, 3-FBT, and TFT from EBC of subject 2, trial 2.*

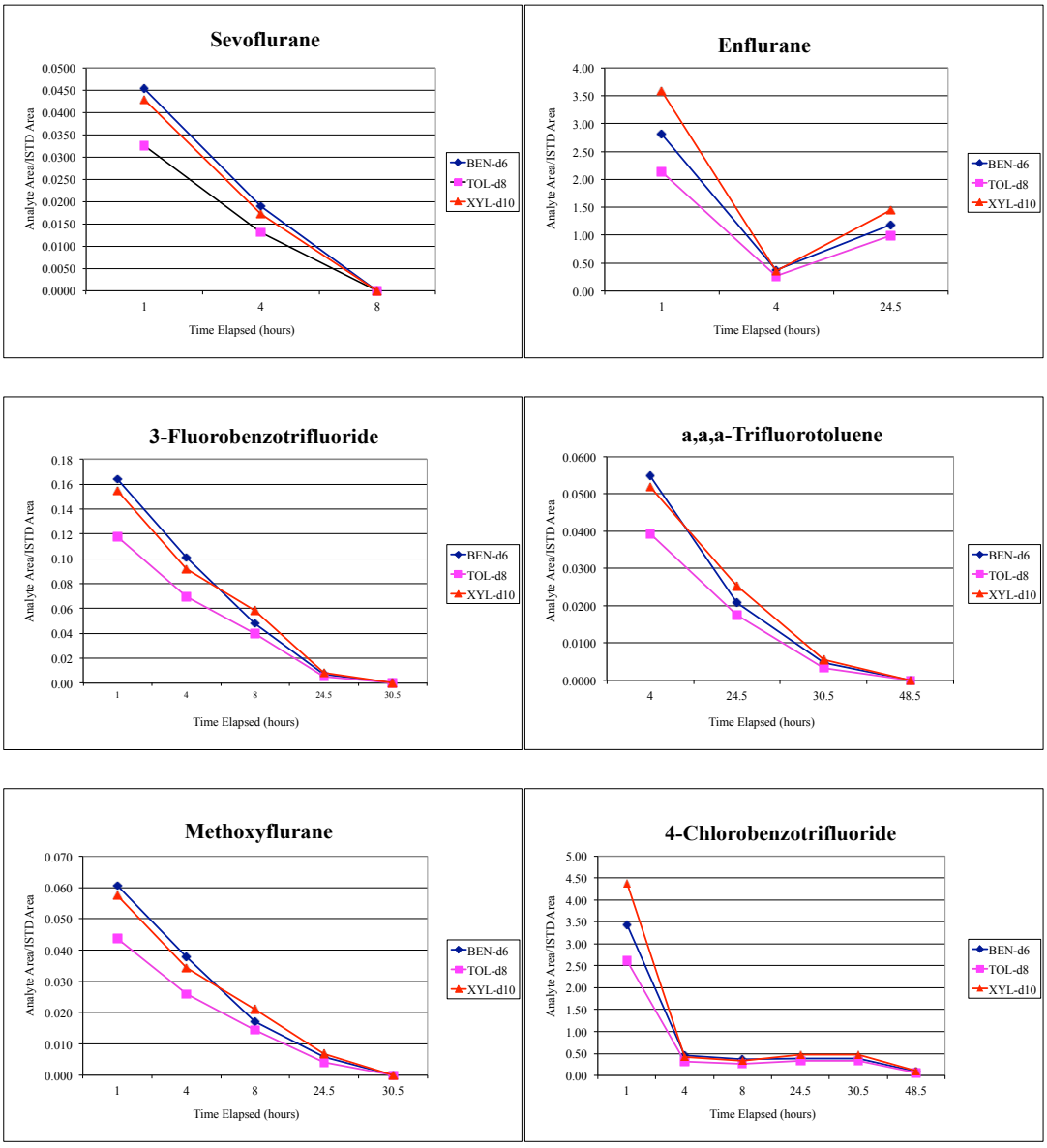

*Each graph contains data points in which the area of the compound was normalized by calculating and graphing ratios of tracer and internal standard vs. time. All 3 internal standards were used and the data points are defined by the legend.

Graph. F.8. Elimination of MET, SEV, ENF, 4-CBT, 3-FBT, and TFT from EBC of subject 2, trial 3.*

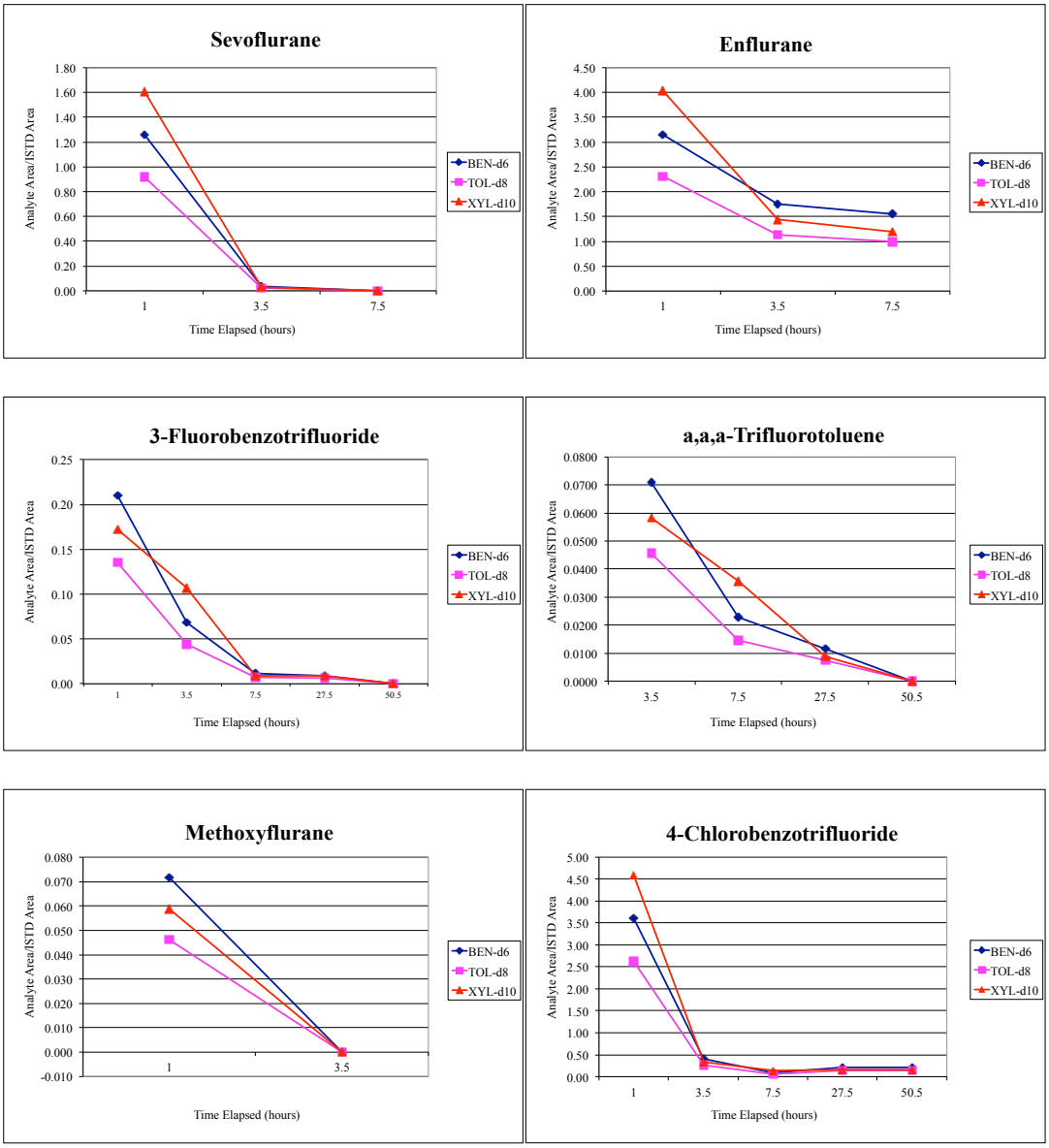

*Each graph contains data points in which the area of the compound was normalized by calculating and graphing ratios of tracer and internal standard vs. time. All 3 internal standards were used and the data points are defined by the legend.